The Meaning of LIF

The Role of Leukaemia Inhibitory Factor in Prostate Cancer-Induced Bone Disease

Christina Jane Turner

Supervisors

Professor Claire M. Edwards

Professor Freddie Hamdy



Nuffield Department of Surgical Sciences

University of Oxford

Trinity 2018

For Mary Turner

2nd November 1925 - 5th April 2016

Declaration

All the work presented in this thesis is the result of my own work unless otherwise stated and does not constitute part of any other thesis. The work herein described was carried out while I was a graduate student of the Nuffield Department of Surgical Sciences working at the Botnar Research Centre, under the supervision of Associate Professor Claire Edwards and Professor Freddie Hamdy.

Acknowledgements

Firstly, I would like to thank Prostate Cancer UK for funding this research.

Secondly, I would like to express my appreciation and thanks to my primary supervisor Professor Claire Edwards, without whom I would never have been given this amazing opportunity. She has allowed me to become a self-sufficient scientist, capable of dealing with problems and setbacks not only during research, but also in life in general. Moreover, she has pushed me to become confident in my abilities and myself, and for that I will always be grateful.

I would also like to thank my second supervisor Professor Freddie Hamdy, who through the Nuffield Department of Surgical Sciences, organised funding for my final year of my DPhil, allowing me to achieve what I have today.

My deepest gratitude goes to Dr Srinivasa Rao. Rao was a previous DPhil student when I first began my journey at the University of Oxford and luckily for me, he had decided to stick around after he finished. Since I started Rao has been my daily mentor, teacher, role model and dearest friend. Words will never convey how thankful I am to him for his patience, guidance and unparalleled wit.

Next, I wish to express my thanks to Dr Emma Morris, who kept me going over the last four years. Through times of hardship and disappointment, she would never be too busy to offer advice, brainstorm ideas or just get me to crack a smile. Her fabulous sense of humour and wonderful personality were what made working in the Edwards' group so

fantastic and I will miss her terribly when I leave.

Special thanks go to fellow DPhil students and partners in crime Aneka Sowman and Jess Whitburn, who made me laugh so much along the way. I could not have asked for two better people to 'discuss' the turmoils of research with. Thanks also go to Quitterie Larrouture and Laura Diment who together with Aneka and Jess made the DPhil room so much fun.

Thanks go to Dr Sam Olechnowicz for all his advice and incredible dry sense of humour, Dr Beatriz Gámez Molina for her technical input, straight talking attitude and kindness, Dr Sarah Gooding for all her advice and Professor James Edwards for his infectious smile and positivity.

To the Oppermann Group I would like to say a big thank you for every reagent ever borrowed and each piece of equipment used, especially in regards to the RNA-seq work. In particular I would like to say a big thank you to Dr Jim Dunford for his excellent laugh and brilliant banter that kept me smiling, Graham Wells for his kindness and personality and Dr Martin Philpott for his help with the Illumina RNA-seq machine.

I would also like to say thank you to Dr Ana Gomes for all her assistance and training on the IVIS imaging machine.

For his incredible, unrelenting support over the last four years, I wish to say a special thanks to my partner, Dr Luke Payne. He has always encouraged me to pursue my dreams and has helped me bear the weight of my DPhil and sporting achievements. He has been by my side through every high and every low and I am extremely lucky to have him in my life.

To my parents, Christopher and Denise Turner. Words will never do justice to the gratitude I feel for everything you have both done for me. The numerous times you have allowed me to vent about situations, the magnitude of times you have supported me and the countless times you have shown me that I can do and be anything, are only a few reasons why I shall ever be indebted to you. Thank you for always being the voice of

reason in times of great stress, I hope that I have made you both very proud.

And to my sister for always making me look good in comparison, just kidding. Thank you for being the kindest, most big-hearted person I know and for giving me all the hugs I needed, but didn't want to admit to.

A big shout out to all the girls from the Oxford University Women's Lightweight Rowing Club, who made my time at Oxford so enjoyable, in particular special thanks to Maline Meiske, Ellie Watts and Hannah Patel for being incredible team mates and friends.

Lastly, I would like to thank my grandparents Roy and Mary Turner, who have always been supportive of me throughout life. My wonderful nanny sadly lost her battle with cancer during this endeavour and I will miss her always. She was and still is the strongest, most witty and selfless person I have ever known. She never stopped believing in me and taught me that there isn't a single thing in this world I cannot achieve if I want it desperately enough. She is the reason I'm the person I am today and without her, none of this would have been possible.

Publications and Achievements

Publications

Turner, C. J. and Edwards, C. M. (2016), 'The role of the microenvironment in prostate cancer-associated bone disease.', *Curr Osteoporos Rep* **14**, 170-177.

Presentations

'Leukaemia inhibitory factor: a novel mediator of prostate cancer-induced bone disease?' - March 2018, Prostate Cancer Meeting, University of Oxford.

'The role of leukaemia inhibitory factor in bone-metastatic prostate cancer' - July 2016, Bone Research Society Meeting, Liverpool, UK.

'The role of leukaemia inhibitory factor in bone-metastatic prostate cancer' - October 2015, Nuffield Department of Surgical Sciences Away Day, University of Oxford.

Posters

'Leukaemia inhibitory factor: a novel mediator of prostate cancer-induced bone disease?' - November 2017, NCRI Cancer Conference, Liverpool, UK. * Abstract Prize.

'Leukaemia inhibitory factor is increased in human bone-metastatic prostate cancer; a novel mediator of prostate-cancer-induced bone disease?' - September 2016, EAU Section of Urological Research Conference, Parma, Italy.

'Leukaemia inhibitory factor is increased in human bone-metastatic prostate cancer; a novel mediator of prostate-cancer-induced bone disease?' October 2016, Nuffield Department of Surgical Sciences Away Day, University of Oxford. * Poster Prize.

Abstract

Bone metastasis is a frequent complication of advanced prostate carcinoma (PCa) and there is an urgent need to elucidate the mechanisms that drive metastasis to identify novel therapeutics and biomarkers. Leukaemia inhibitory factor (LIF) is an IL-6 family cytokine known to be involved in a wide range of biological functions including haematopoiesis and bone formation. Moreover, it has shown to be overexpressed in a number of tumour types including those, which metastasise to bone, but the role in PCa is unknown. The aim of this project is to elucidate the contribution of LIF in PCa bone metastasis.

Using *in silico* analysis I established that increased LIF was associated with disease free survival and freedom from biochemical recurrence in PCa patients. Furthermore, LIF was significantly decreased in metastatic and specifically bone metastatic PCa patients. *In vitro* knockdown of LIF in PCa cells significantly increased migration and invasion. In contrast, long-term overexpression of LIF increased apoptosis, decreased cell proliferation and significantly increased sensitivity to chemotherapy. RNA-seq analysis of PCa cells with overexpression of LIF revealed a significant upregulation of the interferon pathway, *In silico* analysis of murine models of PCa bone disease showed upregulation of LIF in the bone microenvironment, which was supported by *in vitro* co-cultures systems and accompanied by an upregulation of RANKL and a downregulation of OPG. LIF treatment of bone stromal cells caused an increase in differentiation towards osteoblasts at the expense of adipocytes, with LIF serum levels correlating with late stage weight loss in tumour bearing mice as well as leptin levels.

My results indicate that LIF may be a double-edged sword in PCa. LIF is inversely correlated with metastasis in human PCa patients and caused decreased proliferation and increased apoptosis in PCa cells, but with functional effects in cells of the tumour-bone niche that may promote disease progression in advanced PCa.

Contents

List of Figures **14**

List of Tables **17**

1 Introduction **23**

1.1 Prostate cancer . . . 23

1.1.1 Prostate cancer: A history . . . 23

1.1.2 The prostate . . . 25

1.1.3 Risk factors for prostate cancer . . . 25

1.1.4 Diagnosing prostate cancer . . . 26

1.1.5 Prostate specific antigen . . . 27

1.2 Prostate cancer bone metastasis . . . 29

1.2.1 Symptoms of disease . . . 30

1.2.1.1 Pathological fractures . . . 30

1.2.1.2 Bone pain . . . 30

1.2.1.3 Spinal cord compression . . . 30

1.2.1.4 Hypercalcemia . . . 31

1.2.2 Diagnosing bone metastasis . . . 31

1.2.3 Patterns of spread . . . 32

1.2.4 Homing to bone . . . 33

1.2.5 Treatment . . . 35

1.3 The tumour-bone microenvironment . . . 36

1.3.1 Bone . . . 37
1.3.1.1 Osteoblasts . . . 37
1.3.1.2 Osteoclasts . . . 38
1.3.2 Bone marrow adipocytes . . . 40
1.3.3 Mesenchymal stem cells and bone marrow stromal cells . . . 40
1.3.4 Targeting the tumour-bone microenvironment . . . 42
1.4 Prostate cancer bone metastasis *in vivo* models . . . 44
1.5 Leukaemia inhibitory factor . . . 45
1.5.1 LIF in bone . . . 49
1.5.2 LIF in cancer . . . 52
1.5.3 Other biological activities of LIF . . . 56
1.5.3.1 Reproduction . . . 56
1.5.3.2 The neuromuscular system and heart . . . 56
1.5.3.3 The hemopoietic system . . . 57
1.6 Rationale . . . 58
1.7 Research aim and objectives . . . 58

2 Materials and Methods 59

2.1 Cell lines and reagents . . . 59
2.2 Lentiviral production and infection for knockdown . . . 61
2.3 Migration and invasion assays . . . 61
2.3.1 Matrigel transwell invasion assay . . . 61
2.3.2 Transwell migration assay . . . 62
2.3.3 Xcelligence cell migration assay . . . 62
2.4 LIF overexpression construct . . . 63
2.4.1 Inoue method for preparation of competent E.Coli 'ultra-competent' cells . . . 63
2.4.2 Plasmid cloning by restriction enzyme digest . . . 63
2.4.2.1 PCR for amplification of cDNA . . . 63
2.4.2.2 Gel Extraction . . . 64
2.4.2.3 DNA Digest . . . 64

2.4.3 Ligation . . . 64
2.4.3.1 Transformation . . . 65
2.4.3.2 Mini prep . . . 65
2.4.4 Transfection of target cells . . . 66
2.5 RNA isolation . . . 66
2.6 cDNA synthesis . . . 66
2.7 Quantitative real-time polymerase chain reaction (QRT-PCR) . . . 67
2.8 Mycoplasma testing by PCR . . . 69
2.9 Agarose gel electrophoresis . . . 69
2.10 RNA-Seq . . . 69
2.10.1 Transfection of cells for RNA-Seq . . . 69
2.10.2 NEBNext Ultra II RNA library prep for Illumina . . . 70
2.10.3 Qubit . . . 70
2.10.4 Tapestation . . . 70
2.10.5 Next Seq 500 (Illumina) . . . 70
2.11 Bioinformatics . . . 72
2.12 Protein isolation and western blotting . . . 72
2.13 Recombinant LIF treatment of prostate cancer cells . . . 73
2.14 Co-culture . . . 73
2.15 Bicalutamide/DHT treatment . . . 74
2.16 Adipocyte differentiation . . . 74
2.17 Oil Red O staining . . . 74
2.18 Lipid uptake . . . 75
2.19 Mineralisation assay . . . 75
2.20 Alizarin Red S staining quantification . . . 76
2.21 Alkaline phosphotase enzyme assay . . . 76
2.22 Myocyte differentiation . . . 77
2.23 Enzyme-linked immunosorbent assay (ELISA) . . . 77
2.23.1 Human LIF ELISA for *in vitro* samples . . . 77
2.23.2 Human LIF ELISA for *in vivo* and human patient samples . . . 77

2.23.3 Mouse Leptin ELISA . . . 78
2.23.4 Mouse Myostatin ELISA . . . 78
2.24 Cell viability - Alamar blue assay . . . 78
2.25 Vybrant cell labelling . . . 79
2.26 Cell cycle by propidium iodide staining . . . 79
2.27 *In vitro* luciferase assay . . . 79
2.28 *In vivo* model . . . 80
2.28.1 Intracardiac injections . . . 80
2.28.2 Luciferase injections and IVIS® imaging . . . 81
2.28.3 μCT of bones . . . 81
2.28.4 Extraction of *in vivo* bone marrow . . . 81
2.29 Statistical analysis . . . 82

3 LIF expression in prostate cancer 83

3.1 Introduction . . . 83
3.1.1 Big data . . . 84
3.1.2 Prostate cancer biomarkers . . . 85
3.1.3 Prostate cancer *in vivo* model . . . 85
3.1.4 Androgens in prostate cancer . . . 85
3.2 Aims . . . 86
3.3 Results . . . 87
3.3.1 LIF is associated with improved patient survival . . . 87
3.3.2 Circulating LIF does not correlate with metastatic stage . . . 93
3.3.3 LIF expression is not associated with site of establishment in cell lines . . . 97
3.3.4 LIF expression in prostate cancer metastatic *in vivo* model . . . 98
3.3.5 LIF is associated with confluency . . . 103
3.3.6 LIF is not regulated by androgen receptor, but decreases PSA . . . 103
3.4 Discussion . . . 109

4 Effect of LIF in prostate cancer cells 117

4.1 Introduction . . . 117
4.1.1 Cell cycle . . . 118
4.1.2 RNA-seq . . . 119
4.1.3 The interferon pathway . . . 120
4.1.4 Docetaxel treatment in prostate cancer . . . 121
4.2 Aims . . . 122
4.3 Results . . . 123
4.3.1 Effect of LIF knockdown in prostate cancer cells . . . 123
4.3.1.1 LIF knockdown shows significant effects on migration and invasion in prostate cancer cells . . . 126
4.3.2 Effect of LIF overexpression in prostate cancer cells . . . 127
4.3.2.1 Long term LIF overexpression causes slowing of cell growth, proliferation and progression through the cell cycle . . . 130
4.3.2.2 LIF overexpression activates the IFN-γ pathway . . . 136
4.3.2.3 Downstream signalling of LIF . . . 141
4.3.3 LIF overexpression increases chemotherapy sensitivity . . . 143
4.4 Discussion . . . 145

5 The effect of LIF in the bone microenvironment 152
5.1 Introduction . . . 152
5.1.1 RANKL . . . 153
5.1.2 Adipocyte markers . . . 154
5.1.3 Muscle markers . . . 154
5.2 Aims . . . 154
5.3 Results . . . 155
5.3.1 LIF is significantly upregulated in stromal cell co-culture with prostate cancer cells . . . 155
5.3.2 LIF is associated with fat and muscle markers *in vivo* . . . 161
5.3.3 LIF significantly increases mineralisation into osteoblasts at the expense of adipocytes . . . 166
5.3.4 LIF decreases differentiation into muscle cells . . . 173

5.4 Discussion 177

6 Discussion and Future Directions **182**

6.1 Summary of Chapter 3 183

6.2 Summary of Chapter 4 184

6.3 Summary of Chapter 5 185

6.4 Conclusions 187

6.5 Future Directions 189

6.5.1 To determine how LIF affects different stages of disease 189

6.5.2 To investigate if changes in LIF regulation and/or expression between localised and metastatic tumours are due to signalling changes or clonal selection 190

6.5.3 To elucidate if LIF secreted from localised disease primes the bone marrow microenvironment 190

6.5.4 To observe if LIF upregulation as a result of confluency inhibits Hippo/YAP signalling involved in contact inhibition and reduction of migration 191

6.5.5 To investigate prognostic features of innate immune response signatures by the IFN pathway 192

6.5.6 To determine if LIF treatment causes a synergistic effect in combination with chemotherapy treatment 192

Bibliography **194**

7 Appendix **218**

List of Figures

1.1 Digital radiography and multi detector computerised tomography (MDCT) scans of male Egyptian mummy. . . . 24
1.2 Epithelial to mesenchymal transition. . . . 34
1.3 Homing to bone. . . . 35
1.4 A historical view of patient presentation at different stages of disease . . . 36
1.5 Bone cell differentiation . . . 39
1.6 The 'vicious cycle' of bone metastasis. . . . 41
1.7 Schematic representation of therapies used to target the tumour-bone microenvironment . . . 43
1.8 LIFs isoforms . . . 46
1.9 Receptor signaling complexes formed with gp130. . . . 47
1.10 Leukaemia inhibitory factor. . . . 49
1.11 LIFs actions in bone remodelling . . . 52
1.12 LIF expression is increased in patients samples that developed prostate cancer induced bone metastasis . . . 58

2.1 Optimisation of reference genes for qRT-PCR . . . 67

3.1 Elevated LIF mRNA expression is associated with disease free survival. . . 90
3.2 LIF mRNA is decreased in bone metastasis from prostate cancer. . . . 91
3.3 LIF mRNA expression in benign, primary and metastatic prostate cancer. 92

3.4 LIF protein expression is not significantly different in plasma samples from pre-bone metastatic patients compared to non-bone metastatic patients and post-metastatic patients. 94
3.5 LIF expression in cell line is not associated with establishment site 97
3.6 *In vivo* prostate cancer model using PC3-GFP cells 100
3.7 *In vivo* prostate cancer model using PC3 NW1 cells 101
3.8 LIF expression in PC3 NW1 intracardiac murine model 102
3.9 LIF is associated with confluency 103
3.10 Bicalutamide dose and androgen depletion experiment time point optimisation. 106
3.11 Androgen manipulation has no effect of LIF gene expression. 107
3.12 rhLIF decreases PSA protein expression in LNCAPs 108

4.1 pLKO.1 puromycin shRNA construct 124
4.2 pLKO.1 shRNA LIF construct selection 124
4.3 LIF knockdown confirmation in PC3 cells 125
4.4 LIF knockdown in PC3 cells significantly increases migration and invasion 126
4.5 pcDNA 3.1 Hygromycin LIF construct 128
4.6 LIF overexpression confirmation in PC3 NW1 cells 129
4.7 Short term LIF overexpression shows no difference in cell proliferation . . . 130
4.8 Selection of LIF overexpression prostate cancer cells using hygromycin causes cell death 133
4.9 Long term LIF overexpression increases G1 phase of the cell cycle 134
4.10 Long term LIF overexpression slows proliferation of prostate cancer cells . 135
4.11 RNA-Seq of LIF overexpression prostate cancer cells (PC3 NW1) 137
4.12 RNA-Seq of LIF overexpression PC3 NW1 cells 138
4.13 Pathway analysis of differentially expressed genes in RNA-Seq 139
4.14 Confirmation of downstream IFN pathway components after LIF overexpression 140
4.15 Downstream proteins activated by LIF 142

4.16 LIF gene expression is decreased in chemotherapy resistant prostate cancer cells . . . 144
4.17 LIF overexpression increases sensitivity to Docetaxel . . . 144
4.18 Regulation of G1/S phase transition . . . 150

5.1 LIF is significantly upregulated in the stroma after prostate cancer xenograft 155
5.2 Gene expression of LIF is significantly upregulated in bone stromal cells after co-culture with prostate cancer cells . . . 158
5.3 LIF downstream pathways are activated in stromal cells after co-culture with prostate cancer cells . . . 159
5.4 Direct co-culture bone stromal cells with PCa cells after LIF overexpression 160
5.5 LIF is correlation with weight loss . . . 163
5.6 LIF is correlated with fat loss . . . 164
5.7 LIF is correlated with a decrease in muscle markers . . . 165
5.8 LIF significantly increases mineralisation of pre-osteoblasts . . . 166
5.9 rhLIF treatment significantly decreases differentiation into adipocytes . . . 167
5.10 LIF treatment on differentiating fat cells decreases fat markers . . . 168
5.11 LIF secreted from cancer cells significantly decreased LIF and increases RANKL expression in osteoblasts . . . 170
5.12 LIF secreted from cancer cells significantly decreases differentiation into adipocytes . . . 170
5.13 LIF overexpression in PCa cells has no effect on lipid uptake . . . 172
5.14 LIF treatment decreases muscle markers . . . 174
5.15 LIF treatment of differentiated myocytes decreases muscle markers . . . 175
5.16 Conditioned media from high LIF expression cells decreases muscle markers 176

6.1 Working model of LIF in prostate cancer . . . 188

List of Tables

2.1 Establishment sources of PCa cell line 60
2.2 LIF primers for overexpression 64
2.3 Taqman primer list 68
2.4 Sybr primer list 68
2.5 RNA-Seq index list 71
2.6 Antibodies List 73

3.1 Table of non-bone metastatic patients 95
3.2 Table of pre-bone metastatic patients 96
3.3 Establishment sources of PCa cell line 97

7.1 Table of differentially expression genes after RNA-Seq of LIF overexpression prostate cancer cells. 222

List of Acronyms

ADT Androgen deprivation therapy

AKT Protein kinase B

ALP Alkaline phosphatase

AR Androgen receptor

ATP Adenosine triphosphate

BC Before Christ

Bax Bcl-2-like protein 4

BCR Biochemical recurrence

Bim Bcl-2-like protein 11

BMP Bone morphogenetic protein

BPH Benign prostatic hypertrophy

CXCL1 C-X-C chemokine ligand 1

CXCL2 C-X-C chemokine ligand 2

CXCL12 C-X-C motif chemokine 12

CXCR4 C-X-C chemokine receptor type 4

CXCR6 C-X-C chemokine receptor 6

CNTF Ciliary neurotrophic factor

CRPC Castration-resistant prostate cancer

CT1 Cardiotrophin-1

DKK-1 Dickkopft-1

DHT Dihydrotestosterone

DMEM Dulbecco's modified eagle medium

DNA Deoxyribonucleic acid

DRE Digital rectal examination

EGTA Egtazic acid

ELISA Enzyme-linked immune sorbent assay

EMT Epithelial to mesenchymal transition

ET-1 Endothelin-1

FBS Fetal bovine serum

FDA Food and drug administration

FGF Fibroblast growth factor

GEO Gene Expression Omnibus

GFP Green fluorescent protein

G1 phase Gap 1 phase

gp130 Glycoprotein 130

HIF1a Hypoxia-inducible factor 1-alpha

HSC Haematopoietic stem cell

IBMX Isobutylmethylxanthine

IGF Insulin-like growth factor

IHC Immunohistochemistry

IL-6 Interleukin-6

IL-6R Interleukin-6 receptor

IL-8 Interleukin-8

IRF-1 Interferon regulatory factor 1

JAK Janus kinase

kDa Kilodalton

KO Knock-out

LG L-Glutamine

LIF Leukaemia inhibitory factor

LIFR Leukaemia inhibitory factor receptor

MAPK Mitogen-activated protein kinase

MDCT Multidetector computed tomography

MMP-9 Matrix metallopeptidase 9

MRI Magnetic resonance imaging

mRNA Messenger ribonucleic acid

MSC Mesenchymal stem cell

mTOR Mechanistic target of rapamycin

MW Molecular weight

NGF Nerve growth factor

OPG Osteoprotegerin

OSM Oncostatin-M

PBS Phosphate-buffered saline

PCa Prostate carcinoma

PCNA Proliferating cell nuclear antigen

PCA3 Prostate cancer antigen 3

PDGF Platelet-derived growth factor

PET-CT Positron emission tomography - computed tomography

PGE2 Prostaglandin E2

PSA Prostate specific antigen

PTEN Phosphatase and tensin homolog

PTHrP Parathyroid hormone-related protein

PTI-1 Prostate tumour inducing gene-1

p21WAF1 Cyclin-dependent kinase inhibitor 1

PVDF membrane Polyvinyl difluoride membrane

RANK Receptor activator of nuclear factor kappa-B

RANKL Receptor activator of nuclear factor kappa-B ligand

RPMI Roswell park memorial institute medium

RIPA buffer Radioimmunoprecipitation assay buffer

RT-PCR Real time - polymerase chain reaction

RNA Ribonucleic acid

Runx2 Runt-related transcription factor 2

siRNA Small interfering ribonucleic acid

shRNA Short hairpin ribonucleic acid

S phase Synthesis phase

STAT Signal transducer and activator of transcription

TAE buffer Tris-acetate-EDTA buffer

TP53 Tumour protein 53

TRAMP Transgenic adenocarcinoma mouse prostate

TYK2 Non-receptor tyrosine-protein kinase

VEGFA Vascular endothelial growth factor-A

1

Introduction

1.1 Prostate cancer

1.1.1 Prostate cancer: A history

How old is prostate cancer?

Cancer itself is now one of the biggest causes of premature death worldwide. With Cancer Research UK being founded in 2002 and general awareness of this disease ever increasing, it seems hard to think back to a time when cancer was a taboo subject. But how old is it and when did we see the first signs of prostate cancer? Cancer is not a new disease that has developed relatively recently; it has affected people worldwide for centuries. The term 'cancer' originated from the Greek word 'karkinos', meaning crab. Hippocrates (460-370 B.C) originally used it to describe carcinoma with 'finger-like' spreading projections from the main tumour mass. In 2011 Prates *et al* documented what they believed to be the oldest evidence of bone disease from prostate cancer. Using digital x-rays and radiography and multi detector computerised tomography (MDCT), they assessed the remains of three Egyptian mummies. Their interest was drawn to an unnamed wrapped

Ptolemaic mummy (c.285-30BC), whose preserved male perineal anatomy and mummified genitals confirmed his gender. Based on tooth wear, epiphyseal fusion and bone density it was calculated that the male was between 51 and 60 years of age with a height of 1.66m. Multiple focal medullary dense bone lesions were found on the vertebrae, mostly around the lumbar spine. These were generally round in shape and varied in size between 1 and 15mm, similar dense lesions were also found in the pelvis. Considering the typical spread of prostate cancer, the traditional sclerotic bone lesions associated with the disease and the age of the individual it is very likely that the male discovered was suffering from bone metastatic prostate cancer (Prates et al., 2011). However, even this was not the first evidence of bone disease in general, as proven by signs of bone cancer in Egyptian mummies and in ancient manuscripts written almost 3500 years ago. It was noted that there was no cure for cancer, only palliative treatment and according to inscriptions, surface tumours were actually surgically removed in a similar manner as they are today (Sudhakar, 2009). Knowledge is described as 'facts, information, and skills acquired through experience or education; the theoretical or practical understanding of a subject'. The growth in knowledge of cancer biology has led to remarkable progress in early detection, treatment and prevention. Our accumulated knowledge and history of cancer is therefore paramount to our ever-evolving ideas on how to combat this disease.

A **B**

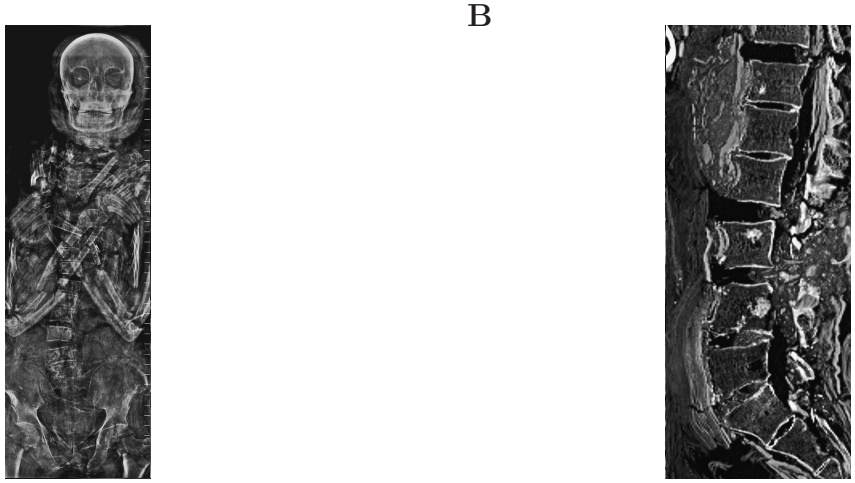


Figure 1.1: **Digital radiography and multi detector computerised tomography (MDCT) scans of male Egyptian mummy.** (**A**) Digital x-ray of the extended upper body of a male Ptolemaic Egyptian mummy, from the Museo Nacional de Arqueologia (MNA) in Lisbon. (**B**) MDCT scans of the lumbar spine, showing sclerotic vertebral bone lesions. Both images were taken from the publication by Prates *et al* 2011 (Prates et al., 2011).

1.1.2 The prostate

The prostate is a male accessory sex gland found only in mammals that functions to produce seminal fluid. Classical descriptions of prostate anatomy began in the late 1800s. Besides the anatomical illustrations published by Andreas Vesalius in 1543, an early description of the male sex organ was reported by Gerard Blasius, put simply as 'glandulae' surrounding the bladder (Timms, 2008). The current understanding of prostate anatomy and development, has largely progressed due to the fascinating nature of the developmental processes that give rise to the prostate and the interest in understanding why high incidence rates of prostatic diseases exist in humans (Marker et al., 2003). The prostate is composed of two main compartments, the stroma and the epithelium, which together ensure normal prostatic development and homeostasis (Verze et al., 2016). The epithelial compartment secretes the prostatic fluid, which contains a number of factors that support sperm maturation necessary for semen liquefaction and sperm motility. Consisting of fibroblasts, myofibroblasts and smooth muscle cells the stromal compartment ensures the appropriate microenvironment for the epithelial compartment (Verze et al., 2016). The stroma provides supportive signals to retain or restore gland homeostasis in healthy conditions or during the regeneration process. Androgens play a crucial role in prostate development and function, but also pathogenesis of disease. Stroma is a mediator of androgenic effects on the epithelium and regulates the fate of stem cells and potentially the initiation and progression of prostate cancer (Berry et al., 2008).

1.1.3 Risk factors for prostate cancer

In 1853 J. Adams described prostate carcinoma (PCa) as a 'very rare disease' (Adams, 1853). It is startling that 165 years later PCa has become that most common type of cancer amongst men in the UK with mortality rates second only to that of lung cancer. However, this dramatic increase in incidence rates is largely attributed to; an increase in life expectancies, better classification of what falls into the category of 'prostate cancer' and environmental or dietary effects of 'western cultures' (Denmeade and Isaacs, 2002).

Currently the mean age of patients with PCa is 72-74 years old, with 85% of patients diagnosed over 65 years old. At 85 the cumulative risk of PCa ranges between 0.5% to

20% worldwide, it is very rare for a male younger than 50 years old to develop this disease (<0.1%), making this a disease increased by age (Grönberg, 2003). Family history of disease is also an important risk factor. In 2003 three separate studies used meta-analysis to evaluate the risk of PCa in relatives of affected men. Since then clustering of familial cohorts has been assessed in new populations. In 2011 Kincinski *et al* published evaluated data to assess the strength of PCa familial aggregation, their study was much larger than previous meta-analysis, but confirmed the same conclusions. They observed more than a two-fold increase in disease incidence rates for all investigated types of familial clustering. Interestingly having an affected brother is associated with a further increased risk than an affected father. Incidence rates also increase with increased numbers of affected family members and furthermore increases the risk for younger family members (aged 65 and under). This suggests the importance of genetic factors and/or environmental factors in early onset PCa (Kiciński et al., 2011). Ethnicity is now also recognised as a risk factor for PCa. Genetic and environmental factors probably account for the predisposition of PCa towards black males, although identifying risk variants have proven difficult. Amundatatir *et al* reported that 8q24 is the most frequently gained chromosomal region in PCa. The gain of this chromosome has been associated with a more aggressive phenotype and poorer prognosis (Amundadottir et al., 2006). At least three distinct loci in separate linkage disequilibrium blocks are present on 8q24, identified by subsequent genome wide association studies. The susceptibility alleles of these loci are more common in men of African and African American origin and thus explains to a certain extent the increased frequency of disease in African ancestry (Kheirandish and Chinegwundoh, 2011).

1.1.4 Diagnosing prostate cancer

The main diagnostic tools for PCa include digital rectal examination, serum prostate-specific antigen (PSA) level and transrectal ultrasound-guided biopsies. Diagnosis depends on the presence of PCa in operative specimens and/or prostate biopsy cores. Ultrasound-guided biopsy has become the standard way to obtain material for histopathological examination (Axel et al., 2008). In 1966 Donald F Gleason created a grading system for PCa based on the architectural pattern of a tumour. The grades assigned range

from 1 to 5 with 1 meaning well differentiated and 5 meaning poorly differentiated. Since PCa are often made up of cancerous cells that have different grades, two grades are assigned for each patient. Poorly differentiated tumours tend to progress quickly while well differentiated tumours progress slowly and intermediate tumours progress at intermediate rates (Gleason, 1992). This scoring system is very useful for predicting the behaviour of PCa, although other factors will contribute towards the staging of disease. Most men presenting with early disease will not have signs or symptoms, however in some cases as the cancer begins to grow towards the urethra, there may be changes in urination, this may include; difficulty urinating, inability to empty the bladder, increased urination or urgency or weak flow upon urination. Older men presenting with lower urinary tract symptoms (LUTS) often request reassurance that their symptoms are not due to PCa, thus PSA testing is commonly used to provide reassurance (Collin et al., 2008). Indeed, this is corroborated by a longitudinal study by Young *et al.* In general practise there are higher testing rates amongst older patients, with high PSA not commonly being followed up by a biopsy, which is required for the diagnosis of PCa. Screening attempts to diagnose disease before symptoms arise, although it is rare for patients with PCa to present with LUTS until the disease is advanced. The results from the study by Young *et al* suggested that in a lot of cases, PSA testing was not used for diagnosis for PCa, but more for investigation and management of LUTS and other benign conditions (Young et al., 2017).

1.1.5 Prostate specific antigen

PSA is an androgen-regulated serine protease that is produced by normal prostate epithelial cells and PCa. It is commonly used as a serum marker for cancer risk (Balk et al., 2003). It is released into seminal fluid, in which it ranges in concentration from 0.3 to 3mg/ml. The majority of PSA is an active serine protease and proteolyses the gel proteins of seminal fluid (semenogelin I (SEMG1) and SEMG2), essentially liquefying the semen and allowing sperm to swim freely. The architecture of a normal prostate keeps PSA confined within it; only a tiny proportion of PSA is able to leak into the circulatory system. In healthy adult males aged $\leq$50 years, concentrations of PSA are 106-fold higher in seminal fluid than in blood, in which the median PSA level is $\approx$0.6 ng/ml. Within the

blood, PSA has little or no catalytic activity, mainly due to the excess presence of protease inhibitors such as α1-antichymotrypsin and α2-macroglobulin, which form stable covalent complexes. In the context of detecting PCa, a PSA level of 4ng/ml or above prompts a recommendation for a prostate biopsy. However the increased blood levels of PSA in PCa patients cannot be explained by increases in PSA expression. During the development and progression of PCa, PSA expression may actually decrease. The increased blood PSA levels reflect increased escape of PSA into blood from the prostate. This results from the disruption of prostate architecture in PCa patients, such as disordering of the basement membrane and loss of basal cell layer, ductal lumen architecture and epithelial cell polarity. In the US, PSA was approved by the food and drug administration (FDA) as a marker to monitor patients with PCa in 1986 and as a diagnosis marker in 1994. As PSA screening has become widespread there has been an increase in the incidence rate of PCa, with a decrease in the proportion of patients with metastatic or locally advanced cancer at diagnosis. However, PSA is also influenced by other prostate disease conditions such as benign prostatic hypertrophy (BPH) and prostatitis as well as age, body mass index and race. One of the main challenges in diagnosis and treatment of PCa is that clinically insignificant PCa is quite common. Many PCas pose no threat to life or health. PSA screening leads to the detection of many of these insignificant cancers, causing patients anxiety and unnecessary treatment (Lilja et al., 2008).

The diagnosis of PCa is currently based on a combination of serum PSA testing and/or digital rectal examination (DRE) and histopathologic evaluation of prostate biopsies. The primary limitation of PSA testing is its lack of specificity. More specific biomarkers are needed not only to improve early detection of PCa, but also to predict metastatic disease. In the past few years, many new promising biomarkers have been identified; however, to date, only a few have reached clinical practice (Hendriks et al., 2017). But PSA testing has developed over the last few decades.

Part of PSA in the blood is complexed and the major part circulates in an unbound form. This unbound form is called freePSA (fPSA) and the free-to-total PSA ratio significantly improves specificity. Moreover, prostate cancer antigen 3 (PCA3), formerly differential display code 3 (DD3), was discovered by Bussemakers *et al.* in 1999. It is a

prostate specific non-coding RNA (Bussemakers et al., 1999) and although PCA3 does not encode a protein, PCA3 ncRNA transcripts originating from prostate cells are detectable and quantifiable in urine. Other urinary detectable biomarkers include the transmembrane protease serine 2-ERG (TMPRSS2-ERG) gene fusion. TMPRSS2-ERG gene fusion seems to be specific for PCa in tissue-based studies and can also be detected in urine after prostate massage. Hessels *et al* determined that, this gene fusion has a 93% specificity and 94% positive predictive value for detection of PCa in post-DRE urine samples in a cohort of 108 men undergoing prostate biopsy. However, TMPRSS2-ERG gene fusions are not yet approved as a PCa biomarker due to the uncertainty of its predictive value of aggressive disease (Hessels et al., 2007).

1.2 Prostate cancer bone metastasis

Bone metastasis is the most frequent complication of progressive disease. The balance between the activities of bone cells determines the phenotype of metastatic bone lesions. The type of bone metastasis is typically referred to as either 'lytic', 'sclerotic' or 'mixed' and this is usually established from the radiographic appearance of the lesions (Coleman, 1997). It is important to note that although PCa is traditionally associated with sclerotic bone metastasis, that this can be a disease of mixed bone lesions. In fact work carried out by Coleman *et al* in 2008 showed that mixed bone metastatic PCa was actually more bone resorptive than breast cancer or multiple myeloma which are normally associated with osteolytic lesions (Coleman et al., 2008). Bone metastasis causes serious morbidity, in 2000 Berruti *et al* reported that 30% of men with hormone refractory PCa and bone metastasis eventually developed skeletal complications. Patients may experience skeletal complications such a bone pain, pathological fracture, spinal cord compression and symptomatic hypercalcemia (Berruti et al., 2000).

1.2.1 Symptoms of disease

1.2.1.1 Pathological fractures

Metastatic destruction of the bone reduces its ability to bear any load resulting in microfractures and subsequently loss of bone integrity. The incidence of rib fractures and vertebral collapse is common causing kyphoscoliosis, loss of height and restrictive lung disease. That being said it is the fracture of a long bone or expansion of the tumour into the spine that causes the most disability amongst patients (Tazi et al., 2003).

1.2.1.2 Bone pain

Bone pain is the most common type of pain arising from cancer and is a significant problem. It is often described as a deep boring sensation that aches or burns, accompanied by intermittent feelings of stabbing pain. Pain may occur around the joints due to mechanical or chemical changes and there is often a disturbance of the innervated periosteum, which can give the pain neurogenic like properties. Clearly bone pain contributes to a decreased quality of life in patients. Moreover, side effects from certain analgesics may in fact be worse than the bone pain itself (Tazi et al., 2003).

1.2.1.3 Spinal cord compression

Spinal cord compression is a common neurologic complication of advanced malignancies, with a frequency amongst patients of between 5 - 10%. PCa is only second to lung cancer as a cause of metastatic spinal cord compression. Involvement of the cord is secondary to local extension of a vertebral metastasis. Tumour compression leads to venous obstruction and development of vasogenic oedema. Back pain is a common symptom of cord compression occurring in 75% to 100% of cases. In the retrospective study conducted by Tazi *et al*, 79% of patients had developed back pain for an average of 60 days before the onset of neurological symptoms. The delay in the diagnosis of spinal cord compression may result in neurological deterioration and progression towards paraplegia. The goal of cord compression treatment is to restore function. Pain relief and prevention of deterioration are the main concerns (Tazi et al., 2003).

1.2.1.4 Hypercalcemia

Hypercalcemia is when the calcium level in blood to rise above normal levels and is a clinically important symptom of bone disease due to the morbidity associated with it. If left untreated moderate-to-severe hypercalcemia causes a number of symptoms including dysfunction of the gastrointestinal tract, kidneys and central nervous system. Hypercalcemia in cancer patients is often caused by increased osteoclastic bone resorption, either from the bone lesions (as with breast cancer or multiple myeloma), or more commonly as a process stimulated by factors such as parathyroid hormone-related protein (PTHrP) (Tazi et al., 2003).

1.2.2 Diagnosing bone metastasis

Diagnosis of bone metastasis currently relies primarily on technetium-99 m (^{99m}Tc) bone scanning and plain x-ray, although it has been shown by positron emission tomography–computed tomography (PET–CT) and magnetic resonance imaging (MRI) that ^{99m}Tc bone scanning frequently underestimates the true prevalence of bone involvement. Even with the use of these techniques specificity and sensitivity for identifying bone metastases varies, with no single approach being considered to be 100% accurate. It has been shown by Abuzallouf *et al* that the likelihood of a positive bone scan increases in patients with a $\geq$20ng/ml PSA level, locally advanced disease or a $\geq$8 Gleason score. Subsequent studies have supported that PSA level and Gleason scores can point towards metastatic disease, although there has been some debate about exact parameters. While PSA and other factors associated with disease progression can provide insight into the risk of bone metastasis, there needs to be a more specific marker to rapidly and accurately predict development of bone metastasis prior to diagnosis with bone scanning. This would allow intervention at the earliest opportunity for high risk patients. The biomarker in question would first need to be present at the initial diagnosis and correlate with the future risk of metastasis. Although several candidates have been described their ability to predict future development of metastasis remains unclear.

In PCa-induced bone disease, disruption of normal bone turnover leads to an increase in factors derived from bone formation (bone-specific alkaline phosphatase, N-terminal

propeptide of procollage type 1), bone resorption (C-telopeptide and N-telopeptide or type 1 collagen and carboxyterminal cross-linked telopeptide of type one collagen) and osteoclastogenesis (osteoprotegerin (OPG) and receptor activator of nuclear factor κ B ligand (RANKL)). All these factors can be measured in the blood or urine and their levels have been shown to be associated with some form of skeletal involvement. Other candidates from proteomic studies include eukaryotic translation factor α I (eEF1α1), which is a truncated form of what is known as the prostate tumour inducing gene (PTI-1). This was found to be elevated in the serum of patients with PCa and in osteoblasts in the vicinity of metastatic PCa cells. Furthermore, serum antiprostasome antibodies have also been identified as potential biomarkers for metastatic risk in 218 patients with PCa. Significant inverse relationships were found between pre-therapy antiprostasome antibody titre and subsequent metastasis to the bone and/or lymph nodes. Thus, in addition to PSA-related parameters there are novel biomarkers that may potentially exist that could predict the future development of bone metastasis. However, their validation in clinical practice is still to be elucidated. As such, we still strive for the ability to identify high risk patients for early intervention to prevent or delay bone metastasis and disease progression (Briganti et al., 2013).

1.2.3 Patterns of spread

Predicting and understanding the patterns of metastasis has historically remained a challenge in cancer. Two theories were formulated in the early twentieth century in a bid to explain specific metastatic patterns of certain tumour types. The 'mechanical' hypothesis describes the spread of the tumour into the lymphatic system followed by a distant spread through the venous system. Whereas the 'seed and soil' hypothesis describes the distribution of distant metastasis from the primary tumour as a plant going to seed. The plant produces seeds that are carried in all directions, but would only survive and grow if they fall on congenial soil (Hess et al., 2006). Since then there have been numerous contributions to the understanding of cancer pathogenesis, metastasis and the dependency of this process on the crosstalk between the tumour and the cancer microenvironment. A key publication by Gundem *et al* in 2015 showed the evolution of metastatic PCa from

primary tumourigenesis to metastasis and castration resistance, using whole genome sequencing. The study indicated that subclones develop metastatic potential within the primary tumour instead of the tumour developing this potential as a whole. Furthermore, they identified that tumour cells frequently spread from one metastatic site to another, as opposed to following a linear timeline of spread from the primary tumour to metastatic site. This work supports the 'seed and soil' hypothesis derived from Stephen Paget: in that rare subclones are able to give rise to disease progression through microenvironmental changes (Turner and Edwards, 2016).

1.2.4 Homing to bone

The initial stages of bone metastasis involve the detachment and migration of tumour cells into nearby blood or lymphatic vessels. Normal prostate epithelial cells are confined to the prostate capsule due to basal cells inside the lumen attaching themselves to the basement membrane, forming a cell layer. Epithelial cells above this base layer then also attach to each other as well as the extracellular matrix. Cell-to-cell adhesion is therefore maintained by different junctions, which are made of protein complexes of cell adhesion molecules. However, during transformation of malignant cells, adhesiveness decreases. Cells are then able to undergo multiple biochemical changes that enable them to assume a mesenchymal phenotype; this process is termed epithelial to mesenchymal transition (EMT) and is now considered to be critical in the development of migration and invasion. The new mesenchymal cells are then able to migrate away from the primary site and into the blood vessels (Jin et al., 2011).

Once cells intravasate, the initial homing to bone is largely regulated by numerous integrins and chemokines produced by stromal cells of the bone marrow. The most well-known interaction is the C-X-C chemokine receptor type 4 (CXCR4), located on tumour cells homing to its ligand, C-X-C motif chemokine 12 (CXCL12), which is expressed on stromal cells and osteoblasts (Autio and Morris, 2013). Furthermore, in addition to producing large amounts of CXCL12, osteoblasts also express anchorage molecules such as angiopoietin and osteopontin (OPN) that encourage tumour cells into the bone microenvironment. OPN has the ability to stimulate haematopoietic stem cell (HSC) and

osteoclast adherence to bone. It has key roles in trans-marrow migration, retention and negative relation of HSCs within the osteoblastic niches. Moreover, in both breast and PCa, OPN has been linked to regulation of metastatic spread and has been found to be highly expressed in metastatic cells and surrounding stromal tissue (Turner and Edwards, 2016) (Kaplan et al., 2006).

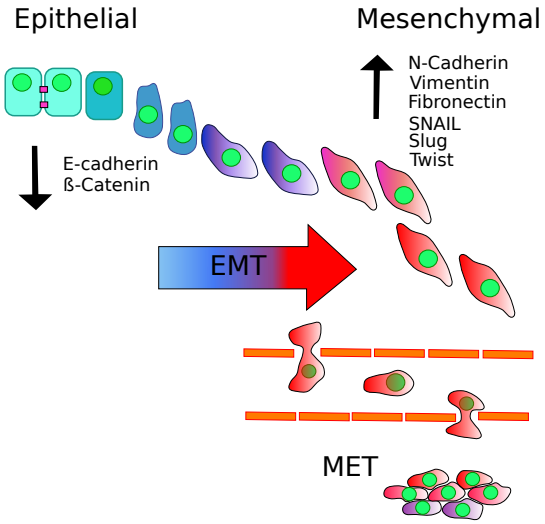


Figure 1.2: **Epithelial to mesenchymal transition.** EMT involves the functional transition of polarised epithelial cells into motile mesenchymal cells. Epithelial and mesenchymal cell markers commonly used to identify epithelial or mesenchymal phenotypes are listed. Initiation of metastasis in cancer requires invasion, which is enabled by EMT. Primary cancer cells lose their cell-cell adhesion through the loss of E-cadherin and are then able to intravasate. Circulating tumour cells then exit the bloodstream to form micro-metastasis where they undergo mesenchymal to epithelial transition (MET) for clonal outgrowth in metastatic sites.

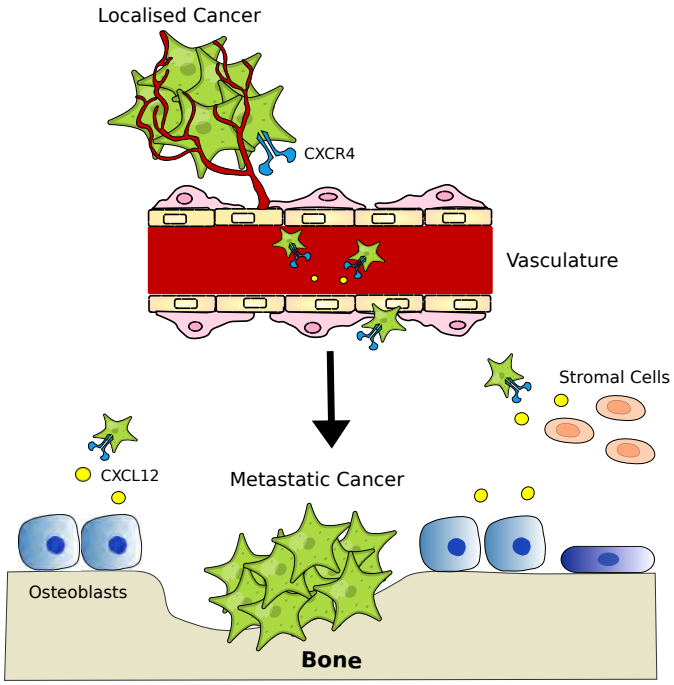


Figure 1.3: **Prostate cancer cells homing to bone.** CXCL12 is highly expressed in the bone marrow and is also secreted by stromal and tumour cells. CXCR4-expressing tumour cells migrate towards a CXCL12 gradient and home towards environments that release CXCL12. The CXCR4/CXCL12 interaction can result in increased proliferation, migration and invasion in tumour cells.

1.2.5 Treatment

The management of localised PCa is usually decided after balancing the benefits and side effects of each option. Active surveillance reduces the probability of overtreating in patients with low risk PCa. This involves monitoring of patients with DRE, PSA testing and/or secondary biopsy, but no active treatment, unless evidence of progression. Radical prostatectomy involves removing the prostate gland and surrounding tissues, however this may be accompanied with affter effects such as incontinence and erectile dysfunction. Localised patients may also be offered radiation therapy (Mottet et al., 2017). In men with metastatic disease, androgen deprivation therapy, (ADT) is prescribed. First line treatment for castration-resistant patients may include, Abiraterone or Enzalutamide (hormone therapies) or Docetaxel (a chemotherapeutic). In the case of relapse post treatment, clinicians may prescribe second line treatment, which will depend upon the first line treatment given. Treatments may include chemotherapy with Cabazitaxel or Docetaxel, with or without anti-androgen drugs such as Enzalutamide (Cornford et al., 2017).

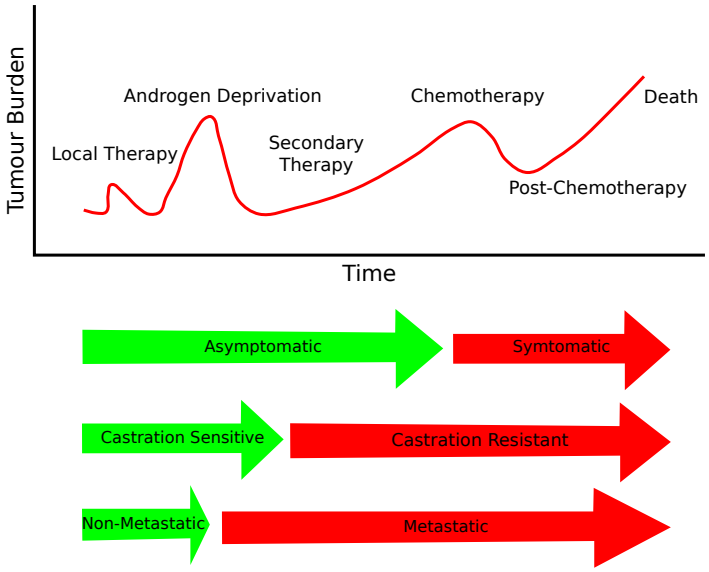


Figure 1.4: **A historical view of patient presentation at different stages of disease.** Surgery and radiation are typically used for patients with localised disease and low tumour burden. However, upon recurrence of disease, often accompanied with a rise in PSA levels, ADT therapy may be given on a continuous or intermittent basis. For the majority of patients PSA levels will subsequently lower and signs of tumour burden will decrease. However, over time many patients will develop castration resistant prostate cancer (CRPC). These patients may go on to have secondary treatment such as androgen synthesis-suppressing agents. Finally for patients who show signs of disease progression it may be necessary to initiate chemotherapy. Chemotherapy may reduce tumour burden and PSA levels, but in a number of cases post chemotherapy, patients will present with clinical deterioration and will ultimately die from their disease.

1.3 The tumour-bone microenvironment

The term 'bone microenvironment' broadly describes the structural and biological system, which encompasses cells of the hematopoietic and mesenchymal lineages, the bone marrow stroma and the extracellular matrix. The bone matrix is a rich source of growth factors, including transforming growth factor-β (TGF-β), insulin growth factors (IGFs), fibroblast growth factor (FGF), platelet-derived growth factor (PDGF) and bone morphogenetic proteins (BMPs). Collectively these growth factors make the bone an alternative site for metastasis, permitting the growth of tumour cells and increasing production and release of cytokines and other bone remodelling factors.

1.3.1 Bone

The adult skeleton is made up of 206 bones, excluding the sesamoid bones. The skeleton serves a variety of functions including providing structural support, protecting internal organs, allowing movement, maintaining mineral homeostasis and acid-base balance, serving as a reservoir of growth factors and cytokines and providing a suitable environment for haematopoiesis (Clarke, 2008).

Bone is a dynamic tissue that relies on the complex interactions between cells of the microenvironment i.e. osteoblasts, which control bone formation and osteoclasts, which control bone resorption, in order to maintain a constant bone mass. Tumour cells use the same regulatory pathways involved in normal bone development and remodelling in order to 'hijack' bone turnover. The dysregulation of bone turnover seen in cancer-induced bone metastasis is the result of the interactions between the tumour and stromal cells of the bone microenvironment (Turner and Edwards, 2016).

1.3.1.1 Osteoblasts

Osteoblasts are the cells that form bone and arise from mesenchymal stem cells (MSCs) (Figure 1.5). Correct osteoblastogenesis relies on a complex network of pathways whose alteration can cause several skeletal abnormalities. Runt-related transcription factor 2 (Runx2) is a 'master regulator' in osteoblast differentiation, driving the initial steps from MSC towards commitment to the osteoblastic lineage (Rucci, 2008). Numerous clinical studies have implicated osteoblasts in the progression of PCa to the bone. Use of bone-homing radiopharmaceuticals inhibit bone metastasis through preferential deposition in sites of increased osteoblastic activity and have shown significant palliative and survival benefits. These observations suggest that direct inhibition of osteoblasts can have an effect on progression of disease. Furthermore, indirect effects can also be seen through the use of bisphosphonates, in which trials have shown reversal of bone loss through inhibition of osteoclast activity, but no effect on cancer progression. This indicates that inhibition of osteoclast activity is not sufficient to influence PCa progression in bone (Logothetis and Lin, 2005).

Osteoblast activation and maturation in multiple myeloma, breast and PCa has been

shown to be stimulated by the Wnt pathway. Evidence suggests that Wnt released by metastatic PCa can stimulate osteoblasts to enhance tumour proliferation, while inhibitor of Wnt signalling; dickkopf-1 (DKK-1) can promote osteolysis, particularly during the early stages of cancer development. Expression of DKK-1 has been found to be upregulated in early PCa with a decline towards advanced bone metastases, suggesting that the initial upregulation is required for the establishment of the tumour, whereas the decrease during bone metastasis can promote Wnt expression, resulting in an increase in osteoblast activity, giving rise to the osteoblastic metastasis traditionally associated with PCa (Turner and Edwards, 2016). Other paracrine factors secreted by PCa that regulate osteoblast proliferation and/or differentiation include: BMP, TGF-β, IGF, PDGF, vascular endothelial growth factor-A (VEGF-A) and endothelin-1 (ET-1) (Logothetis and Lin, 2005). Indeed several members of the TGF-β family have been found to stimulate bone formation. Elevated concentrations of serum TGF-β have been found in bone metastatic PCa patients compared to matched non-bone metastatic controls (Shariat et al., 2001).

1.3.1.2 Osteoclasts

Osteoclasts are multinucleated cells derived from the monocyte/macrophage lineage (Figure 1.5). The differentiation from osteoclast precursors into mature osteoclasts is controlled by receptor activator of nuclear factor κB ligand (RANKL) cFOS and NFκB. Under normal physiological conditions osteoblasts regulate osteoclast activity through maintaining equilibrium between RANKL and its decoy receptor, OPG. The binding of RANKL to receptor activator of nuclear factor κB (RANK) on osteoclast precursors initiates a signalling cascade which results in the activation and differentiation of osteoclasts. This interaction was shown to be a requirement for signalling by Dougall *et al* in 1999, who demonstrated that whole body RANK -/- and RANKL -/- mice developed abnormally dense bones due to the absence of osteoclasts. Dysregulation of RANKL through secretion of Parathyroid hormone-related protein (PTHrP) has become a well-described mechanism in the osteolytic metastasis of breast cancer. RANKL binds to RANK on osteoclast precursors and stimulates the expression of genes such as integrin αvβ3, cathepsin K, matrix metallopeptidase 9 (MMP-9) and H+-ATPase necessary for osteoclast adhesion

and bone degradation. The degradation of bone subsequently promotes the proliferation of tumour cells through the release of growth factors. These growth factors then stimulate proliferation of both osteoblasts and tumour cells creating a vicious cycle (Chantrain et al., 2008). The impairment of the OPG/RANKL and/or RANK crosstalk has been shown in a number of cancers, with the production of soluble RANKL by PCa being suggested as a mechanism by which osteoclastogenesis is initiated (Turner and Edwards, 2016).

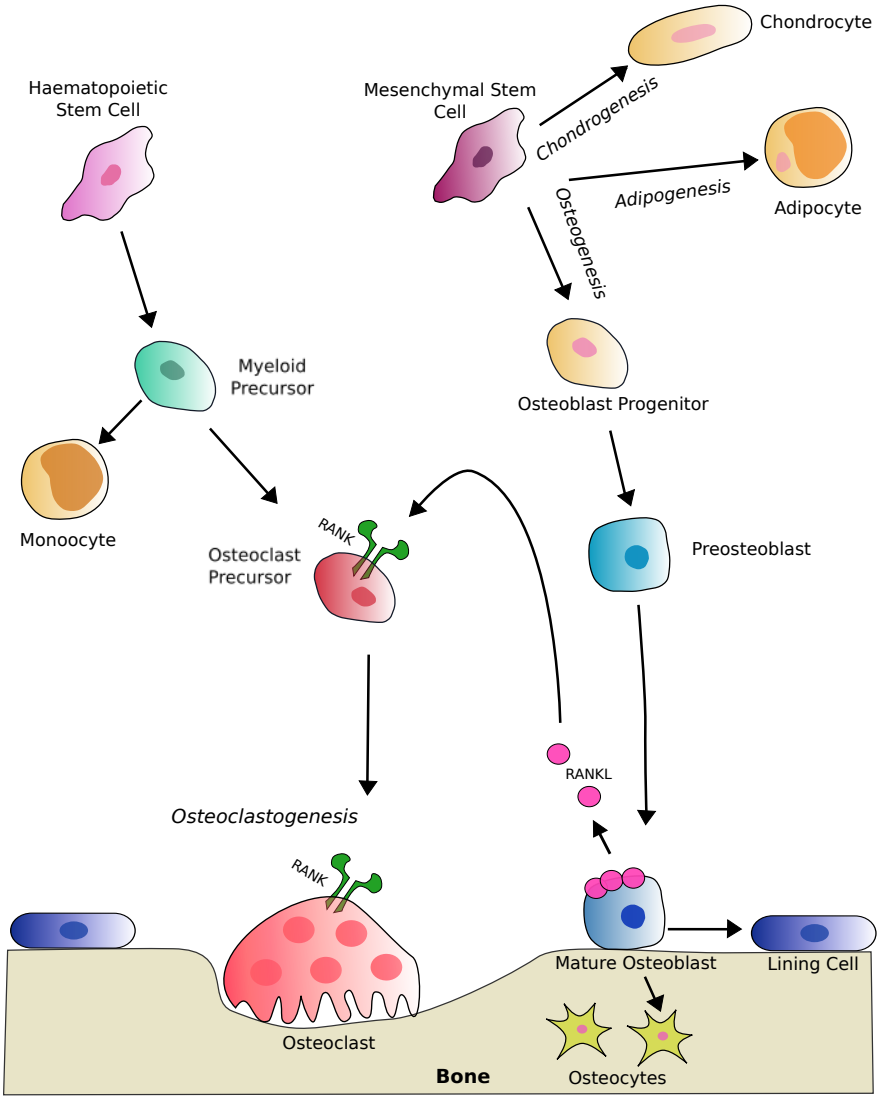


Figure 1.5: **Bone cell differentiation.** Mesenchymal stem cells can differentiate into chondrocytes, adipocytes or osteoblasts depending on the specific stimuli present within the environment. Mature osteoblasts release RANKL, which binds to RANK on osteoclasts precursors, promoting differentiation into osteoclasts. Mature osteoblasts can also differentiate into bone lining cells, which line the bone surface and osteocytes, which are present inside the bone. Haematopoietic stem cells can give rise to myeloid precursor cells, which can differentiate into monocytes and osteoclasts precursors, development into mature osteoclasts is controlled by RANKL.

1.3.2 Bone marrow adipocytes

Bone is a major regulator of energy metabolism. Adipocytes (fat cells) and osteoblasts share common MSC precursors. Adipogenic differentiation plays a pivotal role in the regulation of bone mass and homeostasis, as the MSC lineage can be diverted either towards adipogenesis or osteogenesis depending on the presence of adipogenic (e.g. peroxisome proliferator-activated receptor γ (PPARγ)) or osteogeneic (e.g., Runx2, core-binding factor alpha 1 (Cbfa1)) factors present in the bone microenvironment. A number of studies have suggested that tumour cells can be affected by the presence of adipocytes and adipocyte-associated factors. Increases in adipocyte number can lead to an abundance of lipids, which are critical for signalling, cellular trafficking, and migration. Transformed cells have the ability to utilise and store lipids in order to gain a growth advantage compared to normal epithelial cells. Moreover, adipocytes and associated inflammatory cells secrete adipokines and cytokines, which are known to contribute towards proliferation and survival of cancer cells (Hardaway et al., 2014). Herroon *et al* showed a functional relationship between bone marrow adipocytes and metastatic PCa. They found that increases in invasion were observed in PCa cells when exposed to adipocyte-conditioned media, mediated by fatty acid binding protein 4 (FABP4), suggesting the presence of adipocyte-related factors can lead to an increased progressive phenotype (Herroon et al., 2013). Furthermore, marrow adipocytes have also been found to secrete chemokine C-X-C motif ligand 1 (CXCL1) and chemokine C-X-C motif ligand 2 (CXCL2), which are postulated to activate osteoclasts and thus supply a mechanism to link marrow adipocytes to the vicious cycle of cancer-induced bone disease (Hardaway et al., 2015) (Turner and Edwards, 2016).

1.3.3 Mesenchymal stem cells and bone marrow stromal cells

MSCs are multipotent in nature and thus can give rise to a variety of cell types including: osteoblasts, adipocytes, chondrocytes and fibroblasts. Studies have shown that bone MSCs have the potential to promote the progression of a variety of tumour types (Luo et al., 2014). It is known that MSCs are recruited to the site of the primary tumour to facilitate progression and metastasis. In PCa it has been found that C-X-C chemokine

receptor 6 (CXCR6) is necessary for the recruitment of MSCs. CXCR6 signalling was shown to support recruitment, conversion and activation of MSCs into CXCL12-secreting cancer-associated fibroblasts (CAFs) (Jung et al., 2013). CAFs are known to play key roles in primary cancer growth and metastasis. Li *et al* showed that expression of TGF-β type II receptor was lost in prostate CAFs, indicating that loss of stromal TGF-β responsiveness in the primary site promoted PCa mixed bone metastasis. This was found to be mediated through an increase in expression of cytokines such as, CXCL1 and C-X-C chemokine ligand 16 (CXCL16) (Li et al., 2012) (Turner and Edwards, 2016).

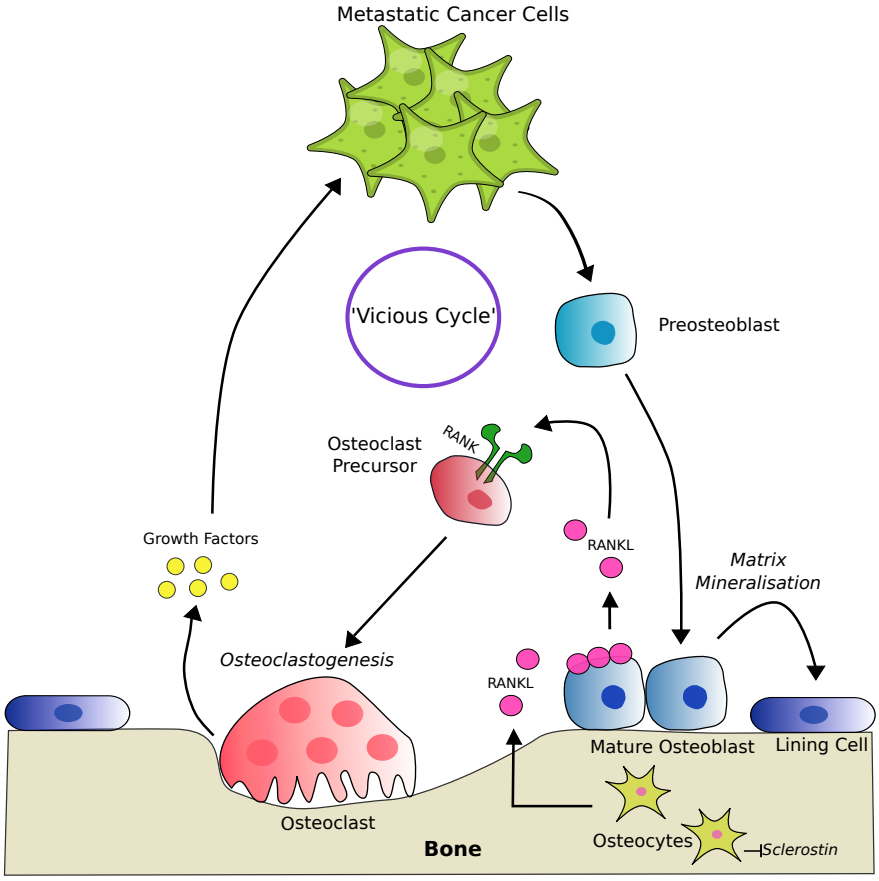


Figure 1.6: **The 'vicious cycle' of bone metastasis.** Metastatic PCa cells promote pre-osteoblasts towards the osteoblastic lineage causing an increase in matrix mineralisation. Cancer cells also upregulate RANKL secretion from mature osteoblasts, which can bind to RANK receptors on osteoclast precursors. This differentiates osteoclast precursors into osteoclasts and increases osteoclastogenesis. Upon bone resorption growth factors are released from the bone matrix and can feed back to the metastatic tumour in order to further its proliferation and survival.

1.3.4 Targeting the tumour-bone microenvironment

Bone metastasis from castration resistant disease can be extremely painful, so agents that target the bone specifically are used as a way of managing symptoms. Zoledronic acid is a bisphosphonate by binds to bone to prevent its breakdown by osteoclasts (Saad et al., 2004). Bisphosphonates are generally well tolerated and have beneficial effects on the management of bone disease and the prevention of bone loss (Coleman and McCloskey, 2011). Denosumab is a humanised monoclonal antibody that binds to and neutralises RANKL, thus inhibiting osteoclast function and bone resorption (Ando et al., 2008). It also inhibits osteoclast differentiation and thus osteoclastogenesis by mature osteoclasts. Phase three studies comparing Denosumab and Zoledronic acid showed that Denosumab delayed onset of skeletal-related events by 8.21 months compared to Zoledronic acid, however neither was shown to improve overall survival (Lipton et al., 2012).

Targeting VEGF signalling in cancer is thought to produce promising effects on the establishment of the tumour within the bone (Roberts et al., 2013). Bevacizumab, a VEGF inhibitor, has been used to in combination with Docetaxel in phase two studies in hormone-refractory PCa patients and showed good PSA responses (Di Lorenzo et al., 2008). These results unfortunately did not transpire to phase 3 study where despite a modest improvement in progression free survival, overall survival did not improve (Kelly et al., 2012). Other VEGF inhibitors currently being evaluated include Sunitinib, Sorafenib and VEGF receptor inhibitors IMS-1121B and anti-VEGFR2.

ET-1 stimulates bone formation and osteoblast proliferation. Evidence suggests that by blocking the ET-1 receptor, osteosclerotic lesions can be prevented. Atrasentan is an ET-1 inhibitor, which prevents the inhibition of DKK1, allowing Wnt signalling to continue (Muralidharan and Smith, 2013). Serum levels of ET-1 have been shown to be increased in bone metastatic PCa patients. However, despite promising initial findings, phase 3 trials have failed to provide clinical benefits from Atrasentan in PCa patients (Todenhofer and Rachner, 2015).

Radium 223 is an alpha emitter that selectively binds to areas of increased bone turnover. By inducing double-strand DNA breaks, Radium 223 is a potent and highly localised cytotoxic treatment and the only bone-targeted treatment used in clinical practise

in PCa that has been associated with improved patient survival (Parker et al., 2013).

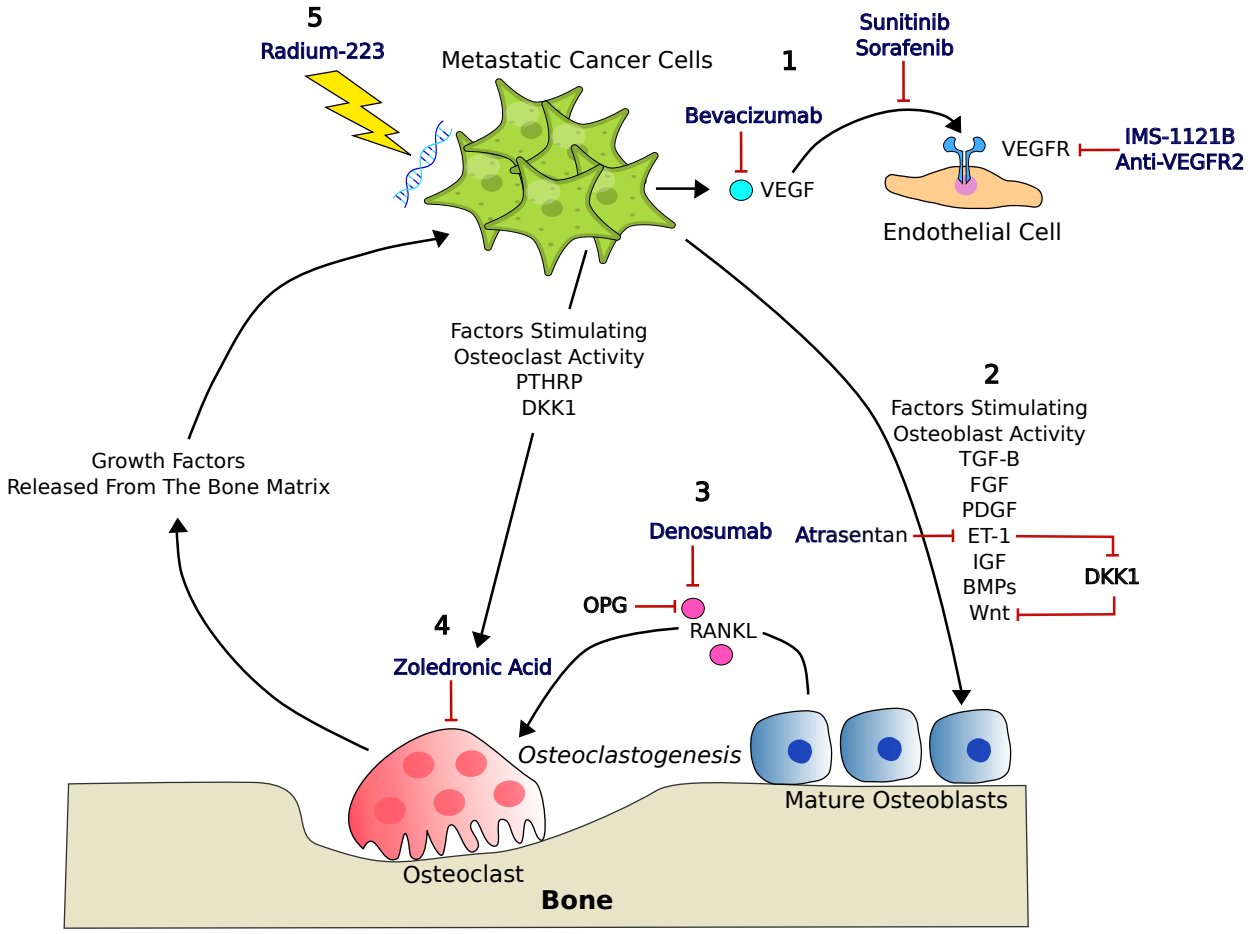


Figure 1.7: **Schematic representation of therapies used to target the tumour-bone microenvironment.** (1) Targeting VEGF. Bevacizumab inhibits VEGF activity by binding to it directly. Sunitinib and/or sorafenib, multiple receptor tyrosine kinase inhibitors, prevent VEGFR binding. IMS-1121B, an anti-VEGFR2 human monoclonal antibody, prevents VEGF binding. (2) Stimulating osteoblastic activity. TGF-β, FGF, PDGF, IGF, ET-1, BMPs and Wnt all stimulate osteoblast activity. ET-1 signalling inhibits DKK1, increasing Wnt. Atrasentan is an ET-1 inhibitor, preventing the inhibition of DKK1, a negative regulator of wnt signalling. (3) Targeting RANKL. Denosumab, a humanised monoclonal antibody that binds to RANKL, inhibiting osteoclast activity and osteoclastogenesis. (4) Targeting osteoclasts. Bisphosphonates, such as zoledronic acid, inhibit mevalonate pathway enzymes and bind to bone minerals to prevent its resorption via osteoclasts. (5) Bone-targeted radiopharmaceuticals. Radium-223 causes double stranded DNA breaks in cancer cells. Short-alpha particle paths allow effective localised cytotoxic cell death with reduced off-target effects. Figure taken from Turner *et al* 2016.

1.4 Prostate cancer bone metastasis *in vivo* models

In vivo animal experiments are essential to PCa research and are particularly important in studying the interactions between tumour cells and their microenvironment. Due to the fact that currently there is no effective cure for metastatic PCa, research is increasingly focused on understanding and preventing metastasis, in particular to the skeleton. As metastasis is complex in it's processes and involves interaction between tumour cells and multiple cells of the microenvironment, pre-clinical *in vivo* models are a reasonable approach to reproduce the organ microenvironment (Fidler, 2003). The most commonly used animal models include transgenic mouse models and human PCa xenografts. A few transgenic mouse models of PCa have been established by targeted disruption of such genes as homeobox protein Nkx3.1(Nkx3.1) and phosphatase and tensin homolog (PTEN). As the mice age, those with homozygous functional deletion of Nkx3.1 display histopathological defects resembling prostate intra-epithelial neoplasia (PIN) (Kim et al., 2002), and prostate-specific deletion of the PTEN gene reproduces natural progression of the disease from prostatic PIN to metastasis (Wang et al., 2003). In addition, the transgenic adenocarcinoma mouse prostate (TRAMP) model was established by transgenic expression of SV40 early genes (T and t antigens) (Greenberg et al., 1995). TRAMP mice also develop high grade PIN within 12 weeks from birth that progresses to poorly differentiated adenocarcinoma within 24–30 weeks. TRAMP mice are helpful in studying lymph node metastasis however, tumours from these animals have neuroendocrine features, which is rare in the clinical setting (Kaplan-Lefko et al., 2003). Furthermore, metastasis to bone, frequently seen in the clinic are rare in TRAMP mice (Hsieh et al., 2007). Overall transgenic mouse models do provide valuable information on the complex pathogenesis of PCa, particularly with regards to dysregulation of specific molecular or genetic changes, although, transgenic tumour models often require a considerable expenditure of time, with large number of animals needed to produce statistically meaningful data (Park et al., 2010). In contrast, human PCa xenograft mouse models provide extremely useful alternative approaches for understanding the specific interactions between various genetically and molecularly altered tumour cells and their microenvironment. Further-

more, they can generate clinically relevant metastasis (i.e. preferential homing) through orthotopic or intra-cardiac injection, in a time scale much shorter than their transgenic counter-parts (Park et al., 2010). As such human PCa xenografts will be used in this thesis.

1.5 Leukaemia inhibitory factor

Leukaemia inhibitory factor (LIF) was originally identified and cloned from the conditioned media of krebs II ascites of tumour cells and was found to induce the differentiation of mouse myeloid leukaemia M1 cells. It was named LIF due its ability to suppress the proliferation of M1 cells. LIF cytokine is a glycosylated protein (molecular weight (MW) of 37–62 kDa) depending on its degree of glycosylation. LIF is encoded by a single gene, which is located on chromosome 11 in mice and chromosome 22q12 in humans. In both species the gene comprises of four exons, although only portions of two encode RNA for the mature protein (Metcalf, 1991). LIF exists in at least three isoforms: a soluble form (LIF-D), an intracellular form found in the nucleus (LIF-I/LIF-T) and/or a third form localised in the extracellular matrix (LIF-M). LIF-D and LIF-M are transcribed from alternative transcripts differing in the first exon, which encodes partially for different signal peptides, which target the mature protein to different locations. LIF-T is a truncated protein due to the absence of the ATG codon in the first exon, leading to translation at the first ATG start codon of exon 2. This isoform has been shown to have pro-apoptotic effects in COS and 293T cell lines. LIF is secreted by numerous cell types including fibroblasts, activated T cells, spleen, macrophages, chondrocytes, bone marrow stromal cells, mesenchymal stem cells, endothelial cells, astrocytes and tumour cells (Trouillas et al., 2009).

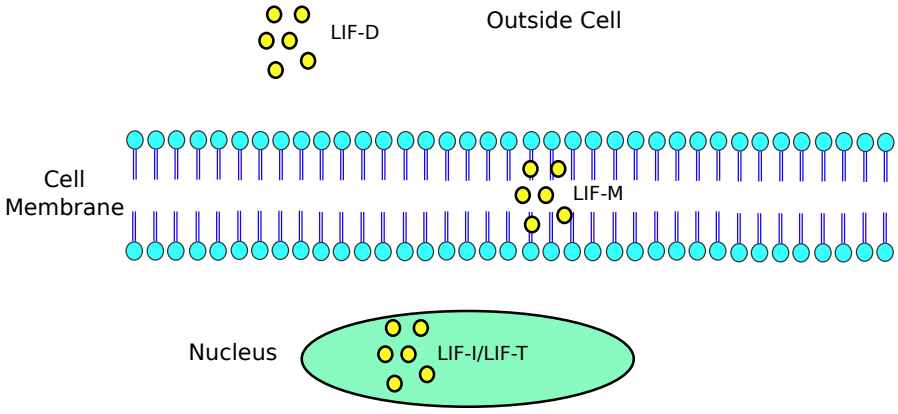


Figure 1.8: **LIFs isoforms.** LIF exists is at least three isoforms: a soluble form (LIF-D), and intracellular form, found in the nucleus (LIF-I/LIF-T) and a localised form in the extracellular matrix (LIF-M).

The LIF receptor (LIFR) comprises of an extracellular portion made up of two hemopoietin receptor domains and a fibronectin type III domain. It also displays homology to the signal transducing subunit glycoprotein 130 (gp130). The binding affinity of LIF to the LIFR subunit interestingly converts to high affinity by association with gp130 (Gough, 1992). Thermodynamically LIF engages with its receptor in a different way to its similar family member, interleukin-6 (IL-6). IL-6 binds to gp130 and interleukin-6 receptor (IL-6R) in an ordered and co-operative process. IL-6 first recruits its specific receptor chain with high affinity and this then recruits gp130. The resulting ternary complexes dimerise to form a signalling hexamer. Alternatively the interaction between LIF and its receptor chains (gp130 and LIFR) is entropically driven with little structural perturbation in either the cytokine or the receptor after binding (Nicola and Babon, 2015).

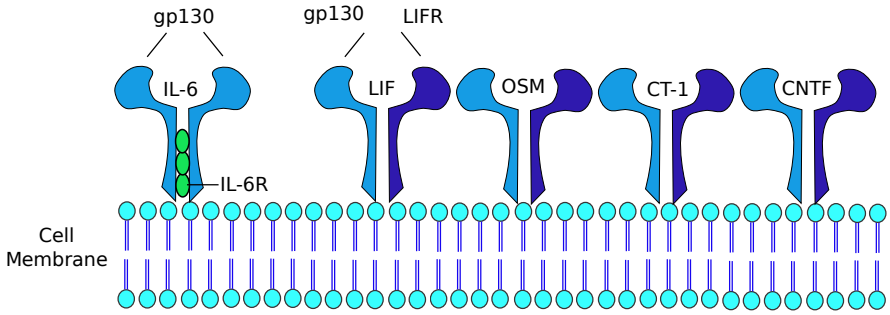


Figure 1.9: **Receptor signaling complexes formed with gp130.** IL-6 binds to a specific B-receptor subunit (IL-6R) and forms a complex that contains gp130 homodimers. The LIFR is used by multiple cytokines including OSM, CT-1 and CNTF, as well as LIF. LIF signals through a trimer of the ligand coupled to LIFR and gp130.

One of the many characteristics of cytokines, is their ability to regulate the expression of other cytokines. Villinger *et al* showed that LIF can induce the expression of proinflammatory cytokines. In response to LIF human articular chondrocytes were shown to express interleukin-1 β (IL-1β), IL-6 and interleukin-8 (IL-8) messenger RNA (mRNA). Similar results were also found in blood monocytes, synoviocytes and epithelial and neuronal human cell lines. Induction of these cytokines have the potential to initiate inflammatory and immunological responses. LIF also has the ability to inhibit lipoprotein lipase (LPL) activity, which can lead to cachexia (Berg et al., 1994).

LIF has been shown to have a variety of proliferation and differentiation affects and downstream signalling is therefore important to establish how LIF effects these. Stimulation of rat hepatoma cells with LIF has shown phosphorylation of janus kinase 1 (JAK1) and primarily activation of signal transducer and activator of transcription 3 (STAT3). In ewing sarcoma (EW1) cells it has also been shown that LIF treatment stimulates phosphorylation of JAK1 and 2, but not non-receptor tyrosine-protein kinase (TYK2). In 1995 Lowe *et al* showed that LIF induces JAK phosphorylation in murine preosteoblast (MC313-E1) cells, specifically JAK1 and signal transducer and activator of transcription 1 (STAT1) and to a lesser extent JAK2 and STAT3. Activation of these STAT proteins was also accompanied by their ability to bind to a STAT binding element derived from

the interferon regulatory factor-1 (IRF-1) gene. Within IRF-1s promoter region is a consensus sequence (TTC/ACNNNAA) that is shared with other early response genes such as FCγR1 that is induced by other members of the IL-6 superfamily including IL-6 and Oncostatin M (OSM). This sequence is also required for the induction of acute phase response genes in hepatocytes by LIF and IL-6. The STAT-binding element of IRF-1 has been shown to allow specific binding of several STAT complexes (Lowe et al., 1995).

Although homozygous LIF-/- mice are viable, they nevertheless present many defects, including a decrease in the survival of HSCs, a substantial loss of motor neurons, as well as an alteration in oligodendrocyte function. Of importance, LIF-/- females do remain fertile, but their blastocysts cannot implant. This implantation defect is due to the absence of LIF production by the uterus. LIF production is normally induced by estradiol via the TP53 loop. There are functional TP53 binding sites in the LIF promoter. Of note, p53 -/- mice display the same implantation defect phenotype as LIF-/- mice. Interestingly, LIF-/- or p53-/- blastocysts develop normally if implanted in a wild-type female or upon direct injection of LIF into the vagina of TP53-/- or LIF-/- mutated mice (Trouillas et al., 2009).

More recent studies using LIF knockout (KO) mice showed its involvement in injury responses, demonstrating the importance of LIF at various stages of neurogenesis and for tissue regeneration after brain or spinal cord injury. Also, LIF is potentially involved in particular contexts of muscle stimulation and regeneration. Furthermore, analysis of LIF KO newborn mice revealed a 40% decrease in bone volume. Double and triple KO model mice with other members of the IL-6 family, such as cardiotrophin-1 (CT1) and ciliary neurotrophic factor (CNTF), also revealed the importance of LIF and CNTF for motor neuron functions. The therapeutic potential of LIF in neurodegenerative and autoimmune diseases, and in reproduction failure treatments has recently been reviewed, stressing the importance of LIF in the different cell contexts (Mathieu et al., 2012).

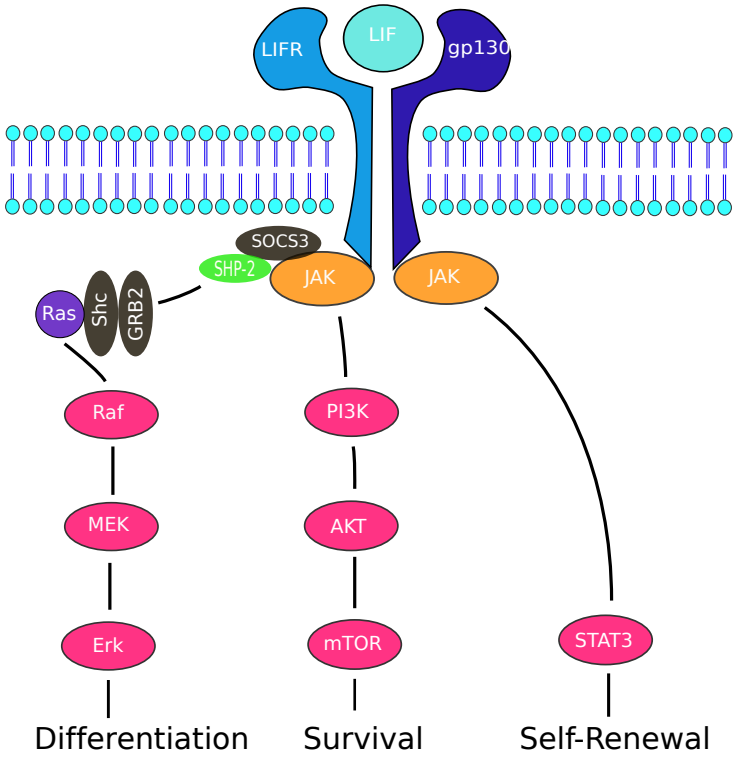


Figure 1.10: **Leukaemia inhibitory factor.** Schematic representation of LIF pathway.

1.5.1 LIF in bone

LIF is a pleiotropic cytokine so unsurprisingly its receptors have been found on a number of organs including the liver, uterus, kidney, central nervous system and bone (Nicola and Babon, 2015). Numerous reports have indicated that LIF can enhance *in vitro* differentiation in osteoblasts or osteoblast precursors isolated from calvaria or bone marrow, accompanied with an increase in osteoblast markers such as alkaline phosphatase (ALP), osteocalcin or bone sialoprotein and increases in bone nodule formulation and extracellular matrix mineralisation (Heymann and Rousselle, 2000) (Bellido et al., 1997). STAT3 activation has been shown to be necessary for LIF-induced osteoblast differentiation and bone formation (Bellido et al., 1998) (Itoh et al., 2006). Similarly IL-6 family cytokines, namely IL-6 and OSM have been shown to reduce proliferation of various osteoblastic cells through the activation of STAT3 and enhanced expression of the cell cycle inhibitor

$p21^{WAF1,CIP1,SDI1}$, this protein is also necessary for the induction of ALP by these cytokines (Bellido et al., 1998). However, other reports have shown inhibitory effects of IL-6 family cytokines on bone formation and marker expression *in vitro*. It is possible that these differing effects depend on the stage of differentiation of the osteoblast; on earlier stage precursor cells for example IL-6 family cytokines may stimulate differentiation, however on more mature cells they would prevent further stimulation (Malaval and Aubin, 2001) (Malaval et al., 2005) (Falconi and Aubin, 2007).

Abe *et al* alluded to a role for LIF in bone resorption *in vitro*, even before it was known as LIF and suggested that it was capable of inducing proliferation and differentiation of immature bone marrow cells and increased bone resorbing activities as measured by calcium release from bone (Abe et al., 1986). LIF has since been shown to stimulate bone resorption by indirect mechanisms, through interactions between osteoblasts and osteoclasts. LIF treatment of co-cultures containing osteoblasts/stromal cells with osteoclast precursors stimulates osteoclast differentiation and activity. LIF was found to induce osteoblastic production of downstream effectors that activate osteoclast differentiation or activity, such as RANKL, IL-1, PTHrP and prostaglandin E2 (PGE2). Data indicated that induction of RANKL is key in their pro-resorption action, with STAT3 being implicated in that induction (Palmqvist et al., 2002) (O'Brien et al., 1999).

In vivo Metcalf and Gearing showed one of the earliest effects of LIF. By engrafting a hemopoietic cell line modified to produce high levels of LIF they sought to induce tissue changes. Remarkable changes were witnessed in the long bones and the sternum of LIF treated animals. An increase in the number of osteoblasts was observed, with an excess in new bone formation, often accompanied with increased bone resorption and calcium deposition in muscle tissue. Furthermore, the mice exhibited obvious signs of weight loss, with loss of all subcutaneous and abdominal fat and generalised organ atrophy. Fatal cachexia developed in as little as 12 days post engraftment (Metcalf and Gearing, 1989). Cornish *et al* showed that by injecting recombinant LIF daily over the right hemicalvaria for 5 days, there was an increase in bone resorption in the LIF treated mice compared to the controls, accompanied by an increase in osteoclast numbers. Fibrotic tissue was laid down with the resorption defects, with accompanying thickening of the periosteum

causing over all thickness of the LIF treated bones to almost double. Osteoblast numbers also increased with LIF treatment. Furthermore, LIF increased periosteal area and total mineralised bone. Thus, this study showed that LIF is capable of accelerating bone turnover locally, further demonstrating its potential to modify bone cell function *in vivo* (Cornish et al., 1993). Reid *et al* assessed the effect of LIF on bone resorption in neonatal mouse calvaria. Both recombinant murine and human LIF stimulated calcium release from the calvaria in a dose dependant manner. This increase in bone resorption was associated with an increase in osteoclast number per mm^2 of bone (Reid et al., 1990). Gimble *et al* differentiated the murine stromal cell line, BMS2 in response to cytokines that share gp130 in their receptor complex. They found that IL-6, IL-11, OSM and LIF all inhibited hydrocortisone-induced adipocyte differentiation in a dose dependent manner. This was based on lipid accumulation and LPL activity. These cytokines were also found to increase ALP enzyme activity in these preadipocyte cells, suggesting that LIF promotes precursor cells towards the osteoblastic lineage at the expense of adipogenesis (Gimble et al., 1994).

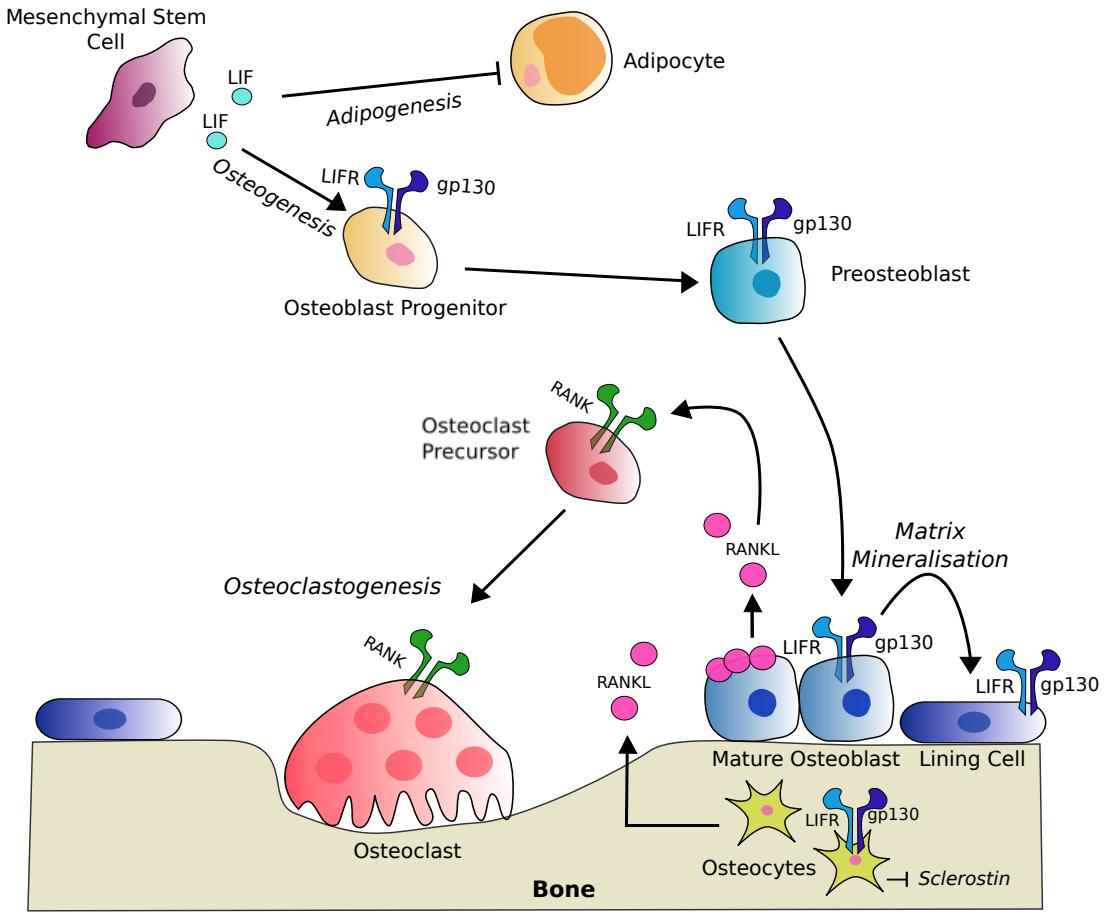


Figure 1.11: **LIFs actions in bone remodelling.** LIF acts on osteoblast precursor cells to differentiate cells towards the osteoblastic lineage and inhibit the production of the osteoblast-inhibitory factor, sclerostin by osteocytes. Osteoblasts produce RANKL, which acts on the receptors of osteoclast precursors to induce differentiation into osteoclasts which resorb bone.

1.5.2 LIF in cancer

LIF is not normally detectable in normal murine or human serum, like other hemopoietic regulators, LIF appears to be a product of stimulation by inductive signals (Metcalf, 1991), one such stimulus is cancer. Studies over the last 20 years indicate that members of the IL-6 family of cytokines, including LIF, contribute to the proliferation and metastasis of several cancers (Shin et al., 2011). In breast cancer it has been found that LIF supports tumourigenesis and metastasis, through the protein kinase B (AKT)- mammalian target of rapamycin (mTOR) pathway. Li *et al* showed that LIF was able to promote cell proliferation and anchorage-independent growth of breast cancer cells *in vitro* and in

xenograft breast tumours *in vivo*. Furthermore, increased LIF promoted invasion and migration both *in vitro* and *in vivo* and was correlated with a poorer relapse free survival in breast cancer patients (Li et al., 2014).

LIF is overexpressed in a large percentage of colorectal cancer cells and downregulates p53 protein levels and function in these cells. This was shown to be mediated by the activation of STAT3, which induces inhibitor of DNA-binding 1 (ID1). ID1 upregulates mouse double minute-2 (MDM2), a key negative regulator of p53, and promotes p53 protein degradation. LIF overexpression promotes cellular resistance towards chemotherapy in cultured colorectal cancer cells and colorectal xenograft tumours in a largely p53-dependent manner. Furthermore, overexpression of LIF is associated with a poor prognosis in colorectal cancer patients (Yu et al., 2014).

In rhabdomyosarcoma, which frequently infiltrates bone marrow, it was found that in LIF stimulated phosphorylation of mitogen-activated protein kinase (MAPK) p42/44, AKT and STAT3, as well as adhesion, chemotaxis and increased resistance to cytostatics. It was also found that rhabdomysarcoma cell lines, that responded to LIF, seeded better to the bone marrow, liver, and lymph nodes of immunodeficient mice than cells that did not respond to LIF and mice inoculated with these responsive cells had more rhabdomyosarcoma cells in the bone marrow and lungs after 6 weeks.

Kuphal *et al* found LIF to be expressed in primary and metastatic melanoma cell lines and in melanoma tissue. They investigated the effect of silencing LIF on cellular melanoma behaviour and found that proliferation; attachment, migration and colony formation were all impaired. Furthermore, it was elucidated that hypoxia, specifically signalling through hypoxia-inducible factor 1-α (HIF-1α) was involved in regulating LIF. Interestingly their data showed that the signalling of LIF was not mediated through the classically described pathway via STAT3, but through BMP4 and BMP7 instead (Kuphal et al., 2013).

However, in colorectal cancer hypoxia induced LIF mRNA expression in human colorectal cancer cells through transactivation of HIF-2α, not HIF-1α. Knockdown of endogenous HIF-2α by small interfering (siRNA) largely abolished the induction of LIF by hypoxia in these cells. Furthermore, there was a strong association found between HIF-2α overexpression and LIF overexpression in human colorectal cancer specimens (Wu et al.,

2015).

Although there is also evidence that suggests that LIF may also be tumour suppressive. p21 plays a crucial role in the cell cycle but has also been shown to confer resistance to apoptosis. Bellido *et al* demonstrated that p21 is a downstream effector of gp130/STAT3 activation and a critical mediator of pro-differentiation and anti-apoptotic effects of IL-6 type cytokines on human osteoblastic cells. Careful manipulation in the activity of cyclins, cyclin dependent kinase 1 (CDK1) and inhibitors of these kinases orchestrate the progression of cells from one phase of the cell cycle to another. Increased expression of CDK inhibitors is now recognised as a mechanism of cell cycle arrest, one of these namely p21. This is able to bind to and inactivate several cyclin/CDK complexes including ones involved in the transition between gap 1 (G1) and synthesis (S) phase and inhibits the replication factor proliferating cell nuclear antigen (PCNA). p21 is implicated in different processes including: DNA damage repair, differentiation and apoptosis. In the first, p21 is stimulated by the tumour suppressor p53, allowing the protein to arrest cells in G1 phase, initiating DNA damage repair before cells continue into S phase. In differentiation and apoptosis, p21 expression occurs independently of p53, resulting in the stopping of cell division and the progression of cells along the differentiation pathway (Bellido et al., 1998).

TGF-β has been shown to regulate the expression of p21, by suppressing the expression of genes important in cell cycle progression and inducing genes crucial for senescence. TGF-β signalling is initiated by the type II receptor (T/βRII), a constitutively auto-phosphorylates serine/theronine kinases, which upon binding recruits and transphosphorylates the type I receptor (TβRI), thus activating its kinase activity. Activated TβRI can then phosphorylate mediators known as receptor-regulated smads (R-smads), smad 2 and smad 3, allowing heterotrimerisation with smad 4 (a common partner). The smad heterotrimer translocates to the nucleus where it can bind DNA and regulate transcription, along with transcription factors, co-activators or co-repressors (Humbert et al., 2015). In cancer the role of TGF-β is complex and has been shown to inhibit cell growth as well as regulate migration and invasion. In breast cancer TGF-β exhibits a dual role: while it acts as a cell cycle inhibitor and pro-apoptotic factor in normal and premalignant

states, these tumour suppressive effects are lost in more advanced tumour and replaced with pro-metastatic effects. In melanoma however, the role of TGF-β is different. While TGF-β acts as a tumour suppressor in normal melanocytes, it also inhibits cell migration and invasion in melanoma at various stages.

Humbert *et al* found through global transcriptome analysis of two human melanoma cell lines, LIF appeared to be strongly upregulated by TGF-β. Previous studies have reported inductions of LIF mRNA and/or protein by TGF-β in Schwann cells and glioblastoma and shown this to be upregulated by binding to a smad binding element in the LIF promoter. Humbert *et al*, define LIF as a downstream target of TGF-β in melanoma and indicate that TGF-β-induced expression of LIF is a prerequisite for tumour suppressive effects. In addition they found that p21 played a significant role in mediating both G1 arrest and apoptosis, but not cell migration downstream of TGF-β. They also found TGF-β-mediated p21 gene expression induced expression of pro-apoptotic genes such as bcl-2-like protein 4 (Bax) and bcl-2-like protein 11 (Bim), leading to cell death (Humbert et al., 2015).

Johnson *et al* showed that in breast cancer, decreased expression of LIFR was associated with cell lines with a higher metastatic potential that readily home to bone. The study suggests that LIFR is important for maintaining tumour cells in a dormant state. This hypothesis, is supported by the previous findings of Sosa *et al* who reported that LIF and LIFR mRNA levels are elevated in dormant squamous cell carcinoma cells (Sosa et al., 2015). STAT3, a downstream effector of LIF has furthermore also been identified as a dormancy-associated gene. In breast cancer patients Johnson *et al* found that LIFR/STAT3 signalling is down-regulated in patients with bone metastases and was associated with a dormancy phenotype as established by the expression of dormancy-associated genes *in vitro*. Thus, LIF may have tumour suppressive effects as well as pro-tumour effects in certain cancer types.

1.5.3 Other biological activities of LIF

1.5.3.1 Reproduction

Implantation is a highly co-ordinated process whereby specialist cells of the embryo, the trophectoderm and trophoblast, establish contact with the uterus of the mother (Carson et al., 2000). Successful embryonic implantation relies on the cross-talk between the embryo and the endometrium. Evidence for the role of LIF in implantation comes from the lack of embryo implantation in transgenic mice, homozygous for LIF gene deficiency. Furthermore, the addition of exogenous LIF to these females throughout the period of implantation restored implantation sites and allowed attachment of a LIF -/- blastocyst. LIF and LIFR mRNA has been shown to be expressed throughout the menstrual cycle with a dramatic increase in the mid to late secretory phase in early pregnancy. LIF is localised in the human endometrial gland, which synthesises and secretes proteins into the uterine lumen. LIF expression has been shown to remain at high levels through the post ovulatory phase, suggesting the need for it throughout preimplantation blastocyte development (Aghajanova, 2004).

1.5.3.2 The neuromuscular system and heart

LIF has been shown to stimulate the development of sensory neurons in cultures of neural crest cells. This was augmented with co-treatment with FGF2 (Murphy et al., 1997), which may act on early precursors that can subsequently become responsive to LIF for survival and/or differentiation, with differentiation becoming dependent on nerve growth factor (NGF) for survival. LIF expression is also increased in nerve injury (Curtis et al., 1994) and similarly LIF was found to promote differentiation of E10 spinal cord motor neurons and reduce motor neuron loss following nerve transection, suggesting LIF may be important in injury responses. LIF has also been seen to reduce muscle atrophy in rats and can stimulate muscle reinnervation (Finkelstein et al., 1996). Proliferation of myoblasts (skeletal muscle precursors) by LIF was found *in vitro* to be at the expense of their differentiation into myotubes (Austin and Burgess, 1991). Furthermore, LIF has effects on the heart; LIF plasmid enhancement has shown recovery from myocardial

infarction in mice with evidence that LIF induced protection against reactive oxygen species and survival pathway in cardiomyocytes. Moreover, it has been suggested that LIF can stimulate cardiac stem cells derived from the bone marrow to migrate to damaged myocardium and stimulate differentiation into endothelial cells and neovascularisation (Nicola and Babon, 2015).

1.5.3.3 The hemopoietic system

LIF promotes the survival and/or proliferation of primitive haematopoietic precursors and primardial germ cells. Escary *et al* showed LIF -/- mice have decreased number of stem cells in the spleen and bone marrow. Furthermore, injection of cells from these mice promoted long-term survival of lethally irradiated wild-type animals, however LIF -/- stem cells remained pluripotent (Escary et al., 1993). In the context of multiple sclerosis (MS) LIF treatment has been shown to boost the number of regulatory T cells (Tregs) in $CD4^+$ T cells isolated by healthy controls and MS patients with low serum concentration of IL-6. Previous findings have suggested that IL-6 inhibits Treg development suggesting an opposing function of LIF and IL-6 (Janssens et al., 2015). LIF has an important role in introducing and/or maintaining epigenetic plasticity within the genome, thus LIF is permissive for epigenetic plasticity. This is prominently seen in stem cells where LIF functions in combination with nanog, a core stem cell transcription factor that, when under the influence of LIF choreographs pluripotency and self-renewal in mouse embryonic stem cells. As cell lineages establish themselves, epigenetic plasticity decreases, culminating in a terminally differentiated cell. This process was thought to be irreversible, however Takahashi and Yamanaka demonstrated that differentiated cells can re-establish a pluripotent state following transfection with core stem cells transcription factors.

1.6 Rationale

The expression and function of LIF in PCa is poorly understood. Previous studies have shown both pro and suppressive effects of LIF in different cancer types. Preliminary studies untaken within the Edwards' lab showed LIF to be upregulated in PCa patient serum samples in pre-bone metastatic patients compared with non-bone metastatic patients via a human obesity cytokine array (RayBiotech). Of the 62 molecules analysed LIF was significantly upregulated, indicating a potential role in disease progression. Taken together with the known role of LIF in bone biology, LIF may play a role in the pathogenesis of PCa-induced bone disease.

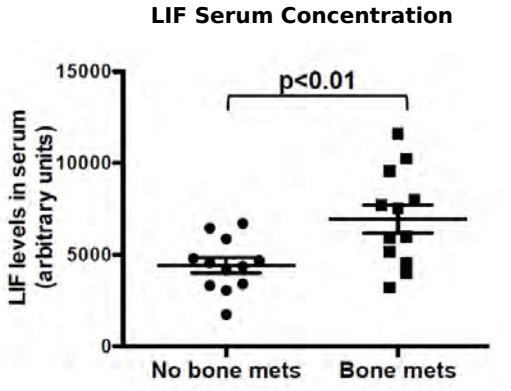


Figure 1.12: Circulating factors in samples from prostate cancer patients with and without bone metastasis was analysed using a human obesity array (RayBiotech). Relative expression was quantified using desitometry. Data is expressed as ± SEM. N = 12. *Data produced by X.Cheng.*

1.7 Research aim and objectives

The main aim of my research is to elucidate the role of LIF in bone metastatic PCa. This will be achieved by the following specific objectives:

- To determine the expression of LIF in prostate cancer.
- To elucidate LIFs effects in prostate cancer cells.
- To investigate the effect of LIF in the bone microenvironment.

2

Materials and Methods

2.1 Cell lines and reagents

PC3 human prostate cancer cell line, 2T3 mouse preosteoblatic cells, 3T3-L1 mouse pre white fat cells, HS-5 and HS27a human stromal cells were obtained from the American type culture collection (ATCC,). ST2 pre bone marrow fat cells were purchased from Riken cell bank (Tsukuba, Japan). PC3, C42B, LNCaP, LN3, VCaP and PC3 NW1 cells were routinely maintained in complete Roswell Park Memorial Institute medium (RPMI) medium (Sigma) consisting of 10% fetal bovine serum (FBS), 5% penicillin-streptomycin (Sigma), 5% vitamins (Sigma), 5% L-glutamine (Sigma), 5% sodium pyruvate (Sigma), 5% non-essential amino acids (Sigma). 2T3, 3T3-L1 and ST2 cells were routinely maintained in complete Dulbecco's modified eagle medium (DMEM) (Sigma) consisting of 10% FBS, 5% penicillin-streptomycin and 5% L-glutamine. ARCaP, ARCaPE, ARCaPM human prostate cancer cell lines were purchased was Novicure Inc, USA (Car. 3421, 3423,

3422 respectively). All three cell lines were routinely maintained in T-medium made from DMEM, plus F-12K powder (Sigma) 4:1, supplemented with 5% FBS, 3g/L sodium bicarbonate (Sigma), 5μg/ml transferrin (Sigma), 0.25μg/ml biotin (Sigma), 25μg/ml adenine (Sigma). C4-2B human prostate cancer cells were a gift from Prof. George Thalmann, University of Bern, Switzerland and maintained in complete RPMI medium (as specified previously). PC3 NW1 cells and were gifted from Dr Penny Ottewell from the University of Sheffield. All other prostate cancer cell lines were a kind gift from Dr. Richard Bryant, University of Oxford. Where possible, cell lines were validated by genotyping and periodic testing for the absence of mycoplasma was conducted. No infected samples, other than the controls, have been detected throughout the project.

Name	Source	Morphology
PC3	Vertebral metastasis	Epithelial
PC3 NW1	Vertebral metastasis	Epithelial
*ARCAP-M	Bone met. ARCAP cell population in mice	Spindle-shaped mesenchymal cells
VCAP	Vertebral metastasis	Epithelial
C42B	Bone metastasis LNCAP tumour in mice	Epithelial-like with thin processes
C42	Sub cut. LNCAP tumour in mice	Epithelial-like
*ARCAPE	Low propensity bone met. cell population in mice	Cobblestone epithelial cells
LNCAP	Lymph node metastasis	Epithelial
LN3	Lymph node metastasis	Epithelial
PNT1A	Prostatic epithelial cells immortilised with SV40	Epithelial

Table 2.1: **Establishment sources and morphology of PCa cell lines.** *Parental ARCAP cell line established from ascites aspirate from a bone metastatic PCa patient. met. = metastasis, cut. = cutaneous.

2.2 Lentiviral production and infection for knock-down

293T cells were seeded at a density of 2.1 x 10^4 cells/cm^2 in a 60mm tissue culture dish (Corning) and incubated at 37°C at 5% CO_2 in a humified incubator for 24hrs. 10μl of FuGEN (Promega) was added into 200μl optiMEM (Sigma) along with 1μg pVSV-G plasmid, 1μg pax plasmid and 1μg lentiviral expression plasmid (LIF shRNA 0008E10, LIF shRNA 0050A6, LIF shRNA 0172G1, LIF shRNA 0211E12 or non-targeting, Sigma). Transfection solutions were incubated at room temperature for 15mins, added to the dish containing cells drop wise and swirled to mix. Plates were incubated overnight at 37°C. 2ml of fresh media was then added to the plates and incubated for a further 24hrs at 37°C. Supernatant was collected after 48hrs after transfection. 4ml of fresh media was then replaced back on the plate and this was incubated for a further 24hrs. The 48hr virus was then filtered through a 0.45μm filter and stored at -80°C. 72hrs after transfection start, supernatant was collected, filtered as previously described and either stored at -80°C or used for infection of target cells. PC3 target cells were seeded for a confluency of 20-30% confluency. 40μl of 400μl/ml Polybrene was added to 2ml of virus (for a final concentration of 8μg/ml). The medium was removed from the target cells and the virus was added with the polybrene. Cells were incubated at 37°C, media was changed after 8hrs, allowed to re-cover overnight and re-transduced the following day. Transduced cells were selected using 5μg/ml Puromycin (Sigma).

2.3 Migration and invasion assays

2.3.1 Matrigel transwell invasion assay

Matrigel (Sigma) was diluted in serum free media (1:15) for use with PC3 cell line, optimisation of matrigel dilution factor is cruicial for other cell lines. Serum Free media RPMI media was added into the wells of a 24 well plate (approx. 500-1000μl) and an 8μm polycarbonate transwell (Appleton Woods) was placed ontop. 100μl of diluted matrigel was

added into the transwell and the plate was then incubated in a humidified incubator at 37°C overnight. Cultured PC3 cells were then seeded at 0.5 x 10^5 in a volume of 200μl of 1% serum medium. 1ml of 20% RPMI growth medium was then added to new wells of the 24 well plate and the transwells now containing the cells placed ontop. It was imperative to ensure that the levels of the medium was the same inside and outside the transwells, otherwise the media may mix predominately by gravity, rather than diffusion. The plate was then placed back in the incubator for 24hrs, medium was removed and cells were fixed using 10% formalin for 10mins. The formalin was then discarded and the transwells were then washed using 1 x PBS. Cells were then permeabilised with 100% methanol for 20mins. Methanol was then discarded and transwells were once again washed with 1 x PBS. Cells were then stained using 1% toluidine blue (in MilliQ water) for 20mins. Membranes were then carefully cut out using a scalpel, wet with xylene/clearene and mounted on a microscope slide with coverslip using DPX mountant (Sigma). Slides were then visualised using a BX40 Olympus microscope.

2.3.2 Transwell migration assay

Transwell migration assay was performed as described above without the addition of matrigel.

2.3.3 Xcelligence cell migration assay

Cells were seeded at 0.5 x 10^5 in 1% serum media into a migration plate (CIM-Plate 16) which is an electronically integrated Boyden chamber with upper and lower chambers. A polyethylene terepthalate microporous membrane is present in the upper chamber, allowing cells to translocate towards the 10% serum media in the lower chamber. The bottom side of the membrane is coated with gold microelectrode sensors that have a reduced ability to conduct electric current when cells adhere to their surface. Thus an 'impedance' signal is generated which enables a quantitative kinetic measurement of cell movement from the upper chamber to the lower chamber. The plate was left at room temperature for 30mins to allow the cells to settle and was then placed into an xCELLigence RTCA DP instrument and left for 33hrs.

2.4 LIF overexpression construct

2.4.1 Inoue method for preparation of competent E.Coli 'ultra-competent' cells

A 200μl pipette tip was placed into glycerol stocks of XL one blue bacteria and transferred to 25ml of autoclaved LB broth in a 250ml flask. The flask was incubated for 8hrs with shaking (300 revolutions per minute (rpm)). Three 1L flasks were then inoculated containing 250ml culture medium as follows; flask 1, 2ml of starter culture, flask 2 1ml starter culture and flask 3, 200μl of starter culture. Flasks were then incubated overnight at room temperature with moderate shaking. The OD600 of all three cultures were read and continued to be monitored until the reading was 0.55. Flasks were then transferred to ice for 10mins. Cells were harvested by centrifugation at 2500xg for 10mins at room temperature in a 50ml falcon tube. The supernatant was then discarded and the tube was dried inverted on a paper towel for 2mins (aspirating any drop remaining). Cells were gently resuspended in 80ml ice-cold inoue transformation buffer. Cells were harvested by centrifugation at 2500xg for 10mins at room temperature. Supernatant was discarded and the tube was dried inverted in paper towels for 2mins (aspirating any drops remaining). Cells were then gently resuspended in 20ml of inoue transformation buffer. 1.5ml of dimethyl sulfoxide (DMSO) was then added and swirled to mix. Cells were then stored on ice for 10mins. Aliquots were quickly dispensed in 500μl volumes into prechilled, sterile eppendorfs. Cells were then snap frozen in liquid nitrogen and stored at -80°C.

2.4.2 Plasmid cloning by restriction enzyme digest

2.4.2.1 PCR for amplification of cDNA

PC3 cells were chosen as they express high levels of LIF. RNA was extracted and cDNA synthesised from these cells as described below. Master mix was made as follows; 25μl 2x iproof high fidelity master mix (Biorad), 23μl cDNA and 2μl of 10μM LIF forward and reverse primer mix (Sigma), primer sequences shown below. A touchdown PCR protocol was then used in a Viriti thermo cycler (Applied Biosystems) using the following

parameters; 0.5°C step down from 70°C to 60°C/cycle in the first 20 cycles, followed by 60°C for the remaining 20 cycles. PCR product was then run on a 1% agarose DNA gel at 100v for approximately 45mins.

Gene Name	Species	Sequence
LIF Forward	Human	AAAAAGCTTATGAAGGTCTTGGCGGCAGG
LIF Reverse	Human	AAGGTACCCTAGAAGGCCTGGGCCAACA

Table 2.2: **LIF primers for overexpression.** Primers were purchased from Sigma.

2.4.2.2 Gel Extraction

Bands were cut from the DNA gel using a clean scalpel upon visualisation using a light box. Pieces of gel were then weighed and instructions from a Qiagen gel extraction kit then followed. Briefly gel was solubilised using buffer QG and 1 volume of isopropanol was added and sample was placed in a QIAquick spin column. Samples were centrifuged at 17,000 x g for 1 min. Flow through was discarded and samples were re-centrifuged after addition of 500μl of buffer QG. Flow through was discarded again and samples were washed using 750μl of buffer PE. Samples were then placed into a clean 1.5ml eppendorf and eluted using 50μl of buffer EB.

2.4.2.3 DNA Digest

Using fast digest HindIII and KPNI restriction enzymes (Thermo) the following DNA digests were made for the PCR product and Plasmid DNA (PCDNA3.1 hygro) in PCR eppendorfs. For the PCR product; 11μl H_2O, 5μl 10x fast green buffer (Thermo), 30μl DNA, 2μl of each enzyme. For the plasmid DNA; 5.2μl H_2O, 2μl 10x fast green buffer, 10μg pcDNA 3.1 Neo DNA, 3μl each enzyme. Eppendorfs were mixed gently and centrifuged before being incubated at 37°C for 15mins. Digested products were then run on a 1% agarose gel and gel extraction was done as described above.

2.4.3 Ligation

For ligation a ratio of 8:1 insert to plasmid was used. pcDNA 3.1 hygro plasmid = 5.6kb, LIF insert = 700bp. 100ng of each was used in a rapid ligation kit (Thermo). Briefly,

100ng linearised vector DNA, 100ng insert DNA, 4μl 5 x rapid ligation buffer, 1μl T4 DNA ligase made up to 20μl with H_2O was placed in a microcentrifuge tube. Tubes were vortexed and spun to collect the drops. Tubes were incubated at 22°C for 5mins. Ligation mix was then used for transformation.

2.4.3.1 Transformation

On ice 1μl of plasmid was added to 50μl of competent cells, this was incubated for 20mins on ice. Samples were then heated to 42°C for 90secs and cooled for 5mins on ice. 1ml of autoclaved LB broth was added to plamid-bacteria mix and incubated at 37°C for 60mins. Samples were then centrifuged at 17,000x g for 2mins. 1ml of solution was discarded and samples were re-suspended in remaining 100μl. Under aseptic conditions samples were plated on an ampicillin LB agar plate and spread using an L rod. Once dry, plates were flipped upside down and grown overnight at 37°C. Once grown individual colonies were picked under aseptic conditions using a 200μl pipette tip, touched to another ampicillin LB agar plate and submerged in 5ml of autoclaved LB broth (with ampicillin). Agar plates were then placed in a 37°C incubator to grow clones over night (then placed in fridge next day) and LB broth was incubated at 37°C on a shaker at 300rpm.

2.4.3.2 Mini prep

N.B. Solutions 1,2 and 3 were taken from Qiagen's maxi prep kit. Cultures were spun down at max speed fo 2mins. The supernatant was discarded and resuspended in 300μl of solution 1 and briefly vortexed. 300μl of solution 2 was added and samples were incubated at room temperature for 5mins. Solution 3 was added and the sample was inverted 6 times. Samples were then spun at 17,000x g for 5mins. The supernatant was transferred to a new tube and 3μl of RNase A (Thermo) was added. This was incubated at 37°C for 1hr. 1.5ml of Chloroform (Sigma) was added and inverted to mix. Samples were centrifuged at 17,000x g for 5mins and the aqueous phase was then transferred to a new tube. Equal volume of isopropanol was added and samples were incubated at room temperature for 10mins. Samples were then spun at 17,000x g for 5mins and supernatant discarded. The pellet was washed with 70% ethanol H_2O, invert mixed and spun at max speed for 2mins. Supernatant was discarded and the pellet was air-dried. Dry pellet was resuspended

in 40μl H_2O. Authenticity of samples was then confirmed by Sanger DNA sequencing, outsourced to the Weatherhall institute of molecular medicine (WIMM), University of Oxford.

2.4.4 Transfection of target cells

Cells were seeded at a density of 3.3 x 10^4 cells/cm^2 and allowed to adhere for 24hrs. Cells were then transfected using 2.5μg of DNA and 9μl of Lipofectamine 2000 transfection reagent (Sigma) in antibiotic free medium. Samples were taken for RNA after 48hrs transfection to confirm overexpression.

2.5 RNA isolation

Total RNA was isolated using the readily available RNeasy kit (Qiagen) according to the manufacturers instructions. Briefly cell membranes were disrupted by 350μl RLT lysis buffer. One volume of 70% ethanol was added to homogenise the lysate. 700μl of the sample was added to a RNeasy spin column and centrifuged for 15secs at 8000 x g. The flow through was discarded and 700μl of buffer RW1 was added to the top of the column. The sample was centrifuged for 15secs at 8000 x g and flow through was discarded. 500μl of buffer RPE was added to the top of the column and the sample was centrifuged for 15secs at 8000 x g and flow through was discarded. 500μl of buffer RPE was added to the top of the column and the sample was centrifuged for 2mins at 8000 x g. Collection tubes were then changed for new 2ml collection tube and columns were centrifuged again at full speed for 1min. Collection tubes were changed for RNase/DNase free 1.5ml eppendorfs. 30μl of RNase/DNase free water was then added to the top of the collection tubes and samples were centrifuged for 1min at 8000 x g to elute the RNA. RNA was quantified using a nanodrop spectrophotometer (Thermo Fisher).

2.6 cDNA synthesis

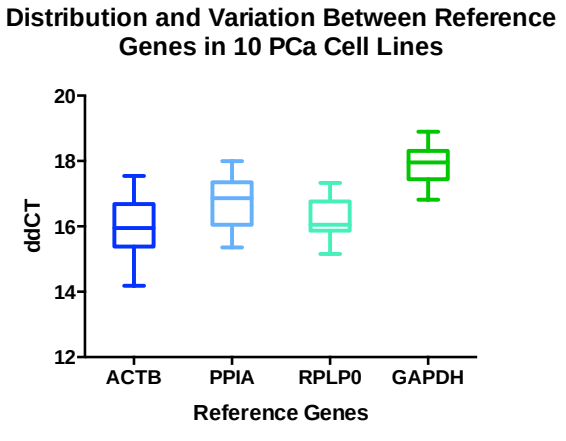
1ug of total RNA was treated with 2μl of 10 x reaction buffer and 1μl of DNase I (Primerdesign, Cat. DNASE-50). To eliminate any contaminating genomic DNA. Sam-

ples were cycled in a thermo cycler (Thermo Scientific) according to manufacturers instructions. 1μg of this was then reverse transcribed using 20μl of Nanoscript 2 (Primerdesign, Cat. RT-premix-48) and cycled in a Veriti thermo cycler (Applied Biosystems) according to manufacturers instructions.

2.7 Quantitative real-time polymerase chain reaction (QRT-PCR)

Taqman real time PCR was performed using Taqman primers (Life Technologies) and Taqman Universal Mastermix (Life Technologies, Cat. 4440041). Briefly, in a 10μl total volume reaction there was; 5μl Taqman Universal Mastermix, 0.5μl of each primer (if multiplexing), 3μl of RNase/DNase free water and 1μl of cDNA. Plate was cycled on a Viia7 (Applied Biosystems) according to manufacturers instruction. Sybr green PCR was performed using sybr green primers (Sigma) and Fast sybr green mastermix (Life Technologies). Briefly, in a 10μl total volume reaction there was; 5μl fast sybr green mastermix, 0.2μl forward primer, 0.2μl reverse primer, 3.6μl RNase/DNase free water and 1μl cDNA. Reference genes for qRT-PCR were optimised as shown below and GAPDH was chosen due to its smallest standard deviation between biological replicates.

A



B

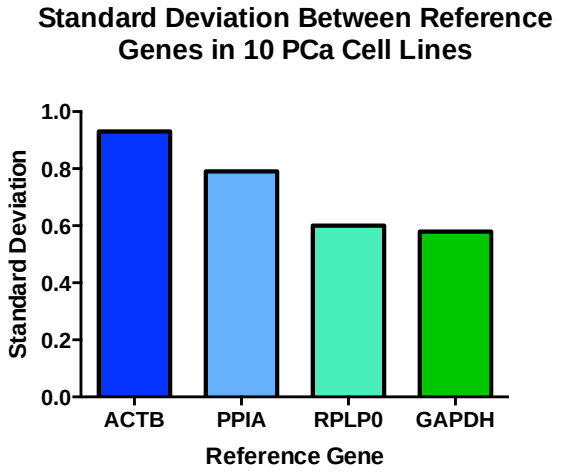


Figure 2.1: **Optimisation of reference genes for qRT-PCR.** (**A**) Distribution and variation of β-actin (ACTB), peptidylprolyl isomerase A (PPIA), ribosomal protein lateral stalk subunit P0 (RPLP0) and Glyceraldehyde 3-phosphate dehydrogenase (GAPDH) in 10 PCa cell lines. (**B**) Standard deviation between biological replicates of reference genes in 10 PCa cell lines.

Gene Name	Species	Probe Number
CDKN1A (P21)	Human	345922
GAPDH	Human	4325792
GAPDH	Mouse	4352339E
LIF	Human	1656268
LIF	Mouse	1312345
LIFR	Human	345922
TnFRSF1 (OPG)	Mouse	651498
TnFSF11 (RANKL)	Mouse	1301196

Table 2.3: **Taqman primer list.** All taqman primer mixes were purchased from Thermo Scientific.

Gene Name	Species	Sequence
Adiponectin Forward	Mouse	AGACCTGGCCACTTTCTCCTCATT
Adiponectin Reverse	Mouse	AGAGGAACAGGAGAGCTTGCAAGA
CEBPα Forward	Mouse	CAGAGGATGGTTTCGGGTCGCT
CEBPα Reverse	Mouse	TAGACGCACCGAGTCCGGCT
Leptin Forward	Mouse	TCACACACGCAGTCGGTAT
Leptin Reverse	Mouse	AGGCTGGTGAGGACCTGTTG
Myogenin Forward	Mouse	GCAATGCACTGGAGTTCG
Myogenin Reverse	Mouse	ACGATGGACGTAAGGGAGTG
Myostatin Forward	Mouse	ACCCATGAAAGACGGTACAAG
Myostatin Reverse	Mouse	TCATCACAGTCAAGCCCAAAG
STAT1 Forward	Human	CTGTATGCCATCCTCGAGAGC
STAT1 Reverse	Human	CTGAGACATCCTGCCACCTT
STAT2 Forward	Human	AAAGCACTGCTAGGCCGATT
STAT2 Reverse	Human	CTCCAGCTGTGAACCATGTCT

Table 2.4: **Sybr primer list.** All sybr green primers were designed using NCBI primer blast and purchased from Sigma.

2.8 Mycoplasma testing by PCR

1ml of cell culture supernatants was centrifuged at 250 x g for 5mins and supernatants were transferred to a fresh eppendorf. Samples were spun at 17,000 x g for 10mins and supernatant was discarded. 50μl of 1 x TE buffer (pH8) was added and samples were heated at 95°C for 3mins. End point PCR per sample was performed using the reaction setup as follows; 0.2μl Jumpstart taq DNA polymerase, 1μl jumpstart buffer, 0.2μl dNTP mix (10mM each), 0.3μl forward primer, 0.3μl reverse primer, 5.5μl RNase/DNase free water and 1μl of test sample. The following PCR program was used; 94°C for 90secs, 94°C for 30secs, 70°C for 30secs, 72°C for 60secs, repeat cycle 20 times, 94°C for 30secs, 60°C for 30secs, 72°C for 60secs, repeat second cycle 20 times,72°C for 4mins, hold at 4°C. PCR products were then run on an agarose electrophoresis gel.

2.9 Agarose gel electrophoresis

Agarose gels were made using 1% agarose (Sigma) and 1 x tris-acetate-EDTA) (TAE) buffer (Sigma). Solution was microwaved for approximately 2mins and swirled to ensure all crystals had dissolved. Once solution was cool to the touch, 2μl (in a 70ml total volume) of 10mg/ml ethidium bromide in H_2O (Sigma) was added, mixed and poured into a mould and allowed to set. 2μl of 6 x DNA loading dye (Thermo) was added to each 10μl PCR product. DNA ladder consisted of; 2μl DNA ladder (Thermo), 1μl 6 x loading dye and 3μl of RNase/DNase free water. Gels were run at 100v for approximately 45mins. DNA bands were visualised under 365nm UV light and images were recorded using a UVITEC gel documentation imaging system.

2.10 RNA-Seq

2.10.1 Transfection of cells for RNA-Seq

PC3 NW1 cells were seeded at a density of 3.3 x 10^4 cells/cm^2 and allowed to adhere fore 24hrs. Cells were the transfected with 2.5μg of DNA and left for 48hrs at which point

samples were taken for RNA.

2.10.2 NEBNext Ultra II RNA library prep for Illumina

Libraries were prepared according to the manufacturers instructions using an NEBnext poly(A) mRNA magnetic isolation module. Firstly mRNA was isolated and fragmented from total RNA using oligo dT beads and a magnetic rack. Beads were mixed with RNA and then washed twice. Samples were heated to 65°C for 5mins. Samples were washed, tris buffer was added and samples were heated once again to 80°C and held at 25°C. Beads were subsequently washed and mRNA was then eluted. First and second strand cDNA synthesis was then performed. Double strand cDNA was purified using NEBnext sample purification beads and DNA was eluted in 0.1 x TE buffer. End prep reaction and adaptor ligation was performed and purification was done using sample purification beads. The quality of the library was assessed on the tapestation system using an Agilient DNA 1000 chip.

2.10.3 Qubit

RNA and DNA quantification was established using a Qubit fluorometer (Life Tech) according to the manufacturers instructions.

2.10.4 Tapestation

The quality of RNA and DNA was established using an Agilent high sensitivity 4200 tapestation system according to the manufacturers instructions.

2.10.5 Next Seq 500 (Illumina)

Samples were run on an Illumina Next seq 500. A next seq 500 v2 kit (75 cycles) (FC-404-2005) was used to multiplex 6 samples. Base index's are listed below. Adaptors were attached to both ends of cDNA fragments to allow pair-end sequencing. Results from RNA-Seq were aligned to the human genome assembly version 38 (hg38 or GRCh38).

Index Number	Sequence
NEBNext i7 Index01	CAAGCAGAAGACGGCATACGAGATCGTGATGTGACTGGAGTTCAGACGTGTGCTCTTCCGATOT
NEBNext i7 Index02	CAAGCAGAAGACGGCATACGAGATACATCGGTGACTGGAGTTCAGACGTGTGCTCTTCCGATOT
NEBNext i7 Index03	CAAGCAGAAGACGGCATACGAGATGCCTAAGTGACTGGAGTTCAGACGTGTGCTCTTCCGATOT
NEBNext i7 Index04	CAAGCAGAAGACGGCATACGAGATTGGTCAGTGACTGGAGTTCAGACGTGTGCTCTTCCGATOT
NEBNext i7 Index05	CAAGCAGAAGACGGCATACGAGATCACTGTGTGACTGGAGTTCAGACGTGTGCTCTTCCGATOT
NEBNext i7 Index06	CAAGCAGAAGACGGCATACGAGATATTGGCGTGACTGGAGTTCAGACGTGTGCTCTTCCGATOT
NEBnext Univ i5 primer	AATGATACGGCGACCACCGAGATCTACACTCTTTCCCTACACGACGCTCTTCCGATOT
NEBNext adapter (Illumina)	GATCGGAAGAGCACACGTCTGAACTCCAGTCUACACTCTTTCCCTACACGACGCTCTTCCGATOT

Table 2.5: **RNA-Seq index list**

2.11 Bioinformatics

Bioinformatics from the RNA-Seq was performed by Srinivasa Rao. Total counts as read from the sequencing (approx 5-6 million) was normalised to the size of the library. Then differentiation expression between samples was analysed in R by using a reference genome. Expression variance between experimental replicates was then plotted, along with a volcano plot and heatmap of upregulated or downregulated genes. All are widely available packages in R.

2.12 Protein isolation and western blotting

Cultured cells were gently washed with 1 x PBS to remove residual growth medium and then either trypsinised using 300μl of trypsin/EDTA and then lysed or lysed directly using 50-100μl of radioimmunoprecipitation (RIPA) protein lysis buffer (Sigma), plus protease inhibitor cocktail (Sigma) and phosphatase inhibitor (Sigma). After incubation for 40mins on ice cells were centrifuged at 12,000x g for 15mins to pellet the cell debris. This supernatant was then transferred to a new eppendorf and the lysate stored at -20°C until future use. The concentration of protein was quantified using a Pierce Bicinchonic Acid (BCA) assay kit (Life Technologies, Cat. 23225). This causes a colourmetric reaction when protein samples are mixed with the working solution. Plates were incubated at 37°C for 30mins and read on a plate reader at wavelength 562nm. Concentrations were calculated using a standard curve obtained from serial dilutions of bovine serum albumin (BSA) provided in the kit. Samples were denatured at 95°C for 5mins in 1 x loading buffer (Life Technologies) and 30μg of each sample was resolved in a 4-20% gradient sodium dodcyl sulphate (SDS)-polyacrylamide gel (Biorad) and transferred to a polyvinylidene difluoride (PVDF) membrane (Biorad) using a semi-dry transfer system (Transblot, Biorad). The membranes were blocked for an hour using 5% BSA in tris-buffered saline with 0.1% tween (TBS-T) and then incubated at a 1:1000 dilution with primary antibody in 5% BSA TBST-T at 4°C overnight. Following this, the membrane was then washed in TBS-T 3 x 10mins each time and then incubated with secondary antibody (either anti-rabbit or anti-mouse) (Cell Signalling) diluted in 5% BSA TBS-T

for 1hr at room temperature. The membrane was then washed again 3 x 10mins in TBS-T as above and then developed using the Novex ECL chemiluminescent substrate reagent kit (Life Technologies Cat. WP20005) using a gel doc system (UVITEC).

Antigen (Name)	Host	Type	Source (Catalogue No.)	Application
Adiponectin	Rabbit	Polyclonal	Abcam (ab3455)	WB 1:1000
Cleaved caspase 3	Rabbit	Monoclonal	Cell signalling (96645)	WB 1:1000
Cleaved caspase 9 (Human)	Rabbit	Monoclonal	Cell signalling (95015)	WB 1:1000
GAPDH	Rabbit	Monoclonal	Cell signalling (51745)	WB 1:1000
Phospho-p44/42 MAPK (Erk 1/2)	Rabbit	Monoclonal	Cell signalling (8544)	WB 1:1000
p44/42 MAPK (Erk 1/2)	Rabbit	Monoclonal	Cell signalling (46959)	WB 1:1000
Phospho-mTOR (Ser2448)	Rabbit	Monoclonal	Cell signalling (55365)	WB 1:1000
mTOR	Rabbit	Monoclonal	Cell signalling (29835)	WB 1:1000
Cleaved PARP (Human) (Asp214)	Rabbit	Monoclonal	Cell signalling (56255)	WB 1:1000
Phospho-STAT3 (Y705)	Rabbit	Monoclonal	Cell signalling (91455)	WB 1:1000
STAT3	Rabbit	Monoclonal	Cell signalling (126405)	WB 1:1000
P21 Waf1/Cip1	Rabbit	Monoclonal	Cell signalling (29475)	WB 1:1000
Phospho-P70 S6 Kinase	Rabbit	Monoclonal	Cell signalling (92345)	WB 1:1000
PSA	Rabbit	Monoclonal	Abcam (ab76113)	WB 1:1000
Anti-Rabbit IgG HRP-Linked	Rabbit		Cell signalling (70745)	WB 1:5000

Table 2.6: **Antibodies List** Abbreviations - WB; western blot.

2.13 Recombinant LIF treatment of prostate cancer cells

PC3 cells were seeded at a density of 2.2 x 10^4 cells/cm^2 and grown for 48hrs before being treated with varying concentrations of rhLIF (50ng/ml, 100ng/ml, 200ng/ml, 400ng/ml or 800ng/ml). LNCAP and VCAP cells were seeded at a density of 2.2 x 10^4 cells/cm^2 and grown for 48hrs before being treated with 100ng/ml of rhLIF.

2.14 Co-culture

2.5 x 10^5 of ARCaPM, 2.2 x 10^4 cells/cm^2 PC3, HS-5, HS27a or 1.1 x 10^4 cells/cm^2 PC3 of 2T3 cells were seeded either directly into a 6 well plate (Corning), or into a 0.4μm

transwell (Scientific Laboratory Supplies). Cells were allowed to settle for 24hrs before transwells were introduced into the wells of the 6 well plate. Cells were then incubated for varying time points up to 48hrs.

2.15 Bicalutamide/DHT treatment

LNCaP cells were seeded at a density of 1.1 x 10^4 cells/cm^2 and incubated at 37°C for 48hrs, after which, media was removed and cells were washed with 1 x PBS. Charcoal-stripped FBS (Gibco) containing medium was then added to each of the wells and incubated at 37°C for 48hrs. Media was subsequently removed and treatments including; Ethanol only control, Bicalutamide only (Abcam, Cat. ICI176334), Bicalutamide + DHT, DHT only and FBS control was added to each well for 8, 16, 24 and 48hrs. RNA and protein was extracted after these time points. A time 0 control after treatment with charcoal-stripped medium was also extracted before treatment.

2.16 Adipocyte differentiation

For differentiation into adipocytes, cells were grown in adipogenic media (10μg/ml insulin, 0.5mM 3-isobutyl-1-methylxanthine (IBMX) and 0.25μm Dexamethasone in DMEM with 10% FBS) for three days before being changed into insulin media (10μg/ml insulin in DMEM with 10% FBS) for another three days. Cells were then changed into normal growth DMEM as described in cell line section for 24hrs.

2.17 Oil Red O staining

Oil Red O working solution was made my adding 3 parts Oil Red O stock solution (60mg in 20ml 100% isoproponal) with 2 parts water, mixed and left undisturbed for 10mins. Solution was then filtered through Whattman No.1 filter paper. Bone marrow pre-adipocytes (ST2) cells or white fat pre-adipocytes (3T3) cells were seeded at a density of 1.1 x 10^4 cells/cm^2 and allowed to adhere for 24hrs. Growth media was then removed from adherent cells, which were washed gently with phosphate-buffered saline (PBS). 10% formalin was

used to fix cells for 1hr. After which time formalin was removed and cells were washed twice with water before 60% isopropanol was added and cells were incubated at room temperature for 5mins. After discarding the isopropanol cells were stained with Oil Red O working solution for 10-20mins after which cells were washed with water until excess stain ceased. Haematoxylin was added to the cells and stained for 1min. Cells were then washed with water until excess stain ceased. Wells were imaged under a Nikon Eclipse TE300 inverted microscope.

2.18 Lipid uptake

PC3 NW1 were seeded at a density of 2.2 x 10^4 cells/cm^2 into glass bottom confocal plates and allowed to adhere for 24hrs. They were then transfected with empty vector of LIF overexpression constructs and left for 48hrs. ST2 adipocytes had been differentiated into adipocytes in parallel with this so that 48hrs post transfection of PCa they were fully differentiated adipocytes. Media from adipocytes (3 wells of a 6 well plate) was removed apart from 500μl that was left in the final well. Cells were then scraped into that media using a cell scraper and media was moved into the next well, scraped and so on. Finally, cells and media were placed in 1.5ml eppendorfs and spun at at 17,000x g for 15mins to pop the cells. After centrifugation, a thick fatty layer could be seen on top of the supernatant. The supernatant was then collected and added to PC3 NW1 empty vector and LIF overexpression cells after 24hrs. Cells were fixed with formalin and stained with Hoescht (1:1000) (Sigma) and Bodipy (1:2000) (Thermo) for 1hr. Cells were then washed twice with PBS and imaged using a Zeiss confocal 710 microscope.

2.19 Mineralisation assay

2T3 cells were seeded at a density of 1.1 x 10^4 cells/cm^2 and allowed to adhere for 48hrs, then differentiated into osteoblasts using osteogenic media for a period of 16 days. Osteogenic media (20mM β glycerophosphate, 50mM ascorbic acid and 1nm Dexamethasone inα minimum essential media (α-MEM) with 10% FBS) was changed every 3 days. At the end of the experiment, cell culture medium was discarded and cells were fixed with

10% formalin (Sigma) for 15mins. Cells were washed with deionised water and stained with Alizarin Red S solution (40nM in water, pH 4.1-4.3) for 30mins. Cells were washed with water until excess stain ceased (approximately 2-3times). Wells were imaged at 20x magnification, under a Nikon inverted microscope.

2.20 Alizarin Red S staining quantification

10% of acetic acid was added to each well of the 6 well plate (Greiner) and incubated at room temperature for 30mins with gentle shaking. Cells were collected using a cell scraper, transferred to a 1.5ml eppendorf and vortexed for 30secs. Samples were then heated to 85°C for 10mins and cooled on ice for 5mins. Samples were centrifuged at 20,000xg for 15mins. 500μl of the supernatant was transferred to a new tube and 200μl of 10% ammonium hydroxide was added to neutralise the acid. 150μl of the sample was aliquoted in triplicate into an opaque-walled, transparent bottom 96 welled plate (Greiner) and absorbance was read at 405nm on a FLUOstar omgea plate reader (BMG Labtech).

2.21 Alkaline phosphotase enzyme assay

Cells were plated in a 96-well plate. The next day the media was aspirated and the cells were washed with 200μl of PBS. 50μl/well of CellLytic M (Sigma) was added to the plate and it was gently shaken for 15mins at room temperature. The plate was then spun down for 15mins at 4°C at 3000xg. 10μl of the supernatant was transferred to a white opaque 96 well plate. 100°C of 1 x 4-methylumbelliferyl phosphate (4-MUP) was added and plates were incubated at 37°C for 30mins. At the same time, 10μl of the same supernatant was used for a corresponding BCA assay (Thermo). Alkaline phosphatase (ALP) fluorescence was read at excitation 340, emission 520 and activity was normalised to BCA total protein.

2.22 Myocyte differentiation

Pre-muscle C2C12 cells were seeded at a density of 1.1 x 10^4 cells/cm^2 and allowed to grow to confluency, at which point cells were treated with differentiation media (DMEM) supplemented with 0.5% FBS, 1% LG and 1% penicillin-streptomycin and cultured for as long as specified.

2.23 Enzyme-linked immunosorbent assay (ELISA)

2.23.1 Human LIF ELISA for *in vitro* samples

A human LIF ELISA (R and D systems, Cat. DY7734-05) was performed according to the manufacturers instructions. Briefly; 100μl of capture antibody in 1 x PBS was added to the 96 well reaction plate and incubated overnight at room temperature. Antibody was aspirated and plates were washed with 400μl of wash buffer, 3 times. Plates were then blocked with 300μl of reagent dilutent for 1hr. After repeating the aspiration/wash step as described earlier, 100μl of sample or standard diluted in reagent dilutent was added to plates and incubated for 2hrs at room temperature. Aspiration/wash step was then repeated and 100μl of detection antibody, diluted in reagent diluent was added and plates were incubated at room temperature for 2hrs. Aspiration/wash step was then repeated and 100μl of working diluted streptavidin-HRP was added to each well and plates were incubated for 20mins at room temperature in the dark. Aspiration / wash step was then repeated and 100μl of substrate solution was added to each well and plates were incubated for 20mins in the dark. 50μl of stop solution was then added to each well and the plate was tapped gently to mix. Optical density was determined for each well immediately using a FLOUstar microplate reader (Omega) set to 450nm.

2.23.2 Human LIF ELISA for *in vivo* and human patient samples

The human LIF platinum ELISA (Invitrogen, Cat. BMS242) was used. Briefly; wells were washed with wash buffer and 50μl of standard or sample was added to the wells and

left to incubate overnight at 4°C on an orbital shaker. The following day, the plate was left at room temperature for 1hr shaking at 400rpm. Wells were washed 4 times with wash buffer and 50μl of biotin-conjugate was added / well. Plates were incubated for 1hr at room temperature shaking at 400rpm. Wells were washed 4 times with wash buffer and 50μl of streptavidin-HRP was added / well and incubated at room temperature for 30mins shaking at 400rpm. Wells were washed 4 times with wash buffer and 50μl of TMB substrate solution was added to wells and incubated for approximately 30mins in the dark. ELISA plates were monitored by reading in a plate reader at 620nm until colour intensity plateaued. Once this occurred plates were stopped using 50μl stop solution and read again at 450nm.

2.23.3 Mouse Leptin ELISA

A mouse/rat Leptin Quantikine ELISA (R and D, Cat. MOB00) was used according to the manufacturers instructions. ELISA protocol was the same as Human LIF ELISA.

2.23.4 Mouse Myostatin ELISA

A GDF-8/Myostatin Quantikine ELISA (R and D, Cat, DSDF80) was used according to the manufacturers instructions. ELISA protocol was the same as Human LIF ELISA.

2.24 Cell viability - Alamar blue assay

Viability of cultured cells *in vitro* was determined using the Alamar Blue assay. In essence a 1mg/ml working solution of resazurin (Sigma, Cat. R7017) was added to the cultured cells at a ratio of 1:10 to the volume of growth medium (eg. 10μl in each well of a 96-well plate containing 100μl of growth medium). The plate was then incubated at 37°C in a humidified incubator for 3hrs. The plate was then read using a fluormeter (Fluostar) (excitation: 545nm, emission: 585nm). The values from the blank wells (growth medium with alamar blue without cells) were then subtracted from the raw fluorescent values to eliminate background fluorescence.

2.25 Vybrant cell labelling

Vybrant cell labelling solutions allow cell populations to be marked in fluorescent colour. This colour is slowly lost during cell division and thus can be used to establish cell proliferation rates. Vybrant DiI solution (Thermo) was used. Briefly, cells were suspended at a density of 1 x 10^6/ml in serum-free media. 5μl of DiI labelling solution was added / ml of cell suspension and incubated for 20mins at 37°C. Cells were then centrifuged at 1500rpm for 5mins and re-suspended in fresh medium. Two more washes were performed and cells were seeded at a density of 2.2 x 10^4 cells/cm^2.

2.26 Cell cycle by propidium iodide staining

Culture cells were washed with 1 x PBS and trypsinised with 300μl of trypsin/EDTA. 700μl of complete media was then added to the well to neutralise the trypsin and cells were collected along with the culture media and washings and spun at 300 x g for 5mins. Cells were then re-suspended in 300μl of 1 x PBS. Cell suspension was then gently vortexed while 700μl of 100% ice cold ethanol was added dropwise. Samples were then incubated on ice for 15mins or overnight at -20°C. Samples were then spun at 300 x g for 5mins at 4°C and cell suspension was re-suspended in 500μl propidium iodide (PI) staining solution (consisting of 50ug/ml PI (Thermo), 0.1mg/ml RNase I (Thermo), 0.05% triton x-100 (Sigma)) for 40mins at 37°C. 500μl of 1 x PBS was then added to the samples and these were spun at 300 x g for 5mins at 4°C. Supernatant was then removed and cells were re-suspended in 500μl of 1 x PBS ready for FACS.

2.27 *In vitro* luciferase assay

Cells were washed with 1 x PBS and 200μl of luciferase lysis buffer was added to each well of a 6 well plate (Lysis buffer consisted of; 25mM Tris/Phosphate, 4mM ethylene glycol-bis(β-aminoethyl ether)-N,N,N',N'-tetraacetic acid (EGTA), 1% triton X-100, 10% glycerol, 2mM dithiotheritol). Cells were scraped from the well using a cell scraper (Sarstedt) and transferred to a 1.5ml eppendorf and centrifuged at highest speed for 5mins at

room temperature. 25μl of the cell extract supernantant was added to 175μl of assay buffer (Assay buffer consisted of; 25mM Tris/Phosphate, 20mM magnesium sulfate ($MgSO_4$), 4mM EGTA, 2mM adenosine triphosphate (ATP), 1mM dithiothreitol). Samples were added to a 96 well microplate, placed in a FLUOstar luminometer (Omega) and injected with 50μl of 1mM luciferin (Promega). Peak-integrated luminescence was measured after a 5sec delay over a 10sec window.

2.28 *In vivo* model

2.28.1 Intracardiac injections

All procedures were conducted in accordance with the Animals Scientific Procedures Act of 1986 (UK) (Project License Number PCCCC8952) issued by the home office. Protocols were approved by the animal welfare and ethical review body of the University of Oxford. Animals were kept in individually-ventilated cages and allowed constant access to food and water.

4 week old athyimc nude mice were purchased from Charles Rivers and acclimatised to their environment for one week prior to experimentation. Animals were anaesthetised using 3% isoflurane and maintained through-out the procedure at 2.5% using a nose cone. Animals were gently taped to a preheated animal stage so that the chest was easily accessible. 1 x 10^5 of PC3-NW1 cells were prepared in sterile 1 x PBS (the viability of these cells were checked before and after the procedure). Anagel ultrasound gel (Medisave) was then administered to the chest of the animal in a single motion to avoid bubbles. The ultrasound probe (visualsonics) 707b was then lowered onto the gel to establish a picture of the heart cavity. Using a 23G needle, cells were then injected into the left ventricle of the heart. After inoculation, animals were gently cleaned of residual ultrasound gel and placed in a preheated recovery chamber and carefully monitored until the animal had fully regained consciousness.

2.28.2 Luciferase injections and IVIS® imaging

Animals were anaesthetised using 3% isoflurane and maintained through-out the procedure at 2.5% using a nose cone. Once anaesthetised mice were injected subcutaneously with VivoGlo^{TM} Luciferin (Promega), at a concentration of 150mg/kg in sterile 1 x PBS using an insulin needle. Subjects were immediately placed inside an IVIS spectrum *in vivo* imaging system (PerkinElmer) and imaged for luciferase activity over time. Optimal luciferase activity was seen at approximately 30mins after injection. Exposure times were adjusted depending on the intensity of the signal. Signal is presented as radiant efficiency so that intensity of signal can be compared from different scanning times.

2.28.3 μCT of bones

Bones were scanned using a Skyscan 1172 (Bruker) machine, performed at 37kV/228 μA, with an isometric resolution of 8.79 μm/pixel using a 0.5mm aluminium filter, rotation of 0.1° with 4 frame averaging. Reconstruction of images was done using NRecon software (SkyScan). Minimum for CS to image conversation was set at 0, maximum for CS to image conversion was set at 0.175000 for all images.

2.28.4 Extraction of *in vivo* bone marrow

Femurs, tibias, spines and jaws were dissected post-mortem. After discarding the skin and muscle, bones were crushed using a pestle and mortar with 2mls of 1 x PBS. Contents were then passed through a 70um cell strainer (Falcon) into a 50ml falcon tube (BD Biosciences). Mortar was then washed with a further 1ml of 1 x PBS and washings were added to the rest of the cell suspension. Tubes were spun at 300 x g for 5mins at 4°C. Bone marrow plasma was then snap frozen in liquid nitrogen and 1ml of 1 x red blood cell lysis buffer was used to re-suspend the cell pellet. This was left on ice for 5mins. Tubes were spun at 300 x g for 5mins at 4°C and washed twice with 1 x PBS + 2% FBS (Gibco). Cells were spun 300 x g for 5mins at 4°C and resuspended in 1 x PBS + 2% FBS. Cells were then halved for RNA extraction (protocol as previously described) of fixed for flow cytometry.

2.29 Statistical analysis

Statistical analysis was performed using Graphpad Prism 6 (Graph Pad Software, CA, USA). Where data was normally distributed statistically significant differences between the means of two or more independent or related groups was established by a one or two way ANOVA respectively with post hoc Tukey or Dunnett's test. A student's T test was used to determine if two sets of data were significantly different from each other and a Pearson correlation coefficient was used to measure the linear correlation between two variables. Data was considered to be significant at $p<0.05$. * = $p<0.05$, ** = $p<0.01$, *** = $p<0.001$. Data are represented as ± standard error mean (SEM), n = 3, unless stated otherwise. *In silico* genomic studies such as microarrays and RNA-Seq data presented in this thesis can yield expression levels of tens of thousands of genes. As such the R project for statistical computing was used along with false discovery rate (FDR) multiple testing correction. FDR is the expected proportion of false positives among all significant tests, allowing the identification of 'candidate positives'.

3

LIF expression in prostate cancer

3.1 Introduction

The LIF pathway has shown contradicting data in relation to patient outcome in different cancer types. LIF itself has been shown to correlate with a poorer prognosis in breast cancer patients, whereas LIFR has been shown to be associated with breast cancer dormancy and ultimately a preferable outcome for patients. In this chapter I aim to investigate the expression of LIF in PCa through *in silico* analysis of PCa patient data sets and establish if LIF can be used as a biomarker of progressive disease.

3.1.1 Big data

The recent rapid increase in the generation of digital data is beginning to enable us to extract new insights from massive data sets, known as big data. Big data is commonly characterised by the '4 Vs'; volume, variety, velocity, and veracity and focuses on associations, rather than on causal relationships. As such, big data can be described as hypothesis-generating, rather than hypothesis-testing, but the potential value of medical big data has been demonstrated in; the delivery of personalised medicine, tailoring diagnostic and treatment decisions and big data-driven population health analyses (Lee and Yoon, 2017). Big data can also be used for focused cancer target mining. With large sequencing datasets in multiple cancer types, platforms such as cBioPortal, oncomine and GEO allow researchers to interactively explore genetic alterations across samples, genes and pathways to link these to clinical outcomes. Using big data approaches, a role for LIF in breast cancer has emerged. In 2014 Li *et al* found that LIF promoted tumourigenesis and metastasis of breast cancer. *In vitro* LIF was found to promote cell proliferation and anchorage-independent growth and was found to increase growth of xenograft breast tumours and promote invasion and migration *in vivo*. Furthermore, overexpression of LIF was significantly associated with a poorer relapse free survival in breast cancer patients (Li et al., 2014). Meanwhile LIFR has been shown to be downregulated in human breast carcinomas and inversely correlates with metastasis. In a study by Chen *et al* they noted that in 1,000 non-metastatic breast cancer tumours, LIFR expression status was correlated with metastasis and recurrence-free disease and overall survival outcome in patients (Chen et al., 2012). Indeed, Johnson *et al* investigated LIFR expression in primary breast cancer patients with a predicted poor prognosis and found that LIFR mRNA levels were significantly lower in those with bone metastasis (Johnson et al., 2016). In this chapter PCa datasets will be used, using samples from benign, primary diseased and metastatic diseased patients to investigate if LIF and/or LIFR can be associated with disease outcome.

3.1.2 Prostate cancer biomarkers

The current limitation of PCa biomarkers still remains the inability to be able to accurately predict patients that will go on to develop metastasis. Li *et al* showed with tissue microarray via immunohistochemisty (IHC) staining in breast cancer specimens, that there was a relationship between LIF expression levels and clinicopathological variables including age at diagnosis, oestrogen receptor levels and progesterone receptor levels. Notably by using Kaplan-Meier survival analysis they concluded that higher expression of LIF was associated with poorer relapse-free survival, suggesting that it could be used as a prognostic marker. In this chapter plasma from non-metastatic, pre-metastatic and post-metastatic cancer patients were used to assess if LIF can be used as a predictor of metastatic disease in PCa.

3.1.3 Prostate cancer *in vivo* model

As discussed in the introduction to this thesis human PCa xenografts have an ability to generate clinically relevant metastasis in a shorter time-scale than transgenic models. Thus, the human PC3 PCa xenograft will be used in this chapter. Athymic nude mice will be used for this model due to their lack of mature T-cells, which enable cross-species xenografted tumour cells to be tolerated by the immune system of the recipient animal. Intracardiac injection of PC3 cells have previously been used to produce skeletal metastases in murine models (Wu et al., 1998). This method is advantageous due to high blood flow compared to tail vein injections (Wu et al., 2013).

3.1.4 Androgens in prostate cancer

The prostate is a primary target organ for androgens and its dependence on them for homeostasis has been thoroughly reviewed. Briefly testosterone, produced by the testis of the fetus and dihydrotestosterone (DHT), produced by local conversion of circulating testoterone by 5α-reductase (an enzyme involved in steroid metabolism), determines the development of the urogenital sinus (UGS) into prostate tissue via the stimulation of the androgen receptor (AR) (Pointis et al., 1979). AR signalling is also important in home-

ostatic maintenance of the adult prostate as well. Androgen deprivation by castration in adult rats has shown prostate shrinkage due to epithelial cell apoptosis (Kyprianou and Isaacs, 1988). AR signalling may play a positive role in adult prostate homeostasis, but it plays a very different role in cancerous prostate tissue. Androgen deprivation therapy (ADT) remains an effective treatment for metastatic PCa, but androgen depletion is frequently associated with the recurrence of PCa. The recurrent disease termed CRPC, although greatly depleted of systemic androgen after castration, still manages to maintain functional AR signalling (Zhou et al., 2015). Interleukin-6 (IL-6) is the head of the family to which LIF belongs. IL-6 is expressed in clinical samples obtained from PCa patients and in multiple cell lines. IL-6 activates both the STAT3 and the MAPK pathways and mechanistically has been shown to regulate AR through these pathways (Culig, 2014). Furthermore, Heemers *et al* show LIFR as an androgen target gene. In the study in which they explored the extent to which co-factors may be affected by androgens through cDNA-mediated annealing, selection, extension, and ligation (DASL) array, they showed LIFR gene expression fold change to be increased by R1881 (a synthetic androgen) treatment by 1.156 and 3.006 using 0.1nM and 1nM respectively (Heemers et al., 2009). This taken together with the finding that LIF is expressed in the murine uterine glands in response to oestrogen stimulation, suggests that the relationship between LIF and AR should be investigated (Ma et al., 2003). The overall goal of this chapter is to elucidate the expression patterns of LIF in PCa and its potential as a biomarker.

3.2 Aims

The aims of work described in this chapter are:

- To determine the expression of LIF and LIFR in PCa patients at different stages of disease.
- To elucidate if LIF can be used as a biomarker of disease.
- To investigate LIF expression in murine models of PCa bone metastasis.
- To observe whether LIF expression in PCa cells is regulated by androgens.

3.3 Results

3.3.1 LIF is associated with improved patient survival

To determine the association of LIF with patient outcomes I used *in silico* analysis of data from Taylor *et al* 2010, due to follow up of patients in the study, allowing survival data to be available (Taylor et al., 2010). 218 tumour samples were obtained from patients treated by radical prostatectomy. Of these 181 were primary tumours and 37 were metastatic tumours. Patients were tracked with history, physical examination and serum PSA testing every 3 months for the first year, 6 months for the second year and annually thereafter. For all analyses described in the study, biochemical recurrence (BCR) was defined as PSA $\geq$0.2 ng/ml on 2 occasions. DNA and RNA were extracted from dissected tissues collected during surgery containing greater than 70% tumour cell content, based on histological assessment and ran using an Affymetrix human exon 1.0 ST array, allowing whole-transcript and exon-level expression data for human primary and metastatic PCa samples and control normal adjacent benign prostate. For *in silico* analysis, whole transcript mRNA gene expression from this study was then analysed using R. The median LIF gene expression (7.013) was used to establish mid-expression, above this 70 patients were categorised as having high levels of LIF and below this, 70 patients were categorised as having low levels of LIF. This median was also used to show the association with BCR. High LIF gene expression was found to be significantly associated with disease-free survival ($p = 0.037$) (Figure 3.1**A**). High LIF gene expression was also found to be associated with the probability of freedom from biochemical recurrence (Figure 3.1**B**). When stratifying these patients into primary/localised vs metastatic disease categories, LIF however, was not shown to be significantly associated with disease state (Figure 3.1**C**). It was found that there was a non-significant increase ($p=0.055$) in LIF mRNA gene expression between benign prostate and primary/localised disease. Interestingly LIFR expression was found to be significantly associated with disease state, adjusted p value <0.001, there was also a significant increase between benign prostate and primary/localised PCa <0.05. However, it is interesting to note the difference in total gene expression between LIF and LIFR. P value was adjusted in R using FDR multiple corrections test against all datapoints within

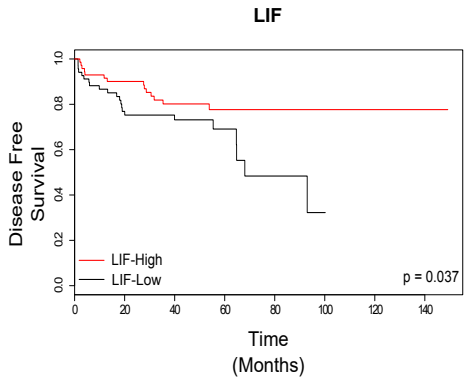
the study.

The data produced by Kumar *et al* 2016 was analysed next (Kumar et al., 2016). This study included 176 localised and metastatic tumours from 63 men with CRPC and matched benign tissue samples from each individual. These samples were laser-capture microdissected which yielded 5,000–10,000 tumour cells per sample. Bone metastases were sampled using a 1mm diameter tissue punch of frozen-embedded tumours. P values from the original Agilent 44K whole human genome expression oligonucleotide microarray were adjusted in R using multiple testing correction against all gene expressions in the dataset. Comparing primary/localised disease with metastatic disease from all metastatic sites, log fold change (log FC) for LIF was -0.3741 with a p value of 0.0195, however once adjusted p = 0.2579 (Figure 3.2**A**). However, when I segregated the bone metastatic population and compared primary/localised patients with those with bone metastasis the log FC for LIF was 0.1075 with a p value of 0.0002 and a significant adjusted p value of 0.0007 (Figure 3.2**B**). The study used three probes for LIFR, all encoded gene transcript variant 1 and 2 and all produce the same downstream protein. As such the log FC for all these probes were averaged. Primary vs metastatic and primary vs bone metastatic samples show 0.2123 and 0.311887 log FCs respectively.

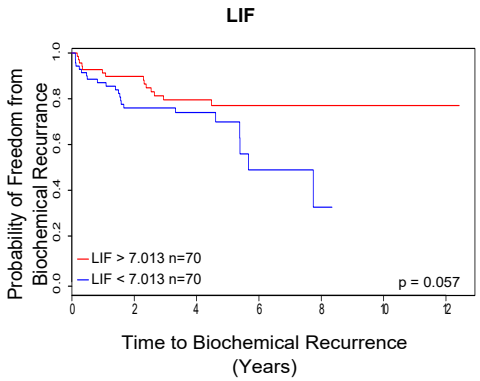
The dataset by Varambally *et al* presented a unique analysis opportunity in that they also profiled, by array, benign prostate tissue as well as primary and metastatic PCa tissue from 13 individual and 6 pooled samples (Varambally et al., 2005). This study conducted an integrative analysis of proteomic alterations and transcriptomic data. The platform used was an Affymetrix human genome U133 Plus 2.0 Array. Comparing benign vs primary PCa LIF had an increased log FC of 0.6786, with a p value of 0.0267, but an adjusted p value of 0.244, making it not significant. Comparing primary vs metastatic PCa for LIF showed a decreased of log FC -1.673, a p value of 0.0162, but an adjusted p value 0.076. This may reflect the small sample size (Figure 3.3**A**). Four probes were used for LIFR in this dataset, again all encoded transcript variants 1 and 2 and all produced the same protein, as such log FC was averaged for all probes. Benign vs primary PCa showed a log FC increase of 0.6877 and primary vs metastatic PCa also showed an increased log FC of 0.1595 (Figure 3.3**B**). Together, these results indicate that low levels of LIF are

associated with decreased survival, freedom from BCR and bone metastasis.

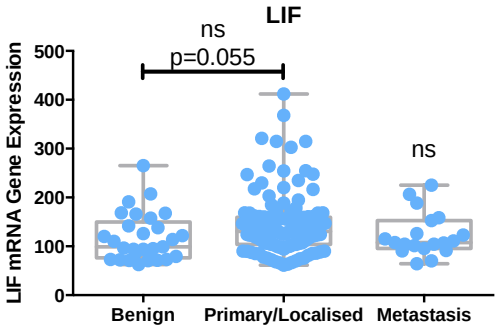
A



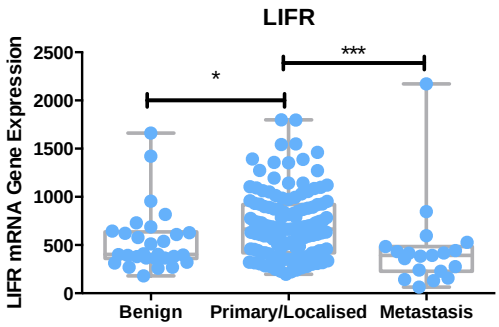
B



C



D

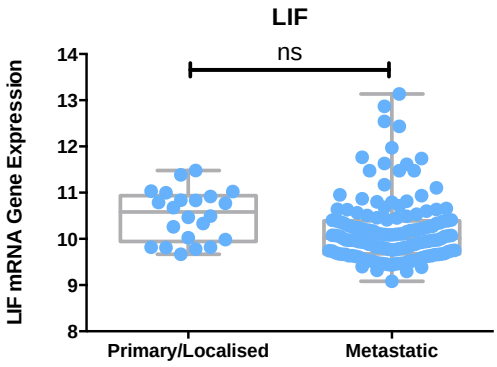


LIF	Log FC	p Value	Adjusted p Value
Benign vs Primary	0.2723	0.0142	0.0556
Primary vs Metastasis	-0.1840	0.1574	0.2901
Benign vs Metastasis	-0.0883	0.5568	0.6466

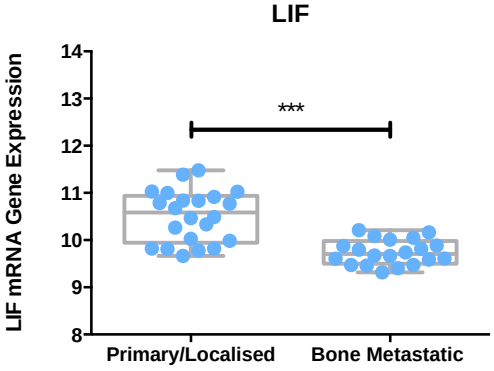
LIFR	Log FC	p Value	Adjusted p Value
Benign vs Primary	0.388	0.009	0.03744
Primary vs Metastasis	-0.876	0.00001	0.0001
Benign vs Metastasis	0.4881	0.0593	0.1272

Figure 3.1: **Elevated LIF mRNA expression is associated with disease free survival.** (**A**) Kaplan-Meier plot using data from Taylor *et al* 2010, re-analysed in R to show survival/disease free progression in patients with PCa shown to have elevated LIF mRNA expression vs those with low LIF expression, p=0.037. (**B**) Kaplan-Meier plot to show probability of freedom from BCR in PCa patients stratified by median expression cut off of 7.013. (**C**) Graph shows whole transcript LIF mRNA expression from benign prostate, primary/localised PCa and metastatic PCa sites. Table shows analysed data in R for differential LIF gene expression. Adjusted p value = adjusted for all datapoints. (**D**) Graph shows LIFR mRNA expression from benign prostate, primary/localised PCa and metastatic PCa sites. Table shows analysed data in R for differential LIFR gene expression. Error bars = standard error mean (SEM).

A

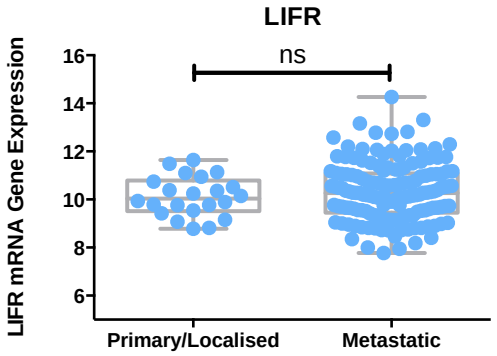


B

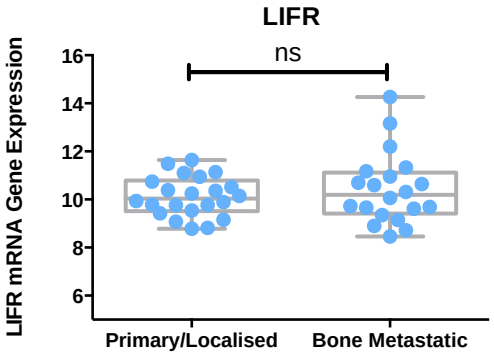


LIF	Log FC	p Value	Adjusted p Value
Primary vs Metastasis	-0.37405	0.195	0.2579
Primary vs Bone Mets	-0.107505	0.0002	0.0007

C



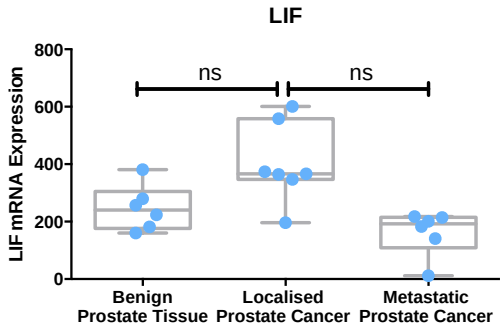
D



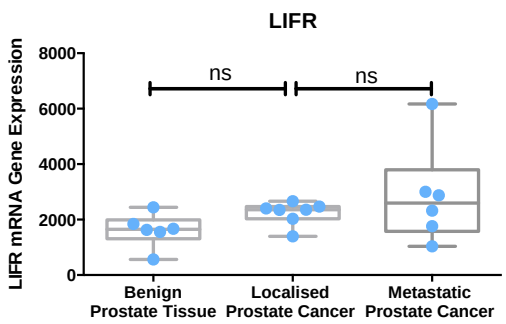
LIFR	Log FC
Primary vs Metastasis	0.2123
Primary vs Bone Mets	0.3119

Figure 3.2: **LIF mRNA is decreased in bone metastasis from prostate cancer.** (**A**) LIF mRNA expression from localised and metastatic PCa sites from Kumar *et al* 2016, re-analysed in R for differential LIF gene expression p= 0.0195, adjusted p= 0.2579. (**B**) LIF mRNA expression from localised and bone metastatic PCa patients analysed for LIF differentiation gene expression p=0.0002, adjusted p=0.0007. Table shows analysed data in R for differential LIF gene expression. (**C**) Graph shows averaged raw LIFR gene expression from 3 LIFR probes from localised and metastatic PCa sites. (**D**) LIFR mRNA expression from localised and bone metastatic PCa. Table shows analysed data in R for differential LIFR gene expression and averaged log FC. Error bars=SEM.

A



B



LIF	Log FC	p Value	Adjusted p Value
Benign vs Primary Prostate Cancer	0.6786	0.0267	0.244
Primary vs Metastatic Prostate Cancer	-1.673	0.0162	0.076

LIFR	Log FC
Benign vs Primary Prostate Cancer	0.6877
Primary vs Metastatic Prostate Cancer	0.1595

Figure 3.3: **LIF mRNA expression in benign, primary and metastatic prostate cancer** (**A**) LIF mRNA expression from benign, localised and metastatic PCa sites from Varambally *et al* 2005. Graph shows raw LIF gene expression, top table shows analysed data in R for differential LIF gene expression. (**B**) LIFR mRNA expression from benign, localised and metastatic PCa sites from Varambally *et al* 2005. Graph shows averaged raw LIFR gene expression from 4 LIFR probes, bottom table shows analysed data in R for differential LIFR gene expression and averaged fold change. Error bars=SEM.

3.3.2 Circulating LIF does not correlate with metastatic stage

Heparin treated plasma samples were made available from the Oxford biobank, these consisted of 29 pre-bone metastatic (M1B) samples that did not have signs of metastasis upon sample collection, but did go on to get bone metastatic disease within 5 years, and matched controls for age and time, that had primary disease. Table 3.1 describes patients with non-bone metastatic disease (M0) and table 3.2 describes patients with pre-bone metastatic disease. Four plasma samples taken from patients post bone-metastasis were also analysed. PSA levels at diagnosis (ng/ml) were found to be significantly increased in patients that were pre-metastatic ($p<0.01$) (Figure 3.4**A**). Circulating LIF protein expression however, was found to be variable, low, and with no significant differences across patient groups (Figure 3.4**B**). Furthermore, there was no significant correlation, using Pearson r or Spearman's rank correlation coefficient, between PSA levels at diagnosis and circulating LIF levels (Figure 3.4**C**). As some LIF concentrations were so low they were undetectable by LIF ELISA, detectable vs non-detectable LIF was graphed to investigate if there was a difference between the detection of LIF in any patient category. Figure 3.4 **D** shows that there was no significant difference in detectable LIF in any patient group.

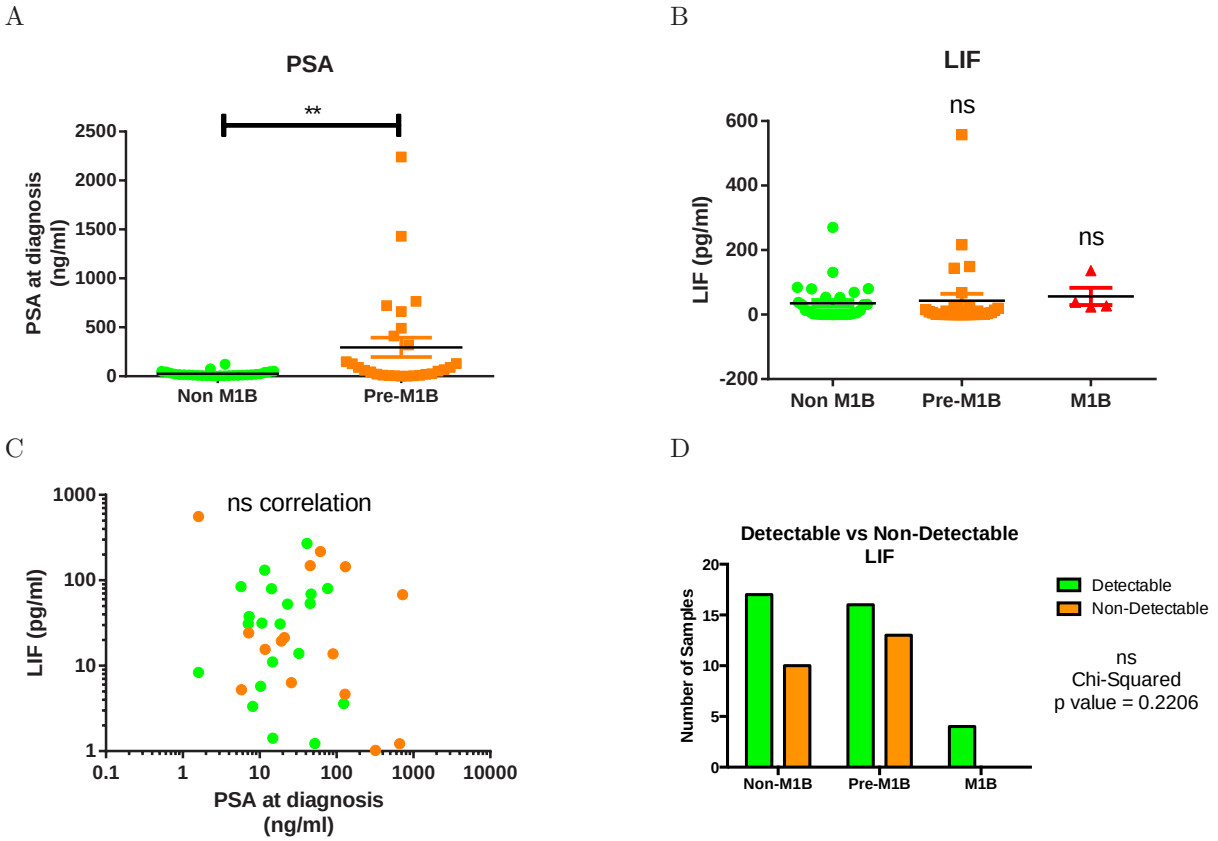


Figure 3.4: **LIF protein expression is not significantly different in plasma samples from pre-bone metastatic patients compared to non-bone metastatic patients and post-metastatic patients.** (**A**) PSA levels at diagnosis (ng/ml) are significantly upregulated in pre-metastatic patients (** = p<0.001). (**B**) LIF protein expression in heparin treated plasma samples of patients with PCa. Patients were either pre-bone metastatic and subsequently went on to develop bone metastasis, non-bone metastatic over the same time period or post-bone metastatic. LIF was not found to be significantly different. Error bars = SEM. (**C**) Log 10 scale, circulating LIF levels (pg/ml) and PSA at diagnosis (ng/ml) in non-bone metastatic and pre-bone metastatic PCa patients. Correlation analysis performed = Pearson's R and Spearman's rank correlations, ns = not significant. (**D**) Detectable vs non-detectable LIF concentrations from ELISA in each patient category. Detectable LIF was quantified as any concentration of above 1pg/ml. Statistical test used, Chi-squared test.

Prompt ID	Matched Study ID	Diagnosis Date	PSA at Diagnosis	Class T Diagnosis	Class N Diagnosis	Class M Diagnosis	P Gleason Diagnosis	S Gleason Diagnosis	Total Gleason Diagnosis	Biopsy Type
600518	600114	13/06/13	7.3	T1c	Unknown	Unknown	3	3	6	Biopsy
600424	600184	16/06/11	10.3	Unknown	Unknown	Unknown	4	4	8	Biopsy
600409	600196	25/10/12	9.8	T1b	N0	M0	5	4	9	TURP Biopsy
600450	600247	20/02/13	1	Unknown	Unknown	M0 Unknown	Unknown	Unknown	Unknown	Unknown
600577	600379	10/06/13	51.5	T3a	N0	M0	4	4	8	Biopsy
600469	600398	21/02/13	18.4	T2c	N0	M0	3	4	7	TURP Biopsy
600492	600447	28/05/13	21.2	T2c	N1	M0	4	5	9	TURP Biopsy
600368	600449	08/08/12	12.9	T2b	Unknown	Unknown	4	5	9	Biopsy
600871	600479	27/02/14	23.1	T3b	N0	M0	4	5	9	Biopsy
600824	600488	28/11/13	20	pT3a	pN0	Unknown	4	5	9	Biopsy
600183	600498	17/08/11	10.7	T2	N1	M0	4	5	9	Biopsy
600552	600529	20/05/13	11.6	Unknown	Unknown	Unknown	4	5	9	Biopsy
600475	600551	14/01/13	4.9	T2a	N0	M0	4	4	8	Biopsy
600355	600586	21/11/12	52.4	T3a	N0	M0	4	4	8	Biopsy
600628	600616	15/07/13	5.7	Unknown	Unknown	Unknown	4	5	Unknown	Biopsy
600644	600666	29/07/13	14.8	Unknown	Unknown	Unknown	4	3	7	Biopsy
600833	600710	12/12/13	123.8	T3b	N0	M0	4	4	8	Biopsy
600182	600820	17/08/11	8.1	T1c	Unknown	Unknown	3	Unknown	3	Unknown
600862	600831	19/05/14	8.9	T3b	N0	M0	4	5	9	Biopsy

Table 3.1: **Table of non-bone metastatic patients.** Heparin treated plasma samples of patients with PCa with primary disease that did not metastasise. Prompt ID refers to specific patients and matched study ID refers to patient IDs that were pre-metastatic patients matched for age and time.

Prompt ID	Matched Study ID	Diagnosis Date	PSA Diagnosis	Class T Diagnosis	Class N Diagnosis	Class M Diagnosis	P Gleason Diagnosis	S Gleason Diagnosis	Total Gleason Diagnosis	ADT Date	Biopsy Type
600114	600518	02/03/11	1.6	T2a	N1	M1b	3	3	6	Unknown	Biopsy
600167	600815	21/07/11	764.8	T3	N1	M1b	4	4	8	24/08/11	Biopsy
600184	600424	31/03/11	320.4	T3	N0	M0	4	4	8	04/05/11	Biopsy
600196	600409	07/09/11	410.8	T2c	N1	M1b	5	4	9	Unknown	Biopsy
600247	600450	Unknown	Unknown	Unknown	Unknown	Unknown	Unknown	Unknown	Unknown	Unknown	Unknown
600379	600577	06/09/12	2239.8	T2c	N1	M1b	4	4	Unknown	06/09/12	Biopsy
600398	600469	13/02/03	Unknown	T3a	N1	M1	3	4	7	06/05/08	Biopsy
600447	600492	22/01/13	4.6	T1b	N1	M1b	4	5	9	02/04/13	TURP Biopsy
600449	600368	13/02/13	9.9	T2c	N1	M1b	4	5	9	26/03/13	Biopsy
600479	600871	10/04/13	52.4	T3/T4	N0	M1	4	5	9	21/05/13	Biopsy
600488	600824	20/03/13	68.6	T3a	N1	M1a	4	5	9	01/04/13	Biopsy
600498	600183	11/04/13	1431.1	pT2c	M1b	4	5	9	Unknown	Biopsy	
600529	600552	29/04/13	5.8	T3a	N0	M1b	4	5	9	11/07/13	Biopsy
600551	600475	20/05/13	25.8	T3b	N0	M1b	4	4	8	01/07/13	Biopsy
600586	600355	20/06/13	128.7	T3b	N0	M0	4	4	8	30/07/14	Biopsy
600616	600628	08/07/13	662.3	T3	N0	M1b	4	5	9	12/08/13	Biopsy
600666	600644	05/08/13	490.2	T2c	N1	M1b	4	3	7	01/09/13	Biopsy
600710	600833	02/09/13	130.2	T3	Unknown	M1b	4	4	8	01/10/13	Biopsy
600820	600182	01/01/04	Unknown	Unknown	N1	M0	Unknown	Unknown	Unknown	01/01/04	Unknown
600831	600862	12/12/13	149.5	Unknown	Unknown	M1b	4	5	9	29/01/14	Biopsy

Table 3.2: **Table of pre-bone metastatic patients.** Heparin treated plasma samples of patients with PCa with pre-metastatic disease that did not have signs of metastasis upon sample collection, but did go on to get bone metastatic disease within 5 years. Prompt ID refers to specific patients and matched study ID refers to patient IDs that were non- bone metastatic patients matched for age and time.

3.3.3 LIF expression is not associated with site of establishment in cell lines

A range of PCa cell lines exist which have been established from multiple sites. Baseline LIF gene expression was investigated in bone metastatic, non-bone metastatic (which were metastatic to other sites) and benign prostate cell lines. Cells were seeded at either 2.2 x 10^4 cells/cm^2 or 2.75 x 10^4 cells/cm^2 to ensure all cell lines reached similar confluencies by 72hrs. The expression of LIF and LIFR was found to be variable throughout the cell lines used, showing no clear association between gene expression and metastatic site (Figure 3.5 **A, B**).

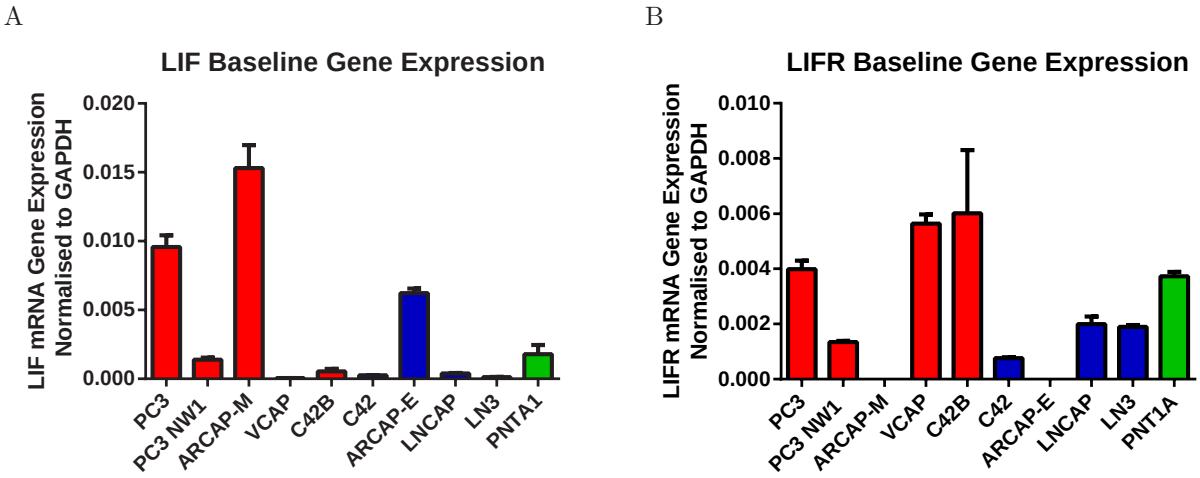


Figure 3.5: **LIF expression in cell line is not associated with establishment site.** (**A**) LIF baseline gene expressions of a variety of cell lines. (**B**) LIFR baseline gene expression in cell lines. Red bars indicate bone metastatic cell lines, blue bars indicate non-bone metastatic cell lines, green bars indicate benign prostate cell lines. Error bars = SEM.

Name	Source	Name	Source
PC3	Vertebral metastasis	C42	Sub cut. LNCAP tumour in mice
PC3 NW1	Vertebral metastasis	*ARCAPE	Low propensity bone met. cell population in mice
*ARCAP-M	Bone met. ARCAP cell population in mice	LNCAP	Lymph node metastasis
VCAP	Vertebral metastasis	LN3	Lymph node metastasis
C42B	Bone metastasis LNCAP tumour in mice	PNT1A	Prostatic epithelial cells immortilised with SV40

Table 3.3: **Establishment sources of PCa cell line.** *Parental ARCAP cell line established from ascites aspirate from a bone metastatic PCa patient. met. = metastasis, cut. = cutaneous.

3.3.4 LIF expression in prostate cancer metastatic *in vivo* model

In vivo murine models play an important role in the study of the aetiology, prevention and treatment of PCa. While tissue culture models are very useful in understanding the biology of PCa, they cannot recapitulate cellular interactions within the tumour microenvironment (Ittmann et al., 2013). In order to investigate LIF levels *in vivo*, an athymic nude mouse model was used. Mice were 4 weeks old upon arrival from Charles Rivers and allowed to acclimatise for 1 week prior to the beginning of the experiment. PC3-GFP and PC3 NW1 PCa cells or PBS control were injected at 1 x 10^5 in a volume of 100μl intracardically into the left ventricle under ultra sound guidance. Mice were then allowed to recover for 2 weeks and were then imaged for fluorescence or luminescence using an IVIS spectrum once a week until experimental end. Fluorescence from PC3-GFP was confirmed prior to injection by fluorescent microscope (Figure 3.6**A**). However, fluorescence wavelengths from PC3-GFP cells were found to not be long enough to be detected by the IVIS spectrum through mouse tissue and gave rise to autofluoresence as depicted by the red colour (Figure 3.5**B**). PC3-GFP were able to be seen post-mortem once tissue covering the ribcage and torso was removed (Figure 3.6**C**). Tumours from the PC3-GFP model were only found in the lungs and liver. FACS sorting of bone marrow cells confirmed no tumour cells had metastasised to the long bones (Figure 3.6**D**).

As such the PC3 NW1 intracardiac model was used to study bone metastasis. These cells had previously been demonstrated to create bone metastasis *in vivo*. The cell line also had a luciferin tag so that tumour growth could be tracked using *in vivo* grade luciferase. Firstly, cells were checked for their luciferase activity (Figure 3.7**A**). Figure 3.7**A** shows PC3 NW1 cells seeded at 1.25 x 10^6 cells/cm^2 with reducing serial dilutions by a factor of 2 in a black walled 96 well plate. Images were taken using the IVIS spectrum and intensity levels of light (total flux) can be seen to be associated with increasing numbers of cells. Using an *in vitro* luciferase assay that quantifies light emission, increased luciferase signal was confirmed from the PC3 NW1 cells compared to PC3 wild type control (Figure 3.7**A**). Some long bone tumours were large enough to emit light 2 weeks after inoculation and continued to increase in intensity until week 5. A common feature that was found in many tumour mice is that they also developed jaw metastasis which can be seen phenotypically

from bulbus tumours on the side of the face (Figure 3.7**B**) and in IVIS scans (Figure 3.7**C**). Weekly IVIS scans show the development of long bone tumours over time, as depicted by tumour mouse 2 in scanning images (Figure 3.7**C**) and quantified using total flux (p/s) (Figure 3.7**D**). This murine model was found to produce osteolytic bone lesions in both the jaw and long bones compared to non-tumour control (Figure 3.7**E**).

Figure 3.8**A** shows luciferase positive prone and supine images from IVIS scans after 5 weeks post inoculation. Bones were taken containing the tumours identified via red arrows and RNA extracted. Human LIF mRNA gene expression was significantly increased in tumour samples compared to non-tumour controls and also when compared to pre-inoculated cells (Figure 3.8**B**). LIF gene expression was found to be correlated with tumour burden as established by total flux, using a Pearson R correlation coefficient (Figure 3.8**C**). Mouse LIF mRNA expression was not detectable via PCR (data not shown). Human LIFR gene expression was also found to be significantly elevated in tumour samples compared to non-tumour controls and was moreover upregulated compared to pre-inoculated cells (Figure 3.8**D**). However, it was not found to be correlated with tumour burden (Figure 3.8**E**). At the protein level, LIF serum concentration was furthermore found to be significantly upregulated in tumour mice compared with non-tumour mice (Figure 3.8**F**). Mouse LIF protein concentration was undetectable via ELISA from *in vivo* serum samples (data not shown).

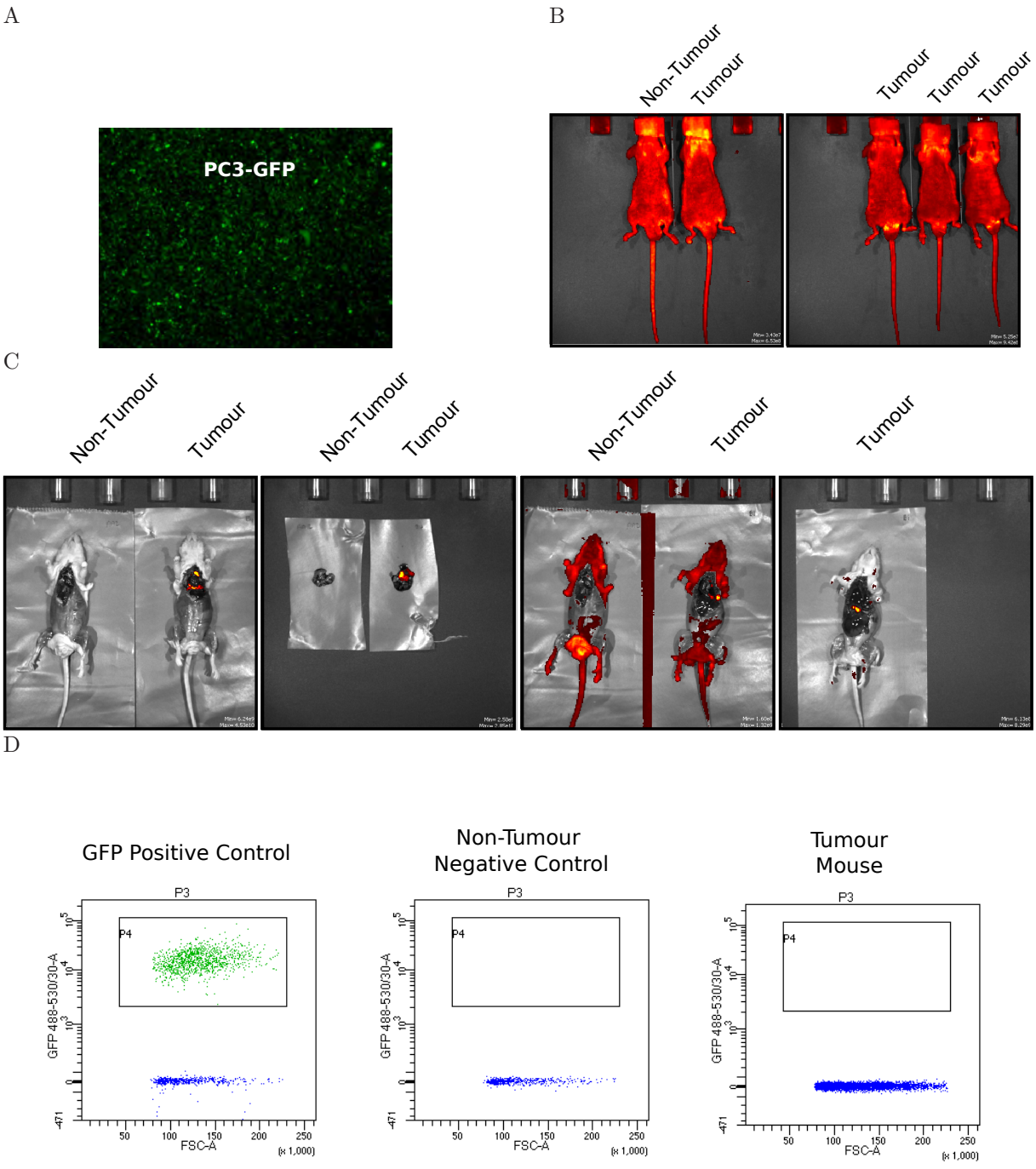


Figure 3.6: ***In vivo* prostate cancer model using PC3-GFP cells** (**A**) Confirmation of fluorescence in PC3-GFP cells prior to injection. (**B**) *In vivo* fluorescence, 6 weeks after injection. Images taken on IVIS Spectrum. (**C**) Fluorescence post mortem. Images taken on IVIS Spectrum. (**D**) FACS plots showing GFP spiked positive bone marrow control, representative non-tumour negative control mouse and representative PC3-GFP tumour mouse.

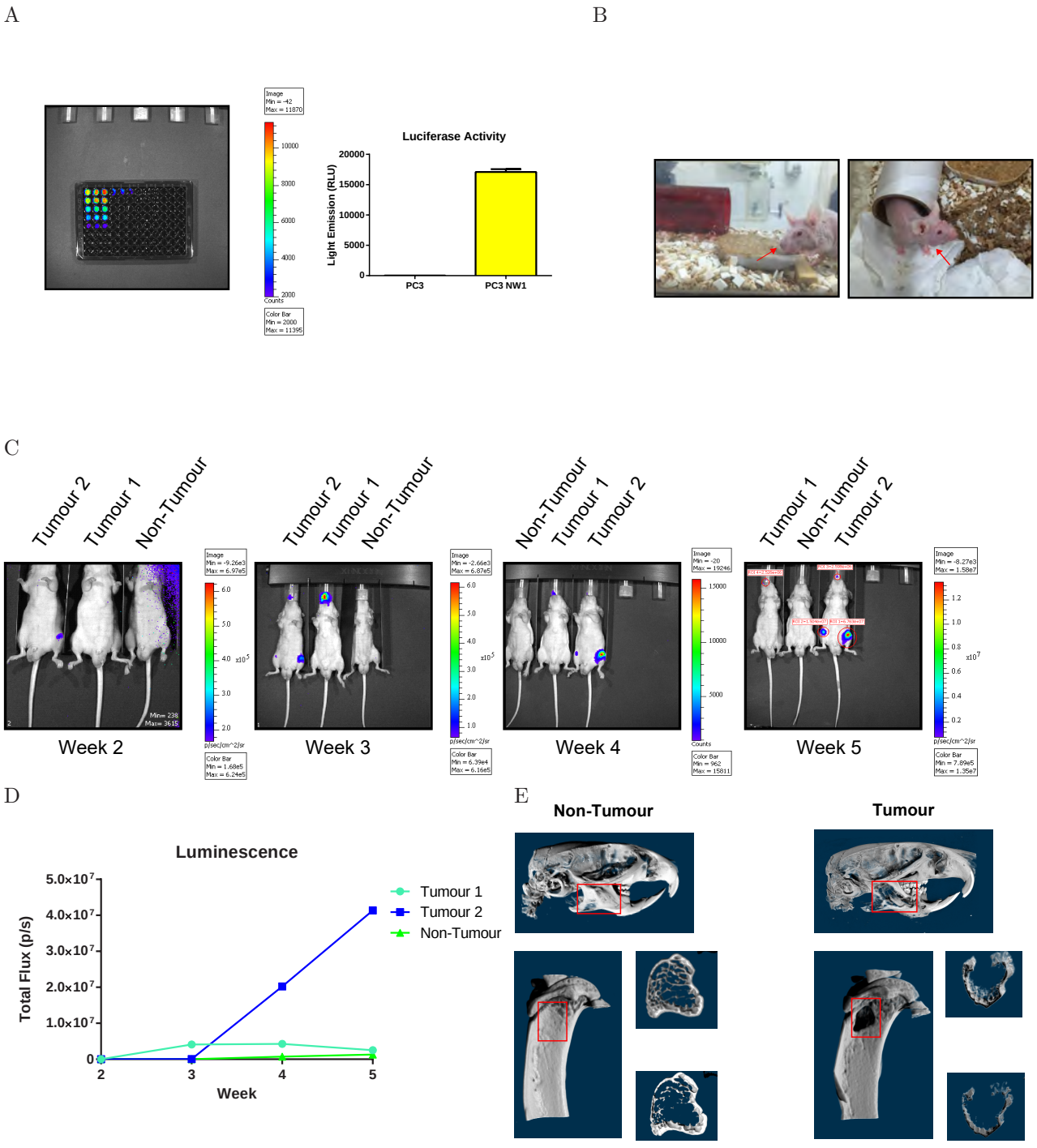


Figure 3.7: ***In vivo* prostate cancer model using PC3 NW1 cells** (**A**) Top figure, confirmation of luciferase activity using serial dilutions of PC3 NW1 cells in black walled 96 well plate. Image taken from IVIS. Bottom figure, *in vitro* confirmation of luciferase activity using luciferase assay. (**B**) Pictures showing bulbus jaw tumours created from PC3 NW1 model. (**C**) Weekly IVIS scans from week 2 to week 5, showing gradual increased tumour burden in long bones. (**D**) Total flux (tumour burden) from tumour and non-tumour mice from week 2 to 5. (**E**) Showing osteolytic lesions found in the jaws and long bones of tumour mice compared to non-tumour mice.

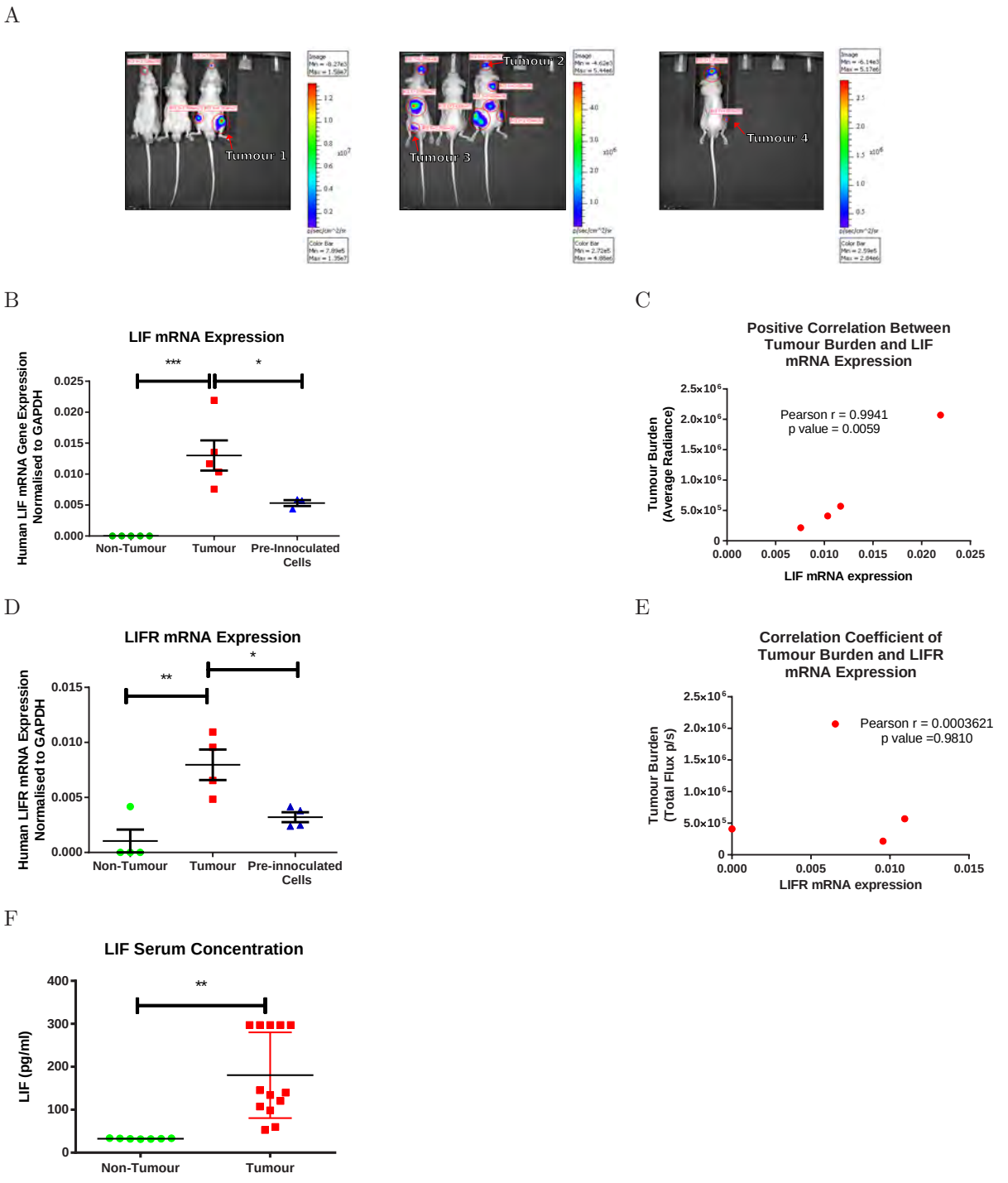


Figure 3.8: **LIF expression in PC3 NW1 intracardiac murine model** (**A**) Luciferase activity in tumour models. Long bones were taken post mortem for tumours indicated. Bones were crushed, strained and RNA extracted. (**B**) Human LIF mRNA gene expression from tumours indicated in above images, plus one not shown. Statistical test used = One-way ANOVA with post hoc Tukey test. Non-tumour vs tumour, p= <0.001, tumour vs pre-inoculated cells, p= <0.05. (**C**) Positive correlation between tumour burden as established by total flux (p/s) and LIF mRNA gene expression using Pearson R correlation coefficient, p=0.0059. (**D**) Human LIFR mRNA gene expression from tumour indicated in above images. Statistical test used = One-way ANOVA with post hoc Tukey test. Non-tumour vs tumour, ** p= <0.01, tumour vs pre-inoculated cells, * p= <0.05. (**E**) Correlation coefficient of tumour burden established by total flux (p/s) and LIFR mRNA gene expression using Pearson R, p= 0.9910. (**F**) LIF serum concentration of non-tumour and tumour mice. Error bars = SEM. Statistical test used = student t test, p=<0.01.

3.3.5 LIF is associated with confluency

While assessing baseline LIF expression of PCa cell lines, it was observed that LIF gene expression could be variable within the same cell line depending on how confluent the cells appeared at the end of the experiment. To confirm this finding a more targeted confluency experiment was performed. Cells were seeded at a high (4.4 x 10^4 cells/cm^2) and low (1.1 x 10^4 cells/cm^2) density and grown for 72hrs, after which low density seeding produced an average cell number of 5.7 x 10^5 and high density seeding produced an average cell number of 1.6 x 10^6. Conditioned media was taken for human LIF ELISA and cells were taken for total protein quantification. RNA was extracted to assess LIF and LIFR gene expression. It was found that LIF RNA and protein expression were significantly associated with higher cell confluency ($p<0.01$) (Figure 3.9**A,B**), however confluency was not found to be associated with LIFR gene expression (Figure 3.9**C**). Interestingly this agrees with the PC3 NW1 *in vivo* model, described previously in this chapter, in that LIF mRNA gene expression was found to correlate with tumour burden. This suggests that as the tumour grows and becomes more confluent as the level of LIF gene expression increases.

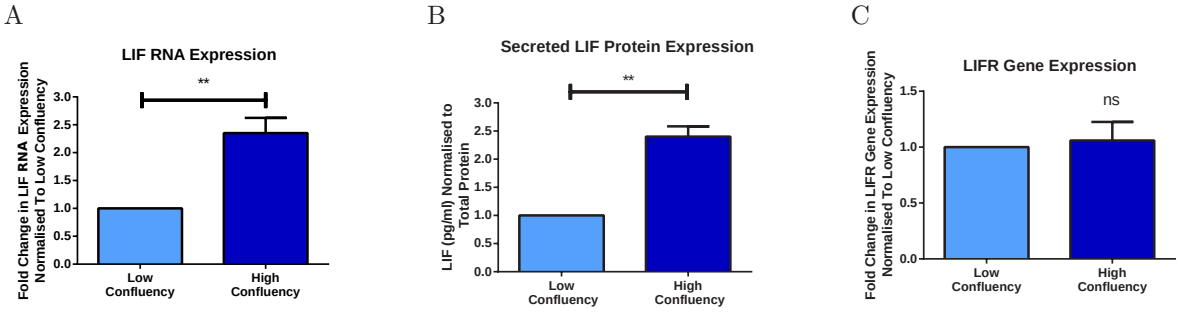


Figure 3.9: **LIF is associated with confluency** (**A**) LIF RNA expression after PC3 cells were cultured for 72hrs at either a high (4.4 x 10^4 cells/cm^2) or low (1.1 x 10^4 cells/cm^2) density. Statistical test used = Student t test, p=<0.001. (**B**) Secreted LIF protein expression after 72hrs as established by Human LIF DuoSet ELISA (R and D). Statistical test used = Student t test, p=<0.001. (**C**) LIFR gene expression. Error bars = SEM. Statistical test used = Student t test, ns= not significant.

3.3.6 LIF is not regulated by androgen receptor, but decreases PSA

Normal development and maintenance of the prostate is dependent on androgens acting through the androgen receptor (AR). AR is known to be important in the development and progression of PCa. The role of androgens and AR signalling has been well characterised in metastatic PCa, where it has been shown that PCa cells are exquisitely adept at maintaining functional AR signalling to drive cancer growth (Zhou et al., 2015). Thus, it was important to establish if androgen manipulation in PCa cells has any effect on the expression of LIF. Bicalutamide is a hormonal therapy drug used to treat PCa through the inhibition of androgens. The LNCaP PCa cell line expresses the AR and hence still has functional androgen signalling. Optimisation of Bicalutamide dose was conducted in LNCaPs using regular growth medium that contains androgens to see the reduction of PSA levels via western blot. 10μM, 20μM and 50μM concentrations of Bicalutamide were tested based on ranges from the literature. It was found that 10μM and 20μM inhibited the expression of PSA protein moderately with 50μM showing a noticeable decrease in PSA levels (Figure 3.10**A**). However, when cells were counted using trypan blue to establish percentage of living cells, the number of viable cells treated with 50μM decreased, suggesting that this concentration of Bicalutamide had a toxic effect on cells (Figure 3.10**B**). In this respect 10μM was chosen as the concentration to continue with as it was the lowest concentration with an inhibitory effect on PSA.

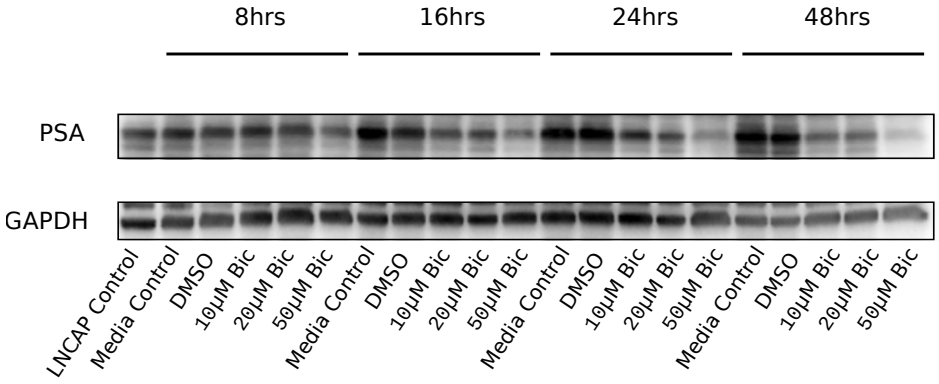
The length of time cells would need to be grown in charcoal stripped media to establish a reduction in PSA expression was then optimised. Androgens are present in FBS that is contained in regular growth medium, to investigate the effect of an increase in androgens on LIF expression it was first important to deplete them from the baseline environment. Charcoal stripped FBS (Sigma) was added to regular growth medium in place of FBS and cells were treated for 24hrs, 48hrs, 72hrs, 96hrs and 8 days with charcoal stripped media. PSA protein expression was depleted after 48hrs (Figure 3.10**C**) and thus this time point was chosen for further investigation as it was the shortest time point that showed a reduction in PSA levels.

LNCaPs were allowed to adhere for 48hrs post seeding, after which they were changed

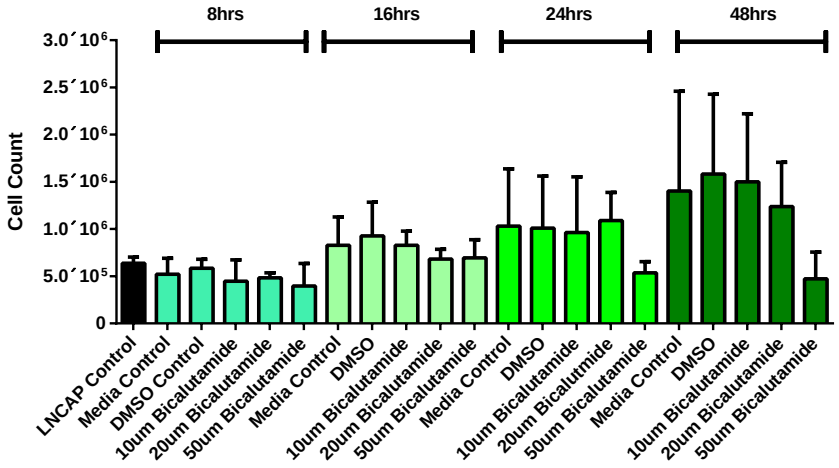
into charcoal stripped medium for 48hrs. Cells were then treated with 10μM Bicalutamide, 10nM DHT (which is a well established dose in these cells), a combination of the two or vehicle control for 8, 16, 24 and 48hrs. PSA protein expression was studied to establish that the treatments worked (Figure 3.11**A**) and mRNA and conditioned media for LIF gene and protein expression was investigated. LIF mRNA gene expression did not change among any of the treatments (Figure 3.11**B**). LIF protein expression was found to be undetectable via ELISA in both controls and the treatments (data not shown).

Given the ability of IL-6 to effect signalling through the AR and subsequently increase expression of androgens, it was also investigated whether treatment with recombinant human LIF (rhLIF) on LNCAPs could have an effect on PSA levels. LNCAPs were grown for 72hrs and treated with 100ng/ml and 200ng/ml rhLIF for 30mins. PSA was decreased in a dose dependent manner by rhLIF (Figure 3.12**A**). IL-6 is able to activate AR signalling through downstream activation of STAT3 and MAPK thus downstream signalling of these pathways as well as mTOR which is also a downstream pathway of LIF, were also investigated in response to LIF treatment. However, these pathways were not found to be activated by LIF in LNCAPs, suggesting LIFs downregulation of PSA levels were through a different mechanism. VCAP cells were used as a positive control for LIF downstream signalling pathways (Figure 3.12**B**).

A



B



C

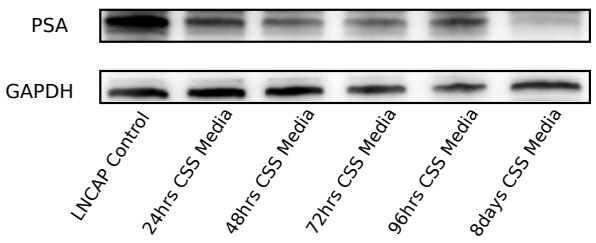
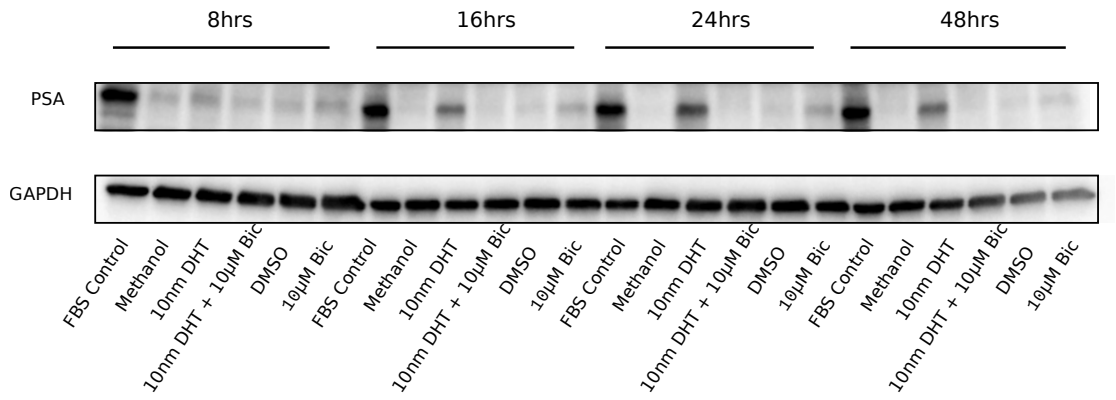


Figure 3.10: **Bicalutamide dose optimisation** (**A**) Western blot showing decreasing PSA protein expression after 8hr, 16hr, 24hr and 48hr time points. (**B**) Cell counts after 10μM, 20μM and 50μM Bicalutamide (bic) treatment for 8hrs, 16hrs, 24hrs and 48hrs. Error bars = SD. **C** Charcoal stripped media time point optimisation. Western blot showing decreasing PSA protein expression after 24, 48, 72, 96hr and 8day time points.

A



B

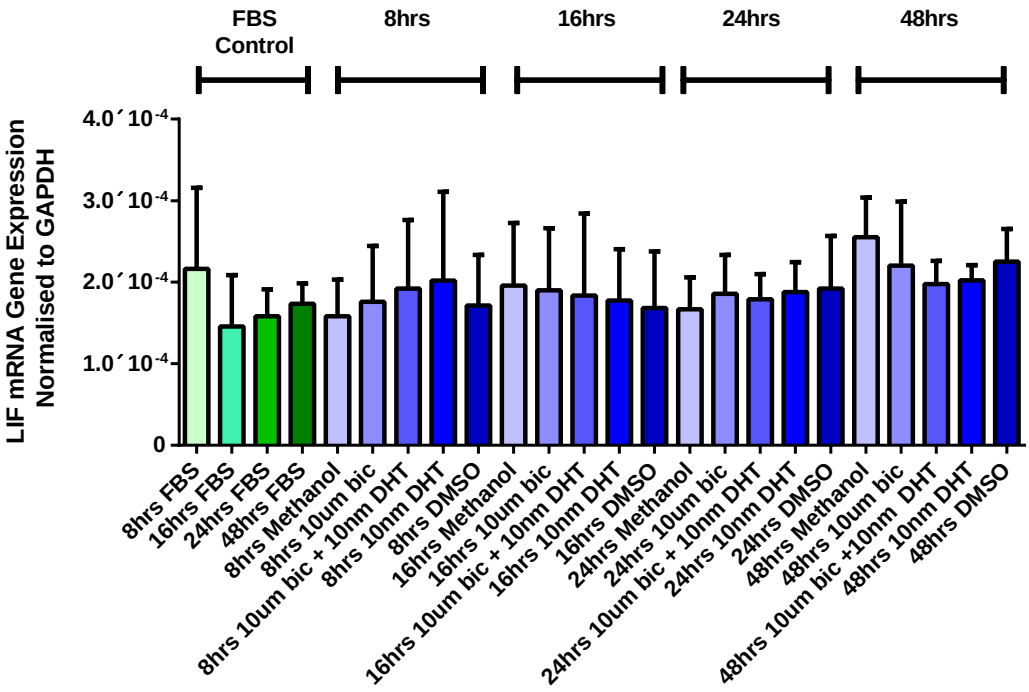
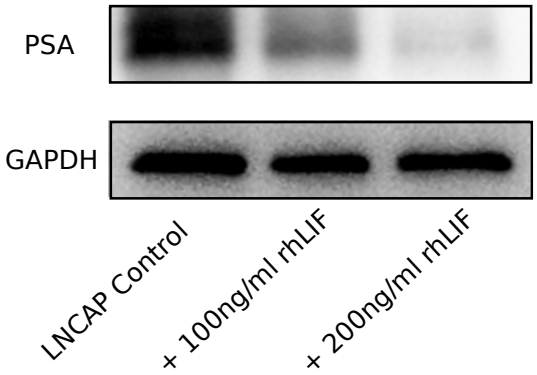


Figure 3.11: **Androgen manipulation has no effect of LIF gene expression.** (**A**) Western blot showing PSA protein expression after treatment with DMSO control, 10μM Bicalutamide (Bic), methanol control or 10nM DHT after 8hrs, 16hrs, 24hrs and 48hrs. (**B**) LIF mRNA gene expression after treatment with DMSO control, 10μM Bicalutamide, methanol control or 10nM DHT after 8hrs, 16hrs, 24hrs and 48hrs. Statistical test used = one way ANOVA with post hoc tukey test. Error bars=SEM.

A



B

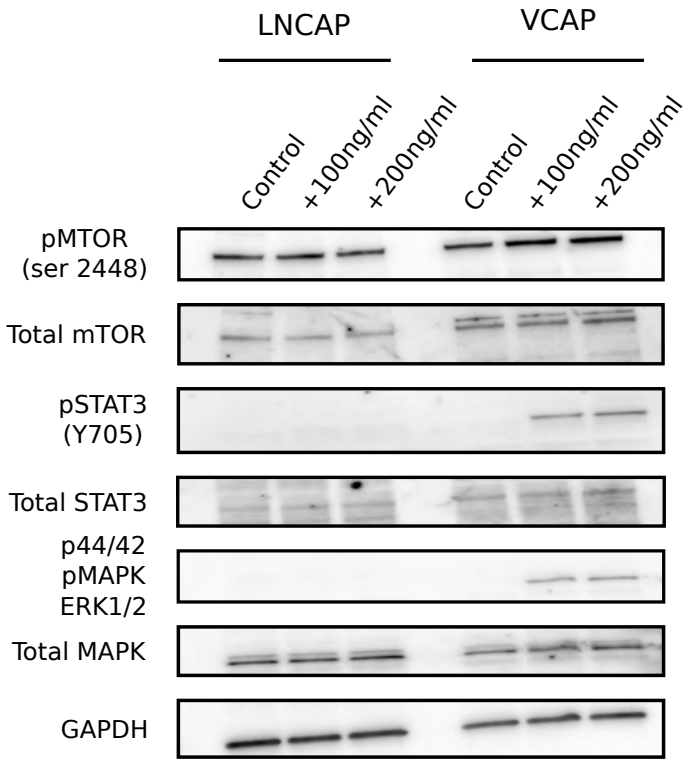


Figure 3.12: **rhLIF decreases PSA protein expression in LNCAPs** (**A**) Western blot showing decreasing PSA protein expression after 30mins of 100ng/ml and 200ng/ml rhLIF. (**B**) Typical downstream signalling pathway of LIF after treatment of LNCAP with 100ng/ml and 200ng/ml rhLIF for 30mins.

3.4 Discussion

The analyses carried out in this chapter provide evidence that LIF is associated with improved patient survival and have generated the hypothesis that LIF may be associated with a better patient prognosis. To elucidate the relationship between LIF and patient outcomes *in silico* analysis of PCa datasets from Taylor *et al*, Kumar *et al* and Varambally *et al* was used. Each dataset gave a unique insight through the types of data that was collected, as is the strength of big data.

Taylor *et al* showed that LIF was associated with disease-free survival and probability of freedom from BCR. Furthermore it appeared that LIF mRNA gene expression was decreased in metastatic patients compared to primary/localised patients, although this was found not be significant upon adjustment. LIFR however, was found to be significantly downregulated in metastatic patients after adjustment. Although, it is important to note that the expression and spread of gene expression signatures for LIFR was far higher than LIF, so although error bars for LIF are smaller and tighter, the interquartile range for LIFR in the primary/localised subset of patients was bigger. LIFR has been identified as a potential tumour suppressor in breast cancer previously. Iorns *et al* used the experimental transformation of normal human mammary epithelial cells by the co-expression of oncogenes and tumour suppressors to provide a disease relevant model for studying breast cell transformation. Using this platform they conducted a genome wide RNAi screen after use of the Expression Arrest^{TM} GIPZ lentiviral shRNA library. LIFR was found to be the highest hit in the list of candidate tumour suppressor genes identified, with the presence of LIFR shRNA in 100% of tumours. Indicating that LIFR may indeed be a tumour suppressor in breast cancer (Iorns et al., 2012). Evidence that the LIF pathway may also be tumour suppressive was provided by Kritikou *et al* in 2003. They showed that in mouse models with LIF deletion, mammary glands exhibit delayed involution and reduced apoptosis. They suggest that as the upstream activator of STAT3 which through its activation and subsequent downstream activation of the ERK1/2 survival pathway, LIF potentiates the subsequent pro-apoptotic effect of STAT3 (Kritikou et al., 2003). To investigate the clinical relevance of this *in vivo* finding, Iorns *et al* then analysed expres-

sion dataset from Oncomine Research and ran meta-analysis of the expression of LIFR in normal and cancerous breast tissue. They found that LIFR expression was significantly decreased in breast cancer samples (median expression -0.82) compared to normal breast samples (median expression 0.42, $p< 0.0001$) and inversely correlated with tumour grade ($p< 0.0001$), suggesting that the loss of LIFR occurs during breast tumourigenesis (Iorns et al., 2012). The results in this chapter show a similar occurrence with LIFR being significantly downregulated in metastatic samples compared to primary/localised samples in the Taylor *et al* data set. LIF shows a similar pattern, but it isn't until you separate the subset of bone metastatic patients in the dataset from Kumar *et al* that you see a significant adjusted p value of 0.0007 between primary and bone metastatic patients, suggesting an increased effect in bone metastasis.

In the dataset by Varambally *et al* LIF appears to show a tendency to be upregulated in primary PCa compared to benign tissue, with a subsequent decrease in expression between primary and metastatic disease, although after adjustment this was not found to be significant. Metcalf *et al* reported that LIF is not detectable in normal murine or human serum, but is a product of stimulation. They suggested that cancer was one such inductive signal (Metcalf, 1991). Indeed, increased LIF expression has been noted in many solid tumours including breast, skin colorectal and nasopharyngeal cancers (Nicola and Babon, 2015), and so there is a strong body of evidence that LIF expression is indeed upregulated in primary cancer. What the Varambally dataset lacks, is number of samples. This is a very small dataset and so it would be difficult to detect significant correlations within the data. This data lends its support to the subsequent downregulation of LIF expression in metastatic tumours compared to primary, but once again is not found to be significant once p value adjusted.

In 2014 Li *et al* analysed 374 breast cancer patient samples for the expression of LIF via immunohistochemistry (IHC). Even though only 54.8% of tumour samples were found to be positive for LIF, they concluded a correlation between LIF and a poorer relapse free survival in breast cancer patients. Tumours were considered to be positive for LIF staining when more than 10% of tumour cells were positive for LIF staining. Thus, in this cohort size a large amount of specimens are segregated into the negative category.

Moreover, a lack of positive staining for a molecule of interest cannot by interpreted as a complete absence of said molecule. Furthermore, the background setting threshold is arbitrarily set and thus it cannot be formally concluded that a molecule of interest is absent in the tissues investigated. Thus, the pitfalls of IHC are potentially so numerous that it can become impossible to determine with certainty whether an antibody produces a specific staining pattern based on intensity. Correct interpretation of IHC must rely on additional information about the expression and localisation of the molecule of interest. This limitation applies particularly to ubiquitous secreted molecules, such as signalling molecules, such as LIF, present at low concentrations in numerous cell types (Jean-Marc, 2008). Furthermore, using IHC to assess the expression levels of LIF only reveals the expression signature of intracellular LIF. This is only one part of the total LIF expression as LIF is a secreted protein (Haines et al., 2000). While it is useful to essentially separate LIF expression in the tumour from the microenvironment, secreted LIF cannot be investigated. In this chapter circulating levels of LIF in PCa patients were evaluated using plasma samples from non-metastatic, pre-metastatic and post-metastatic patients. Similar to the study conducted by Li *et al* LIF expression amongst all patients was generally low. This meant that patients with a 'positive' LIF expression caused a large spread in the data. The amount of 'negative' results (as defined as LIF expression undeterminable by Human LIF ELISA) also reduced the experiment specimen number, making results difficult to interpret. The results presented here showed that LIF did not correlate with disease state. Although the limitations of using secreted LIF as a marker include that LIF expression maybe from tumour, microenvironment or the number of other cell types that express LIF and thus this may 'dilute' any expression pattern that may be present. In addition, it has been demonstrated not only in other cancer types, but also in PCa by Varambally *et al* that LIF expression is upregulated in cancer diseased state compared to a benign tumour or 'normal' state of being. In the ELISA presented in this chapter there was no benign or 'normal' control group so it cannot be said LIF is not still upregulated in cancer diseased states. What can be concluded is that circulating levels of LIF cannot be used as a predictor of prognosis in PCa patients.

Athymic mice, such as the mice used in this chapter, lack mature T-cells, which enable

cross-species 'xenografted' tissues, including tumour cells, to be tolerated by the immune system of the animal (Wu et al., 2013). Athymic nude mice were used *in vivo* with the addition of human PC3-GFP and PC3 NW1 cells to induce bone metastasis from PCa. PC3 cells are androgen insensitive and can form osteolytic metastases after intra-cardiac and intratibial injection (Wu et al., 2013). After prostatic or intra-cardiac injection, bone metastasis sites include the skull, ribs, pelvis, femur and tibia, mandible, and occasionally the brain and spinal cord. PC3-GFP cells grown subcutaneously and then sectioned into small fragments and surgically implanted into the mouse prostate have previously shown murine bone metastasis (Yang et al., 1999). However, PC3-GFP cells used in this chapter failed to produce bone metastasis to the long bones and a disadvantage of this model was the spread of metastasis to soft tissue, which is uncharacteristic of PCa. A variant of PC3s which has a higher incidence of metastasis (PC3M) also forms osteolytic metastases which can be seen frequently within the mandible via intracardiac injection, with is likely to be a result of increased bone turnover in the jaw. The PC3 NW1 cells tagged with luciferase can also be seen to produce a higher incidence of metastasis compared to the PC3-GFP cells and caused mandible metastasis in almost all recipients. Mandibular metastases in PCa is uncommon but can still occur to devastating effect (Simmons et al., 2014). The PC3 NW1 variant cells were easily trackable using luciferin injection and IVIS imaging and showed a progression to long bone metastatic growth from 2 weeks post injection to experimental end point at 5 weeks.

It was found that human LIF and LIFR gene expression from tumours as well as circulating levels of LIF were higher in tumour mice compare with non-tumour mice. This may not be surprising as it would seem logical that the expression of any human gene or secreted protein was increased in mice where human tumour cells were inoculated. There was however, an increase in both LIF and LIFR gene expression between the levels found in pre-inoculated cells compared with tumour cells that had been passaged through the murine model. This maybe due to confluency, as LIF gene expression was found to be associated with increased confluency *in vitro* so too was it found to be associated with tumour burden *in vivo*. Tumour burden was categorised as increased total flux as established by the IVIS, which was shown to be increased as cell number increased. This

was shown using a serial dilution prior to experimental start. As such tumour burden can be a reading of confluency and this chapter has established an association between LIF gene expression and confluency.

Mouse LIF and LIFR gene expression and systemic mouse LIF were found to be undetectable in either non-tumour or tumour samples. One of the reasons for this may be due to lower baseline levels being found in mice tissue compared to human. Using BioGPS, a centralised gene annotation portal that enables researchers to access distributed gene annotation resources (Wu et al., 2016), it was found that LIF and LIFR baseline gene expression across a variety of tissue types was higher in humans than in mice (data not shown), suggesting that it may be more difficult to detect LIF expression in mice than humans.

Chen *et al* identified LIFR as a breast cancer metastasis suppressor upstream of Hippo signalling. Restoring LIFR expression in highly malignant tumour cells suppressed metastasis by triggering a Hippo kinase cascade that lead to phosphorylation, cytoplasmic retention and functional inactivation of the transcriptional co-activator YES-associated protein (YAP). Conversely, loss of LIFR in non-metastatic breast cancer cells induced migration, invasion and metastatic colonisation through activation of YAP (Chen et al., 2012). The Hippo pathway plays a prominent role in numerous human carcinomas. Specifically, YAP, which can lead to excessive cell proliferation and inhibition of apoptosis, which can give rise to tumourigenesis. YAP is strongly elevated in multiple types of human malignancies including breast, lung, small intestine, colon and liver cancers (Kim and Myung, 2018) and YAP has been shown to regulate motility, invasion, and castration-resistant growth of PCa cells (Zhang et al., 2015). Inactivation of YAP by the Hippo pathway has been shown to induce cell contact inhibition and tissue growth control Zhao *et al*. YAP expression is frequently elevated in PCa which may cause evasion of contact inhibition, thus providing a growth advantage for YAP overexpressing cancer cells (Zhao et al., 2007).

The capacity of cells to regulate proliferation in a cell-cell context is a fundamental requirement for organisation and maintenance of tissues in multicellular organisms. Contact inhibition of growth is not restricted just to tissues but is a property that is exhibited by primary cells of many types including smooth muscle, fibroblasts, endothelial

and epithelial cells. Increasing amounts of cell-cell contact in adherent cells eventually block the growth factor and integrin stimulated proliferation of cells *in vitro* (Nelson and Daniel, 2002). In this chapter it was found that both LIF gene and protein expression was upregulated in response to confluency. Not only has LIFR been shown to be upstream of the Hippo pathway but more recently a proteomics study by Ali *et al* showed LIF to also be upstream of the Hippo pathway (Ali et al., 2017). Although, it was not found that LIFR gene expression is upregulated in response to high confluency, one possible mechanism as to why LIF gene and protein expression increases may be due to contact inhibition. As cells become confluent LIF may be activated to initiate Hippo signalling in a bid to phosphorylate YAP and thus deactivate it to slow proliferation. However, contact inhibition is overcome in tumours and is now regarded as a hallmark of cancer. This abolishment can also be seen in various types of cancer cells in culture (Hanahan and Weinberg, 2011).

Thus, another mechanism that could be involved in the upregulation of LIF is the loss of invasiveness. YAP transcriptional activity has more recently been linked to metastasis in melanoma, lung and breast cancer. Sharif *et al* found that by altering the density at which the cancer cells are propagated, enhanced or reduced the vascular invasiveness of commonly studied cancer cell lines. When PC3 cells were grown at a high density for a short period of time (up to 15hrs), their invasiveness was significantly reduced. This non-invasive phenotype was not caused by a difference in cell proliferation rates or apoptosis and was reversed by switching cells to a low-density growth condition (Sharif et al., 2015). This mechanism may be more likely and LIFs effect on invasion will be discussed in the following chapter.

LNCaP is an androgen-responsive human CaP cell line, derived from a lymph node CaP metastasis. LNCaPs have AR mutations and have been shown to be sensitive to anti-androgens and oestrogen as well as to androgens. IL-6 can confer androgen-like activity on LNCaP cells. IL-6 binds to its receptor, which is composed of a ligand-binding and a signal-transducing subunit and activates the STAT and MAPK pathways (Culig et al., 2002). Lin *et al* 2001, found that in the absence of androgen, IL-6 increased PSA mRNA levels. Furthermore, Bicalutamide, abolished the IL-6 effect. Pretreatment

of LNCaP cells with p38 mitogen-activated protein kinase (MAPK), MAP/extracellular signal-regulated protein kinase kinase 1/2, and ErbB2 MAPK inhibitors (SB202190, PD98059, or tyrphostin AG879 respectively) blocked IL-6-mediated induction of the PSA promoter, demonstrating that IL-6 activity was dependent on the MAPK pathway. IL-6 also activated the AR gene promoter, resulting in increased AR mRNA and protein levels in LNCaP cells (Lin et al., 2001). In 2002 Culig also found that IL-6 induced expression of the PSA gene and that inhibitors of MAPK downregulated IL-6s induced AR activity (Culig et al., 2002). The results displayed in this chapter demonstrate that rhLIF treatment on LNCaPs downregulated PSA protein levels in a dose dependent manner. Not only was this effect the opposite to what is seen using IL-6, the MAPK STAT3 and mTOR pathways were not found to be activated in response to LIF treatment. This not only suggests that LIF maybe downregulating PSA expression through a different mechanism other than MAPK, but that the downstream signalling pathways typically seen to be activated in response to LIF were not activated in LNCaPs. Androgen deprivation therapy (ADT) is widely accepted as first-line treatment of symptomatic metastatic PCa. There is also compelling evidence that neoadjuvant ADT increases disease-specific and overall survival in men with high-grade, clinically localised PCa who undergo radiotherapy (Perlmutter and Lepor, 2007). It has been demonstrated that AR is expressed in primary PCa as well as metastatic disease. Not only is it expressed, but also it is transcriptionally active in recurrent PCa under androgen-deprivation conditions. Mechanisms, which allow activation of the AR are complex, but hypotheses include; mutations on the AR gene, cross-talk with other signalling pathways (such as IL-6) and interaction with MAPK signalling. The androgen signalling cascade obviously plays an important role in PCa and thus there are various strategies to inhibit AR activation and function (Karantanos et al., 2013). As LIF has been shown to downregulate the androgen receptor target gene, PSA, perhaps it has the ability to inhibit AR function, although further investigation would be needed to conclude this. Moreover, it is important to note that although Heemers *et al* showed LIFR as an androgen target gene, LIF was not found to be activated by manipulation of androgen levels, suggesting that it is an upstream not a downstream effector (Heemers et al., 2009).

The analyses performed in this chapter have shown that LIF gene expression is associated with patient survival and decreased probability of biochemical recurrence. Furthermore, LIF was found to not be regulated by the AR, but did decrease PSA in PCa cells, although no correlation was found between LIF and LIFR in patient plasma samples.

4

Effect of LIF in prostate cancer cells

4.1 Introduction

IL-6 family cytokines, including LIF have previously been shown to contribute to the proliferation and metastasis of several cancers (Shin et al., 2011), with breast cancer supporting a role for LIF in tumourigenesis and metastasis (Li et al., 2014). However, in melanoma it has been shown to produce tumour suppressive effects through p21 activation, a functional regulator of the cell cycle (Humbert et al., 2015). To investigate the effect of LIF in PCa cells, expression levels may be altered using contructs or treatment with recombinant LIF (rhLIF). Functional effects on cell viability, growth, migration and invasion and sensitivity to chemotherapy will be evaluated in this chapter to establish if LIF has a pro-survival or suppressive effect on PCa cells.

4.1.1 Cell cycle

The cell cycle is a ubiquitous process involved in the growth and proliferation of cells. The process involves many checkpoint proteins that direct a cell through mitosis. Central to this are the cyclin-dependent kinases (CDKs) that regulate the progression of a cell through the different stages of the cell cycle; growth phase 1(G_1), synthesis phase (S), growth phase 2 (G_2) and mitosis (M). In G_1 phase the cell is preparing for DNA synthesis, in S phase cells are synthesising DNA and in G_2 cells are preparing for mitosis. G_0 or sub G_1 phase was originally used to indicate cells that were not cycling, but is now used to indicate apoptotic cells (Schafer, 1998). In cancer, there are fundamental alterations in the genetic control of cell division, resulting in unrestricted cell proliferation. Mutations mainly occur in two classes of genes: oncogenes and tumour suppressor genes. In normal cells, the products of oncogenes operate at different levels along the proliferation pathway. Whereas mutated versions of oncogenes can promote tumour growth. Inactivation of tumour suppressor genes such as retinoblastoma (Rb) and p53 results in the dysfunction of proteins that would normally inhibit cell cycle progression. Cell cycle deregulation associated with cancer occurs through the mutation of proteins important at different levels of the cell cycle. Aberrant activation of CDKs, is a mutation frequently seen in human cancers (Vermeulen et al., 2003). Progression through the cell cycle is monitored by checkpoints that sense possible defects during DNA synthesis and chromosome segregation. Activation of these checkpoints induces cell cycle arrest through modulation of CDK activity. Cell cycle arrest allows cells to repair defects, thus preventing their transmission to resulting daughter cells. The DNA damage checkpoint protects cells from constant assault by exogenous as well as endogenous genotoxic agents such as; chemicals, free radicals, ionizing radiation, by-products of intracellular metabolism or medical therapy, that induce alterations within the DNA. These alterations are sensed by a signalling pathway that ultimately leads to CDK inhibition and cell cycle arrest. If repair is somehow unsuccessful due to either excessive DNA damage or genetic defects in either the checkpoint or the DNA repair machinery, cells may enter senescence or undergo apoptosis. Alternatively an accumulation of DNA alterations may result in genomic instability leading to cell transformation and oncogenesis (Malumbres and Barbacid, 2009). Humbert *et al*

define LIF as a downstream target of TGFβ and indicated that LIFs activation by TGFβ was a prerequisite of tumour suppressive effects in melanoma. Furthermore, they showed that TGF-β induced LIF expression led to a STAT3-dependent activation of p21, causing effects on G1 arrest and apoptosis. This suggests that LIF may have suppressive effects on the cells cycle.

4.1.2 RNA-seq

The transcriptome is the complete set of transcripts in a cell. Understanding the transcriptome is critical for interpreting functional elements of the genome and understanding development of disease. RNA-sequencing (RNA-Seq) uses deep-sequencing technology. Briefly, total RNA or fractionated, such as poly(A)+, is converted into a library of cDNA fragments with adaptors attached to one or both ends. Each molecule is then sequenced in a high throughout manner to obtain short sequences from one end (single-end sequencing) or both ends (pair-end sequencing). The reads are typically between 30-400bp in length, depending on the DNA-sequencing technology used. Following sequencing, the results are either aligned to a reference genome or transcripts or assembled again without the genomic sequence to produce a genome-scale transcription map, encompassing the transcriptional structure and / or level of expression for each gene (Wang et al., 2009). Some advantages RNA-Seq has when compared with other transcriptomic methods, such as microarrays, are; that the required amount of starting RNA is low, the range to quantify gene expression levels is higher, background noise is relatively low and the cost for mapping transcriptomes of large genomes is actually lower compared to other methods (Wang et al., 2009).

Cancer as a disease is highly heterogeneous. Several types of DNA alterations, chromosomal rearrangements or DNA variations may give rise to human cancers. In recent years, the introduction of next-generation sequencing platforms has had a large-scale, positive impact in cancer research. In particular, RNA-Seq is an extremely useful tool to begin to answer the multitude of questions regarding carcinogenesis in humans, in order to quantify and establish the changing expression levels of transcripts during development of disease and under different manipulated conditions (Costa et al., 2013). As such, in this

chapter RNA-Seq will be used after manipulation of LIF levels in PCa cells to establish changing downstream levels of transcripts.

4.1.3 The interferon pathway

Type I interferons (IFNs) activate intracellular antimicrobial responses and influence the development of innate and adaptive immune responses. Canonical type I IFN signalling activates the JAK/STAT pathway, leading to transcription of IFN-stimulated genes. Type I IFNs are polypeptides that are secreted by infected cells and function as; inducers of intrinsic cell antimicrobial states in infected and neighbouring cells to limit the spread of infectious agents, modulator of the innate immune reponses and activators of the adaptive immune system thus, promoting the development of antigen-specific T and B cell responses. In the canonical type I IFN-induced signalling pathway interferon-α receptor (IFNAR) engagement was shown to activate receptor-associated proteins; JAK1 and TYK2, which phosphorylate the latent cytoplasmic transcription factors STAT1 and STAT2. Tyrosine-phosphorylated STAT1 and STAT2 dimerise and translocate to the nucleus, where they assemble with IFN-regulatory factor 9 (IRF9) to form a trimolecular complex called IFN-stimulated gene factor 3 (ISGF3). ISGF3 then binds to its cognate DNA sequences, which are known as IFN-stimulated response elements (ISREs), thereby directly activating the transcription of IFN-stimulated genes (Ivashkiv and Donlin, 2014).

Research by Slaney *et al* has demonstrated that type I IFN secreted by tumour cells can actually induce an anti-metastatic immune response that prevents breast cancer metastasising to the bone. Furthermore, analysis of bone metastatic mouse models and breast cancer patients has shown that tumour cell type I IFN signalling is greatly suppressed, suggesting that this pathway needs to be downregulated in order for tumour cells to relocate (Slaney et al., 2013). Moreover, as a downstream effector of the IFN pathway, STAT1 is generally considered to be a tumour suppressor. A correlation of STAT1 expression with good prognosis has been shown in several types of cancers, including colorectal cancer, hepatocellular carcinoma, oesophageal cancer, pancreatic cancer, soft tissue sarcoma and metastatic melanomas. The effects of STAT1 range from cell cycle inhibition and sensitisation to apoptotic stimuli resulting in cell death. Mechanistically, STAT1 can

transcriptionally regulate the expression of cell cycle effectors, pro-apoptotic proteins and death-receptors and their ligands (Meissl et al., 2017). However, there is also increasing evidence for tumour promoting functions of STAT1. Acquired therapy resistance is a characteristic for late stage cancer and metastasis and is primarily responsible for therapy failure. Although STAT1 generally acts pro-apoptotic and potentiates effects of genotoxic agents, there is also evidence that high STAT1 expression and/or activation can confer therapy resistance. Indeed Patterson *et al* found that siRNA knockdown of STAT1 in DU145 Docetaxel resistant PCa cells was enough to re-sensitise cells to treatment (Patterson et al., 2006). As LIFs involvement in this pathway will be discussed later in this chapter, the consequences on chemotherapy resistance will also be investigated.

4.1.4 Docetaxel treatment in prostate cancer

Docetaxel (Taxotere) is approved for the treatment of patients with locally advanced or metastatic breast, non-small-cell lung cancer and/or androgen-independent metastatic PCa (Engels et al., 2005). Docetaxel kills cells by disrupting the function of microtubules, which are essential for cell survival. It also inhibits the anti-apoptotic gene Bcl2 and encourages expression of the cell-cycle inhibitor, p27. Thus, Docetaxel prevents new cells from forming, causes existing cells to undergo apoptosis and stop other cells from maturing and replicating. As with all cytotoxic agents its actions aren't specifically aimed at tumour cells and so 'healthy' cells may be adversely affected too, resulting in drug-related side effects (Baker et al., 2009). Many patients initially respond to androgen-ablative therapy but, with time, develop fatal androgen-independent disease. This realisation lead to the testing of cytotoxic chemotherapy as treatment for hormone-refractory PCa. A large number of single-agent Phase II studies have been conducted with numerous chemotherapeutics. In general, response rates of <10% have been observed in these single-agent studies. A fall in serum PSA is the main indicator of response in these studies. Thus, using this criteria, chemotherapy combinations have subsequently resulted in a >50% decline in serum PSA levels in a significant proportion of patients. Combination therapies have included agents such as Docetaxel and clinical data indicates a survival advantage in patients treated with chemotherapy combinations (Denmeade and Isaacs, 2002). In

this chapter, it will be investigated whether the combination of LIF manipulation with chemotherapy treatment can give an increased apoptotic effect in PCa cells.

4.2 Aims

The aims of work described in this chapter are:

- To manipulate LIF expression to observe effects on; cell viability, growth, migration and invasion and sensitivity to chemotherapy
- To investigate downstream signalling in response to LIF overexpression constructs and recombinant LIF treatment.

4.3 Results

4.3.1 Effect of LIF knockdown in prostate cancer cells

In order to see the functional effects that arise from PCa-derived LIF, wild type PC3 cells which have a high baseline gene expression of LIF were used to create a stable LIF knockdown (KD) cell line. Creation of the cell line utilised a pLKO.1 puromycin with shRNA construct (Sigma). Four LIF shRNAs were chosen from Sigma and transfected with envelope and packing vectors (pCMV-VSV-G and psPAX2) into HEK293T cells. GFP constructs were also transfected into HEK293T cells as an efficiency control (Figure 4.1). After 48hrs the virus was collected, filtered and used to transduce, with the addition of Polybrene, into PC3 target cells. GFP virus was used as a transduction efficiency control (Figure 4.1). Transfection efficiency of each shRNA construct was established by qRT-PCR. LIF shRNA, 005086 was selected for future experiments due to its increased ability to reduce LIF mRNA expression compared to non-targeting control. (Figure 4.2). Stable LIF KD cells were selected out using 5μg/ml puromycin over a month (as described in the literature). Confirmation of LIF KD at the gene (60%) and protein level (70%) is shown in Figure 4.3, LIF KD had no effect on LIFR gene expression (Figure 4.3**C**) and no short-term effect on viability (Figure 4.3**D,E**).

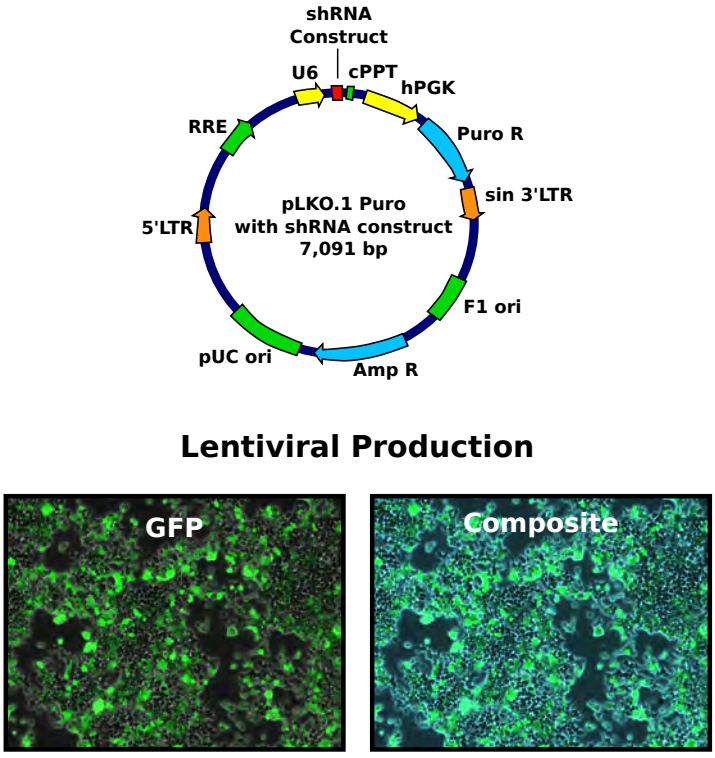


Figure 4.1: **pLKO.1 puromycin shRNA construct.** pLKO.1 puromycin construct, identifying region where LIF shRNA (Sigma) was inserted using envelope and packing vectors (pCMV-VSV-G and psPAX2). Lentivirus was produced in HEK293T cells, GFP pictures show efficiency of lentiviral production. Lentiviral transduction was performed in PC3 cells. GFP pictures show efficiency of lentiviral transduction.

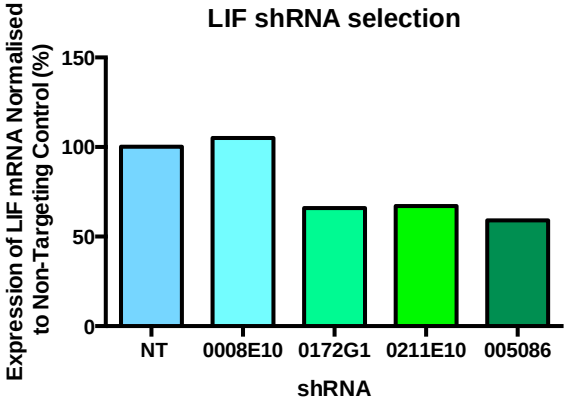


Figure 4.2: **pLKO.1 shRNA LIF construct selection.** Four LIF shRNA constructs were chosen from Sigma and transfected into PC3 PCa cells. Expression of LIF mRNA was then investigated compared to non-targeting control. shRNA 005086 was selected for further experiments.

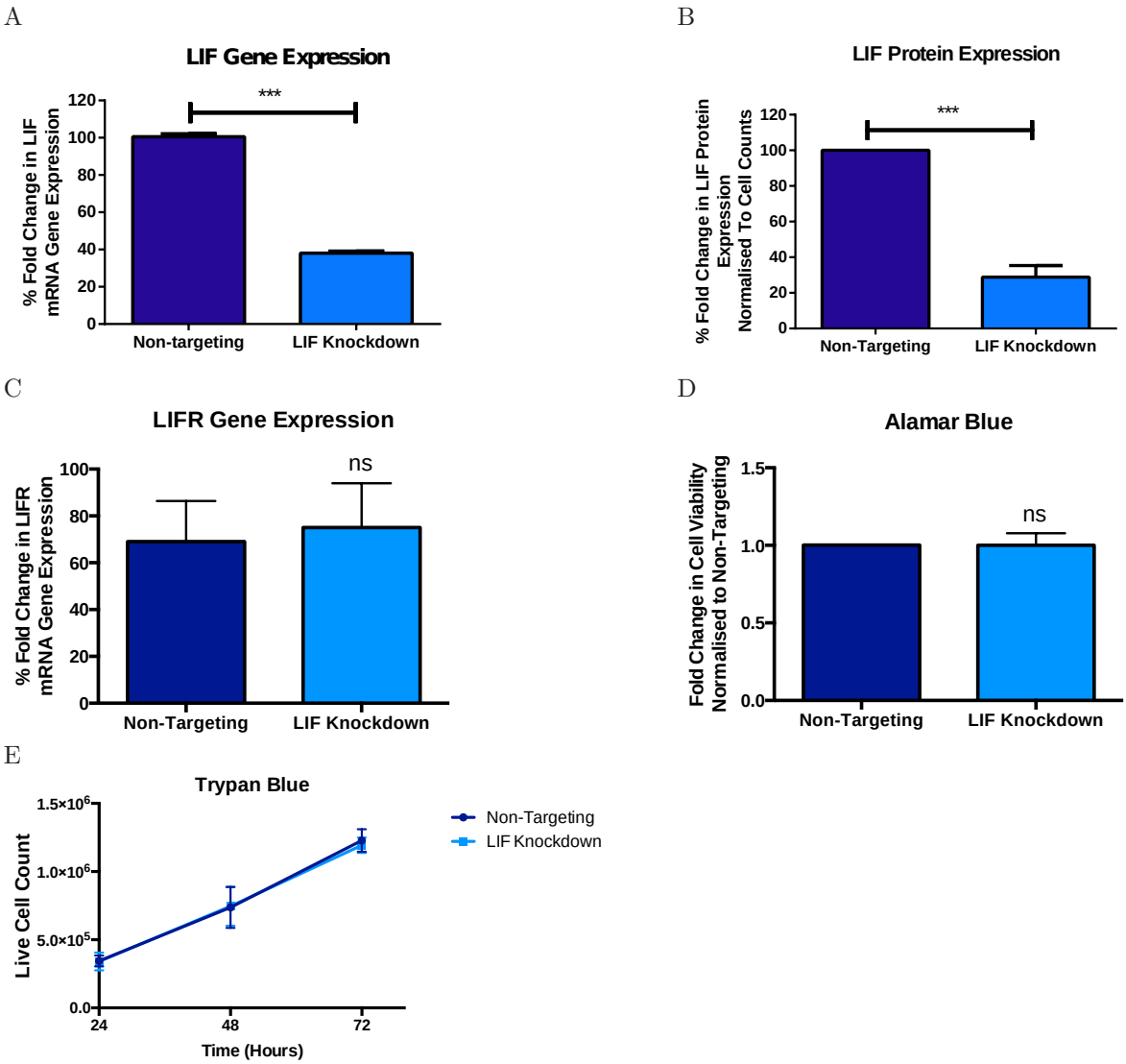


Figure 4.3: **LIF knockdown confirmation in PC3 cells.** (**A**) LIF mRNA gene expression after puromycin selection, showing 60% knockdown. (**B**) LIF protein expression after puromycin selection, showing 70% knockdown. (**C**) LIFR mRNA gene expression showing no significant (ns) difference between LIF knockdown and non-targeting control. (**D**) Fold change in cell viability, showing no significant difference between LIF knockdown or non-targeting control. (**E**) Live cell count by trypan blue over time. Statistical test used = Student t test, *** p= < 0.001. Error bars = SEM.

4.3.1.1 LIF knockdown shows significant effects on migration and invasion in prostate cancer cells

LIF KD cells and non-targeting control PC3 cells were seeded at 2.6 x 10^5 cells/cm^2 in 1% serum media into a migration plate (CIM-Plate 16) for the xCELLigence RTCA DP instrument and left for 33hrs. Impedance readings were taken every hour. LIF KD significantly increased the migration of cells compared to non-targeting control cells (Figure 4.3**A**). To validate this finding, KD cells and non-targeting control were seeded at 1.5 x 10^5 cells/cm^2 into transwell boden chambers and allowed to migrate to or invade through matrigel for 24hrs. Cells were stained with toluidine blue and counted using image J. Again, LIF KD cells were found to migrate and invade significantly more compared with non-targeting control (Figure 4.3 **B**,**C**).

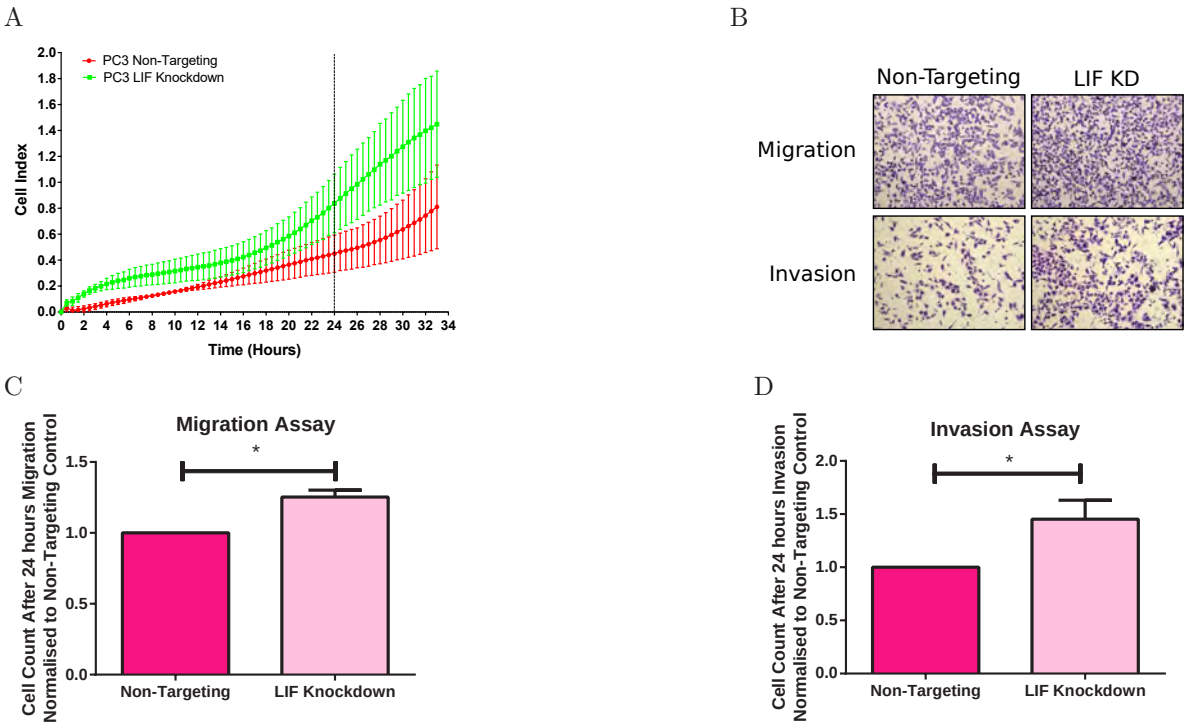


Figure 4.4: **LIF knockdown in PC3 cells significantly increases migration and invasion** (**A**) XCELLIGENCE real-time cell analysis was used to measure cell movement over 33hrs. Dotted line represents doubling time. Statistical test used = Two way ANOVA, column factor = <0.001 ***. N=3. (**B**) Representative microscope images showing transwell migration and invasion assay after LIF KD and non-targeting control. (**C**) 24hrs transwell migration assay. Statistical test used = student t test * p = <0.05. (**D**) 24hrs transwell invasion assay. Statistical test used = Student t test * p=<0.05.

4.3.2 Effect of LIF overexpression in prostate cancer cells

During the generation of the LIF KD cell line, it was found that the wild type PC3-GFP cells did not produce bone metastasis *in vivo*. The decision was then made to change to the PC3 NW1 model, which produced reliable bone metastasis to the long bones *in vivo*. It was preferable to make the manipulated cell line in cells that would also produce an appropriate disease model *in vivo*. However, upon further study of the PC3 NW1 cells, it was found that they had a low baseline level of LIF compared to their wild type counterpart. As such KD in these cells would have been inappropriate and thus it was decided to overexpress LIF in these cells instead and investigate the resulting functional effects. Methods to create the overexpression construct are described in the materials and methods section under 'making LIF overexpression construct'. Figure 4.4 shows the structure of the pcDNA 3.1 construct used, agarose gel confirmation of initial LIF PCR amplification, confirmation of linearisation by restriction enzymes and LIF positive colonies post transformation. Positive colonies were then sent for confirmation via Sanger DNA sequencing at he WIMM, University of Oxford.

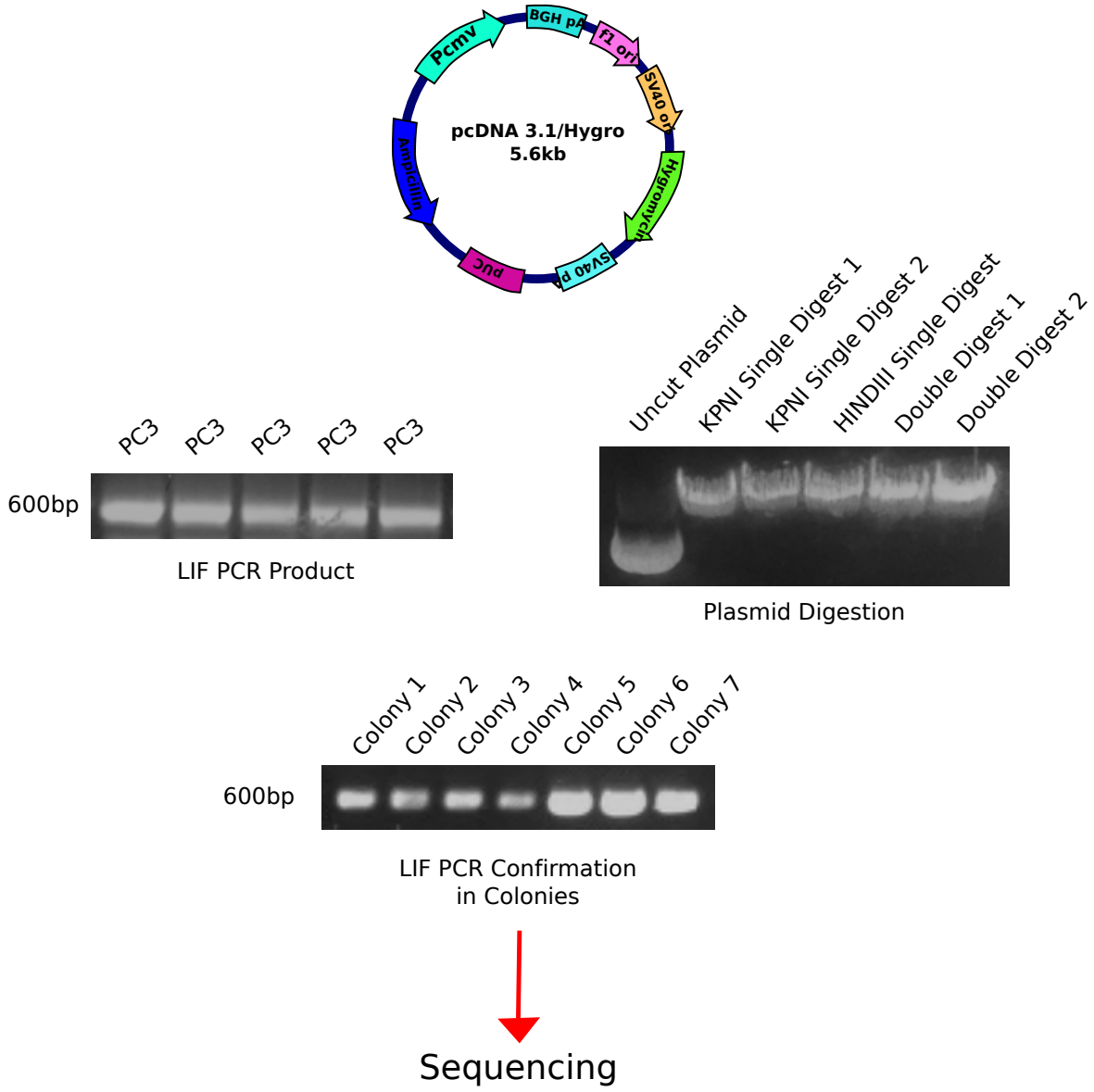


Figure 4.5: **pcDNA 3.1 Hygromycin LIF construct.** pcDNA 3.1 Hygromycin construct was used to insert LIF DNA from PCR amplification from PC3 cells. DNA gel shows positive PCR amplification of LIF. LIF DNA and pcDNA 3.1/Hygro constructs were then digested using restriction enzymes, KPNI and HindIII, confirmation as shown in DNA gel. After ligation and transformation, colonies were extracted and confirmed for the presence of LIF DNA through PCR (as shown by DNA gel). Positive colonies were then sent for confirmation via sequencing.

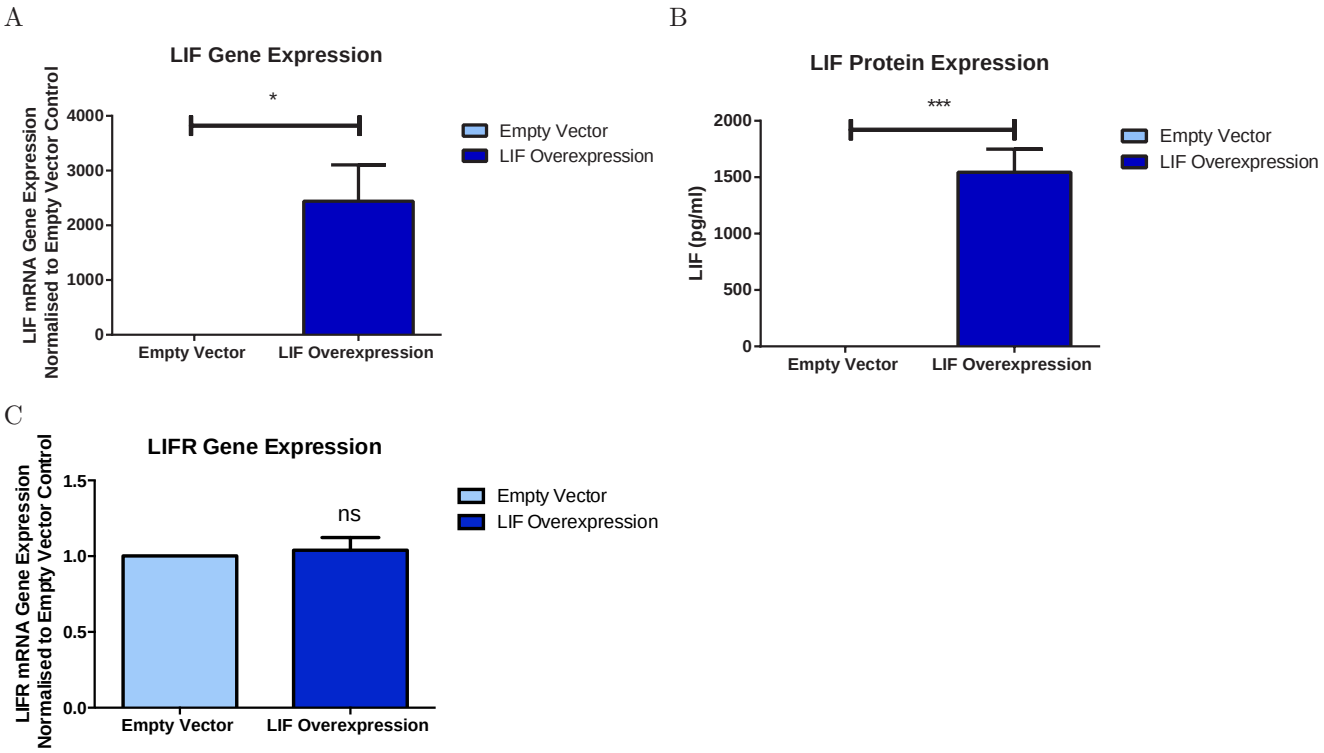


Figure 4.6: **LIF overexpression confirmation in PC3 NW1 cells.** (**A**) LIF mRNA gene expression after transient transfection. (**B**) LIF protein expression after transient transfection. (**C**) LIFR mRNA gene expression after transient transfection. Statistical test used = Student t test, * p=<0.05, *** p= < 0.001, ns = not significant. Error bars = SEM.

Positive constructs were transfected into PC3 NW1 cells using 2.5μg of DNA per transfection as described in the materials and methods section under 'transfection of target cells'. Figure 4.5 shows significant confirmation of LIF overexpression at the gene and secreted protein level with no significant change on LIFR gene expression. After LIF overexpression was confirmed, cells were changed into 200μg/ml hygromycin selection media to select out stably overexpressed and control cells. Selection media was changed every 48hrs for two weeks. It was observed that LIF overexpression cells began to die substantially more after this length of time compared to empty vector control. Due to the high level of initial overexpression it was concluded that this was not a transfection problem. Thus, it was investigated whether long-term LIF overexpression could cause cell death in PCa cells.

4.3.2.1 Long term LIF overexpression causes slowing of cell growth, proliferation and progression through the cell cycle

Firstly, the viability of LIF overexpression and empty vector control cells was investigated after short-term transient transfection. Cells were seeded at 3.3 x 10^4 cells/cm^2 and allowed to adhere for 24hrs prior to transfection 24hrs after transfection, PC3 NW1 cells were seeded into a 96 well plate for 24, 48, 72 and 96hrs Alamar blue assays. This showed no difference in cell viability between LIF overexpression or empty vector control over these time points (Figure 4.6**A**). Secondly the production of apoptotic proteins was investigated. Cells were seeded and transfected as described above and after 48hrs transfection, samples were taken for protein. Interestingly, empty vector control cells produced higher amounts of apoptotic protein markers than LIF overexpression cells (Figure 4.6**B**).

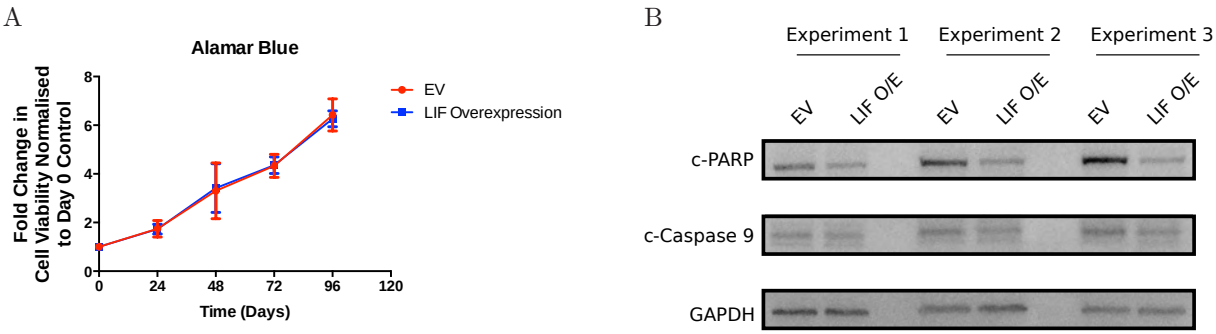


Figure 4.7: **Short term LIF overexpression shows no difference in cell proliferation.** Cells were seeded at a density of 3 x 10^5 and transfected with LIF overexpression or empty vector control for 24hrs. Cells were then seeded into a 96 well plate and alamar blue was added at day 0, 24hrs, 48hrs, 72hrs or 96hrs. (**A**) Graph showing alamar blue cell viability after 24, 48, 72 or 96hrs, normalised to day 0 control. (**B**) Cells were seeded and transfected as described above, but left until 48hrs post transfection. At which point cells were taken for protein. Western shows three separate experiments of LIF overexpression and empty vector control looking at apoptotic proteins. EV = empty vector, LIF O/E = LIF overexpression.

However, this did not explain the observations seen after selection. Thus, cells were seeded and transfected as described before and 48hrs post transfection, 200μg/ml of hygromycin selection media was added to cells and grown for 6, 8 and 11 days, replacing the selection media every 48hrs. At which point cells were taken for flow cytometry to establish if LIF overexpression was causing cells to undergo apoptosis. Cells were stained with propidium iodide (PI) to look at cell cycle. PI is a fluorogenic compound that binds stoichiometrically to nucleic acid (Wallen et al., 1982)(Pollack and Ciancio, 1990)(Ormerod et al., 1992). Fluorescence emission is proportional to the nucleic acid content of a cell. This method was originally used to measure apoptosis in mouse thymocytes (Nicoletti et al., 1991) and has been shown to provide a quick and simple flow cytometry method to measure cell cycle and apoptosis. By measuring cellular DNA content (after removal of RNA) it allows quantification of sub G1/G0 phase (apoptotic cells), G1 phase (haploid), G2 (diploid) and S phase (replicating DNA) cells. It was found that selection of LIF overexpression cells caused an increase in sub G1/G0 phase compared to empty vector control, increasing over the three time points (Figure 4.7 **A,B,C**). This suggests that LIF overexpression causes cell death over a prolonged period of time when exposed to hygromycin and also a decrease in total cycling cells as shown by the decrease in G1 phase and decreased counts of cells in different cell phases (Figure 4.7**D**). Although, it is important to note that due to the presence of selection media, increased cell death may be increased sensitivity to hygromycin. Therefore, a longer overexpression through re-transfection was investigated.

Cells were seeded and transfected as described previously, except 48hrs after transfection, cells were re-seeded and re-transfected for 9 days. After this period of time cells were then either taken for flow cytometry to look at cell cycle or labelled with 1,1'-Dioctadecyl-3,3,3',3'- Tetramethylindocarbocyanine Perchlorate (DiI) to investigate cell proliferation. Cell cycle analysis revealed that LIF overexpression did indeed cause a significant increase in sub G1 / G0 phase. Furthermore, this was accompanied with a significant increase in G1 phase and significant decrease in S and G2 phase compared with empty vector control (Figure 4.8). This suggested that LIF overexpression cells were being held in G1 phase for longer than the empty vector control cells and thus would not complete a cell cycle at the

same rate, suggesting that their proliferation was being impaired. It is important to note the G1 phase difference between LIF overexpression cells that were selected for and LIF overexpression cells that were consistently re-transfected. Selected LIF overexpression cells had a considerably more profound effect on induction of apoptosis and as selection went on, the number of counts with cells at each phase of the cell cycle decreased.

Whereas, consistent transfection of LIF caused an increase in G1 and a significant decrease in other phases, counts in each phase remained comparable to empty vector control. This could account for the difference seen between the two experiments, hence, cells were also stained with DiI (Thermo), a lipophilic membrane stain that diffuses laterally to stain the entire cell. With every cell division fluorescence produced by the stain halves, and so comparative proliferation rates can be observed. After staining, cell were re-seeded at a density of 2.2 x 10^4 cells/cm^2 to ensure cells did not get too confluent as this would prohibit proliferation. 24hrs later cells were re-transfected again and cells were allowed to proliferate for 72 or 96hrs. Samples were then taken for flow cytometery. Figures 4.9**A, B** shows a significant difference in DiI stain between LIF overexpression and empty vector control cells at both time points, with figure 4.9**C** showing LIF overexpression cells to have more DiI stain compared to empty vector control by flow cytometry. It was also found that at 96hrs, LIF overexpression samples had a significantly lower live cell count compared with empty vector control (Figure 4.9 **D, E**).

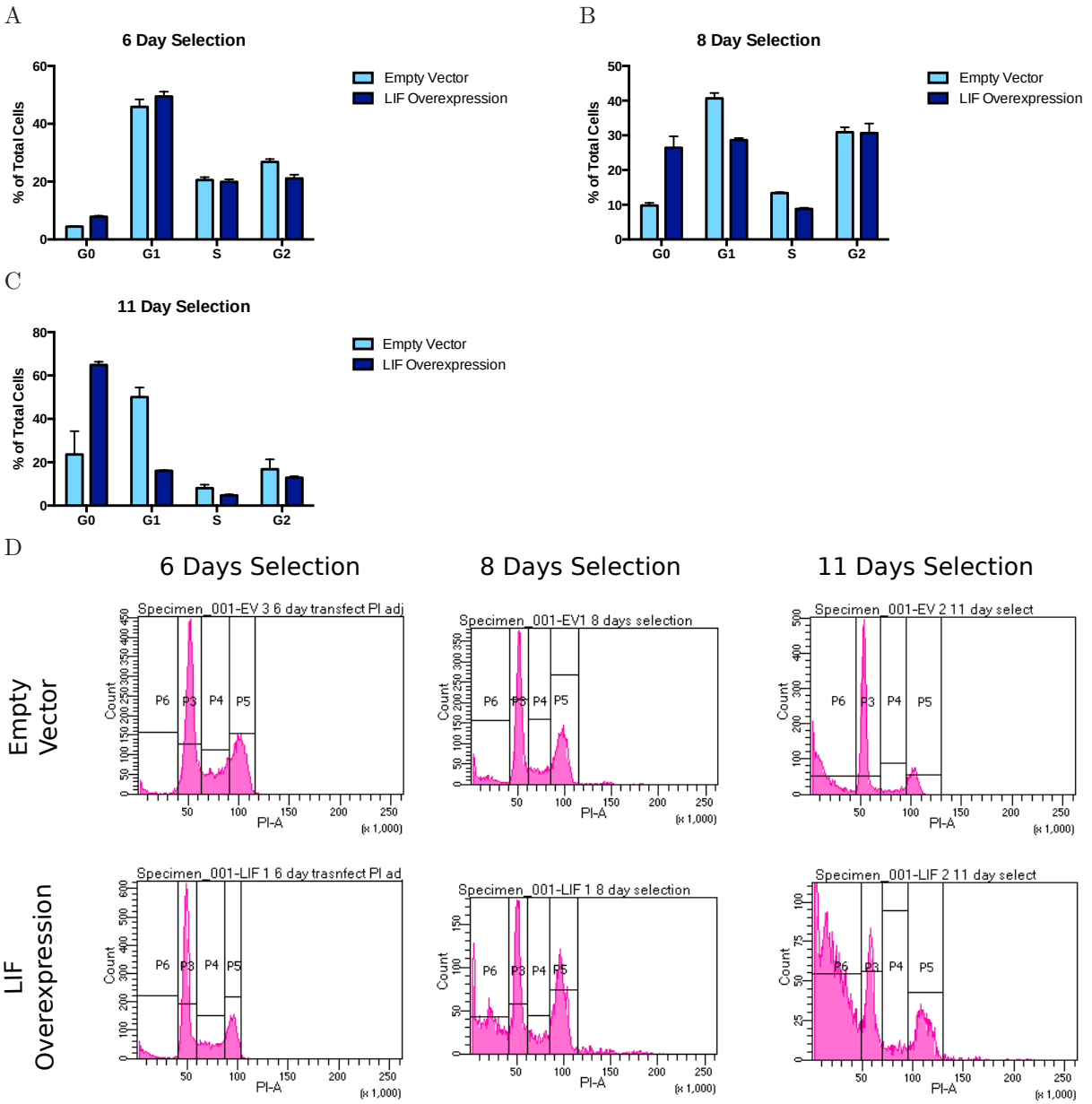
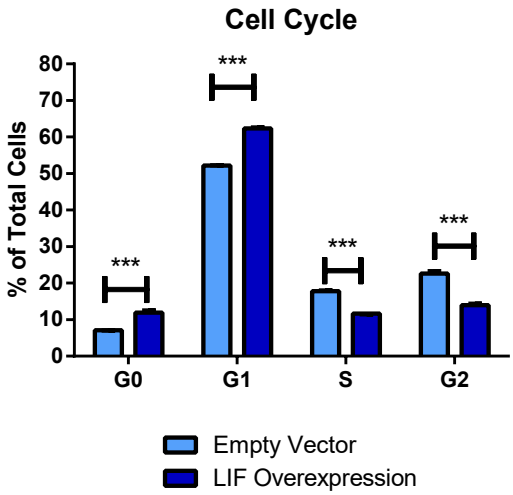
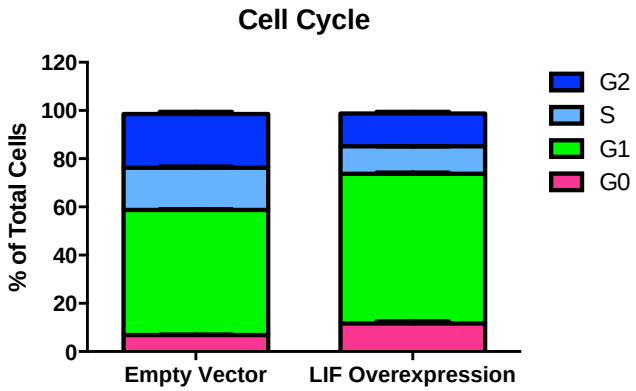


Figure 4.8: **Selection of LIF overexpression prostate cancer cells using hygromycin causes cell death.** PC3 NW1 PCa cells were seeded at 3.3 x 10^4 cells/cm^2 and transfected 24hrs later. They were then left to recover for 48hrs and selected using 200μg/ml for 6,8 or 11 days. Changing selection media every 48hrs. (**A**) Graph showing % of total cells in each phase of the cell cycle after 6 days of selection. (**B**) Graph showing % of total cells in each phase of the cell cycle after 8 days of selection. (**C**) Graph showing % of total cells in each phase of the cell cycle after 11 days of selection. Error bars = Standard Deviation. N=2. (**D**) Cell cycle plots from flow cytometry showing LIF overexpression and empty vector control after 6, 8 and 11 days of selection.

A



B



C

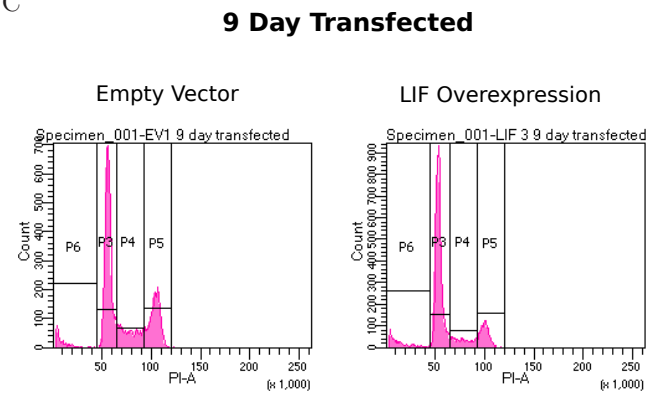


Figure 4.9: **Long term LIF overexpression increases G1 phase of the cell cycle.** Cells were seeded at 3.3 x 10^4 cells/cm^2 and transfected 24hrs later. They were then left to recover for 48hrs, re-seeded at 3.3 x 10^4 cells/cm^2 and transfected again. This process continued until cells were taken for flow cytometry after being transfected for 9 days. (**A**) Graph showing % of total cells in each phase of the cell cycle after 9 days of transfection. (**B**) Graph showing % of total cells in each phase of the cell cycle after 9 days of transfection. (**C**) Representative cell cycle plots from flow cytometry showing LIF overexpression and empty vector control after 9 days transfection. Statistical test used = Two way ANOVA, *** p= < 0.001. Error bars = SEM.

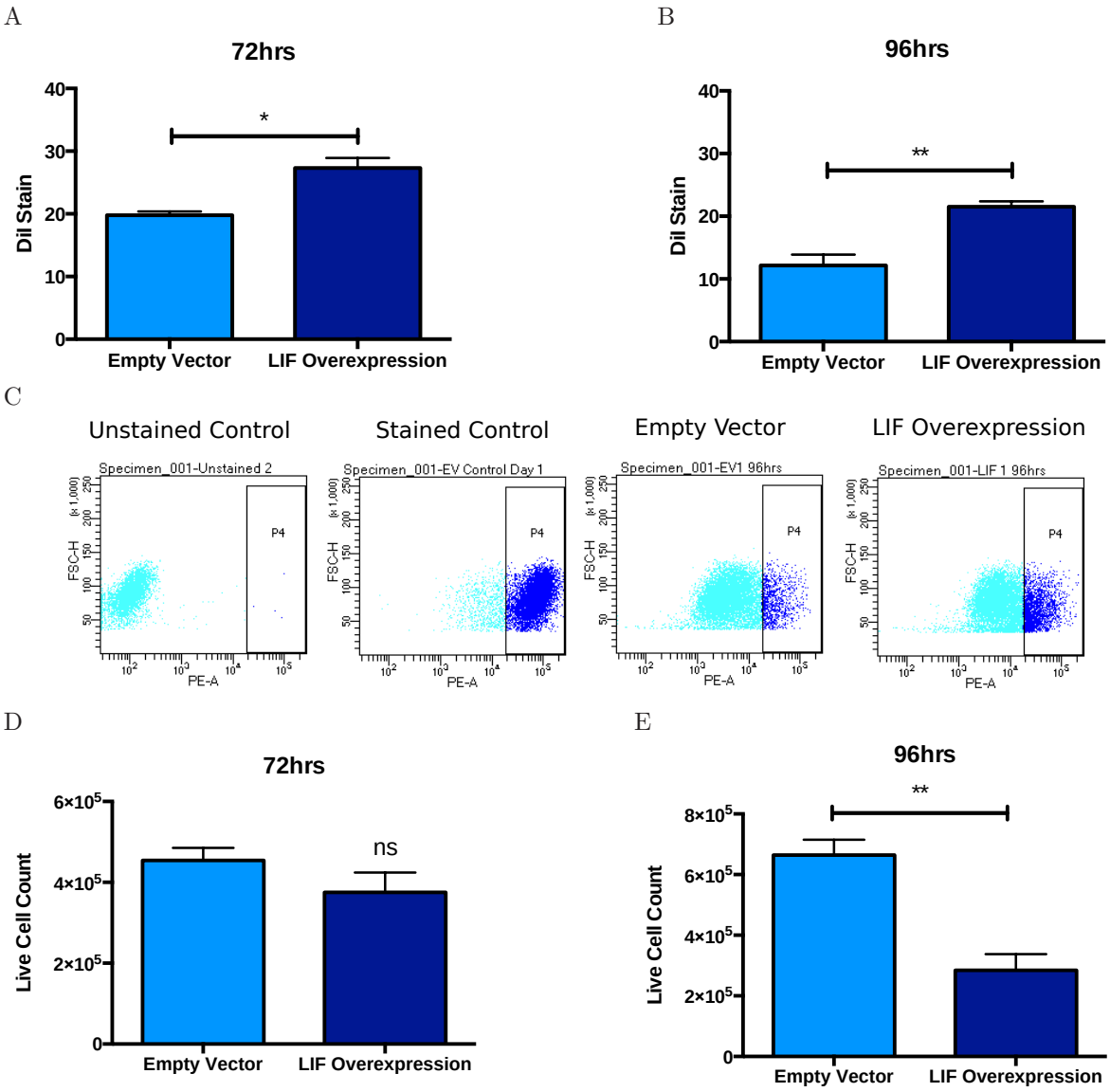


Figure 4.10: **Long term LIF overexpression slows proliferation of prostate cancer cells.** Cells were transiently transfected for 11 days prior to experimental start. Cells were then stained with DiI (thermo) and seeded at 2.2 x 10^4 cells/cm^2. (**A**) 72hrs DiI stained LIF overexpression and empty vector control. (**B**) 96hrs DiI stained LIF overexpression and empty vector control. Statistical test used = student t test, * p <0.05, ** p<0.01. Error bars = SEM. (**C**) Flow cytometry plots showing unstained control cells and positive DiI control cells taken immediately after staining. Representative plot for empty vector and LIF overexpression cells after 96hrs DiI stain. (**D**) Live cell counts as established by trypan blue staining of cells, prior to flow cytometry. 72hrs after DiI stain. (**E**) 96hrs after DiI stain. Statistical test used = Student t test, ** p<0.01. Error bars = standard error mean (SEM).

4.3.2.2 LIF overexpression activates the IFN-γ pathway

As LIF overexpression was observed to have a tumour suppressive effect on PCa cells, it was next investigated what downstream signalling pathways could have a role in this. Methods on how samples were prepared and how the RNA-Seq was run can be found in the material and methods section under 'RNA-Seq'. Figure 4.11 shows a heat map produced from the top 30 differentially expression genes after p value adjustment, with figure 4.12**A** showing a volcano plot depicting a graphical visualisation of high and low expressional changes as a result of LIF overexpression. Figure 4.12**B** shows a little variability of overexpression levels of LIF overexpression samples, however with biological replicates, this is to be expected. As can be seen from the raw fold change table, LIF upregulation is clearly still the highest changed gene between LIF overexpression samples and empty vector control, with an adjusted p value of <0.001 (Appendix, Table 7.1). Pathway analysis using Reactome showed that the most differentially expressed pathway was the IFN type I pathway (Figure 4.13). IFNs are a group of signalling proteins made and released by host cells typically in response to the presence of pathogens, but can also be released in response to tumour cells.

Confirmation of upregulation of STAT1 and STAT2 was acquired via q-RTPCR, showing significant upregulation in response to LIF overexpression ($p>0.01$ and $p>0.001$ respectively) (Figure 4.14**A**,**B**). The RNA-Seq also revealed a downregulation of parathyroid hormone like hormone (PTHLH), which encodes for the parathyroid hormone related protein (PTHrP). PTHrP has been reported to have an important role in the vicious cycle of local bone destruction which characterises osteolytic bone metastasis (Guise, 2002). Taken together with LIFs role in normal bone development, it was assessed whether LIF overexpression PCa cells displayed increased signs of stemness. Using an alkaline phosphatase (ALP) assay the level of ALP enzyme activity was assessed in wild type PC3 NW1 cells, empty vector, LIF overexpression and 2T3 positive control cells. It was found that there was no significant difference between any of the PCa cell types (Figure 4.12**C**) Although, when expression of PTHLH was confirmed via q-RTPCR, the decrease in LIF overexpression cells was found to be not significant (Figure 4.12**D**).

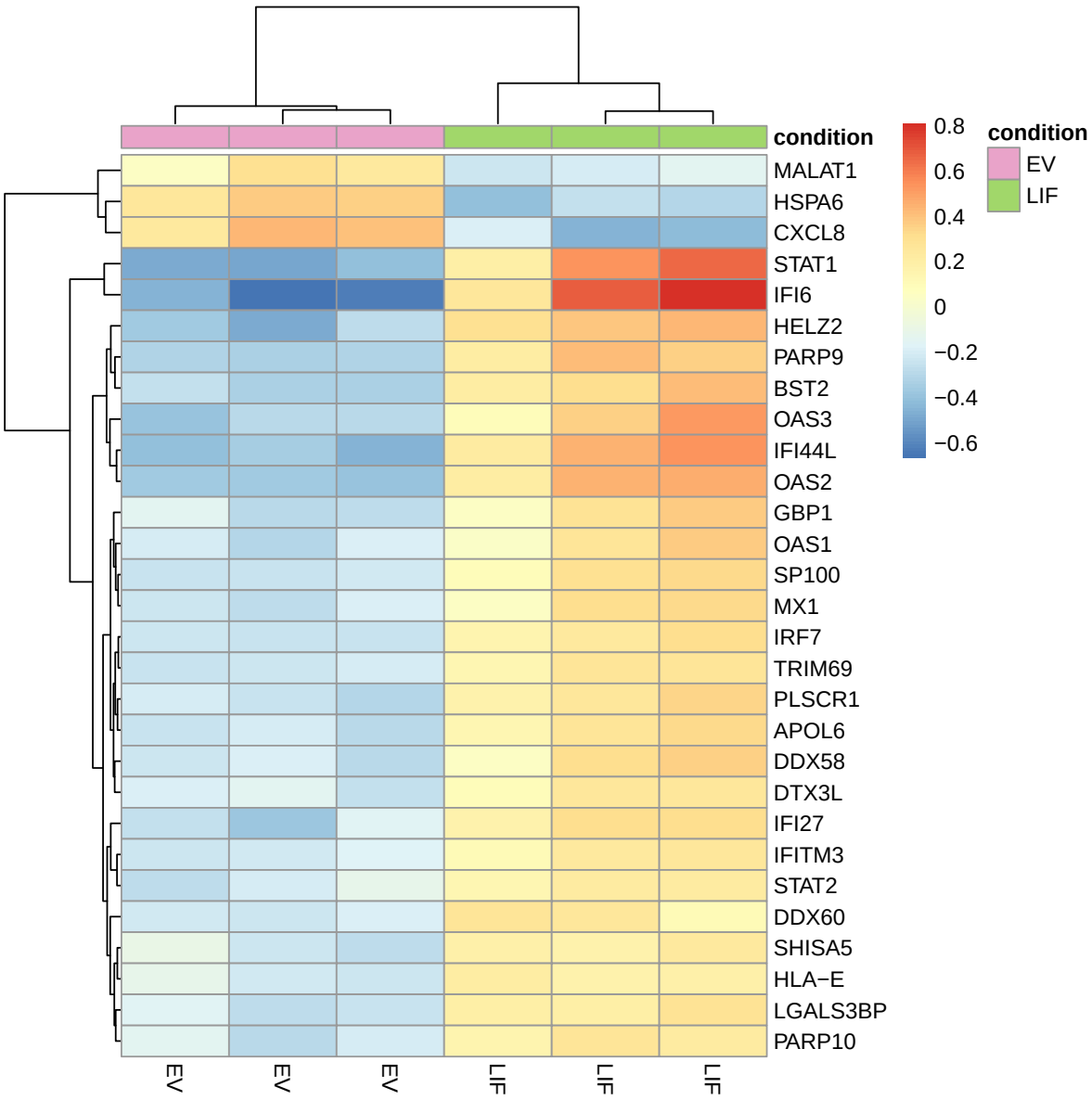
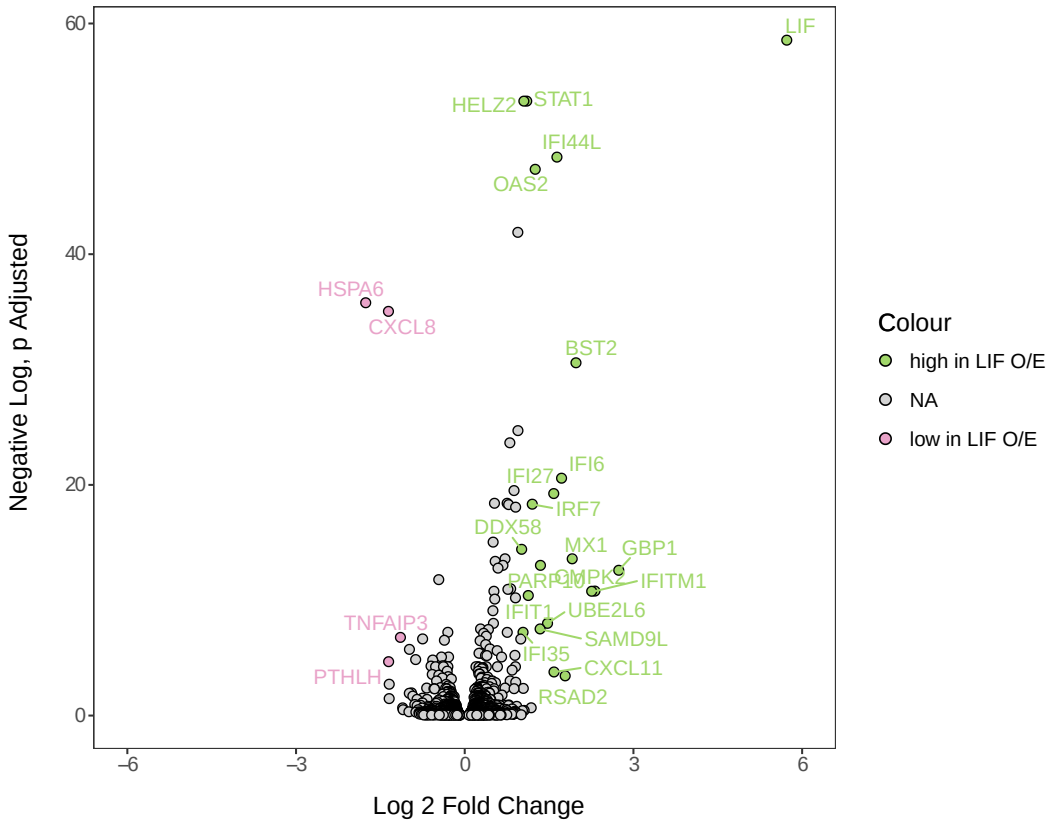


Figure 4.11: **RNA-Seq of LIF overexpression prostate cancer cells (PC3 NW1).** Heatmap showing top 30 differentially expressed genes after p value adjustment. Heatmap produced by S.Rao from data collected by the author of this thesis.

A



B

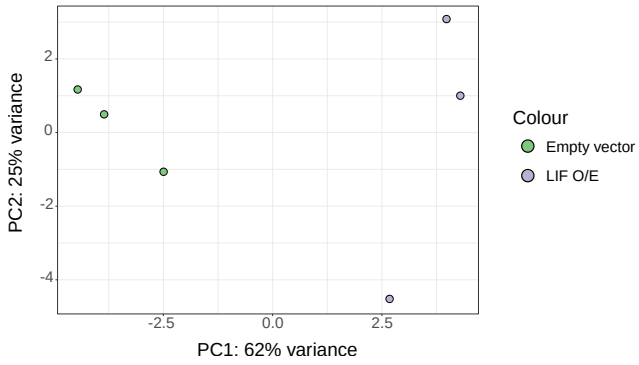


Figure 4.12: **RNA-Seq of LIF overexpression PC3 NW1 cells.** (**A**) Volcano plot, showing high expression of genes in LIF overexpression (O/E) cells (green) and low expression of genes in O/E cells (pink). (**B**) Expression variance between experimental replicates. N=3. Volcano plot produced by S.Rao from data collected by the author of this thesis.

Most significant pathways

The following table shows the 25 most relevant pathways sorted by p-value.

Pathway name	Entities				Reactions	
	found	ratio	p-value	FDR*	found	ratio
Interferon alpha/beta signaling	42 / 184	0.013	1.11e-16	1.37e-14	19 / 20	0.002
Interferon Signaling	53 / 392	0.028	1.11e-16	1.37e-14	53 / 66	0.006
Cytokine Signaling in Immune system	63 / 1,055	0.075	1.11e-16	1.37e-14	115 / 639	0.053
Immune System	75 / 2,663	0.189	1.11e-16	1.37e-14	233 / 1,526	0.127
Interferon gamma signaling	19 / 250	0.018	5.83e-12	5.72e-10	9 / 15	0.001
Antiviral mechanism by IFN-stimulated genes	13 / 94	0.007	1.20e-11	9.86e-10	25 / 31	0.003
Attenuation phase	8 / 47	0.003	2.51e-08	1.76e-06	3 / 5	4.17e-04
HSF1-dependent transactivation	8 / 59	0.004	1.41e-07	8.02e-06	4 / 8	6.68e-04
ISG15 antiviral mechanism	9 / 83	0.006	1.49e-07	8.02e-06	16 / 16	0.001
Regulation of HSF1-mediated heat shock response	10 / 113	0.008	1.91e-07	9.34e-06	7 / 14	0.001
HSF1 activation	7 / 43	0.003	2.59e-07	1.14e-05	1 / 7	5.84e-04
OAS antiviral response	5 / 15	0.001	4.43e-07	1.82e-05	9 / 15	0.001
Cellular response to heat stress	10 / 135	0.01	9.44e-07	3.49e-05	12 / 29	0.002
Negative regulators of DDX58/IFIH1 signaling	5 / 36	0.003	3.00e-05	0.001	11 / 13	0.001
Cellular responses to stress	15 / 514	0.037	1.48e-04	0.005	31 / 184	0.015
Regulation of IFNA signaling	4 / 28	0.002	1.74e-04	0.005	5 / 5	4.17e-04
DDX58/IFIH1-mediated induction of interferon-alpha/beta	6 / 96	0.007	3.74e-04	0.011	39 / 46	0.004
TRAF3-dependent IRF activation pathway	3 / 17	0.001	6.43e-04	0.017	6 / 9	7.51e-04
Cellular responses to external stimuli	15 / 601	0.043	7.57e-04	0.019	31 / 254	0.021
Interleukin-6 family signaling	3 / 30	0.002	0.003	0.077	8 / 33	0.003
Deubiquitination	8 / 288	0.02	0.007	0.159	18 / 77	0.006
NF-kB activation through FADD/RIP-1 pathway mediated by caspase-8 and -10	2 / 13	9.25e-04	0.007	0.159	5 / 5	4.17e-04
TRAF6 mediated IRF7 activation	3 / 43	0.003	0.009	0.173	11 / 11	9.18e-04
Ovarian tumor domain proteases	3 / 43	0.003	0.009	0.173	7 / 14	0.001
Signaling by Interleukins	13 / 640	0.046	0.009	0.179	57 / 491	0.041

* False Discovery Rate https://reactome.org

Figure 4.13: **Pathway analysis of differentially expressed genes in RNA-Seq** Pathway analysis was completed using Reactome, a freely available pathway analysis software.

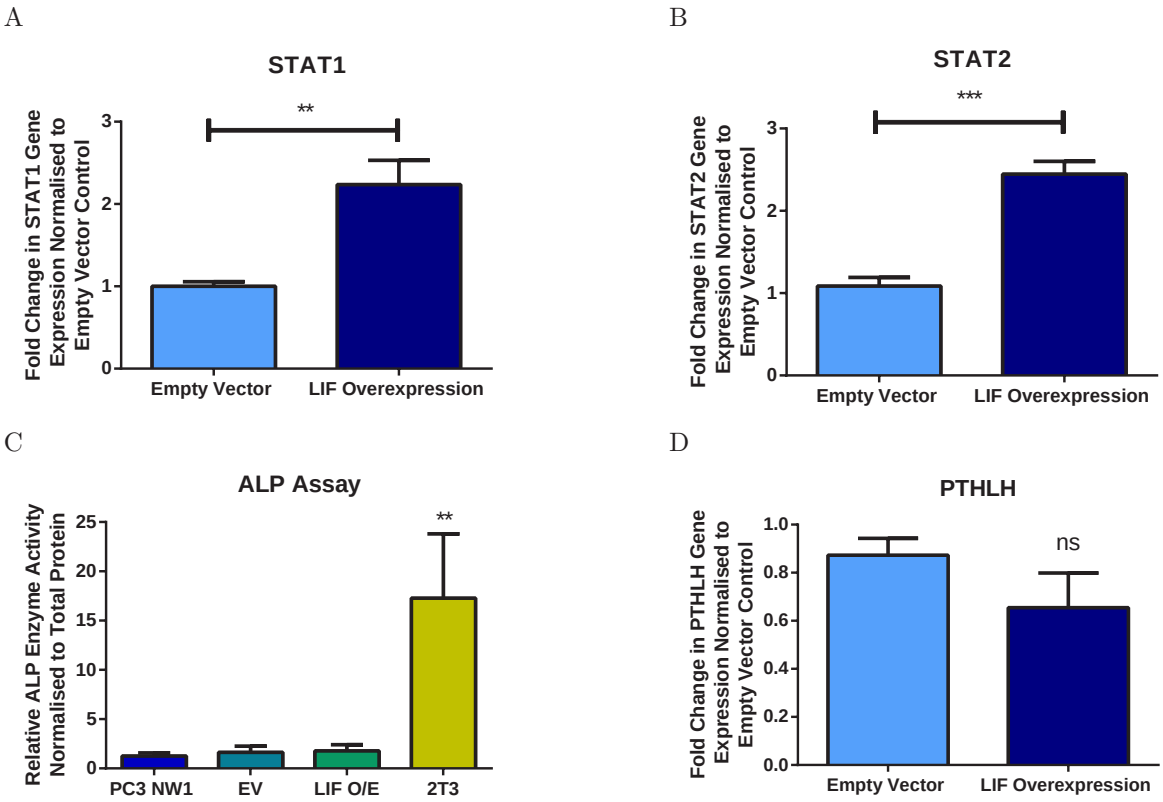


Figure 4.14: **Confirmation of downstream IFN pathway components after LIF overexpression.** (**A**) q-RTPCR confirming STAT1 gene expression is significantly upregulated after LIF overexpression. (**B**) q-RTPCR confirming STAT2 gene expression is significantly upregulated after LIF overexpression. Statistical test used = student t test, ** p=<0.01, *** p= < 0.001. (**C**) ALP assay showing ALP activity in PC3 NW1 control, empty vector (EV), LIF overexpression cell (LIF O/E) or 2T3 positive control cells. Statistical test used = One way ANOVA with Tukey post hoc test, ** p<0.01. (**D**) q-RTPCR showing PTHLH gene expression after LIF overexpression. Statistical test used = Student t test, ns = not significant. Error bars = SEM.

4.3.2.3 Downstream signalling of LIF

The literature reports that LIF exerts its biological functions mainly through the activation and regulation of the JAK/STAT3, EKR1/2 and mTOR signalling pathways (Yu et al., 2014). As such it was investigated whether the same signalling pathways are activated in response to LIF in PCa. PC3 cells were treated with rhLIF at 50ng/ml, 100ng/ml, 200ng/ml, 400ng/ml or 800ng/ml for 30mins. The initial short time point was chosen due to the short 6hr half-life of LIF. It was observed that the downstream target of (pMTOR) (ser2448), p70 S6 kinase (p70 S6K) was upregulated in response to LIF treatment with all concentrations when compared to PC3 untreated control (Figure 4.15**A**). However, this was not seen directly through phosphorylation of mTOR. 100ng/ml was chosen for further analysis due to its ability to activate P70 S6K protein expression at a relatively low dose. The time course for which LIF was treated for was then optimised. Cells were treated with 100ng/ml rhLIF for 15mins, 30mins, 1hr or 2hrs. It was found that 30mins was in fact the optimal time point for looking at downstream signalling proteins in response to LIF (Figure 4.15**B**). LIF treatment was found to have varying effects on p70 S6K expression, showed decreased expression compared to control at 15mins and 2hrs, and activation at 30mins. p44/42 MAPK Erk 1/2 however was only activated at 30mins, this activation was lost at later time points. STAT3 is another signalling pathway described in the literature to be downstream of LIF, although is not present in PC3 cells and so is not shown (Figure 4.15**C**).

Previously in this chapter it was found that LIF overexpression had a significant effect on the cell cycle, with long term transient transfection of LIF increasing G1 phase. p21 has been reported to be involved in maintaining G1 cell cycle arrest when the checkpoint is triggered. Cells exposed to stress can trigger the G1 checkpoint that causes growth arrest until conditions become more favourable (El-Deiry, 2016). As such it was investigated whether LIF treatment would upregulate p21 expression. Cells were treated with 100ng/ml rhLIF for 30mins; it was found that LIF treatment increased p21 protein expression (Figure 4.15**D**).

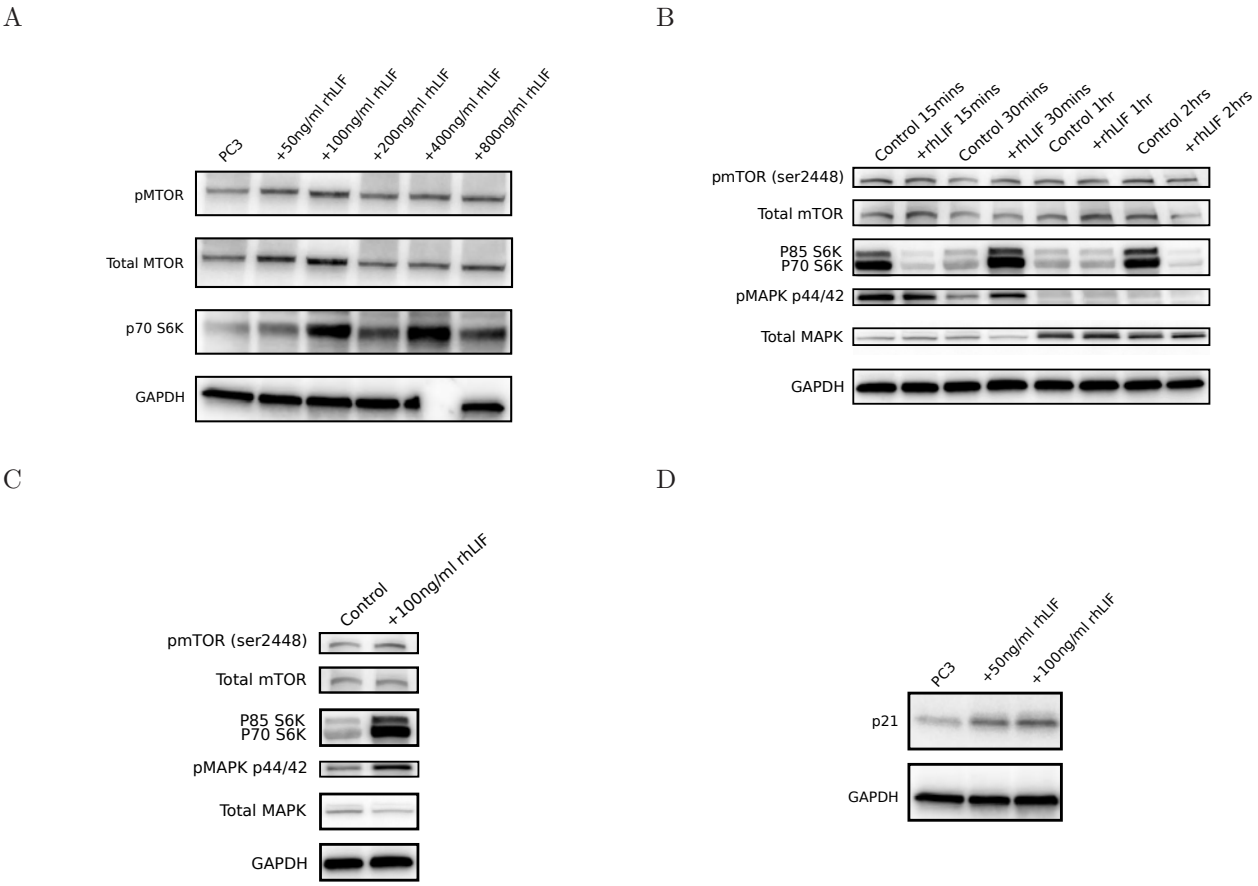
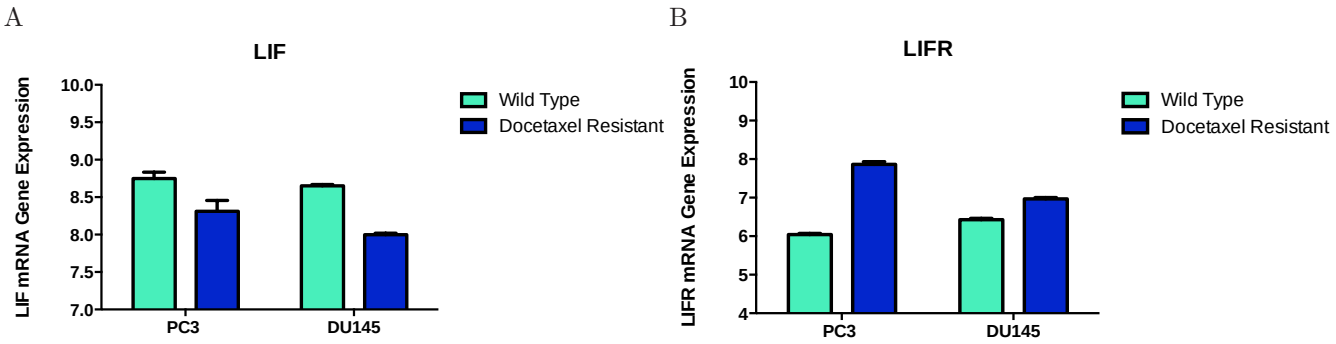


Figure 4.15: **Downstream proteins activated by LIF treatment.** PC3 cells were seeded at a density of 2.2 x 10^4 cells/cm^2 and grown for 48hrs, at which point cells were treated with recombinant human LIF(rhLIF) at varying concentrations for varying time points. (**A**) Western blot showing optimisation of rhLIF concentration. PC3 cells treated with 50ng/ml, 100ng/ml, 200ng/ml, 400ng/ml or 800ng/ml rhLIF for 30mins. (**B**) Western blot showing optimisation of treatment time. PC3 cells treated with 100ng/ml rhLIF for 15mins, 30mins, 1hr or 2hrs. (**C**) Western blot showing downstream activated proteins after 100ng/ml rhLIF treatment for 30mins. (**D**) Western blot showing p21 activation after rhLIF for 30mins.

4.3.3 LIF overexpression increases chemotherapy sensitivity

It has been shown in other solid tumour types; such as breast cancer that IFN-related DNA damage resistance signature (IRDS) is associated with resistance to chemotherapy and/or radiation across different cancer cell lines. In particular STAT1 has been recognised to mediate experimental resistance (Weichselbaum et al., 2008). Previously in this chapter it was observed that LIF overexpression in PCa cells caused downstream upregulation of STAT1. Furthermore, it was also shown that prolonged LIF overexpression in PCa cells could slow the cell cycle. Chemotherapy, such as Docetaxel, is more effective on more highly proliferative cells such as tumour cells and although this toxic treatment is not specifically targeted against cancer cells it tends to kill more tumour cells than healthy tissue due to the quick cancer turnover. If LIF overexpression cells are proliferating slower then this could also potentially cause resistance to chemotherapeutics.

In silico analysis was used on a dataset by Aguilera *et al*, who converted DU145 and PC3 cells into Docetaxel resistant subtypes. Whole genome arrays were then used to compare global gene expression between these cell lines and their wild type counterparts. It was found that LIF gene expression was significantly decreased in PC3 and DU145 Docetaxel resistant cells compared to control, $p<0.05$ and $p<0.001$ respectively. LIFR however, was significantly upregulated in both PC3 ($p<0.001$) and DU145 ($p<0.001$) compared to control (Figure 4.16). This suggests that LIF maybe lost in chemoresistance and may in fact render LIF overexpression cells sensitive to Docetaxel treatment. This was investigated by using long-term overexpression of LIF in PC3 NW1 cells. Cells were grown and re-transfected for 9 days, at which point cells were reseeded into 96 well plates and treated with 0.25nm, 0.5nm, 1nm, 2nm, 4nm, 8nm and 16nm of Docetaxel for 24, 48 or 72hrs. Interestingly it was found that LIF overexpression cells were more sensitive to Docetaxel treatment at all three time points. At 24hrs LIF overexpression shows a significant decrease in % viability at 16nm of Docetaxel ($p<0.05$). Whereas, at 48 and 72hrs LIF overexpression shows a significant decrease in % viability at 4nm, 8nm and 16nm ($p<0.01$, $p<0.001$, $p<0.001$) (Figure 4.17). This suggests that although LIF may slow the cell cycle, it still renders cancer cells sensitive to drug treatment.



Cell Line	Gene	Log FC	p value	Adjusted p value
PC3	LIF	-0.4393448	0.003883421	0.01473565
PC3	LIFR	1.8226423	0.000000000065	0.000000007
DU145	LIF	-0.65227509	0.000004	0.00007
DU145	LIFR	0.53905176	0.00004	0.0003

Figure 4.16: **LIF gene expression is decreased in chemotherapy resistant prostate cancer cells.** (**A**) LIF mRNA gene expression from PC3 and DU145, wild type and Docetaxel resistant cells. Data from Aguilera *et al* was re-analysed in R for differential gene expression. PC3, p=<0.01, adjusted p=0.05. DU145, p=<0.001, adjusted p=<0.001. (**B**) LIFR mRNA gene expression from PC3 and DU145, wild type and Docetaxel resistant cells. Error bars = SEM.

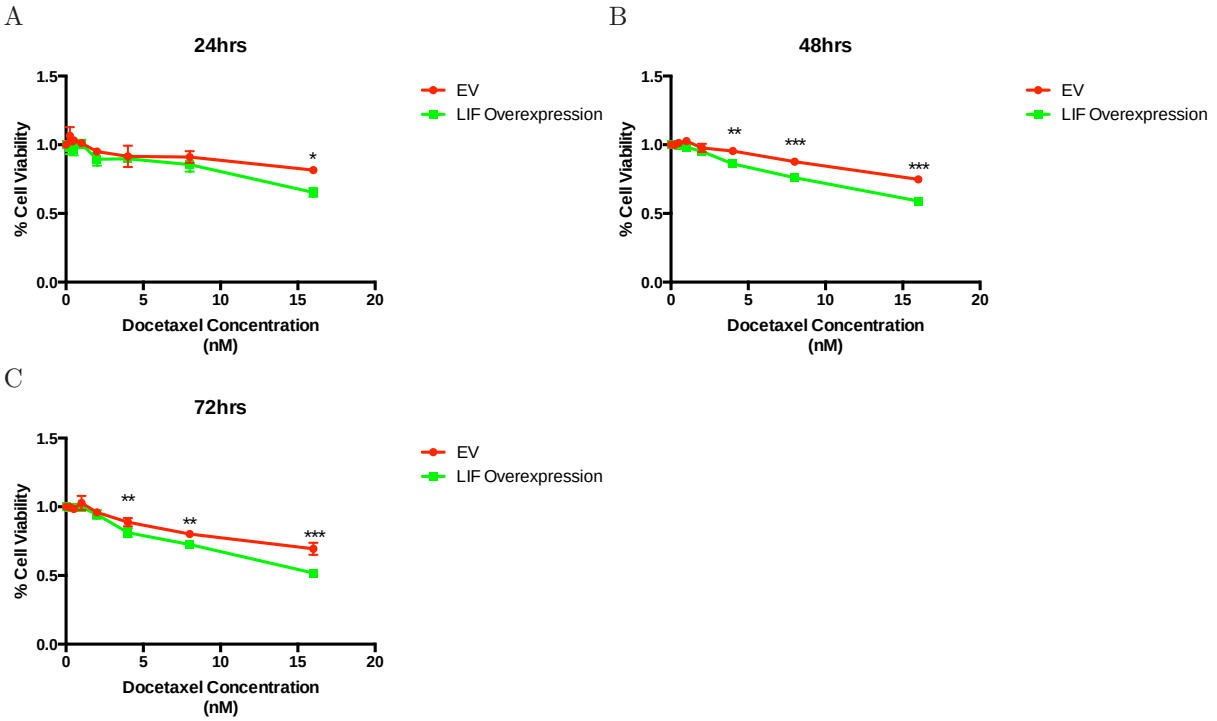


Figure 4.17: **LIF overexpression increases sensitivity to Docetaxel.** Cells were transiently transfected with LIF overexpression construct or empty vector control for 24hrs. Cells were reseeded and treated with increasing doses of Docetaxel for 24, 48 and 72hrs. (**A**) % viability of cells after 24hrs treatment with Docetaxel. (**B**) % viability of cells after 48hrs treatment with Docetaxel. (**C**) % viability of cells after 48hrs treatment with Docetaxel. Error bars = SEM. Statistical test used for all graphs = Two way ANOVA with Sidak's multiple comparisons post hoc test. * p = <0.05, ** p<0.01, *** p<0.001.

4.4 Discussion

The analyses carried out in this chapter provide evidence that LIF may act as a tumour suppressor in PCa cells. LIF overexpression was found to activate the IFN pathway, which has been previously shown to mediate growth inhibition and control apoptosis. Moreover, long term LIF overexpression was shown to significantly induce apoptosis and increase G1 phase of the cell cycle. Thus, to elucidate how LIF may be involved in disease, a LIF shRNA construct was made and validated in PC3 NW1 PCa cells. Surprisingly LIF KD had no effect on cell viability or growth, but had a significant positive effect on migration and invasion, despite LIF signalling being linked with cellular pathways involved in differentiation, cell survival and self-renewal. This links with *in silico* analysis of patient cohorts shown in the previous chapter in which decreased expression of LIF was associated with metastatic disease. Moreover, results from the PCa *in vivo* models also presented in the previous chapter, showed PC3 NW1, which possess a lower baseline gene expression of LIF, caused increased bone metastasis compared to wild type PC3s. Both patient and *in vivo* data support the finding that LIF KD increased migration and invasion *in vitro*. Treatment of breast cancer cells with LIF however, has been shown to increase migration and invasion ability of tumour cells (Li et al., 2014). Furthermore, overexpression of LIF was found to promote the proliferation of cultured human breast cancer cells and increase the growth of xenograft tumours formed by many human tumour cells.

These effects were hypothesised to be controlled by the mTOR pathway, which is frequently activated in breast cancer. Activation of mTOR and its downstream targets p70 S6K and eukaryotic translation initiation factor 4E (eIF4E) binding protein play important roles in promoting cell growth, proliferation and metastasis. By blocking mTOR signalling Li *et al* largely abolished the promoting effect of LIF on invasion and migration of breast cancer cells (Li et al., 2014). However, I found that LIF treatment also activated the downstream mTOR effector, p70 S6K, but still found that KD of LIF increased migration and invasion, suggesting that there may be another mechanism in PCa. As discussed in the previous chapter, LIF maybe linked with a loss of invasiveness through

the Hippo/YAP pathway. I found that LIF expression was linked with cell density, Sharif *et al* reported that in PC3 cells invasiveness was lost upon high density growth, with no effect on proliferation or apoptosis. Cells were seeded at a density that ensured a confluent starting point before migration. If LIF is upregulated as a result of confluency then it stands to reason that LIF maybe upregulated before migration and invasion even begins, thus inhibiting their movement. Whereas, in LIF KD cells they are able to migrate and invade more freely.

In this chapter it was shown that LIF overexpression caused subsequent activation of the IFN pathway via RNA-seq. IFNs can inhibit cell growth and control apoptosis, activities which have been shown to suppress cancer as well as infection (Stark et al., 1998). STAT1 which was also found to be significantly upregulated in response to LIF overexpression has previously been shown to be important in mediating the growth inhibitory effects of IFNα or IFNγ (Bromberg et al., 1996). Depending upon the stimuli or cell type, STAT1 can modulate a vast spectrum of cell death, comprising of both apoptotic and non-apoptotic pathways (Kim and Lee, 2007). CDK inhibitors p21 and p27 can be induced in an IFN/STAT1 dependent manner in different cell types. Furthermore, STAT1 also induces the transcription of Bcl-2 family members, which respond to cellular stress and act to preserve mitochondrial integrity. Furthermore, evidence also suggests that IFNγ can induce non-apoptotic cell death through the induction of the autophagosome. In human hepatocellular carcinoma cell lines and in primary hepatic carcinoma cells, IFNγ was shown to induce autophagosome formation, with its inhibition reducing IFNγ-induced cell death. Thus, upregulation of the IFN pathway and consequently STAT1 can indicate cell death in a number of ways.

This chapter has shown that long term overexpression of LIF via transient transfection is able to slow the cell cycle by causing cells to arrest in G1 phase and increase the number of cells in the sub G1/G0 phase of the cell cycle, accordant with increased apoptosis. However, when LIF overexpression cells were selected using hygromycin, this produced a different cell cycle profile. While it did indeed produce large amounts of cells in sub G1/G0 phase, overtime it also decreased the number of cells cycling through the cell cycle as shown by the reduction of percentage of cells in each phase and the total cell count. One possible

explanation for this is that the pcDNA construct used to produce LIF overexpression may have poor transfection efficiency. If the construct is only transfecting a small amount of cells, albeit to produce large amounts of LIF expression, then during selection the vast majority of cells will be susceptible to hygromycin treatment. Hygromycin inhibits protein translation by inhibiting translocation of mRNA and tRNAs on the ribosome, thus causing a potent effect in cells without resistance (Borovinskaya et al., 2008). Any drop in transfection efficiency must be caused by the introduction of LIF into the construct, as empty vector control cells appear to have a high tolerance to selection. In future, it would be beneficial to try an adenovirus or lentiviral system to see if transfection efficiency could be increased and hopefully produce the same phenotype as was produced when using long term transient overexpression. Furthermore, if stable cell lines were able to be produced, due to the inhibitory nature of LIF on the cell cycle, it would be advantageous to create an inducible construct that could be used *in vivo* to investigate the effect of LIF overexpression at each stage of tumour growth and development.

It is important to note that sub G1 signals may not always reflect individual apoptotic cells. Necrotic cells sometimes exhibit some degree of DNA degradation, which may result in hypodiploid nuceli. Moreover, the sub G1/G0 peak can also represent nuclear fragments, clumps of chromosomes, micronuclei or nuclei with normal DNA content, but with different chromatin structure and depleted accessibility of fluorochrome to DNA (i.e. cells undergoing differentiation). Thus, the presence of a sub G1/G0 peak does not confirm the presence of apoptotic cells (Darzynkiewicz et al., 2001). To further confirm that apoptosis is occurring in response to LIF overexpression, one could examine the morphology of apoptotic bodies (Wyllie et al., 1984), biochemically, through DNA fragmentation on a agarose gel (Sellins and Cohen, 1987) or terminal deoxynucleotidyl transferase assay to specifically demonstrate DNA breaks (Gavrieli et al., 1992). However, the effect seen on G1 phase taken together with the increased p21 expression in response to LIF treatment (Figure 4.13) and the function of STAT1 as a cell growth inhibitor, suggests that STAT1 maybe involved in this tumour suppressing function.

In general, STAT1 is considered a tumour suppressor, although there is increasing evidence for tumour-promoting functions of STAT1. Radiotherapy and chemotherapy

are effective treatment methods for many types of cancer, but resistance is a common occurrence. Recent findings indicate that IFN signalling can be induced in response to cancer therapies (Weichselbaum et al., 2008). Weichselbaum *et al* report that expression of IFN-stimulated genes creates an IFN-related DNA damage resistance signature (IRDS), which correlates with resistance to radiotherapy and chemotherapy across different tumour types such as; breast cancer, head and neck cancer, prostate cancer, lung cancer, glioma, myeloma (Weichselbaum et al., 2008). Cheon *et al* described how a high dose of IFNβ can activate cellular responses so that anti-viral, pro-apoptotic and anti-proliferative proteins are highly expressed. Negative feedback mechanisms are extremely important to terminate the expression of these genes after IFN stimulation. Sustained expression of many initial proteins is harmful to cell survival. In 2009, Cheon *et al* discovered increased expression of proteins encoded by genes that were sustained for days after IFN stimulation, thus providing a selective advantage to the cells that can tolerate them (Cheon and Stark, 2009). IFNβ signalling induces the phosphorylation of STAT1 and 2 in combination with IFN response factor 9 (IRF9), which together form a tripartite transcription factor, IFN-stimulate gene factor 3 (ISGF3), which in turn can drive the expression of $>$ 100 IFNβ stimulated genes. In 2013, Cheon *et al* showed that prolonged exposure of cells to constant low levels of IFNβ, that is often seen in cancer, led to increased expression of ISGF3 dependent proteins and constitutive resistance to DNA damage (Cheon et al., 2013). I have described results in this chapter that show significant upregulation of the IFN pathway and specific effectors STAT1 and 2 leading to pro-apoptotic and anti-proliferative effects in PCa cells, much the same as described by Cheon *et al*.

After dissemination from a primary tumour to metastatic site, cancer cells can resume growth immediately or enter a state of dormancy. In tumours that are progressively growing, activation of the ERK pathway allows for G0/G1/S phase transition and cell division. Despite that ERK is primarily involved in the induction of proliferation and also differentiation in some case, high levels of p38 is thought to be a negative growth regulator that may actually supress cell proliferation by inhibiting ERK and inducing G1 arrest and apoptosis (Chen et al., 2000) (Aguirre-Ghiso et al., 2001) (Takenaka et al., 1998). Aguirre-Ghiso *et al* showed that in human head and neck carcinoma, ERK MAPK/p38 stress

activated protein kinase (SAPK) activity ratio predicted whether cells would proliferate or enter a state of dormancy *in vivo*, with a high ERK/p38 ratio favouring tumour growth and a high p38/ERK ratio inducing tumour growth arrest (dormancy) (Aguirre-Ghiso et al., 2003). As I found that MAPK ERK 1/2 protein was increased in response to rhLIF treatment in PCa cells, it would be interesting to investigate the ratio of this to p38 protein expression. Increased p38 expression in relation to ERK expression may explain one mechanism by which LIF is able to produce G1 cell cycle arrest, giving rise to a 'dormant' phenotype.

In this chapter I have demonstrated that long term transient transfection of LIF caused cell cycle arrest in G1 phase. The typical regulation of the G1/S phase transition of the cell cycle is shown in figure 4.16. Treatment with rhLIF on PCa cells resulted in increased p21 protein expression. p21 can inhibit the phosphorylation of the CDK2/cyclin E1 complex, which prevents degradation of cyclin E1. Thus, to further investigate the effect of LIF on G1, expression of cyclin E1 protein expression could be observed in response to rhLIF treatment (Figure 4.16).

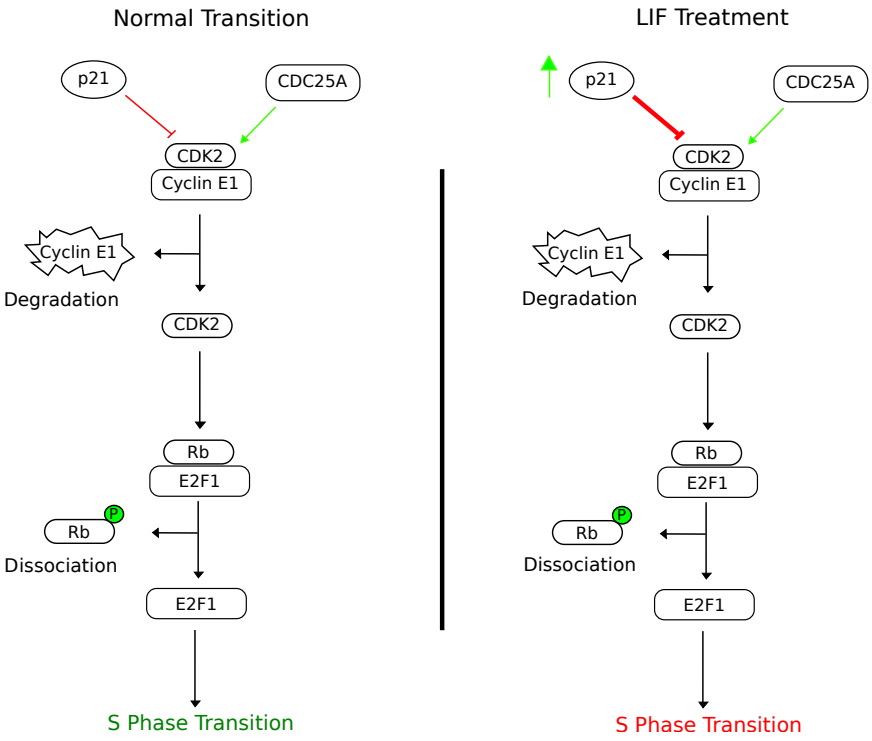


Figure 4.18: **Regulation of G1/S phase transition.** rhLIF treatment causes upregulation of p21 protein, which inhibits the phosphorylation of the CDK2/cyclin E1 complex by CDC25A. This in turn blocks, cyclin E1 from degrading, which prevents CDK2 from phosphorylating the Rb/E2F1 complex. Thus, stopping Rb dissociation and subsequence S phase transition.

p21 was initially considered to be a tumour suppressor, based on its ability to block proliferation of cells. However, it is now considered to have dual functions in cancer with a dark side that can promote disease. Morris-Hanon *et al* studied the functions of both p21 and p27 in five patient-derived glioma stem cell-enriched cell lines. They found that not only was p21 and p27 functional in glioma stem cells, but that they also negatively regulated cell cycle progression in both unstressed conditions and in response to chemotherapeutics. The lack of these proteins can impair the cell cycle, rendering cells more vulnerable to DNA damage as was shown by siRNA silencing of these proteins and subsequent genotoxic stress showing improved sensitisation (Morris-Hanon et al., 2017). As such these proteins can be seen to convey resistance to DNA damage in this cancer type and so in this chapter I also sought to investigate the effect of LIF on chemotherapy resistance. Interestingly I found using *in silico* analysis that LIF expression decreased in a dataset of Docetaxel resistant PCa cells. Furthermore, long term overexpression of

LIF in PCa with subsequent treatment with Docetaxel, rendered LIF overexpression cells more sensitive. This is however, a relatively short time course of Docetaxel treatment and so it is unknown whether prolonged exposure to Docetaxel would continue to render LIF overexpression cells more sensitive. Obviously in patients initial chemotherapy treatment often produces favourable results to begin with but it is prolonged exposure to a therapy that causes resistance. As such there is a future piece of work that could be done to tease apart the prognostic features of LIF expression and the innate immune response signatures within clinical datasets.

Moreover, as long term overexpression of LIF has been shown to cause cell death in PCa cells, it would be interesting to use rhLIF as a treatment in an *in vivo* setting. Firstly, to further investigate the role of LIF in the mechanism of PCa homing to the bone. An experiment injecting 5mg/kg rhLIF for 1 week prior and 2 week post inoculation of PC3 NW1 cells. Secondly, to evaluate LIF's role in tumour development *in situ*, rhLIF, would be injected 2 weeks before experimental end point, with long bones being taken for FACS analysis.

The experiments performed in this chapter, have shown that LIF is involved in PCa migration and invasion, and cell cycle. Furthermore, whole transcriptome analysis of LIF's effects in PCa shows 93 differentially regulated genes. Interestingly these outcomes may be different in different cancer types. The next chapter of this thesis investigates the effect of LIF in the bone microenvironment.

5

The effect of LIF in the bone microenvironment

5.1 Introduction

The role of the tumour microenvironment in cancer development and progression is widely recognised as an important area of research. Progressive PCa has a specific propensity to metastasise to bone and thus the bone microenvironment has become an important research focus. As LIF has a direct effect on bone remodelling under normal physiological conditions, this chapter will explore if LIF has any effect on the tumour-bone microenvironment.

5.1.1 RANKL

Unlike other solid tumours such as breast and lung, which produce osteolytic bone lesions, PCa bone metastasis is typically osteoblastic with mixed osteolytic lesions as well. Bone lesions occur through the remodelling of the bone matrix by osteoblasts and osteoclasts. The RANKL pathway is one of many that is abused by PCa. RANKL is normally expressed by osteoblasts and other stromal cells to regulate osteoclastic activity. It binds to RANK receptors on preosteoclasts in order to stimulated them into mature osteoclasts (Sturge et al., 2011). In PCa RANKL is frequently overexpressed either by the tumour itself or indirectly through osteoblasts. This causes a feedback loop that increases the rate of bone turnover which can be seen in the form of mixed bone lesions in PCa (Josson et al., 2010).

Furthermore, PCa cells may also respond to growth factors secreted by osteoblasts or growth factors released from the bone matrix upon bone resorption. Lang *et al* demonstrated the growth-promoting effect on PCa epithelial cells after treatment with conditioned medium from cultured osteoblasts (Lang et al., 1995). Thus, as cancer cells are constantly interacting and acquiring survival advantages from their microenvironment, it is critical to investigate these interactions to improve treatment and overall survival of patients. LIF has been shown to induce the osteoblastic production of RANKL (Palmqvist et al., 2002) (O'Brien et al., 1999). Metcalf and Gearing showed LIFs *in vivo* effects in the form of an increase in the number of osteoblasts, with an excess in new bone formation, accompanied with increased bone resorption and signs of weight loss, in the form of subcutaneous and abdominal fat loss (Metcalf and Gearing, 1989). Human MSCs are multipotent cells present in adult marrow, these can replicate as undifferentiated cells and have the potential to differentiate into bone, cartilage, fat, tendon, muscle and marrow stroma (Pittenger et al., 1999). LIF has been shown to be expressed by MSCs and thus in this chapter I will investigate the effect of LIF on cells of the bone microenvironment (Chapman et al., 2006).

5.1.2 Adipocyte markers

Adiponectin is an adipocyte-derived hormone that plays a role in the function of insulin and energy homeostasis (Saltiel, 2001). Serum levels of adiponectin are normally decreased in humans or animals that are obese or are insulin resistant (Arita et al., 1999). *In vivo*, it has been shown to improve fatty acid utilisation in the liver and skeletal muscle of mice and produces weight loss without affecting food intake (Fruebis et al., 2001). Whereas, leptin, another hormone produced by adipocytes, displays effects on energy homeostasis by suppressing food intake and stimulating energy expenditure (Scarpace et al., 2002). It is mainly produced in white adipose tissue, with circulating levels of leptin correlated with adiposity (Ahima and Flier, 2000). As adiponectin and leptin are well established indicators of adipocytes, these will be used to establish effects on adipocytes in this chapter.

5.1.3 Muscle markers

Differentiation of skeletal muscle tissue involves the initial determination of mesoderm cells towards the myogenic lineage, followed by proliferation and then irreversible withdrawal from the cell cycle. Associated with this is the expression of muscle-specific genes, culminating in the formation of differentiated multinucleated myotubes. Myogenin is a muscle family regulatory factor involved in the co-ordination of skeletal muscle development or myogenesis and repair (Tapscott and Weintraub, 1991). Whereas, myostatin is a negative regulator of differentiation into myotubes (Langley et al., 2002). Thus, myogenin and myostatin will be used in this chapter as markers of muscle.

5.2 Aims

The aims of work described in this chapter are:

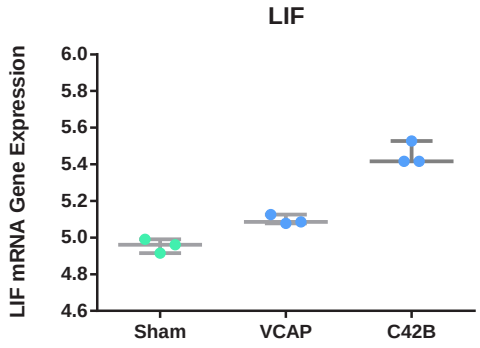
- To investigate the effect of LIF in the PCa/bone microenvironment using *in silico* analysis and *in vitro* co-culture systems.
- To determine if LIF expression and/or treatment alters the bone microenvironment.

5.3 Results

5.3.1 LIF is significantly upregulated in stromal cell co-culture with prostate cancer cells

To begin to investigate the importance of LIF in the tumour-bone microenvironment, I used *in silico* analysis of data from Ozdemir *et al* 2014 (Ozdemir et al., 2014). They used intra-osseous xenografts of C42B or VCAP PCa cells injected into the bone marrow cavity of the left tibia of male CB17 SCID mice. Sham-operated animals were used as controls. VCAP xenograft mice were sacrificed after 6 weeks and C42B after 8 weeks, with sham controls also being sacrificed at the same time points. They found that LIF was significantly upregulated in the bone marrow microenvironment in both C42B (p=<0.01) and VCAP (p=<0.001) xenografts compared to sham animals (Figure 5.1). Interestingly, despite a difference in baseline LIF expression between (low) C42B and (high) VCAP cells, that I found in chapter 3 of this thesis, both cell lines induced an upregulation in LIF in the study by Ozedemir *et al*, suggesting LIF expression in the PCa cells may not be important in regard to LIF upregulation in the microenvironment.

A



B

Sham vs Cell line injected	Log FC	p Value	Adjusted p Value
VCAP	0.9788	0.0003	0.0009
C42B	1.0759	0.0006	0.0017

Figure 5.1: **LIF is significantly upregulated in the stroma after prostate cancer xenograft.** *In silico* analysis of data from Ozdemir *et al* 2014, showing LIF gene expression in *in vivo* samples extracted from the stroma in xenograft models using osteoinductive prostate cancer cells (VCAP and C42B) (**A**) Graph showing raw LIF gene expression. (**B**) Table showing differential LIF gene expression analysis normalised to sham injected. Error bars=SEM.

To investigate this further pre-osteoblastic 2T3 were co-cultured directly with PC3 PCa cells for a period of 48hrs. Using species specific TaqMan probes it was established that there was a significant upregulation in LIF gene expression of the 2T3 stromal cells, but not in the PC3 cancer cells (Figure 5.2**A,B**). This was accompanied by a significant upregulation of RANKL and downregulation of OPG, the ratio of which is an important determinate of bone mass and skeletal integrity (Boyce and Xing, 2007) (Figure 5.2**C,D**). To further confirm that this was not limited to one stromal cell line or a result of direct co-culture, LIF upregulation was then investigated using Boyden chamber transwells. Figure 5.2**E** shows transwell co-culture of PC3 with human HS-5 and HS27a stromal cells after 48hrs. LIF was significantly upregulated in HS-5 cells ($p < 0.05$) and in HS27a cells ($p < 0.01$) after co-culture with PC3 PCa cells. PCa cells however, were found to have no significant upregulation. To ensure that this was not limited to PC3 cells, another bone metastatic PCa cell line, ARCAP-M cells, was used in transwell co-cultures with HS-5 and HS27a cells. Once again LIF gene expression was significantly upregulated in HS-5 ($p<0.01$) and HS27a ($p<0.001$) cells after co-culture with ARCAP-M cells showing no significant upregulation after co-culture (Figure 5.2**F**).

As LIF upregulation was seen specifically in the stromal cells after both direct and transwell co-culture, it was then investigated if LIF downstream signalling pathways were activated in response to co-culture. It was found that in the 2T3 stromal cells co-cultured with PC3 cells there was an upregulation of downstream mTOR effector p70 S6K and p44/42 pMAPK (ERK1/2), two pathways that are typically upregulated by LIF signalling. In the PC3 cancer cells, there was an upregulation in pmTOR (ser 2448) signalling and p70 S6K, but not the MAPK pathway (Figure 5.3).

As *in silico* analysis showed that LIF was significantly upregulated in the bone microenvironment after PCa inoculation, regardless of their baseline LIF expression, it was next investigated whether the LIF upregulation, along with RANKL and downregulation of OPG, was LIF independent. To investigate this, PC3 NW1 empty vector and LIF overexpression cells were used in direct co-culture with 2T3 cells. Since PC3 NW1 have a lower basal LIF expression than wild type PC3 cells, it was first necessary to confirm that direct co-culture with PC3 NW1 could also induce upregulation of RANKL (Figure

5.4**A**), downregulation of OPG (Figure 5.4**B**) and upregulation of LIF (Figure 5.4**C**). However, when co-cultured with empty vector or LIF overexpression cells, LIF was found to be decreased in LIF overexpression cell co-culture compared to empty vector control (Figure 5.4**D**). RANKL expression after co-culture was also found to be significantly downregulated in LIF overexpression cell co-culture compared to empty vector (Figure 5.4**E**). OPG was found not to be significant although LIF overexpression cell co-culture did have a large spread of data with large error bars (Figure 5.4**F**). This error effected the RANKL/OPG ratio analysis as seen in figure 5.4**G**. This ratio has a trend to decrease in the LIF overexpression cell co-culture condition, however an outlier is causing increased error and so the experiment would need to be conducted again to confirm the trend of this ratio.

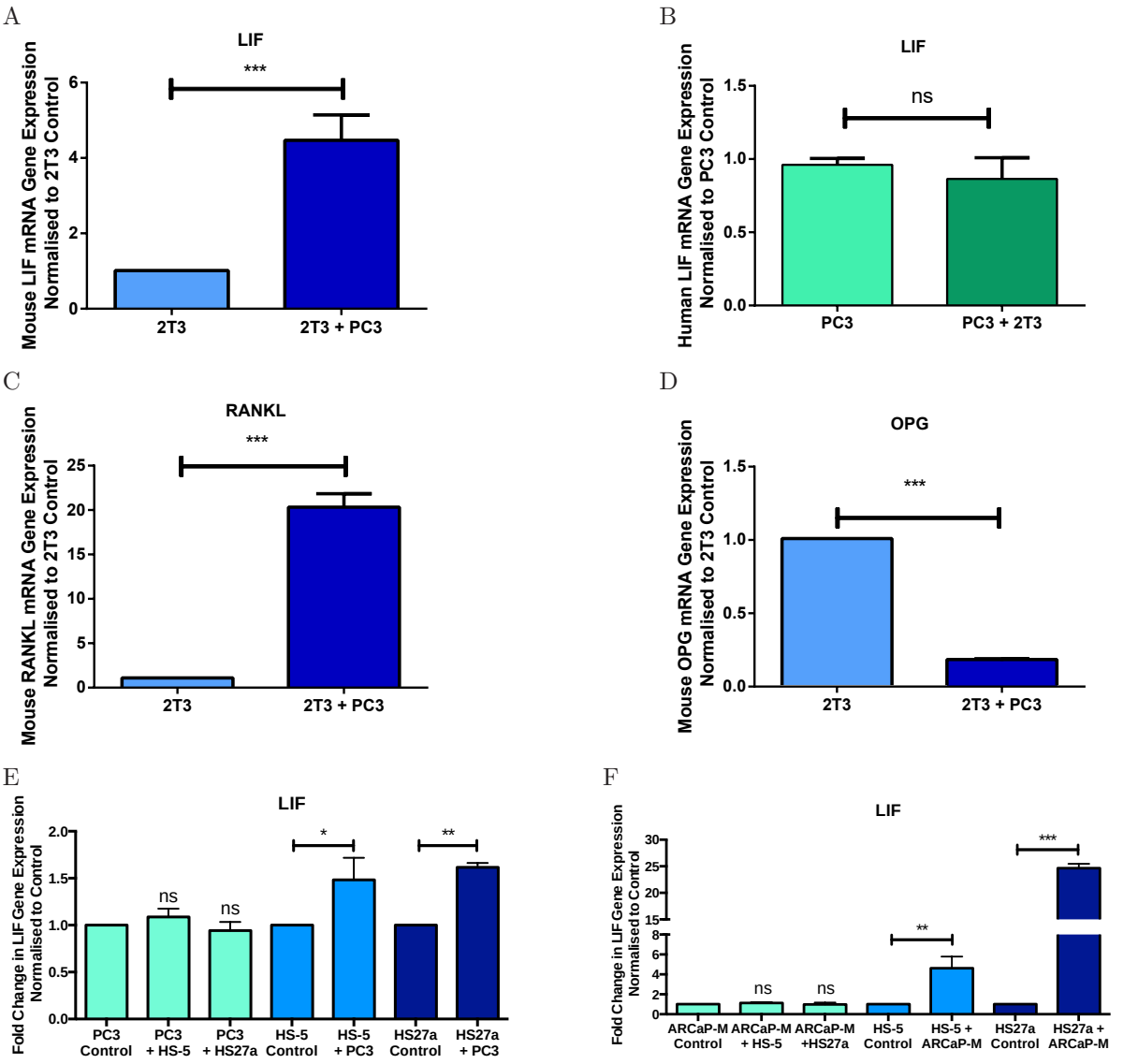


Figure 5.2: **Gene expression of LIF is significantly upregulated in bone stromal cells after co-culture with prostate cancer cells.** Human bone metastatic PC3 cells were co-cultured directly with mouse stromal 2T3 cells for 48hrs. (**A**) Mouse LIF mRNA expression in 2T3 cells with and without co-culture. (**B**) Human LIF mRNA expression in PC3 cells with and without co-culture. (**C**) Mouse RANKL mRNA expression in 2T3 cells with and without co-culture. (**D**) Mouse LIF mRNA expression in 2T3 cells with and without co-culture. Statistical test used = student t test, *** $p<0.001$, ns = not significant. (**E**) Human LIF mRNA expression after transwell co-culture with PC3 prostate cancer and HS-5 or HS27a human stromal cells. (**F**) Human LIF mRNA expression after transwell co-culture with ARCaP-M prostate cancer and HS-5 or HS27a human stromal cells. Statistical test used = One way ANOVA with tukey post hoc test, * $p<0.05$, ** $p<0.01$, *** $p<0.001$. Error bars = standard error mean (SEM).

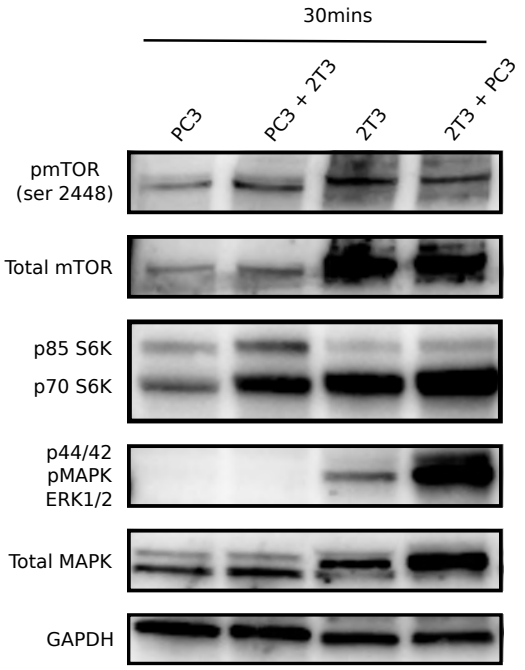


Figure 5.3: **LIF downstream pathways are activated in stromal cells after co-culture with prostate cancer cells.** PC3 or 2T3 cells were seeded at 2.2 x 10^4 cells/cm^2 separately in either a 6 well plate or transwell insert and grown for 48hrs. Transwells were then added on top of the 6 well plate for 30mins, after which point protein was extracted.

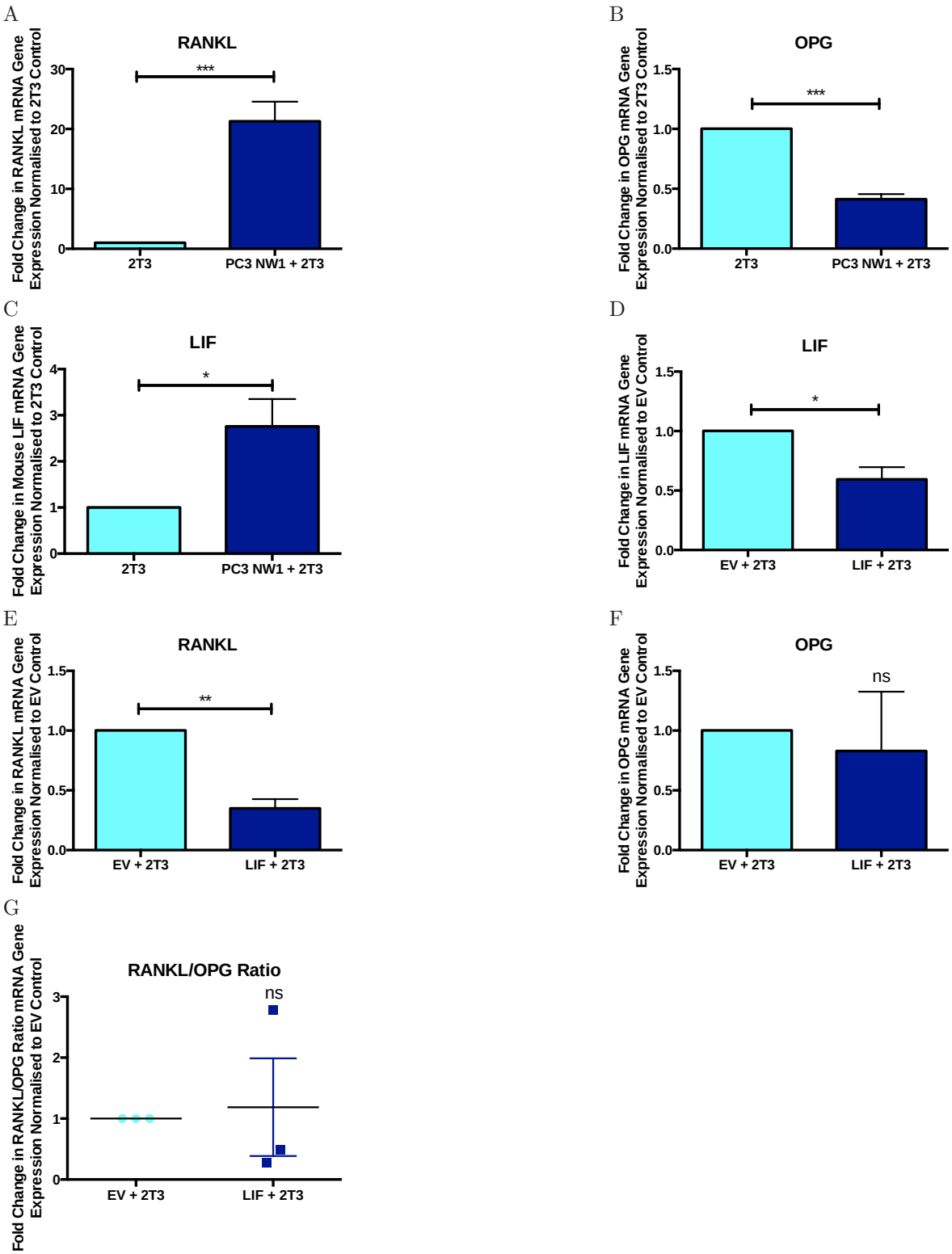


Figure 5.4: **Direct co-culture bone stromal cells with PCa cells after LIF overexpression.** Human bone metastatic PC3 NW1, empty vector or LIF overexpression cells were co-cultured directly with mouse stromal 2T3 cells for 48hrs. (**A**) Mouse RANKL mRNA expression in 2T3 cells with and without co-culture. (**B**) Mouse mRNA expression in 2T3 cells with and without co-culture. (**C**) Mouse LIF mRNA expression in 2T3 cells with and without co-culture. (**D**) Mouse LIF mRNA expression in 2T3 cells with and without co-culture with empty vector and LIF overexpression cells. (**E**) Mouse RANKL mRNA expression in 2T3 cells with and without co-culture. (**F**) Mouse OPG mRNA expression in 2T3 cells with and without co-culture. (**G**) RANKL/OPG ratio mRNA gene expression in 2T3 cells with and without co-culture. Statistical test used = Statistical test used = student t test, * <0.05, **p<0.01, *** p<0.001, ns = not significant. Error bars = standard error mean (SEM).

5.3.2 LIF is associated with fat and muscle markers *in vivo*

During PCa *in vivo* experiments, weight was monitored consistently throughout. It was noticed that circulating LIF levels appeared to be associated with smaller mice. At the end of experiment before sacrifice, animals were weighed, which showed a significant difference between non-tumour and tumour mice (Figure 5.5**A**). Weight difference was calculated by using baseline weight prior to inoculation of cancer cells and weight taken just before sacrifice. When weight difference was correlated with circulating LIF concentration it was found to be significant ($p< 0.05$) (Figure 5.5**B**). However, for some ELISA measurements of LIF concentration the optical density (OD) was read at the top end of the scale, thus samples were too concentrated to be told apart from each other. Due to the volume of blood required for the three ELISAs it was not possible to repeat LIF concentrations. Thus, for LIF correlation with weight, leptin and myostatin, statistics are shown with the addition of these samples and without. Figure 5.5**C** shows that removal of these high LIF datapoints the correlation between LIF and weight difference is no longer significant.

Weight loss through late stage cancer can occur through the loss of adipose and/or skeletal muscle tissue (Kir and Spiegelman, 2016). Due to the correlation between LIF and weight it was postulated that LIF could potentially correlate with fat as well, hence leptin and adiponectin were measured as indicators of adiposity. It was found that leptin serum concentrations were significantly lower in tumour mice compared to non-tumour controls (Figure 5.6**A**) and correlated with circulating LIF levels ($p<0.05$) including high LIF datapoints (Figure 5.6**B**). However, upon removal of the high LIF datapoints this correlation was found no longer to be significant (Figure 5.6**C**). Serum samples were also assessed for secreted levels of adiponectin. Figure 5.6**D** shows adiponectin as a high molecular weight (HMW), hexamer or trimer, with decreased levels of adiponectin in tumour mice compared to non-tumour controls. This suggests that LIF is associated with fat and that fat markers are decreased in late stage diseased animals. Although, weight loss can not only be a consequence of fat loss, it can also occur in response to muscle loss. Hence, a muscle marker, myostatin was used to establish if diseased mice also lost muscle.

Myostatin is a myokine that is released from myocytes (muscle cells) and causes a feedback loop to inhibit differentiation into more muscle cells. Myostatin serum concen-

trations were significantly decreased in tumour mice compared to non-tumour controls (Figure 5.7**A**). Furthermore, when correlated with circulating LIF levels, including high LIF data points, it was found to be statistically significant ($p<0.05$) (Figure 5.7**B**). However, this correlation was not found to be significant when high LIF datapoints were removed (Figure 5.7**C**). Using the high LIF datapoints, it would suggest that LIF is associated with both fat and muscle markers, which are decreased in late stage diseased animals. Although these concentrations would need to be re-measured in order to draw final conclusions.

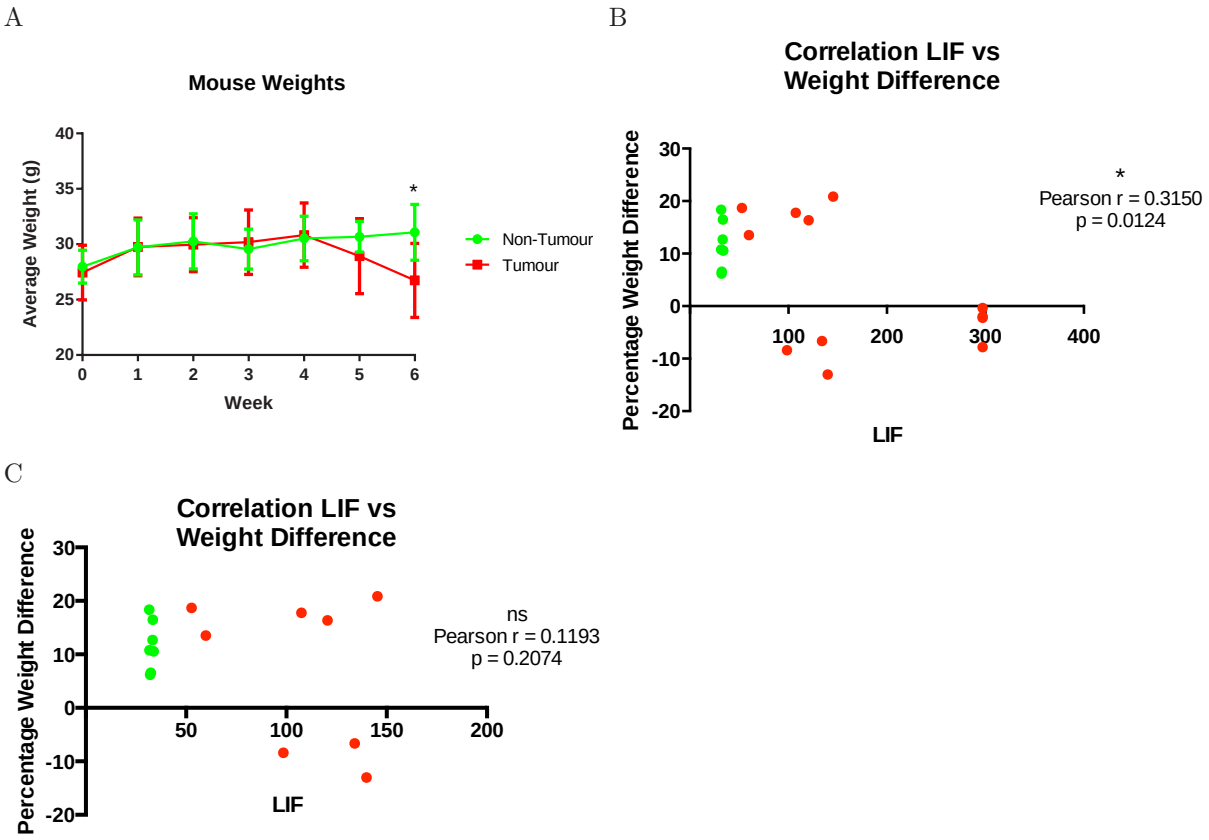


Figure 5.5: **LIF is correlation with weight loss.** (**A**) Graph showing average mouse weights over experiment. Statistical test used = two way ANOVA with Sudak's post hoc test, * $p<0.05$. Error bars = SEM. (**B**) Pearsons correlation between LIF (pg/ml) and weight difference from baseline to experimental end, * $p<0.05$. (**C**) Pearsons correlation between LIF (pg/ml) and weight difference from baseline to experimental end, excluding maximised values of LIF.

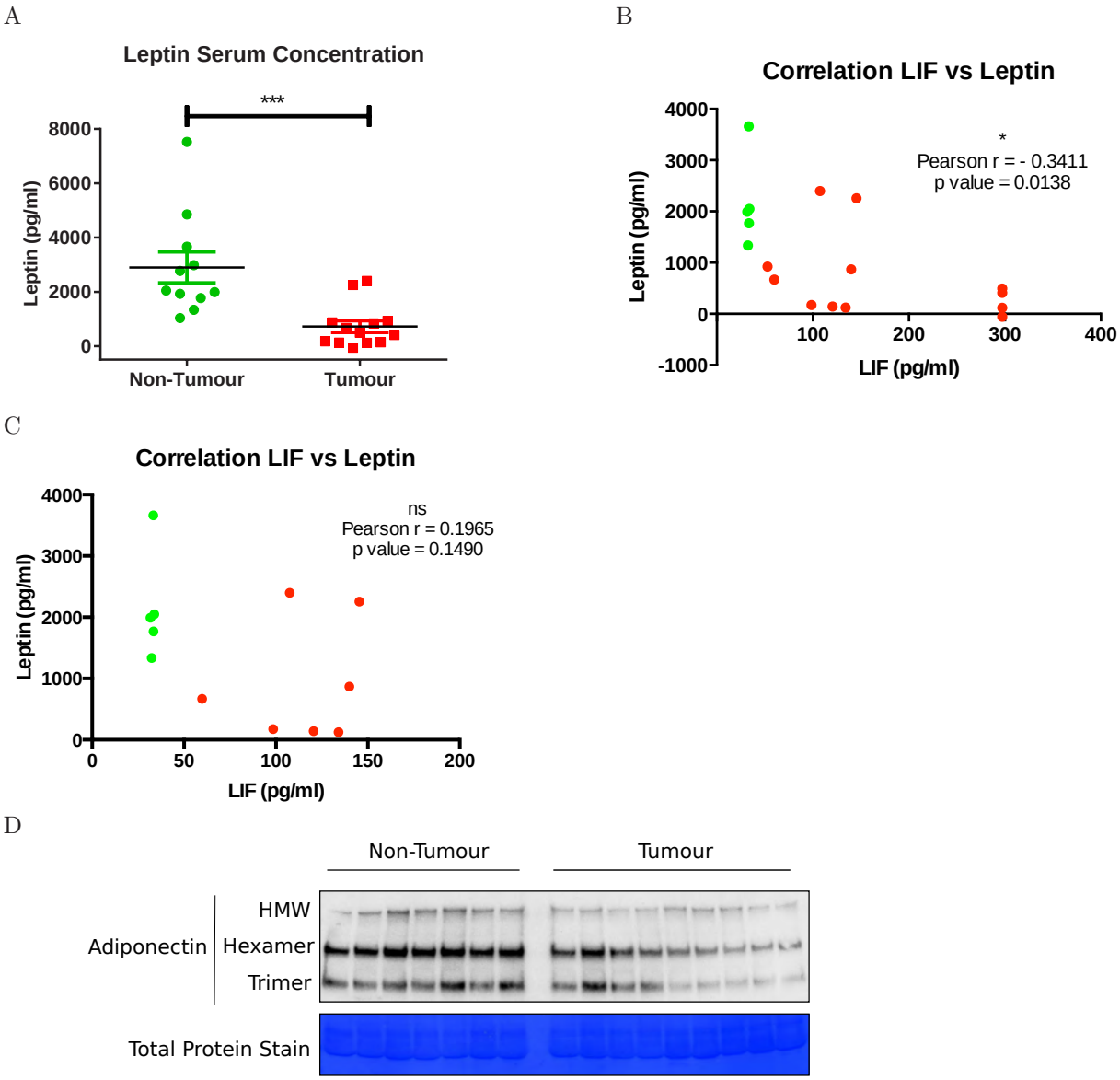


Figure 5.6: **LIF is correlated with fat loss.** (**A**) Mouse leptin protein expression of non-tumour and tumour mice using a mouse Quantikine ELISA (R and D). Statistical test used = student t test, *** $p<0.001$. Error bars = SEM. (**B**) Pearsons correlation between leptin serum concentration (pg/ml) and LIF serum levels (pg/ml). **C** Pearsons correlation between leptin serum concentration (pg/ml) and LIF serum levels (pg/ml), excluding maximised values of LIF. (**D**) Western blot showing circulating levels of adiponectin from mouse serum.

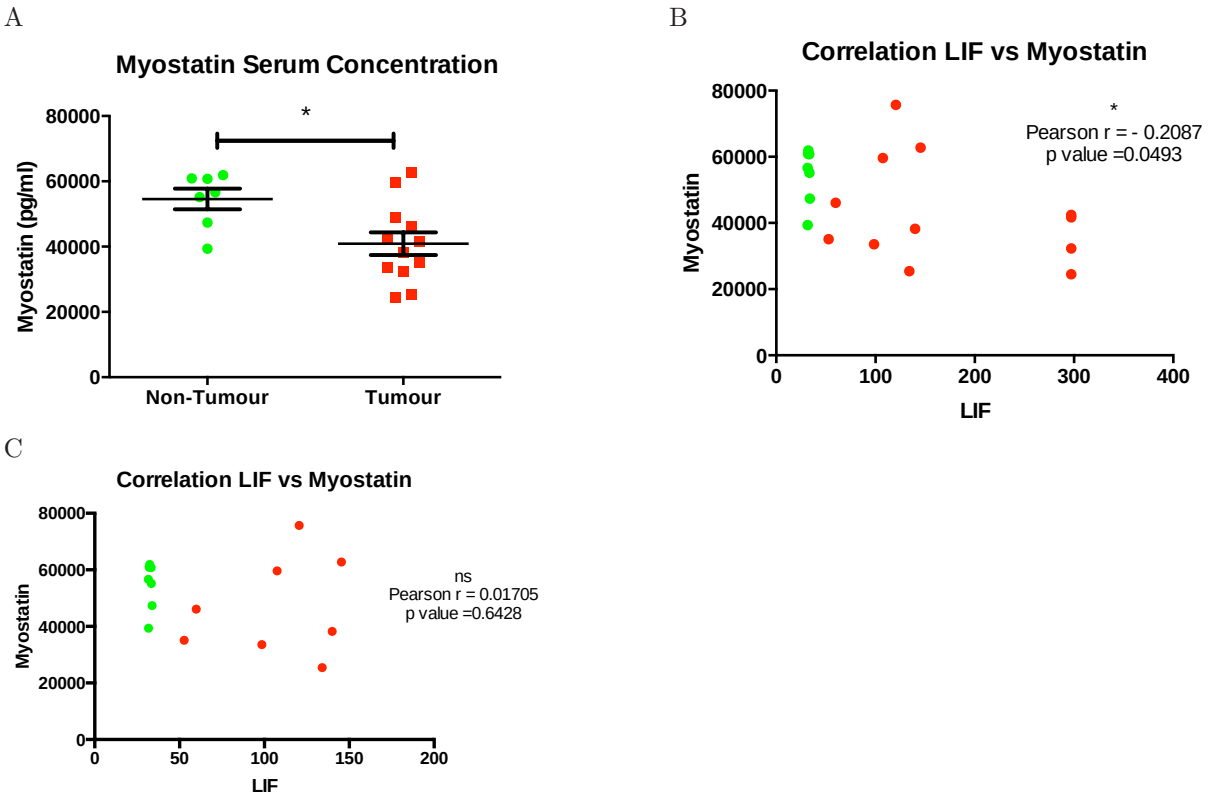


Figure 5.7: **LIF is correlated with a decrease in muscle markers.** (**A**) Mouse myostatin protein expression of non-tumour and tumour mice using a mouse Quantikine ELISA (R and D). Statistical test used = student t test, * $p<0.05$. Error bars = SEM. (**B**) Pearsons correlation between myostatin serum concentration (pg/ml) and LIF serum levels (pg/ml). (**C**) Pearsons correlation between myostatin serum concentration (pg/ml) and LIF serum levels (pg/ml), exclusing maximised values of LIF.

5.3.3 LIF significantly increases mineralisation into osteoblasts at the expense of adipocytes

LIF has been shown to be involved with both bone formation and bone resorption under normal homeostatic conditions. As LIF was found to correlate with decreased fat markers *in vivo*, I examined the effect of LIF on adipogenesis and osteoblastogenesis. 2T3 cells were differentiated into osteoblasts using osteogenic media for a period of 16 days with and without the presence of LIF. Media and treatment were changed every 24hrs. LIF treatment significantly increased the quantity of mineralisation (as established by Alizarin Red staining) ($p<0.001$) (Figure 5.8).

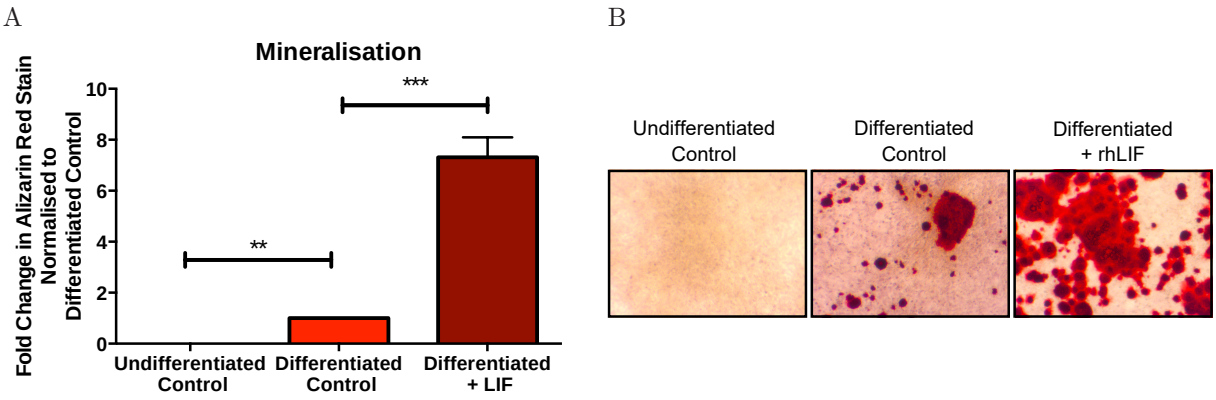


Figure 5.8: **LIF significantly increases mineralisation of pre-osteoblasts.** (**A**) Graph showing Alizarin red quantification (450nm OD). Statistical test used = One-way ANOVA with post hoc tukey test. Error bars = SEM. (**B**) Representative microscope pictures of Alizarin staining of undifferentiated, differentiated and differentiated + 100ng/ml rhLIF 2T3 cells.

As LIF was found to increase differentiation into osteoblasts, as osteoblasts and adipocytes share a common precursor, the differentiation into adipocytes was then investigated. Bone marrow pre-adipocytes (ST2) cells or white fat pre-adipocytes (3T3) were differentiated using adipogenic media. LIF treatment was initiated at day 0 from the initial addition of adipogenic media, 24hrs after or 48hrs after. Adipogenic media and LIF treatment was reapplied every 24hrs. LIF treatment of bone marrow ST2 pre-adipocytes caused a significant decrease in differentiation into adipocytes when added with the differentiation media ($p<0.01$), 24hrs later ($p<0.01$) or 48hrs later ($p<0.05$) (Figure 5.9**A,B**). Furthermore, LIF treatment on white fat 3T3 pre-adipocytes also caused a significant decrease in differentiation into adipocytes when added with the differentiation

media (p<0.001), 24hrs later (p<0.001) or 48hrs later (p<0.001) (Figure 5.9**C,D**).

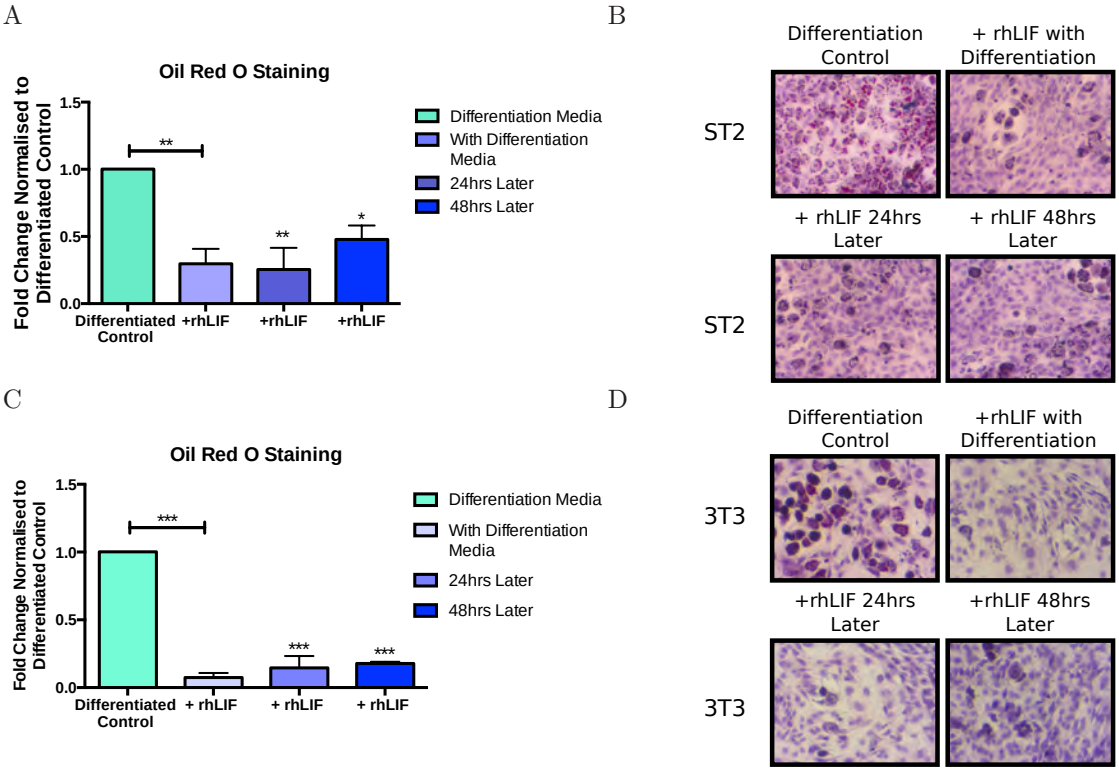


Figure 5.9: **rhLIF treatment significantly decreases differentiation into adipocytes.** ST2 (bone marrow pre-adipocytes) or 3T3 (white fat pre-adipocytes) were seeded at a density of 1 x 10^5. 24hrs later they were treated with adipocyte differentiation media with or without LIF. 24hrs later the differentiation media was changed, LIF treatment was changed on the with differentiation media condition and LIF treatment started on the 24hrs later condition. 24hrs after that differentiation media was changed and LIF treatment re-applied on, with differentiation media and 24hrs later condition and LIF treatment started on the 48hrs later condition. 24hrs later, differentiation media was changed for insulin only medium for 72hrs, with re-treatment of LIF every 24hrs. Cells were then changed into full media for 24hrs. Cells were then changed into full media for 24hrs before staining. (**A**) Quantification of oil red o staining of ST2 cells, using image J from microscope picture. (**B**) Representative microscope pictures, showing differentiation of ST2 cells into adipocytes with and without LIF treatment. (**C**) Quantification of oil red o staining of 3T3 cells, using image J from microscope picture. (**D**) Representative microscope pictures, showing differentiation of 3T3 cells into adipocytes with and without LIF treatment. Statistical test used = One way ANOVA with Dunnetts post hoc test, ** p<0.01, * p<0.05. Error bars = SEM.

The effect of LIF on adipocyte-related gene expression was then investigated (Figure 5.10). LIF treatment of 3T3 cells showed a significant decrease in adiponectin gene expression when treated with the differentiation media (p<0.01), 24hrs later (p<0.01) or 48hrs later (p<0.01) (Figure 5.10**A**). Furthermore, LIF treated also showed a significant decrease in CEBPα, a transcription factor that co-ordiantes the differentiation of adipocytes, in 3T3 cells. LIF treatment with differentiation media showed a significant decrease of p<0.05 and 48hrs later showed a p<0.01 decrease, 24hrs later however, was

not found to be significant (Figure 5.10**B**). Leptin gene expression after LIF treatment of 3T3 cells was unchanged (Figure 5.10**C**). Differentiation into bone marrow adipocytes from ST2 cells showed a significant decrease of adiponectin with initial addition of differentiation media ($p<0.05$), however, was not significant at any other time point (Figure 5.10**D**). Whereas, CEBPα was found to be significantly decreased with differentiation media ($p<0.001$), 24hrs later ($p<0.001$) and 48hrs later ($p<0.001$) (Figure 5.10**E**). In all experiments the gene expression of the differentiation control was significantly higher compared to the undifferentiation control, confirming that differentiation into fat cells had taken place. As adipocytes and osteoblasts share a common precursor cells (MSC), these results suggest that LIF favours the differentiation into osteoblasts rather than adipocytes.

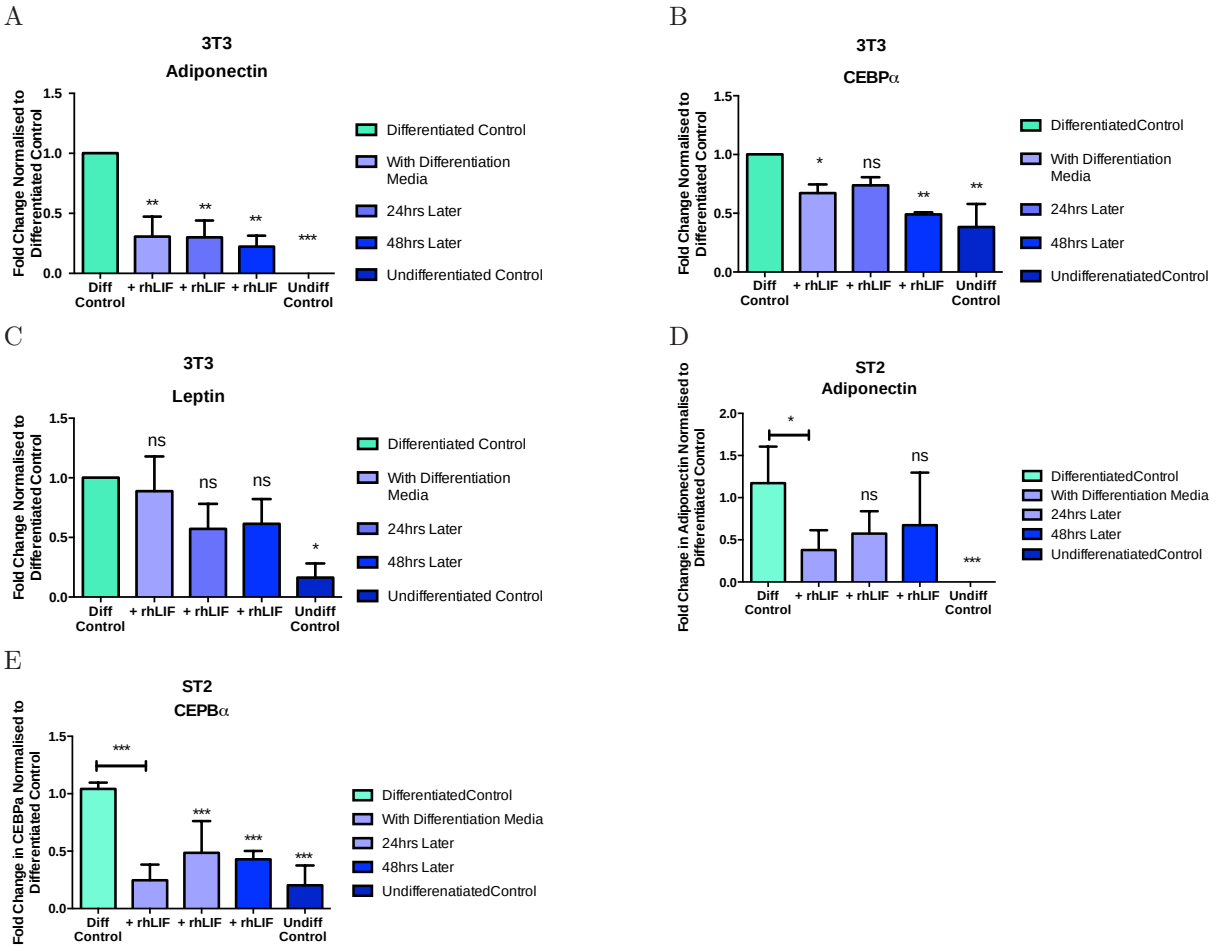


Figure 5.10: **LIF treatment on differentiating fat cells decreases fat markers.** (**A**) Mouse adiponectin mRNA gene expression after 3T3 differentiation with rhLIF. (**B**) Mouse CEBPα mRNA gene expression after 3T3 differentiation with rhLIF. (**C**) Mouse leptin mRNA gene expression after 3T3 differentiation with rhLIF. (**D**) Mouse adiponectin mRNA gene expression after ST2 differentiation with rhLIF. (**E**) Mouse CEBPα mRNA gene expression after ST2 differentiation with rhLIF. Statistical test used = One way ANOVA with Dunnetts post hoc test, *** $p<0.001$, ** $p<0.01$, * $p<0.05$. Error bars = SEM.

The results presented thus far show observations of the direct effects of rhLIF. To investigate the effects of LIF secretion from PCa cells, I used the PC3 NW1 empty vector and LIF overexpression model. Pre-osteoblastic 2T3 cells were differentiated into mature osteoblasts using osteogenic media. After which cells were treated with and without the addition of empty vector conditioned media (CM) or LIF overexpression CM. CM was taken after PC3 NW1 cells were cultured for 48hrs after transient transfection with constructs. It was found that LIF gene expression was significantly decreased in differentiated 2T3 cells treated with LIF overexpression CM. RANKL was found to be significantly upregulated in 2T3 cells treated with LIF overexpression CM compared to empty vector control ($p<0.05$), suggesting that RANKL upregulation is a consequence of LIF expression. OPG was found not to be significantly changed in any treatment type (Figure 5.11**A**). All experiments were found to be significantly different from the undifferentiated control (Figure 5.11**B**). The RANKL/OPG ratio was then analysed and found not to be significant in LIF CM treated conditions when compared to empty vector control (Figure 5.11**C**).

The effects of empty vector and LIF overexpression CM was then investigated on differentiation into adipocytes. ST2 cells were differentiated into adipocytes using adipogenic media with the presence of empty vector or LIF overexpression CM. Quantification of oil red o showed a significant decrease between ST2s cells differentiated with empty vector CM compared to LIF overexpression CM ($p<0.05$) (Figure 5.12**A,B**).

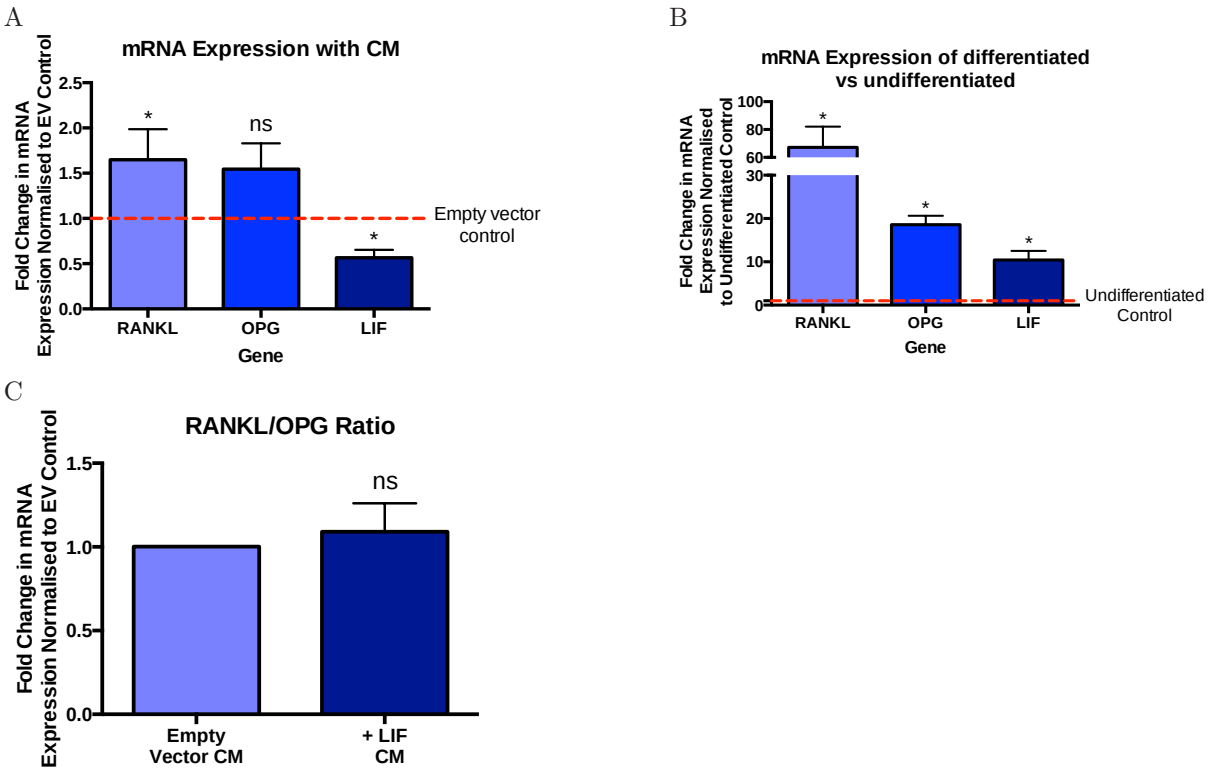


Figure 5.11: **LIF secreted from cancer cells significantly increases LIF and RANKL expression in osteoblasts.** 2T3 cells were seeded at a density of 1.1 x 10^4 cell/cm^2 and differentiated into mature osteoblasts for 16 days using osteogenic media. Mature osteoblasts were then treated with conditioned media from empty vector control PC3 NW1 cells or LIF overexpression PC3 NW1 cells for 48hrs. (**A**) Mouse RANKL, OPG and LIF mRNA gene expression of mature osteoblasts compared to EV treated control. (**B**) Mouse RANKL, OPG and LIF mRNA gene expression of mature osteoblasts compared to undifferentiated control. (**C**) RANKL/OPG ratio of empty vector CM treated osteoblasts vs LIF overexpression CM treated. Statistical test used = student t test, * $p<0.05$. Error bars = SEM.

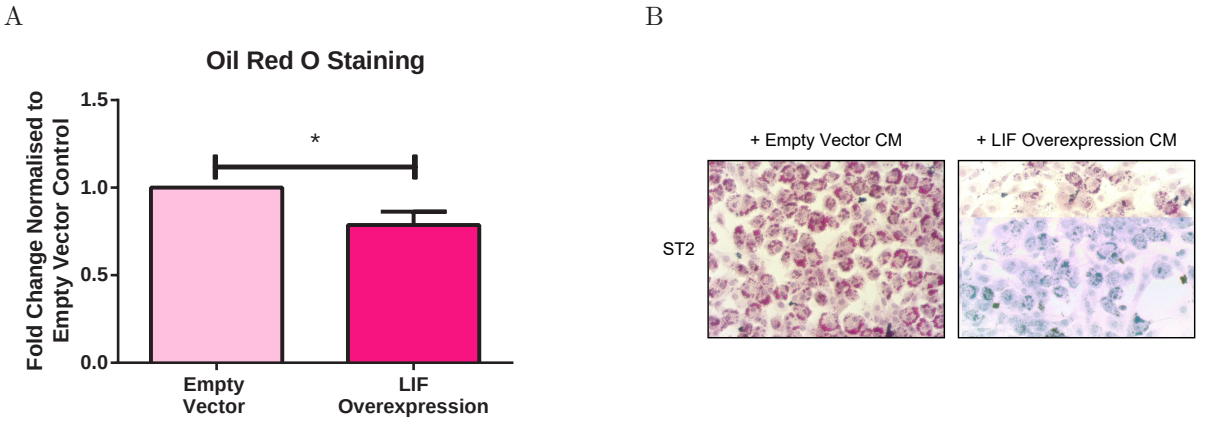


Figure 5.12: **LIF secreted from cancer cells significantly decreases differentiation into adipocytes.** ST2 cells were seeded at a density of 2.2 x 10^4 cells/cm^2 and allowed to adhere for 24hrs. After 24hrs cells were treated with differentiation media with empty vector of LIF overexpression conditioned medium. Cells were allowed to differentiate for 1 week, replacing media and treatment every 24hrs. (**A**) Graph showing quantified oil red o stain in empty vector treated vs LIF overexpression treated. Statistical test used = student t test, * $p<0.05$. (**B**) Representative microscope images showing ST2 cells differentiated into adipocytes with the addition of empty vector or LIF overexpression conditioned media.

Bone marrow-derived lipids from adipocytes have previously been shown to stimulate proliferation and invasion of prostate tumour cells and upregulate genes involved in fatty acid transport (Herroon et al., 2013). In this chapter it has been shown that PCa LIF overexpression CM decreased oil red o staining of ST2 differentiated adipocytes. Furthermore, in the previous chapter it has been suggested that LIF overexpression in PCa cells may cause a growth disadvantage and thus LIF overexpression PCa may have hindered lipid uptake. Thus, to test if LIF was capable of causing decreased lipid uptake an experiment was performed where PC3 NW1 were transfected with empty vector or LIF overexpression constructs and treated with lipids harvested from mature adipocytes. It was found that there was no difference in the amount of bodipy stain (lipid stain) in empty vector PC3 NW1 cells when compared to LIF overexpression PC3 NW1 cells (Figure 5.13). However, when LIF treatment was found to reduce that amount of oil red o in adipocytes, it is important to note that oil red o stains the lipids inside cells and while this is used as a method of quantifying differentiation into mature adipocytes, it does not account for lipids that may be released into the media. It is possible that LIF expression may have caused release of lipids from adipocytes into the surrounding media. Epidemiologic studies have suggested that dietary fat may contribute to PCa (Suburu and Chen, 2012). The majority of mammalian tissues satisfy their lipid requirements through the uptake of free fatty acids (FFAs) and lipoproteins from the blood. Fatty acid and cholesterol biosynthesis is usually restricted to certain cell types, such as adipocytes. However, in the context of cancer increased lipid biosynthesis is frequently seen in these cells (Baenke et al., 2013). As such it would need to be investigated if LIF was causing lipid release from adipocytes that may confer a preferable environment for PCa cells.

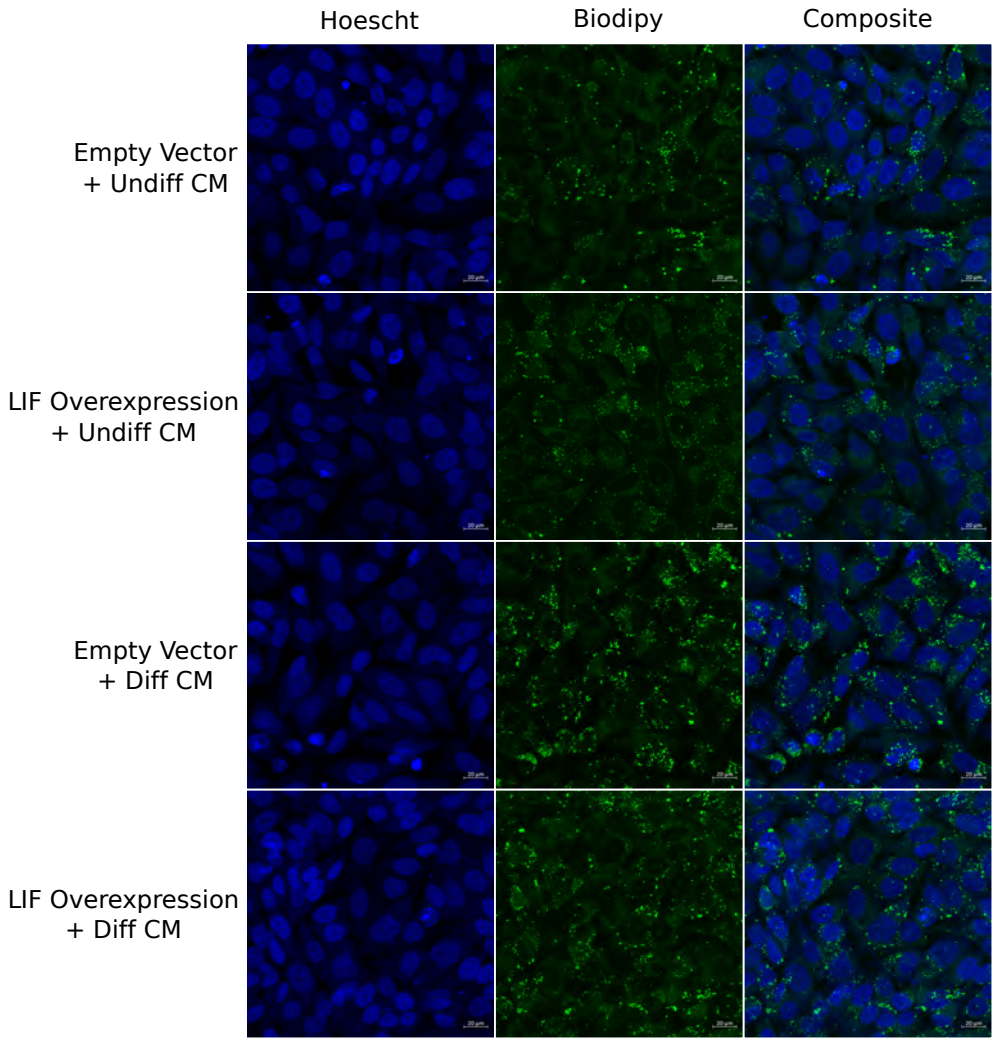


Figure 5.13: **LIF overexpression in PCa cells has no effect on lipid uptake.** Mouse ST2 cells were differentiated into adipocytes over a period of 7 days using adipogenic media or left undifferentiated over the same time period. Cells were then scraped into their media and spun at 17,000x g for 15mins. Supernatant was taken and added to empty vector or LIF overexpression PCa cells for 24hrs. Cells were fixed using formalin and stained with Hoescht (1:2000) or Bodipy (1:1000). Pictures were taken using a Zeiss confocal 710 microscope. Undiff CM = Undifferentiated adipocyte conditioned media, Diff CM = Differentiated adipocyte conditioned media.

5.3.4 LIF decreases differentiation into muscle cells

Weight loss due to late stage cancer as seen previously in this chapter with the PC3 NW1 *in vivo* tumour model, can also be due to muscle wasting, with or without fat loss and is a pivotal feature of cancer cachexia (Aversa et al., 2017). Metcalf *et al* showed *in vivo* that muscle atrophy can be a consequence of LIF overexpression (Metcalf and Gearing, 1989). As I have already established a role for LIF in the reduction of differentiation into fat cells and a reduction in fat markers, I can turn my attention to LIF's involvement in muscle development. C2C12 cells were differentiated for a total of 1 week. During this time period cells were also treated with 100ng/ml rhLIF at the same time as the initial addition of differentiation media, 24hrs later or 48hrs later. Myocyte differentiation was confirmed by elevated expression of muscle markers and formation of myotubes through blind testing of microscope images (Figure 5.14). LIF caused a significant decrease in myogenin and myostatin gene expression when added with differentiation media ($p<0.001$), 24hrs later ($p<0.01$) or 48hrs later ($p<0.05$) (Figures 5.14**A,B**). Figure 5.14**C** also shows confirmation of differentiation with white arrows in differentiation control depicting fully formed myotubes. LIF treatment resulted in a decrease in myotube formation (Figure 5.14**C**).

As LIF treatment had a significant effect on differentiation into myotubes and expression of muscle markers during differentiation, it was then examined whether LIF treatment would have any effect on muscle markers or number of myotubes if treatment was begun after cells were already differentiated. Cells were seeded and differentiated for 1 week. Differentiated C2C12 cells were then treated with 100ng/ml rhLIF for 96hrs, 72hrs or 48hrs. Media with rhLIF was changed every 24hrs. It was found that rhLIF treatment decreased the expression of muscle markers and decreased the number of visible myotubes (Figure 5.15).

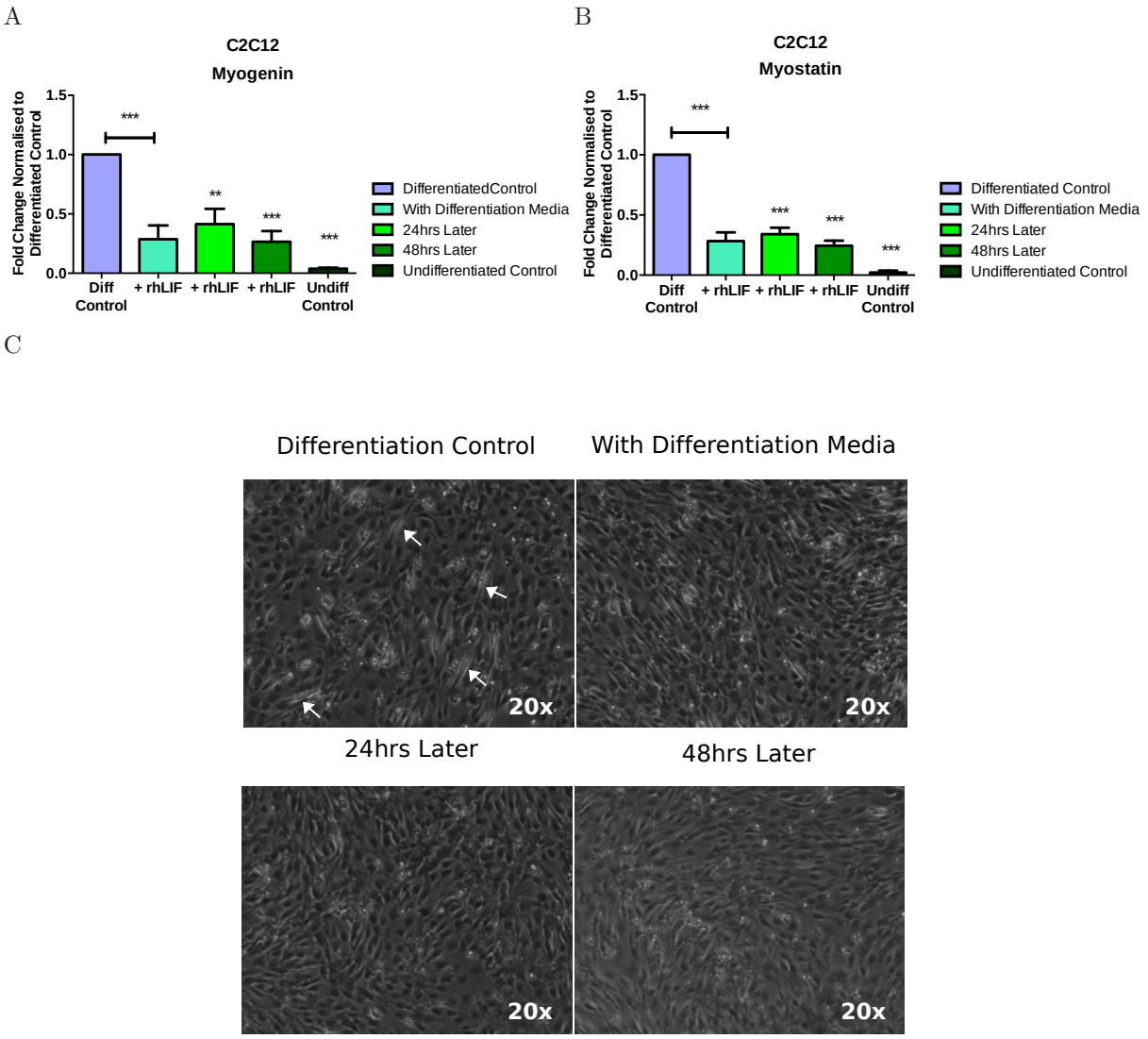


Figure 5.14: **LIF treatment decreases muscle markers.** (**A**) Mouse myogenin mRNA gene expression differentiated into myotubes with and without 100ng/ml rhLIF treatment. (**B**) Mouse myostatin mRNA gene expression differentiated into myotubes with and without 100ng/ml rhLIF treatment. Statistical test used = One way ANOVA, with post hoc Dunnett test, *** $p<0.001$. Error bars = SEM. (**C**) Representative microscope pictures showing C2C12 cells differentiated into myotubes using 0.5% FBS media with and without LIF treatment. Arrows indicate differentiated myotubes, as confirmed by blind testing of microscope images.

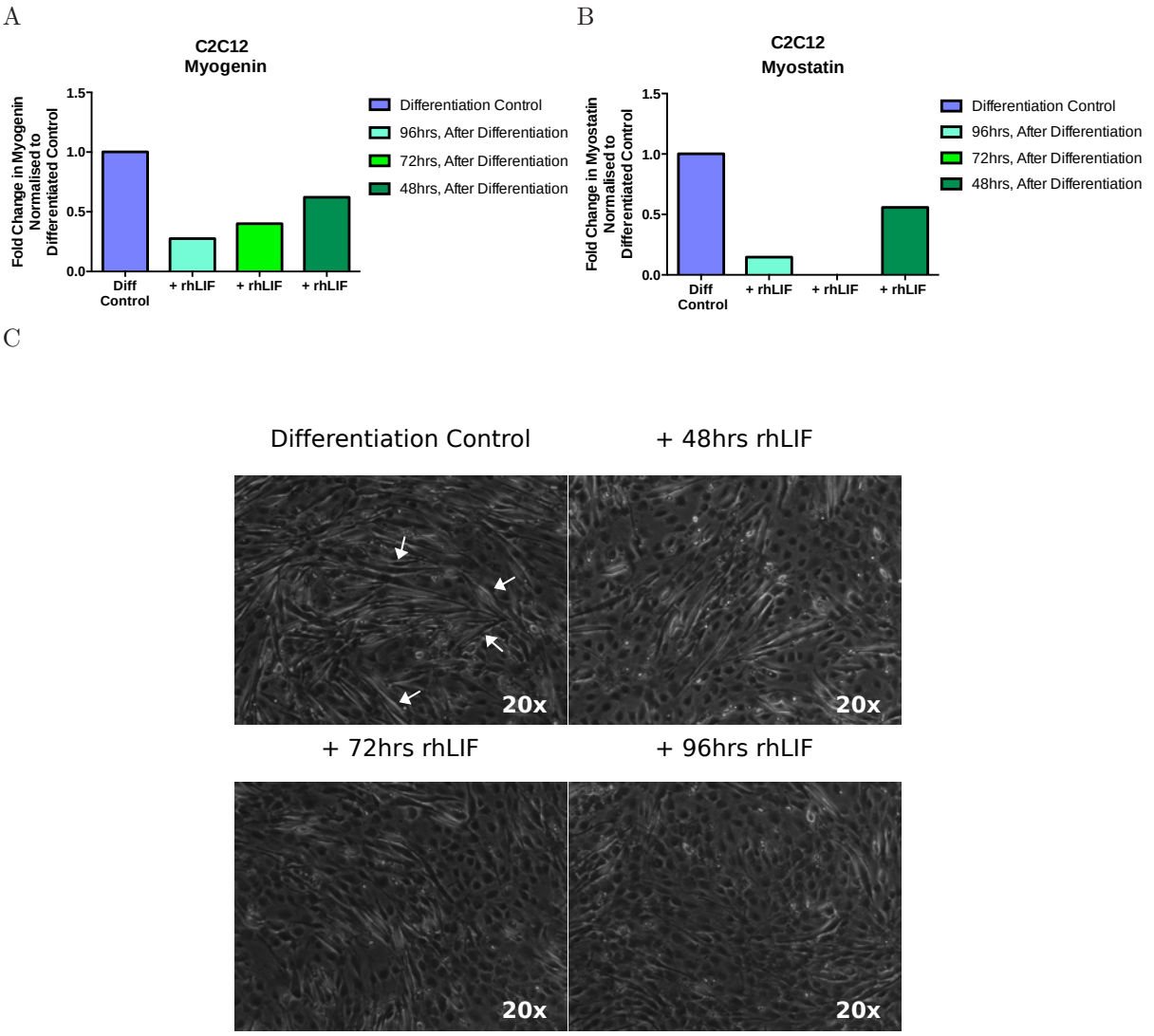


Figure 5.15: **LIF treatment decreases muscle markers.** (**A**) Mouse myogenin mRNA gene expression after differentiation into myotubes with and without 100ng/ml rhLIF treatment. (**B**) Mouse myostatin mRNA gene expression after differentiation into myotubes with and without 100ng/ml rhLIF treatment. N=1. (**C**) Representative microscope pictures showing C2C12 cells after differentiation into myotubes using 0.5% FBS media with and without LIF treatment. Arrows indicate differentiated myotubes, as confirmed by blind testing of microscope images.

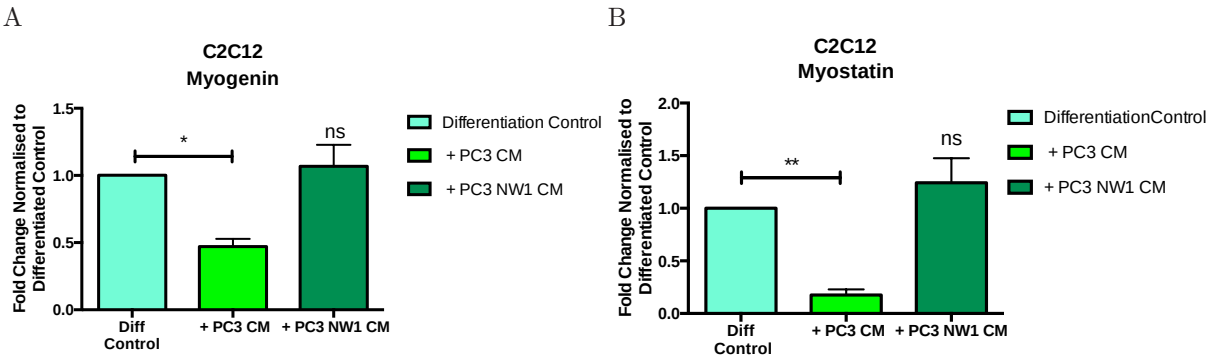


Figure 5.16: **Conditioned media from high LIF expression cells decreases muscle markers.** (**A**) Mouse myogenin mRNA gene expression differentiated into myotubes with and without CM from PC3 or PC3 NW1 cells. (**B**) Mouse myostatin mRNA gene expression differentiated into myotubes with and without CM from PC3 or PC3 NW1 cells. Statistical test used = One way ANOVA, with post hoc Dunnett test, ** $p<0.01$ * $p<0.05$. Error bars = SEM.

It was then investigated whether LIF from conditioned media from PCa could also influence differentiation in myotubes. Conditioned media from wild type PC3 cells, which have a high baseline level of LIF and PC3 NW1 wild type cells, which have a low baseline level of LIF were cultured to confluency for 48hrs, at which point conditioned media was taken. C2C12 cells were differentiated for 1 week. During this time period cells were also treated with PCa conditioned media with the initial addition of differentiation media, 24hrs later or 48hrs later. Figure 5.16 shows expression of muscle markers, myogenin and myostatin after treatment. PC3 conditioned media showed a significant decrease in both myogenin and myostatin expression ($p<0.05$ and $p<0.01$) compared to differentiation control and PC3 NW1 conditioned media treatment (Figure 5.16).

5.4 Discussion

Results from previous chapters in this thesis have shown that LIF in PCa is associated with improved patient survival and cancer suppression. The analyses carried out in this chapter however, suggests that LIF could be a double-edged sword when it comes to metastatic disease. To elucidate the expression of LIF in the tumour-bone microenvironment, I used *in silico* analysis of PCa xenografts from Ozdemir *et al.* This revealed that LIF was significantly upregulated in the bone microenvironment after intra-tibial inoculation with PCa VCAP or C42B cells. In the PC3 NW1 *in vivo* model discussed in chapter 3, mouse bones were also taken for RNA to assess gene expression. Mouse LIF in the microenvironment was assessed in those samples, but unfortunately expression was too low to be detected (data not shown). However, it is important to note that the study conducted by Ozdemir *et al* inoculated PCa cells intratibially, whereas the PC3 NW1 model was an intracardiac model and thus differences in gene expression may lie in the method of inoculation. Furthermore, different cell lines were used and so differences may also be introduced there.

Based on this *in silico* finding, I then assessed co-cultures of PCa and bone stromal cells to reproduce this effect *in vitro*. Using both direct and transwell co-culture systems and a range of PCa and bone stromal cells I was able to induce significant LIF upregulation specifically in the bone stromal cells in every condition. Interestingly this was accompanied by an upregulation of RANKL and downregulation of OPG. RANKL activates mature osteoclasts and osteoclastogenesis through binding to RANKL on osteoclast precursor cells, whereas OPG negatively regulates RANKL by also binding to RANK and reducing the half-life of RANKL bound to the membrane, therefore inhibiting bone resorption induced by osteoclasts (Tat et al., 2006). The RANKL/RANK/OPG triad is a key regulator for normal bone metabolism. The interaction and concentrations of RANKL and OPG have a direct relationship and in the case of cancer can cause growth of bone metastasis. RANKL has been implicated in the skeletal metastasis from lung, breast and prostate tumours. The osteolytic lesions and hypercalcemia seen in these solid tumours are associated with excessive osteoclast activation mediated by RANKL/RANK

interactions (Wittrant et al., 2004). Huang *et al* demonstration that RANKL mRNA and protein expression was upregulated in 90% of skeletal lesions in patients with lung, breast, thyroid and prostate cancer (Huang et al., 2002). Thus, the results seen in this chapter suggest that co-culture of PC3 and 2T3 cells gives rise to an osteolytic phenotype, which is probably unsurprising considering that PC3 cells give rise to osteolytic bone disease (Sanchez-Sweatman et al., 1998-1999). LIF has been shown to upregulate RANKL mRNA in mouse calvaria (Palmqvist et al., 2002) and this could be the case in the co-cultures described here.

The MAPK pathway functions to regulate key transcriptional mediators of osteoblast differentiation. ERK along with p38 MAPKs phosphorylates RUNX2, the master regulator of osteoblast differentiation. ERK can also activate ribosomal protein S6 kinase (RSK2), which in turn phosphorylates activating transcription factor 4 (ATF4), a transcriptional regulator of late-stage osteoblast synthetic functions (Greenblatt et al., 2013). Thus, LIFs activation of p44/42 MAPK (ERK1/2) downstream signalling proteins could be one mechanism that leads to the differentiation of osteoblasts that can be seen in this chapter using rhLIF, but also shows increased bone formation seen in PCa patients. However, in order to investigate whether or not this upregulation of RANKL in co-culture systems was due to LIF, the PC3 NW1 LIF overexpression model was utilised. PC3 NW1 wild type cells already have a lower baseline level of LIF compared to wild type PC3 cells and were shown to induce the same phenotype when co-cultured with 2T3 stromal cells. When using empty vector or LIF overexpression cells however, RANKL upregulation was not found to be significant, likely reflecting the spread of data. It was found however, that there was a significant downregulation of OPG, suggesting that this effect seen in stromal cells in response to PCa co-culture was independent of LIF.

LIF has previously been reported to decrease obesity. Jansson *et al* found that using an ovariectomised mouse model, daily injections of 30mg/kg of LIF for 15 days significantly reduced the weight of white fat depots and serum leptin levels (Jansson et al., 2006). In this chapter I found that LIF correlated with the weight difference seen between baseline and sac date, with tumour mice having significant weight loss compared to non-tumour mice in the final week of the experiment. LIF was also significantly correlated with leptin

serum levels, suggesting that in these tumour mice LIF is correlated with leptin and weight loss. Taken together with the findings from Jansson *et al*, it would suggest that LIF could be one mechanism of causation of *in vivo* late-stage weight loss from PCa.

The incidence of skeletal metastasis and mortality rates for PCa increases with obesity, a condition that increases bone marrow adiposity. Interestingly anorexia nervosa can also increase bone marrow adiposity, a condition that can be seen in late-stage cancer patients (cachexia) (Bredella et al., 2009). Bone marrow adipocytes are metabolically active components of the bone marrow and Herroon *et al* has previously shown the promoting effect of marrow fat on the growth and progression of skeletal prostate tumours. They have shown that lipids produced by the adipocytes in the marrow induced the expression of the lipid chaperone fatty acid binding protein 4 (FABP4) and stimulated their growth and invasiveness (Herroon et al., 2013). Results in this chapter demonstrated that treatment with LIF overexpression PCa conditioned media on differentiating adipocytes caused a significant reduction in oil red o staining. This stain targets lipids, however lipids can also be seen using brightfield microscopy prior to staining, which appear as little bubbles and thus can be used to identify an adipocyte cell. Prior to staining it was observed that there did not appear to be a noticeable difference in adipocyte number between adipocytes treated with empty vector conditioned media compared with LIF overexpression. The difference was only noticeable when specifically staining for lipids, furthermore stained lipids appeared smaller than those treated with empty vector conditioned media. It was found that there was significantly less lipid present in adipocytes after LIF overexpression treatment, post staining. As lipids appeared smaller after LIF overexpression treatment it was hypothesised that perhaps LIF could be preventing their growth, either through preventing differentiation as seen previously in this chapter or by another mechanism.

Adipocytes have evolved to store and release fatty acids. They can accommodate massive storage of triacylglycerol (TAG) during energy abundance and release free fatty acids into the plasma for the use by other tissues during times of energy need (Thompson et al., 2010). Co-culture with adipocytes and tumour cells has previously been shown to lead to a transfer of free fatty acids released by the adipocytes (Wen et al., 2017).

Increase amounts of fatty acids and lipids can promote tumour growth and progression, and in the case of breast cancer, adipocytes and cancer cells directly interact with each other to exchange molecules such as growth factors, chemokines, and interleukins in a reciprocal manner (Blücher and Stadler, 2017). As oil red o only stains lipids that are being stored in adipocytes, it would not account for any lipids that had been released into the surrounding media and thus I hypothesised that perhaps LIF overexpression conditioned media may stimulate adipocytes to release lipids instead of storing them. Considering the work by Herroon *et al* this would create a growth advantage for PCa cells. As such a study was designed using empty vector and LIF overexpression cells to investigate the quantity of lipid uptake. I found that there was no difference between PCa cells, suggesting that LIF has no effect on lipid uptake. However, considering that I have shown that LIF expression is correlated with patients with primary disease and that conditioned media from LIF overexpression cells was able to reduce lipid staining in adipocytes, future research would need to investigate if primary PCa can prime the bone microenvironment to create a lipid rich site for metastasis. Firstly, it would need to be established if LIF overexpression conditioned media does indeed release lipids into the media in which the adipocytes are grown, for which Bodipy stain could be used.

Cancer cachexia is the systematic loss of body weight that is not diet dependent and not only involves significant loss of fat stores but also muscle mass. In colon cancer, Seto *et al* found that JAK/STAT and ERK signalling was stimulated in C2C12 cells using conditioned media from mouse colon carcinoma C26 cells. Moreover, they showed that LIF was the cytokine that induced these signalling pathways as well as causing muscle atrophy in myotubes differentiated from C2C12 cells (Seto et al., 2015). In this chapter I have shown that specific treatment with rhLIF can decrease the differentiation into myotubes from C2C12 cells and the expression of muscle markers. Moreover, it has also been demonstrated that conditioned media from PCa cells containing a high amount of LIF, compared to conditioned media from PCa cells with a low expression of LIF, also decreased expression of muscle markers. Furthermore, in line with the work by Seto *et al* I also treated differentiated C2C12 cells with rhLIF to establish if reversal of differentiation could occur. Although this experiment was only done once, it can be used

as a proof of principle that rhLIF treatment on already differentiated C2C12 cells can indeed reduce the number of myotubes seen via microscopy and reduce the expression of muscle markers. However, the results shown in this chapter show a reduction of myotube number compared to control, whereas muscle atrophy as described by Seto *at al* showed a reduction in myotube diameter, which suggests that our results point to a reversal of differentiation rather than atrophy. Indeed Mastroyiannopoulos *et al* showed that through down-regulation of myogenin in terminally differentiated mouse myotubes from C2C12 cells, induced re-entry into the cell cycle as shown by initiation of DNA synthesis and increased cyclin D1 and cyclin E2. This suggests that through down-regulation of myogenin, differentiation of myotubes can be reversed, a mechanism that can be applied in this chapter through decrease of myogenin via rhLIF treatment (Mastroyiannopoulos et al., 2012).

The results presented in this chapter have shown that LIF could potentially be a double-edged sword in the tumour-bone microenvironment. LIF was shown to promote differentiation into osteoblasts and increase RANKL expression, which could give rise to the mixed bone lesions seen in PCa. Furthermore, LIF was shown to be correlated with weight loss through a decrease in fat and muscle, which could be associated with late-stage weight loss from cancer.

6

Discussion and Future Directions

Bone metastasis from PCa is a common consequence of advanced disease, occurring in more than 80% of cases. After metastasis patients are faced with a 5-year survival rate of 25%, with a median survival of approximately 40 months (Mundy, 2002). At first diagnosis of metastatic disease is a multidisciplinary approach and may take the form of systemic chemotherapy, hormone therapy and bisphosphonates (Janjan et al., 2009). Initially metastatic disease is largely sensitive to ADT, but progression to castration-resistant disease can be rapid, in as little as 18-20 months post treatment initiation (Eisenberger and Walsh, 1999). Bone metastasis can cause distressing symptoms among patients including bone pain, skeletal fracture, spinal cord compression and/or muscle weakness (Smith et al., 2009). Once the disease progresses use of localised radiotherapy or radiopharmaceuticals may be considered (Janjan et al., 2009), but ultimately prognosis for these patients is not positive. There is therefore a need to understand the mechanisms that drive metastasis in order to identify novel therapeutic strategies. The focus of this

study was the role of LIF in PCa-induced bone disease. LIF is known to be involved in a wide range of biological functions including haematopoiesis and bone formation and has been shown to be overexpressed in a number of cancer types. This thesis describes the expression of LIF in PCa, its function in PCa cells and its role in the bone marrow microenvironment.

6.1 Summary of Chapter 3

Chapter 3 of this thesis elucidated LIF expression in PCa patients. Contradictory to previously published work in breast cancer, LIF was found to be associated with disease free survival and freedom of BCR in PCa patients. LIF mRNA expression was furthermore found to be significantly decreased in bone metastatic PCa patients. The LIF pathway has been shown to have conflicting results in tumourigenesis in breast cancer. On the one hand, LIF has been shown to correlate with a poorer relapse free survival in patients, but on the other, Kritikou *et al* showed that LIF deletion in murine mammary glands resulted in delayed involution and a reduction in apoptosis. They suggested that the downstream effector of LIF, STAT3 potentiates it's pro-apoptotic effects and pointed to the loss of LIFR being a key player in tumourigenesis, by showing that LIFR was significantly decreased in breast cancer samples compared to normal and was inversely correlated with tumour grade. In PCa however, I found that LIFR was not consistently decreased in metastatic patients. Whereas LIF, while not always significant after sample number adjustment, appeared to be consistently decreased in each dataset that was investigated.

I found circulating levels of human LIF in *in vivo* models to be significantly higher in tumour mice compared to non-tumour mice, which may not be surprising considering that a human xenograft murine model was used. However, it was found that *in vitro* LIF gene and secreted protein expressions were significantly upregulated in response to tumour cell confluency, and this may be one explanation for what was seen *in vivo*. Through a recent proteomics study, LIF was found to be upstream of the Hippo pathway, which can cause functional inactivation of YAP. YAP can lead to excessive proliferation and inhibition of apoptosis in cancer and has been shown to be upregulated in a number of tumour types.

Inactivation of YAP has been linked with contact inhibition and thus one mechanism for the upregulation of LIF. Another mechanism could be loss of invasiveness. YAP has been linked to metastasis in melanoma, lung and breast cancer, but Sharif *et al* showed that growing PC3 to a high density significantly reduced their invasiveness.

I also demonstrated that treatment with rhLIF on LNCaP cells (which are androgen-responsive), downregulated PSA protein levels in a dose dependent manner. Comparing the typical downstream pathways of LIF and pathways shown to be used by IL-6 to upregulated PSA (STAT and MAPK), it was found that LNCaP showed differential expression compared to VCaP cells. In response to LIF VCaPs show upregulation of the mTOR, STAT3 and MAPK pathways, which are all known typical signalling pathways downstream of LIF. Whereas LNCaPs did not show phosphorylation of STAT3 or MAPK in response to LIF treatment, suggesting that the downregulation of PSA must be through a different mechanism to the one seen with IL-6.

6.2 Summary of Chapter 4

Chapter 4 provided evidence that LIF could be a tumour suppressor, supporting my earlier findings that LIF was positively associated with disease free survival and increased probability of freedom from BCR. LIF KD in PCa cells showed a significant increase in migration and invasion that was found to be independent of proliferation. As discussed previously, loss of invasiveness could be linked with YAP signalling. In this study cells were seeded to confluency before migration or invasion began. From the results of the previous chapter, if LIF is upregulated in response to confluency and this is involved in loss of invasiveness, then LIF KD cells would have a migration and invasion advantage.

Moreover, long-term LIF overexpression in PCa cells produced cell cycle arrest in G1 phase with an increase in non-proliferative cells in sub G1/G0. rhLIF treatment of PCa cells increased protein expression of p21 in a dose dependent manner which corresponds with the inhibition of G1/S phase transition. Proliferation of LIF overexpression cells long term was shown to be slowed, supporting the cell cycle arrest finding. Johnson *et al* indicated an important role for LIFR in maintaining tumour cells in a dormant state in breast cancer. They suggest that STAT3 signalling in response to LIF confers a dormancy

phenotype (Johnson et al., 2016). In addition to this LIF and LIFR mRNA levels have been shown to be elevated in dormant squamous cell carcinoma cells and that LIFR levels are increased in sub G1/G0 phase cells (Oki et al., 2014) (Sosa et al., 2015). This taken together with the results presented in this thesis suggests that LIF confers cell cycle arrest that may result in a dormant phenotype in PCa cells.

Long-term LIF overexpression was furthermore found to increase sensitivity to Docetaxel. *In silico* analysis revealed that in PC3 and DU145 PCa cells, LIF was significantly decreased in Docetaxel resistant cells and I provided evidence that overexpression of LIF prior to chemotherapy induction, significantly increased their sensitivity to the drug. In the RNA-seq of LIF overexpression PCa cells it was found that the IFN pathway was significantly upregulated, with the typical pathway effector, STAT1 also significantly upregulated. STAT1 is primarily known as a tumour suppressor and can induce cyclin-dependent kinase inhibitors p21 and p27 in a number of cell types, causing cell cycle arrest. Furthermore, STAT1 can upregulate pro-apoptotic regulator such as, BAK and a number of caspases, which play essential roles in programmed cell death. I found that long term LIF overexpression increased apoptosis, this suggests that treatment had an additive effect on the sensitivity to cellular stress posed by Docetaxel.

6.3 Summary of Chapter 5

Chapter 5 suggests that LIF could be a double-edged sword in bone metastatic PCa. *In silico* analysis revealed that upon investigation of the bone marrow microenvironment after human xenograft *in vivo*, LIF gene expression was significantly upregulated compared to control. This was confirmed through my *in vitro*, however unfortunately I was unable to investigate this *in vivo*. PCa cells co-cultured with bone marrow stromal cells gave rise to an upregulation in LIF gene expression specifically in bone stromal cells. This was accompanied by an upregulation of RANKL and a downregulation of OPG, the ratio of which is an important determinant of bone mass and skeletal integrity (Boyce and Xing, 2007). The RANKL pathway is frequently overexpressed in PCa either by the tumour itself or indirectly through osteoblasts and this in turn causes a feedback loop which increases the rate of bone turnover, which can be seen in the form of mixed bone

lesions (Josson et al., 2010). LIF treatment was found to increase differentiation into osteoblasts and decrease differentiation into adipocytes, suggesting that this may occur at the expense of the adipocytes, considering that they share a common precursor (MSCs). Furthermore, conditioned media from LIF overexpression PCa cells specifically was shown to increase RANKL gene expression, raising the possibility that PCa cells do not need to be in close proximity or in contact with stromal cells to increase this expression. As previously described in chapter 3, LIF gene expression is higher in patients with primary PCa. There could therefore be a scenario where as primary PCa cancer secretes LIF, this in turn primes the bone microenvironment to upregulate RANKL.

I also found that LIF was correlated with a weight difference in tumour mice, and with leptin serum levels, a hormone produced by adipocytes (Scarpace et al., 2002). LIF has previously been shown to decrease obesity. With daily LIF injections into mice showing significantly reduced weight of white fat depots and serum leptin levels (Jansson et al., 2006). Cancer cachexia is defined as the systematic loss of body weight that is not diet dependent and not only involves significant loss of fat stores but also muscle mass. The murine model described in this chapter showed a significant loss of weight in cancer mice towards the end of the experiment, this may be due to fat loss, but may also be a loss of muscle. Myostatin is a muscle marker, serum protein levels of which were found to be significantly decreased in the *in vivo* model. I found that *in vitro* LIF treatment of C2C12 cells decreased differentiation into mature myotubes and that this was also the case using PCa conditioned media with high and low baseline levels of LIF. The JAK/STAT and ERK signalling pathways were previously shown to be activated in response to conditioned media treatment from mouse colon carcinoma C26 cells. Seto *et al* showed that LIF induced these signalling pathways as well as causing muscle atrophy in differentiated C2C12 cells (Seto et al., 2015). Together, these suggest that LIF may cause a decrease in weight from late-stage cancer through fat and muscle loss.

6.4 Conclusions

Conclusions that can be drawn from this thesis are; LIF is significantly upregulated in primary PCa, which renders cells sensitive to initial chemotherapy treatment. Furthermore, LIF overexpression cells were shown to grow significantly slower than their empty vector counterpart, which fits with the slow growing nature of primary PCa. Secreted LIF from PCa cells can signal to mature osteoblasts to increase RANKL gene expression, which can upregulate osteoclastogenesis giving rise to osteolytic lesions. Treatment with rhLIF on pre-osteoblastic 2T3 cells also showed that LIF can promote differentiation into mature osteoblasts which could give rise to the sclerotic lesions seen in PCa. Knockdown of LIF increased invasion and migration in PCa cells, with decreased LIF expression seen in metastatic PCa patients, suggesting that LIF is downregulated in metastatic disease. Co-culture systems of metastatic cells and stromal cells upregulated RANKL expression independently of LIF expression and thus metastatic cells can also cause an increase in bone turnover. Upon resorption of the bone matrix, growth factors are released which can be feedback to the cancer cells. Treatment of PCa cells increased p21 expression in a dose dependant manner, with long-term overexpression causing G1 cell cycle arrest and a decrease in cellular proliferation. LIF may induce a slow growing, dormant phenotype in cancer cells, but may also prime the bone osteoblastic niche to create a favourable environment for metastatic cancer growth. Transwell co-culture experiments revealed that downstream signalling of typical LIF pathways such as the JAK/STAT, MAPK and mTOR pathways that were activated in stromal cells are involved in osteoblast differentiation and bone formation, which in turn could induce sclerotic bone lesions (Li, 2013), (Greenblatt et al., 2013), (Chen and Long, 2015) (Figure 6.1). Thus, it is concluded that LIF is a double-edged sword in PCa bone disease, and while it may produce a favourable phenotype in primary disease, it may also produce a negative one in the bone microenvironment. The challenges found in detecting circulating LIF rule out a role as a biomarker, however blockage of LIF specifically in the bone microenvironment may represent a novel therapeutic strategy.

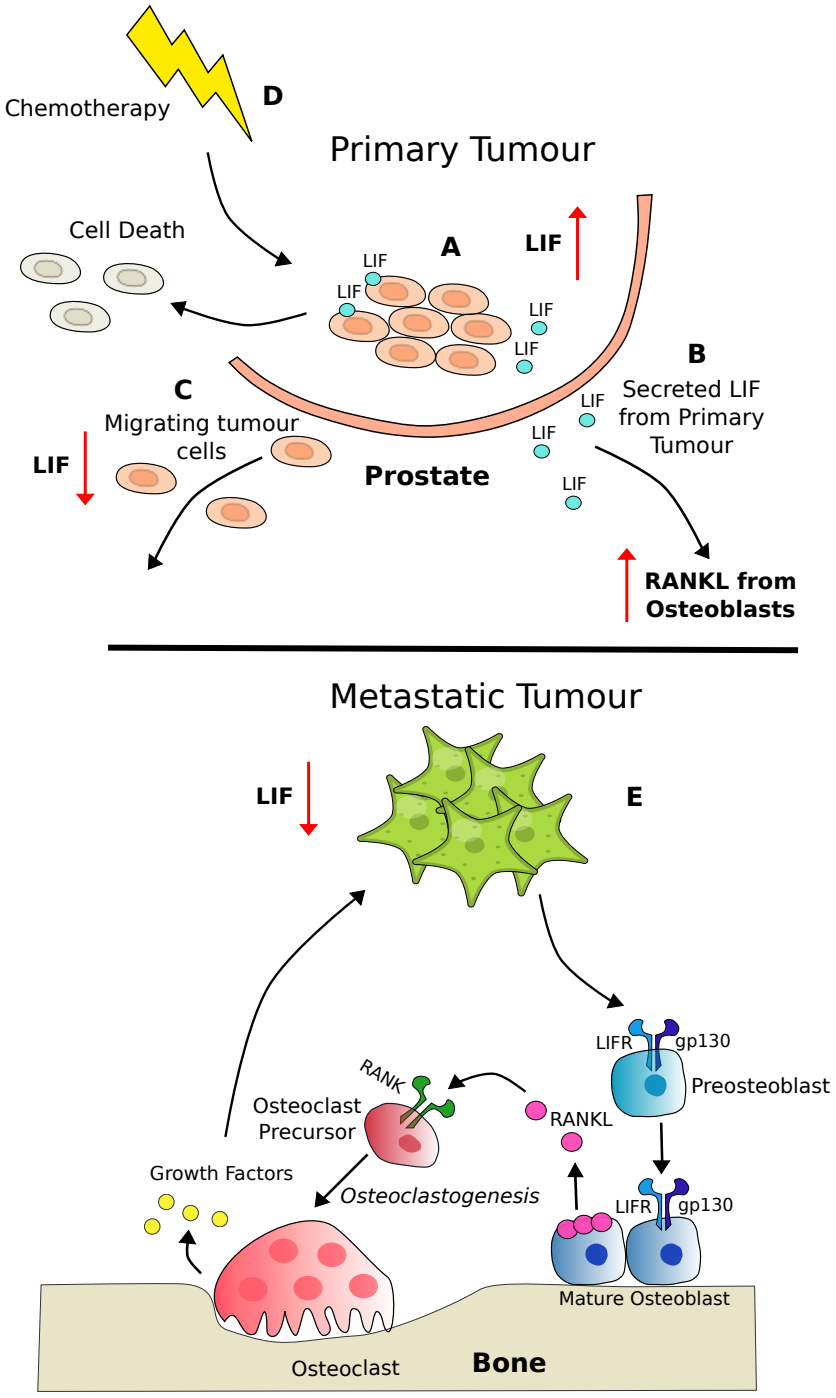


Figure 6.1: **Working model of LIF in prostate cancer.** Primary prostate cancer overexpresses LIF (**A**), which is secreted from the tumour cells and circulates the body. Upon arriving at the bone, LIF can promote pre-osteoblasts into mature osteoblasts, which in turn upregulate RANKL (**B**). RANKL can bind to RANK on osteoclast precursors, differentiating them into mature osteoclasts. These can resorb bone, releasing growth factors. In order for the primary tumour to metastasise, cancer cells downregulate LIF expression, causing an increase in migration and invasion (**C**). LIF expression within the primary tumour renders these cells sensitive to chemotherapy treatment, causing cell death (**D**). Once tumour cells have metastasised to the bone they can also increase bone turnover independently of LIF (**E**).

6.5 Future Directions

6.5.1 To determine how LIF affects different stages of disease

As discussed in previous chapters, LIF may act as a tumour suppressor. LIF overexpression caused significant cell death during selection of stable clones using hygromycin. An explanation for this may be that only a few cells within the whole population have been efficiently transfected. These cells may give rise to a very high level of LIF expression, but once hygromycin selection is initiated, cells that have not been efficiently transfected die off. As such a lentiviral or adenoviral system may give rise to better transfection efficiency, stable clones from which should give rise to the same phenotype as seen through consistent transient transfection. As the PCa cells that were used to create the overexpression construct work very efficiently *in vivo*, it would be interesting to produce a transducible construct that could be used *in vivo*, to investigate the effect of LIF expression in PCa cancer cells at different stages of disease. Moreover, as rhLIF was shown to induce p21 expression, which is associated with inhibition of the G1/S phase transition causing cell cycle arrest, it would also be beneficial to evaluate the effectiveness of rhLIF as a treatment for PCa *in vivo*. As I have shown the potential of LIF to have different effects at different stages of disease, I could create an experiment where rhLIF could be used to answer different questions. The first would involve the intracardiac model, as described in this thesis, rhLIF would be inoculated along with the tumour cells and injected daily for a period of two weeks; developing tumours would then be surveilled using IVIS luminesce imaging. This would answer the question of whether LIF has any effect on the initial homing to bone. The next question would be, if LIF has any effect on tumour development, two approaches could be taken for this. Firstly, an intra-cardiac model could be used and cancer cells inoculated as described before, but instead of injecting rhLIF with initial inoculation, tumours would be allowed to develop for two weeks before injection of rhLIF proceeds. An intra-tibial injection could also be used to isolate tumour development from bone homing in which cells are injected directly into the long bone and followed by treatment with rhLIF to observe if tumour growth is established.

6.5.2 To investigate if changes in LIF regulation and/or expression between localised and metastatic tumours are due to signalling changes or clonal selection

LIF expression from *in silico* analysis of human patient samples showed LIF to be highly expressed in localised/primary disease, whereas in metastatic samples LIF expression was found to be reduced. This change in regulation could either be through reduced signalling or the outgrowth of LIF reduced cancer cells within the primary tumour. Although LIFR expression was found to be reduced in metastatic samples in the Taylor *et al* dataset, the Kumar *et al* dataset showed differences in expression between different probes and thus averaged to be not significant. As such it may be likely that LIF reduced clones may exist within the primary tumour that produce an increase in migration and invasion. This could be investigated through primary PCa biopsies of multiple sites. Immuno-staining would reveal if the expression of LIF was uniformly high or show differences in LIF levels in the primary tumour. This could potentially be clinically followed up showing if tumour with specific LIF expression signatures were more or less likely to give rise to metastasis.

6.5.3 To elucidate if LIF secreted from localised disease primes the bone marrow microenvironment

LIF secreted into the conditioned media from overexpression cancer cells was found to significantly increase the expression of RANKL in mature osteoblasts, suggesting that cancer cells do not need to be in contact or in close proximately to cause this effect. Upregulation of RANKL can give rise to increased bone turnover, which is often seen in bone disease from PCa. In breast cancer it has been shown that inoculation of mice with breast cancer conditioned media gave rise to osteolytic lesions without the presence of cancer cells. Cox *et al* 2015, showed osteolytic lesion formation and cortical bone loss after injection of hypoxic tumour-conditioned media in a tumour-free model (Cox et al., 2015). This suggests that secreted proteins from the tumour can upregulate osteoclastogenesis before the tumour metastasises. I have shown that LIF can promote differentiation into mature osteoblasts and that conditioned media from LIF overexpression cells can increase

RANKL gene expression. This fits with the sclerotic bone lesions formed from rapid increases in bone formation and the osteolytic lesions formed from increases in RANKL, promoting osteoclastogenesis, often seen in PCa. To further investigate this, conditioned media from LIF overexpression and empty vector control PCa cells could be injected into murine models, to establish if bone lesions occur without the presence of cancer cell inoculation.

6.5.4 To observe if LIF upregulation as a result of confluency inhibits Hippo/YAP signalling involved in contact inhibition and reduction of migration

Chen *et al* identified LIFR as a breast cancer metastasis suppressor upstream of the Hippo pathway (Chen et al., 2012). They found that restoring LIFR expression in malignant tumour cells suppressed metastasis by triggering a Hippo kinase cascade that lead to phosphorylation and inactivation of YAP. The inactivation of YAP by the Hippo pathway has been shown to induce contact inhibition and tissue growth control (Zhao et al., 2007). Increased YAP expression has also been linked to metastasis in melanoma, lung and breast cancer (Sharif et al., 2015). Sharif *et al* 2015 showed that by increasing the density of PCa cells their invasiveness significantly reduced. I have shown that LIF is increased with confluency and increased cell density. I have also shown that decreased LIF expression, increased cell migration and invasion in PCa cells. To further investigate this, PCa cells could be grown to confluency as described in chapter 3 and downstream signalling of the Hippo/YAP pathway could be investigated. Treatment of PCa cells with rhLIF would also show if the Hippo/YAP pathway was downstream of LIF. Furthermore, I could determine if the increases in migration and invasion in PCa cells after downregulation of LIF expression was due to increases in YAP signalling through western blot and qRT-PCR.

6.5.5 To investigate prognostic features of innate immune response signatures by the IFN pathway

LIF overexpression was found to induce the innate immune/Type 1 interferon pathway. It has been shown that physiological levels of IFNs inhibit tumour development (Kaplan et al., 1998). High doses of IFNs are now used for cancer therapy due to their anti-proliferative and pro-apoptotic abilities. However, high doses of IFNβ can activate cellular responses so that anti-viral, pro-apoptotic and anti-proliferative proteins are highly expressed. Sustained expression of many of these initial proteins is harmful to cell survival and thus provides a selective advantage to the cells that can tolerate them (Cheon and Stark, 2009). Constant low levels of IFNβ are often seen in cancer and can lead to resistance to DNA damage and can associate with a poorer prognosis (Cheon et al., 2013). As such it would be worth investigating the prognostic features of the IFN pathway activation within clinical datasets described in this thesis using *in silico* analysis.

6.5.6 To determine if LIF treatment causes a synergistic effect in combination with chemotherapy treatment

Two or more treatments that produce similar effects will sometimes exhibit enhanced effect together, producing an additive effect. A synergistic effect enhances the effect to greater than their individual effects, allowing lower doses to be administered and thus reducing adverse reactions (Tallarida, 2011). It was found that LIF overexpression PCa cells significantly increased sensitivity to the chemotherapeutic agent Docetaxel. rhLIF has previously been used in a phase I study on patients with advanced cancer. The study investigated pharmacokinetics, and biological effects and demonstrated haematopoietic recovery after chemotherapy in patients treated with rhLIF. This study however, did not investigate whether rhLIF treatment aided in treatment with chemotherapy (Gunawardana et al., 2003). Thus, there is a precedence that rhLIF can be well tolerated in humans and as our data suggests could be used to increase sensitivity to chemotherapy. As such it would be interesting to investigate a dose range of chemotherapy and rhLIF treatment alone and together to determine if; rhLIF treatment gives rise to the same effect as LIF

overexpression and whether treatment of these two compounds increases apoptotic effects in PCa cells.

Bibliography

Abe, E., Tanaka, H., Ishimi, Y., Miyaura, C., Hayashi, T., Nagasawa, H., Tomida, M., Yamaguchi, Y., Hozumi, M. and Suda, T. (1986), 'Differentiation-inducing factor purified from conditioned medium of mitogen-treated spleen cell cultures stimulates bone resorption.', *Proceedings of the National Academy of Sciences of the United States of America* **83**, 5958–5962.

Adams, J. (1853), 'The case of scirrhous of the prostate gland with corresponding affliction of the lymphatic glands in the lumbar region and in the pelvis', *Lancet* **1**.

Aghajanova, L. (2004), 'Leukemia inhibitory factor and human embryo implantation.', *Ann N Y Acad Sci* **1034**, 176–183.

Aguirre-Ghiso, J. A., Estrada, Y., Liu, D. and Ossowski, L. (2003), 'Erk-mapk activity as a determinant of tumor growth and dormancy; regulation by p38s-apk', *Cancer Research* **63**, 1684.

Aguirre-Ghiso, J. A., Liu, D., Mignatti, A., Kovalski, K., Ossowski, L. and Hunter, T. (2001), 'Urokinase receptor and fibronectin regulate the erkmapk to p38mapk activity ratios that determine carcinoma cell proliferation or dormancy in vivo', *Molecular Biology of the Cell* **12**, 863–879.

Ahima, R. S. and Flier, J. S. (2000), 'Leptin', *Annual Review of Physiology* **62**, 413–437.

Ali, S. A., Kaur, G., Kaushik, J. K., Malakar, D., Mohanty, A. K. and Kumar, S. (2017), 'Examination of pathways involved in leukemia inhibitory factor (lif)-induced cell growth arrest using label-free proteomics approach.', *J Proteomics* **168**, 37–52.

Amundadottir, L. T., Sulem, P., Gudmundsson, J., Helgason, A., Baker, A., Agnarsson, B. A., Sigurdsson, A., Benediktsdottir, K. R., Cazier, J.-B., Sainz, J., Jakobsdottir, M., Kostic, J., Magnusdottir, D. N., Ghosh, S., Agnarsson, K., Birgisdottir, B., Le Roux, L., Olafsdottir, A., Blondal, T., Andresdottir, M., Gretarsdottir, O. S., Bergthorsson, J. T., Gudbjartsson, D., Gylfason, A., Thorleifsson, G., Manolescu, A., Kristjansson, K., Geirsson, G., Isaksson, H., Douglas, J., Johansson, J.-E., Balter, K., Wiklund, F., Montie, J. E., Yu, X., Suarez, B. K., Ober, C., Cooney, K. A., Gronberg, H., Catalona, W. J., Einarsson, G. V., Barkardottir, R. B., Gulcher, J. R., Kong, A., Thorsteinsdottir, U. and Stefansson, K. (2006), 'A common variant associated with prostate cancer in european and african populations.', *Nat Genet* **38**, 652–658.

Ando, K., Mori, K., Rédini, F. and Heymann, D. (2008), 'Rankl/rank/opg: key therapeutic target in bone oncology', *Current Drug Discovery Technologies* **5**, 263–268.

Arita, Y., Kihara, S., Ouchi, N., Takahashi, M., Maeda, K., Miyagawa, J.-i., Hotta, K., Shimomura, I., Nakamura, T., Miyaoka, K., Kuriyama, H., Nishida, M., Yamashita, S., Okubo, K., Matsubara, K., Muraguchi, M., Ohmoto, Y., Funahashi, T. and Matsuzawa, Y. (1999), 'Paradoxical decrease of an adipose-specific protein, adiponectin, in obesity', *Biochemical and Biophysical Research Communications* **257**, 79–83.

Austin, L. and Burgess, A. W. (1991), 'Stimulation of myoblast proliferation in culture by leukaemia inhibitory factor and other cytokines.', *J Neurol Sci* **101**, 193–197.

Autio, K. A. and Morris, M. J. (2013), 'Targeting bone physiology for the treatment of metastatic prostate cancer.', *Clin Adv Hematol Oncol* **11**, 134–143.

Aversa, Z., Costelli, P. and Muscaritoli, M. (2017), 'Cancer-induced muscle wasting: latest findings in prevention and treatment', *Therapeutic Advances in Medical Oncology* **9**, 369–382.

Axel, H., Gunnar, A., Michel, B., Steven, J., B, M. V., Peter, S. H. and Filliberto, Z. (2008), 'Eau guidelines on prostate cancer', *European Urology* **53**, 68 – 80.

Baenke, F., Peck, B., Miess, H. and Schulze, A. (2013), 'Hooked on fat: the role of lipid

synthesis in cancer metabolism and tumour development.', *Dis Model Mech* **6**, 1353–1363.

Baker, J., Ajani, J., Scotte, F., Winther, D., Martin, M., Aapro, M. S. and von Minckwitz, G. (2009), 'Docetaxel-related side effects and their management.', *Eur J Oncol Nurs* **13**, 49–59.

Balk, S. P., Ko, Y.-J. and Bubley, G. J. (2003), 'Biology of prostate-specific antigen.', *J Clin Oncol* **21**, 383–391.

Bellido, T., Borba, V. Z., Roberson, P. and Manolagas, S. C. (1997), 'Activation of the janus kinase/stat (signal transducer and activator of transcription) signal transduction pathway by interleukin-6-type cytokines promotes osteoblast differentiation.', *Endocrinology* **138**, 3666–3676.

Bellido, T., O'Brien, C. A., Roberson, P. K. and Manolagas, S. C. (1998), 'Transcriptional activation of the p21(waf1,cip1,sdi1) gene by interleukin-6 type cytokines. a prerequisite for their pro-differentiating and anti-apoptotic effects on human osteoblastic cells.', *J Biol Chem* **273**, 21137–21144.

Berg, M., Fraker, D. L. and Alexander, H. R. (1994), 'Characterization of differentiation factor/leukaemia inhibitory factor effect on lipoprotein lipase activity and mrna in 3t3-l1 adipocytes.', *Cytokine* **6**, 425 – 432.

Berruti, A., Dogliotti, L., Bitossi, R., Fasolis, G., Gorzegno, G., Bellina, M., Torta, M., Porpiglia, F., Fontana, D. and Angeli, A. (2000), 'incidence of skeletal complications in patients with bone metastatic prostate cancer and hormone refractory disease: predictive role of bone resorption and formation markers evaluated at baseline', *The Journal of Urology* **164**, 1248 – 1253.

Berry, P. A., Maitland, N. J. and Collins, A. T. (2008), 'Androgen receptor signalling in prostate: effects of stromal factors on normal and cancer stem cells.', *Mol Cell Endocrinol* **288**, 30–37.

Blücher, C. and Stadler, S. C. (2017), 'Obesity and breast cancer: Current insights on

the role of fatty acids and lipid metabolism in promoting breast cancer growth and progression', *Frontiers in Endocrinology* **8**, 293.

Borovinskaya, M. A., Shoji, S., Fredrick, K. and Cate, J. H. D. (2008), 'Structural basis for hygromycin b inhibition of protein biosynthesis.', *RNA* **14**, 1590–1599.

Boyce, B. F. and Xing, L. (2007), 'Biology of rank, rankl, and osteoprotegerin.', *Arthritis Res Ther* **9**, S1.

Bredella, M. A., Fazeli, P. K., Miller, K. K., Misra, M., Torriani, M., Thomas, B. J., Ghomi, R. H., Rosen, C. J. and Klibanski, A. (2009), 'Increased bone marrow fat in anorexia nervosa', *The Journal of Clinical Endocrinology and Metabolism* **94**, 2129–2136.

Briganti, A., Suardi, N., Gallina, A., Abdollah, F., Novara, G., Ficarra, V. and Montorsi, F. (2013), 'Predicting the risk of bone metastasis in prostate cancer', *Cancer Treatment Reviews* **40**, 3–11.

Bromberg, J. F., Horvath, C. M., Wen, Z., Schreiber, R. D. and Darnell, J. E. J. (1996), 'Transcriptionally active stat1 is required for the antiproliferative effects of both interferon alpha and interferon gamma.', *Proc Natl Acad Sci U S A* **93**, 7673–7678.

Bussemakers, M. J., van Bokhoven, A., Verhaegh, G. W., Smit, F. P., Karthaus, H. F., Schalken, J. A., Debruyne, F. M., Ru, N. and Isaacs, W. B. (1999), 'Dd3: a new prostate-specific gene, highly overexpressed in prostate cancer.', *Cancer Res* **59**, 5975–5979.

Carson, D. D., Bagchi, I., Dey, S. K., Enders, A. C., Fazleabas, A. T., Lessey, B. A. and Yoshinaga, K. (2000), 'Embryo implantation', *Developmental Biology* **223**, 217 – 237.

Chantrain, C. F., Feron, O., Marbaix, E. and DeClerck, Y. A. (2008), 'Bone marrow microenvironment and tumor progression.', *Cancer Microenviron* **1**, 23–35.

Chapman, G., Banks, J., Fanning, L., Kozik, M., Finney, M., Weitzel, R., Greco, N., Sakthivel, R. and Laughlin, M. J. (2006), 'Leukemia inhibitory factor (lif): Marrow-derived human mesenchymal stem cell (humsc) secretion and potential impact on umbilical cord

blood (ucb) cd133+ hematopoietic stem cells (hsc) differentiation.', *Blood* **108**, 4262–4262.

Chen, D., Sun, Y., Wei, Y., Zhang, P., Rezaeian, A. H., Teruya-Feldstein, J., Gupta, S., Liang, H., Lin, H.-K., Hung, M.-C. and Ma, L. (2012), 'Lifr is a breast cancer metastasis suppressor upstream of the hippo-yap pathway and a prognostic marker.', *Nat Med* **18**, 1511–1517.

Chen, G., Hitomi, M., Han, J. and Stacey, D. W. (2000), 'The p38 pathway provides negative feedback for ras proliferative signaling.', *J Biol Chem* **275**, 38973–38980.

Chen, J. and Long, F. (2015), 'mtorc1 signaling promotes osteoblast differentiation from preosteoblasts', *PLoS ONE* **10**, e0130627.

Cheon, H., Holvey-Bates, E. G., Schoggins, J. W., Forster, S., Hertzog, P., Imanaka, N., Rice, C. M., Jackson, M. W., Junk, D. J. and Stark, G. R. (2013), 'Ifnβ-dependent increases in stat1, stat2, and irf9 mediate resistance to viruses and dna damage', *The EMBO Journal* **32**, 2751–2763.

Cheon, H. and Stark, G. R. (2009), 'Unphosphorylated stat1 prolongs the expression of interferon-induced immune regulatory genes.', *Proc Natl Acad Sci U S A* **106**, 9373–9378.

Clarke, B. (2008), 'Normal bone anatomy and physiology.', *Clin J Am Soc Nephrol* **3**, S131–9.

Coleman, R. E. (1997), 'Skeletal complications of malignancy', *Cancer* **80**, 1588–1594.

Coleman, R. E., Guise, T. A., Lipton, A., Roodman, G. D., Berenson, J. R., Body, J.-J., Boyce, B. F., Calvi, L. M., Hadji, P., McCloskey, E. V., Saad, F., Smith, M. R., Suva, L. J., Taichman, R. S., Vessella, R. L. and Weilbaecher, K. N. (2008), 'Advancing treatment for metastatic bone cancer: Consensus recommendations from the second cambridge conference', *Clinical cancer research : an official journal of the American Association for Cancer Research* **14**, 6387–6395.

Coleman, R. E. and McCloskey, E. V. (2011), 'Bisphosphonates in oncology.', *Bone* **49**, 71–76.

Collin, S. M., Metcalfe, C., Donovan, J., Lane, J. A., Davis, M., Neal, D., Hamdy, F. and Martin, R. M. (2008), 'Associations of lower urinary tract symptoms with prostate-specific antigen levels, and screen-detected localized and advanced prostate cancer: a case-control study nested within the uk population-based protect (prostate testing for cancer and treatment) study.', *BJU Int* **102**, 1400–1406.

Cornford, P., Bellmunt, J., Bolla, M., Briers, E., De Santis, M., Gross, T., Henry, A. M., Joniau, S., Lam, T. B., Mason, M. D., van der Poel, H. G., van der Kwast, T. H., Rouvière, O., Wiegel, T. and Mottet, N. (2017), 'Eau-estro-siog guidelines on prostate cancer. part ii: Treatment of relapsing, metastatic, and castration-resistant prostate cancer', *European Urology* **71**, 630–642.

Cornish, J., Callon, K., King, A., Edgar, S. and Reid, I. R. (1993), 'The effect of leukemia inhibitory factor on bone in vivo.', *Endocrinology* **132**, 1359–1366.

Costa, V., Aprile, M., Esposito, R. and Ciccodicola, A. (2013), 'Rna-seq and human complex diseases: recent accomplishments and future perspectives.', *Eur J Hum Genet* **21**, 134–142.

Cox, T. R., Rumney, R. M. H., Schoof, E. M., Perryman, L., Høye, A. M., Agrawal, A., Bird, D., Latif, N. A., Forrest, H., Evans, H. R., Huggins, I. D., Lang, G., Linding, R., Gartland, A. and Erler, J. T. (2015), 'The hypoxic cancer secretome induces pre-metastatic bone lesions through lysyl oxidase', *Nature* **522**, 106 –110.

Culig, Z. (2014), 'Proinflammatory cytokine interleukin-6 in prostate carcinogenesis', *American Journal of Clinical and Experimental Urology* **2**, 231–238.

Culig, Z., Klocker, H., Bartsch, G. and Hobisch, A. (2002), 'Androgen receptors in prostate cancer.', *Endocr Relat Cancer* **9**, 155–170.

Curtis, R., Scherer, S. S., Somogyi, R., Adryan, K. M., Ip, N. Y., Zhu, Y., Lindsay, R. M. and DiStefano, P. S. (1994), 'Retrograde axonal transport of lif is increased

by peripheral nerve injury: correlation with increased lif expression in distal nerve.', *Neuron* **12**, 191–204.

Darzynkiewicz, Z., Bedner, E. and Smolewski, P. (2001), 'Flow cytometry in analysis of cell cycle and apoptosis.', *Semin Hematol* **38**, 179–193.

Denmeade, S. R. and Isaacs, J. T. (2002), 'A history of prostate cancer treatment', *Nature Reviews Cancer* **2**, 389 – 396.

Di Lorenzo, G., Figg, W. D., Fossa, S. D., Mirone, V., Autorino, R., Longo, N., Imbimbo, C., Perdona, S., Giordano, A., Giuliano, M., Labianca, R. and De Placido, S. (2008), 'Combination of bevacizumab and docetaxel in docetaxel-pretreated hormone-refractory prostate cancer: a phase 2 study.', *Eur Urol* **54**, 1089–1094.

Eisenberger, M. A. and Walsh, P. C. (1999), 'Early androgen deprivation for prostate cancer?', *N Engl J Med* **341**, 1837–1838.

El-Deiry, W. S. (2016), 'p21(waf1) mediates cell cycle inhibition, relevant to cancer suppression and therapy', *Cancer research* **76**, 5189–5191.

Engels, F. K., Sparreboom, A., Mathot, R. A. A. and Verweij, J. (2005), 'Potential for improvement of docetaxel-based chemotherapy: a pharmacological review.', *Br J Cancer* **93**, 173–177.

Escary, J.-L., Perreau, J., Duménil, D., Ezine, S. and Brûlet, P. (1993), 'Leukaemia inhibitory factor is necessary for maintenance of haematopoietic stem cells and thymocyte stimulation', *Nature* **363**, 361 – 364.

Falconi, D. and Aubin, J. E. (2007), 'Lif inhibits osteoblast differentiation at least in part by regulation of has2 and its product hyaluronan.', *J Bone Miner Res* **22**, 1289–1300.

Fidler, I. J. (2003), 'The pathogenesis of cancer metastasis: the 'seed and soil' hypothesis revisited.', *Nat Rev Cancer* **3**, 453–458.

Finkelstein, D., Bartlett, P., Horne, M. and Cheema, S. (1996), 'Leukemia inhibitory factor is a myotrophic and neurotrophic agent that enhances the reinnervation of muscle in the rat', *Journal of Neuroscience Research* **46**, 122–128.

Fruebis, J., Tsao, T.-S., Javorschi, S., Ebbets-Reed, D., Erickson, M. R. S., Yen, F. T., Bihain, B. E. and Lodish, H. F. (2001), 'Proteolytic cleavage product of 30-kda adipocyte complement-related protein increases fatty acid oxidation in muscle and causes weight loss in mice', *Proceedings of the National Academy of Sciences* **98**, 2005.

Gavrieli, Y., Sherman, Y. and Ben-Sasson, S. A. (1992), 'Identification of programmed cell death in situ via specific labeling of nuclear dna fragmentation.', *J Cell Biol* **119**, 493–501.

Gimble, J. M., Wanker, F., Wang, C. S., Bass, H., Wu, X., Kelly, K., Yancopoulos, G. D. and Hill, M. R. (1994), 'Regulation of bone marrow stromal cell differentiation by cytokines whose receptors share the gp130 protein.', *J Cell Biochem* **54**, 122–133.

Gleason, D. F. (1992), 'Histologic grading of prostate cancer: a perspective.', *Hum Pathol* **23**, 273–279.

Gough, N. M. (1992), 'Molecular genetics of leukemia inhibitory factor (lif) and its receptor.', *Growth Factors* **7**, 175–179.

Greenberg, N. M., DeMayo, F., Finegold, M. J., Medina, D., Tilley, W. D., Aspinall, J. O., Cunha, G. R., Donjacour, A. A., Matusik, R. J. and Rosen, J. M. (1995), 'Prostate cancer in a transgenic mouse.', *Proc Natl Acad Sci U S A* **92**, 3439–3443.

Greenblatt, M. B., Shim, J.-H. and Glimcher, L. H. (2013), 'Mitogen-activated protein kinase pathways in osteoblasts.', *Annu Rev Cell Dev Biol* **29**, 63–79.

Grönberg, H. (2003), 'Prostate cancer epidemiology', *The Lancet* **361**, 859–864.

Guise, T. A. (2002), 'The vicious cycle of bone metastases.', *J Musculoskelet Neuronal Interact* **2**, 570–572.

Gunawardana, D. H., Basser, R. L., Davis, I. D., Cebon, J., Mitchell, P., Underhill, C., Kilpatrick, T. J., Reardon, K., Green, M. D., Bardy, P., Amor, P., Crump, D., Ng, S., Nation, R. L. and Begley, C. G. (2003), 'A phase i study of recombinant human leukemia inhibitory factor in patients with advanced cancer.', *Clin Cancer Res* **9**, 2056–2065.

Haines, B. P., Voyle, R. B. and Rathjen, P. D. (2000), 'Intracellular and extracellular leukemia inhibitory factor proteins have different cellular activities that are mediated by distinct protein motifs', *Molecular Biology of the Cell* **11**, 1369–1383.

Hanahan, D. and Weinberg, R. A. (2011), 'Hallmarks of cancer: The next generation', *Cell* **144**, 646–674.

Hardaway, A. L., Herroon, M. K., Rajagurubandara, E. and Podgorski, I. (2014), 'Bone marrow fat: linking adipocyte-induced inflammation with skeletal metastases.', *Cancer Metastasis Rev* **33**, 527–543.

Hardaway, A. L., Herroon, M. K., Rajagurubandara, E. and Podgorski, I. (2015), 'Marrow adipocyte-derived cxcl1 and cxcl2 contribute to bone osteolysis in metastatic prostate cancer', *Clinical & experimental metastasis* **32**, 353–368.

Heemers, H. V., Regan, K. M., Schmidt, L. J., Anderson, S. K., Ballman, K. V. and Tindall, D. J. (2009), 'Androgen modulation of coregulator expression in prostate cancer cells', *Molecular Endocrinology* **23**, 572–583.

Hendriks, R. J., van Oort, I. M. and Schalken, J. A. (2017), 'Blood-based and urinary prostate cancer biomarkers: a review and comparison of novel biomarkers for detection and treatment decisions.', *Prostate Cancer Prostatic Dis* **20**, 12–19.

Herroon, M. K., Rajagurubandara, E., Hardaway, A. L., Powell, K., Turchick, A., Feldmann, D. and Podgorski, I. (2013), 'Bone marrow adipocytes promote tumor growth in bone via fabp4-dependent mechanisms.', *Oncotarget* **4**, 2108–2123.

Hess, K. R., Varadhachary, G. R., Taylor, S. H., Wei, W., Raber, M. N., Lenzi, R. and Abbruzzese, J. L. (2006), 'Metastatic patterns in adenocarcinoma.', *Cancer* **106**, 1624–1633.

Hessels, D., Smit, F. P., Verhaegh, G. W., Witjes, J. A., Cornel, E. B. and Schalken, J. A. (2007), 'Detection of tmprss2-erg fusion transcripts and prostate cancer antigen 3 in urinary sediments may improve diagnosis of prostate cancer.', *Clin Cancer Res* **13**, 5103–5108.

Heymann, D. and Rousselle, A.-V. (2000), 'gp130 cytokine family and bone cells', *Cytokine* **12**, 1455 – 1468.

Hsieh, C.-L., Xie, Z., Yu, J., Martin, W. D., Datta, M. W., Wu, G.-J. and Chung, L. W. K. (2007), 'Non-invasive bioluminescent detection of prostate cancer growth and metastasis in a bigenic transgenic mouse model.', *Prostate* **67**, 685–691.

Huang, L., Cheng, Y. Y., Chow, L. T. C., Zheng, M. H. and Kumta, S. M. (2002), 'Tumour cells produce receptor activator of nf-kappab ligand (rankl) in skeletal metastases.', *J Clin Pathol* **55**, 877–878.

Humbert, L., Ghozlan, M., Canaff, L., Tian, J. and Lebrun, J.-J. (2015), 'The leukemia inhibitory factor (lif) and p21 mediate the tgfβ tumor suppressive effects in human cutaneous melanoma', *BMC Cancer* **15**, 200.

Iorns, E., Ward, T. M., Dean, S., Jegg, A., Thomas, D., Murugaesu, N., Sims, D., Mitsopoulos, C., Fenwick, K., Kozarewa, I., Naceur-Lombarelli, C., Zvelebil, M., Isacke, C. M., Lord, C. J., Ashworth, A., Hnatyszyn, H. J., Pegram, M. and Lippman, M. (2012), 'Whole genome in vivo rnai screening identifies the leukemia inhibitory factor receptor as a novel breast tumor suppressor', *Breast Cancer Research and Treatment* **135**, 79–91.

Itoh, S., Udagawa, N., Takahashi, N., Yoshitake, F., Narita, H., Ebisu, S. and Ishihara, K. (2006), 'A critical role for interleukin-6 family-mediated stat3 activation in osteoblast differentiation and bone formation', *Bone* **39**, 505–512.

Ittmann, M., Huang, J., Radaelli, E., Martin, P., Signoretti, S., Sullivan, R., Simons, B. W., Ward, J. M., Robinson, B. D., Chu, G. C., Loda, M., Thomas, G., Borowsky, A. and Cardiff, R. D. (2013), 'Animal models of human prostate cancer: The consensus report of the new york meeting of the mouse models of human cancers consortium prostate pathology committee', *Cancer research* **73**, 2718–2736.

Ivashkiv, L. B. and Donlin, L. T. (2014), 'Regulation of type i interferon responses', *Nature reviews. Immunology* **14**, 36–49.

Janjan, N., Lutz, S. T., Bedwinek, J. M., Hartsell, W. F., Ng, A., Pieters, R. S., Ratanatharathorn, V., Silberstein, E. B., Taub, R. J., Yasko, A. W. and Rettenmaier, A. (2009), 'Therapeutic guidelines for the treatment of bone metastasis: A report from the american college of radiology appropriateness criteria expert panel on radiation oncology', *Journal of Palliative Medicine* **12**, 417–426.

Janssens, K., Van den Haute, C., Baekelandt, V., Lucas, S., van Horssen, J., Somers, V., Van Wijmeersch, B., Stinissen, P., Hendriks, J. J. A., Slaets, H. and Hellings, N. (2015), 'Leukemia inhibitory factor tips the immune balance towards regulatory t cells in multiple sclerosis.', *Brain Behav Immun* **45**, 180–188.

Jansson, J.-O., Moverare-Skrtic, S., Berndtsson, A., Wernstedt, I., Carlsten, H. and Ohlsson, C. (2006), 'Leukemia inhibitory factor reduces body fat mass in ovariectomized mice.', *Eur J Endocrinol* **154**, 349–354.

Jean-Marc, F. (2008), 'Is my antibody-staining specific? how to deal with pitfalls of immunohistochemistry', *European Journal of Neuroscience* **28**, 2365–2370.

Jin, J.-K., Dayyani, F. and Gallick, G. E. (2011), 'Steps in prostate cancer progression that lead to bone metastasis.', *Int J Cancer* **128**, 2545–2561.

Johnson, R. W., Finger, E. C., Olcina, M. M., Vilalta, M., Aguilera, T., Miao, Y., Merkel, A. R., Johnson, J. R., Sterling, J. A., Wu, J. Y. and Giaccia, A. J. (2016), 'Induction of lifr confers a dormancy phenotype in breast cancer cells disseminated to the bone marrow', *Nature cell biology* **18**, 1078–1089.

Josson, S., Matsuoka, Y., Chung, L. W. K., Zhau, H. E. and Wang, R. (2010), 'Tumor-stroma co-evolution in prostate cancer progression and metastasis.', *Semin Cell Dev Biol* **21**, 26–32.

Jung, Y., Kim, J. K., Shiozawa, Y., Wang, J., Mishra, A., Joseph, J., Berry, J. E., McGee, S., Lee, E., Sun, H., Wang, J., Jin, T., Zhang, H., Dai, J., Krebsbach, P. H., Keller, E. T., Pienta, K. J. and Taichman, R. S. (2013), 'Recruitment of mesenchymal stem cells into prostate tumours promotes metastasis.', *Nat Commun* **4**, 1795.

Kaplan, D. H., Shankaran, V., Dighe, A. S., Stockert, E., Aguet, M., Old, L. J. and Schreiber, R. D. (1998), 'Demonstration of an interferon γ-dependent tumor surveillance system in immunocompetent mice', *Proceedings of the National Academy of Sciences of the United States of America* **95**, 7556–7561.

Kaplan-Lefko, P. J., Chen, T.-M., Ittmann, M. M., Barrios, R. J., Ayala, G. E., Huss, W. J., Maddison, L. A., Foster, B. A. and Greenberg, N. M. (2003), 'Pathobiology of autochthonous prostate cancer in a pre-clinical transgenic mouse model.', *Prostate* **55**, 219–237.

Kaplan, R. N., Psaila, B. and Lyden, D. (2006), 'Bone marrow cells in the 'pre-metastatic niche': within bone and beyond.', *Cancer Metastasis Rev* **25**, 521–529.

Karantanos, T., Corn, P. G. and Thompson, T. C. (2013), 'Prostate cancer progression after androgen deprivation therapy: mechanisms of castrate-resistance and novel therapeutic approaches', *Oncogene* **32**, 5501–5511.

Kelly, W. K., Halabi, S., Carducci, M., George, D., Mahoney, J. F., Stadler, W. M., Morris, M., Kantoff, P., Monk, J. P., Kaplan, E., Vogelzang, N. J. and Small, E. J. (2012), 'Randomized, double-blind, placebo-controlled phase iii trial comparing docetaxel and prednisone with or without bevacizumab in men with metastatic castration-resistant prostate cancer: Calgb 90401.', *J Clin Oncol* **30**, 1534–1540.

Kheirandish, P. and Chinegwundoh, F. (2011), 'Ethnic differences in prostate cancer', *British Journal of Cancer* **105**, 481–485.

Kiciński, M., Vangronsveld, J. and Nawrot, T. S. (2011), 'An epidemiological reappraisal of the familial aggregation of prostate cancer: A meta-analysis', *PLOS ONE* **6**, 1–7.

Kim, H.-B. and Myung, S.-J. (2018), 'Clinical implications of the hippo-yap pathway in multiple cancer contexts', *BMB Reports* **51**, 119–125.

Kim, H. S. and Lee, M.-S. (2007), 'Stat1 as a key modulator of cell death.', *Cell Signal* **19**, 454–465.

Kim, M. J., Bhatia-Gaur, R., Banach-Petrosky, W. A., Desai, N., Wang, Y., Hayward, S. W., Cunha, G. R., Cardiff, R. D., Shen, M. M. and Abate-Shen, C. (2002), 'Nkx3.1 mutant mice recapitulate early stages of prostate carcinogenesis.', *Cancer Res* **62**, 2999–3004.

Kir, S. and Spiegelman, B. M. (2016), 'Cachexia & brown fat: A burning issue in cancer', *Trends in cancer* **2**, 461–463.

Kritikou, E. A., Sharkey, A., Abell, K., Came, P. J., Anderson, E., Clarkson, R. W. E. and Watson, C. J. (2003), 'A dual, non-redundant, role for lif as a regulator of development and stat3-mediated cell death in mammary gland', *Development* **130**(15), 3459–3468.

Kumar, A., Coleman, I., Morrissey, C., Zhang, X., True, L. D., Gulati, R., Etzioni, R., Bolouri, H., Montgomery, B., White, T., Lucas, J. M., Brown, L. G., Dumpit, R. F., DeSarkar, N., Higano, C., Yu, E. Y., Coleman, R., Schultz, N., Fang, M., Lange, P. H., Shendure, J., Vessella, R. L. and Nelson, P. S. (2016), 'Substantial interindividual and limited intraindividual genomic diversity among tumors from men with metastatic prostate cancer.', *Nat Med* **22**, 369–378.

Kuphal, S., Wallner, S. and Bosserhoff, A. K. (2013), 'Impact of lif (leukemia inhibitory factor) expression in malignant melanoma.', *Exp Mol Pathol* **95**, 156–165.

Kyprianou, N. and Isaacs, J. t. (1988), 'Activation of programmed cell death in the rat ventral prostate after castration', *Endocrinology* **122**, 552–562.

Lang, S. H., Miller, W. R. and Habib, F. K. (1995), 'Stimulation of human prostate cancer cell lines by factors present in human osteoblast-like cells but not in bone marrow.', *Prostate* **27**, 287–293.

Langley, B., Thomas, M., Bishop, A., Sharma, M., Gilmour, S. and Kambadur, R. (2002), 'Myostatin inhibits myoblast differentiation by down-regulating myod expression.', *J Biol Chem* **277**, 49831–49840.

Lee, C. H. and Yoon, H.-J. (2017), 'Medical big data: promise and challenges', *Kidney Research and Clinical Practice* **36**, 3–11.

Li, J. (2013), 'Jak-stat and bone metabolism', *JAK-STAT* **2**, e23930.

Li, X., Sterling, J. A., Fan, K.-H., Vessella, R. L., Shyr, Y., Hayward, S. W., Matrisian, L. M. and Bhowmick, N. A. (2012), 'Loss of tgf-beta responsiveness in prostate stromal cells alters chemokine levels and facilitates the development of mixed osteoblastic/osteolytic bone lesions.', *Mol Cancer Res* **10**, 494–503.

Li, X., Yang, Q., Yu, H., Wu, L., Zhao, Y., Zhang, C., Yue, X., Liu, Z., Wu, H., Haffty, B., Feng, Z. and Hu, W. (2014), 'Lif promotes tumorigenesis and metastasis of breast cancer through the akt-mtor pathway', *Oncotarget* **5**, 788 – 801.

Lilja, H., Ulmert, D. and Vickers, A. J. (2008), 'Prostate-specific antigen and prostate cancer: prediction, detection and monitoring.', *Nat Rev Cancer* **8**, 268–278.

Lin, D. L., Whitney, M. C., Yao, Z. and Keller, E. T. (2001), 'Interleukin-6 induces androgen responsiveness in prostate cancer cells through up-regulation of androgen receptor expression.', *Clin Cancer Res* **7**, 1773–1781.

Lipton, A., Fizazi, K., Stopeck, A. T., Henry, D. H., Brown, J. E., Yardley, D. A., Richardson, G. E., Siena, S., Maroto, P., Clemens, M., Bilynskyy, B., Charu, V., Beuzeboc, P., Rader, M., Viniegra, M., Saad, F., Ke, C., Braun, A. and Jun, S. (2012), 'Superiority of denosumab to zoledronic acid for prevention of skeletal-related events: a combined analysis of 3 pivotal, randomised, phase 3 trials.', *Eur J Cancer* **48**, 3082–3092.

Logothetis, C. J. and Lin, S.-H. (2005), 'Osteoblasts in prostate cancer metastasis to bone.', *Nat Rev Cancer* **5**, 21–28.

Lowe, C., Gillespie, G. A. and Pike, J. W. (1995), 'Leukemia inhibitory factor as a mediator of jak/stat activation in murine osteoblasts.', *J Bone Miner Res* **10**, 1644–1650.

Luo, J., Ok Lee, S., Liang, L., Huang, C.-K., Li, L., Wen, S. and Chang, C. (2014), 'Infiltrating bone marrow mesenchymal stem cells increase prostate cancer stem cell population and metastatic ability via secreting cytokines to suppress androgen receptor signaling.', *Oncogene* **33**, 2768–2778.

Ma, W., Song, H., Das, S. K., Paria, B. C. and Dey, S. K. (2003), 'Estrogen is a critical determinant that specifies the duration of the window of uterine receptivity for implantation', *Proceedings of the National Academy of Sciences of the United States of America* **100**, 2963–2968.

Malaval, L. and Aubin, J. E. (2001), 'Biphasic effects of leukemia inhibitory factor on osteoblastic differentiation.', *J Cell Biochem Suppl* **36**, 63–70.

Malaval, L., Liu, F., Vernallis, A. B. and Aubin, J. E. (2005), 'Gp130/osmr is the only lif/il-6 family receptor complex to promote osteoblast differentiation of calvaria progenitors.', *J Cell Physiol* **204**, 585–593.

Malumbres, M. and Barbacid, M. (2009), 'Cell cycle, cdks and cancer: a changing paradigm', *Nature Reviews Cancer* **9**, 153 – 166.

Marker, P. C., Donjacour, A. A., Dahiya, R. and Cunha, G. R. (2003), 'Hormonal, cellular, and molecular control of prostatic development.', *Dev Biol* **253**, 165–174.

Mastroyiannopoulos, N. P., Nicolaou, P., Anayasa, M., Uney, J. B. and Phylactou, L. A. (2012), 'Down-regulation of myogenin can reverse terminal muscle cell differentiation', *PLoS ONE* **7**, e29896.

Mathieu, M.-E., Saucourt, C., Mournetas, V., Gauthereau, X., Thézé, N., Praloran, V., Thiébaud, P. and Bœuf, H. (2012), 'Lif-dependent signaling: New pieces in the lego', *Stem Cell Reviews* **8**, 1–15.

Meissl, K., Macho-Maschler, S., Muller, M. and Strobl, B. (2017), 'The good and the bad faces of stat1 in solid tumours.', *Cytokine* **89**, 12–20.

Metcalf, D. (1991), 'The leukemia inhibitory factor (lif)', *The International Journal of Cell Cloning* **9**, 95–108.

Metcalf, D. and Gearing, D. P. (1989), 'Fatal syndrome in mice engrafted with cells producing high levels of the leukemia inhibitory factor.', *Proc Natl Acad Sci U S A* **86**, 5948–5952.

Morris-Hanon, O., Furmento, V. A., Rodriguez-Varela, M. S., Mucci, S., Fernandez-Espinosa, D. D., Romorini, L., Sevlever, G. E., Scassa, M. E. and Videla-Richardson, G. A. (2017), 'The cell cycle inhibitors p21(cip1) and p27(kip1) control proliferation but enhance dna damage resistance of glioma stem cells.', *Neoplasia* **19**, 519–529.

Mottet, N., Bellmunt, J., Bolla, M., Briers, E., Cumberbatch, M. G., De Santis, M., Fossati, N., Gross, T., Henry, A. M., Joniau, S., Lam, T. B., Mason, M. D., Matveev, V. B., Moldovan, P. C., van den Bergh, R. C. N., Van den Broeck, T., van der Poel, H. G., van der Kwast, T. H., Rouvière, O., Schoots, I. G., Wiegel, T. and Cornford, P. (2017), 'Eau-estro-siog guidelines on prostate cancer. part 1: Screening, diagnosis, and local treatment with curative intent', *European Urology* **71**, 618–629.

Mundy, G. R. (2002), 'Metastasis to bone: causes, consequences and therapeutic opportunities.', *Nat Rev Cancer* **2**, 584–593.

Muralidharan, A. and Smith, M. T. (2013), 'Pathobiology and management of prostate cancer-induced bone pain: recent insights and future treatments.', *Inflammopharmacology* **21**, 339–363.

Murphy, M., Dutton, R., Koblar, S., Cheema, S. and Bartlett, P. (1997), 'Cytokines which signal through the lif receptor and their actions in the nervous system.', *Prog Neurobiol* **52**, 355–378.

Nelson, P. J. and Daniel, T. O. (2002), 'Emerging targets: molecular mechanisms of cell contact-mediated growth control.', *Kidney Int* **61**, 99–105.

Nicola, N. A. and Babon, J. J. (2015), 'Leukemia inhibitory factor (lif).', *Cytokine Growth Factor Rev* **26**, 533–544.

Nicoletti, I., Migliorati, G., Pagliacci, M. C., Grignani, F. and Riccardi, C. (1991), 'A rapid and simple method for measuring thymocyte apoptosis by propidium iodide staining and flow cytometry', *Journal of Immunological Methods* **139**(2), 271–279.

O'Brien, C. A., Gubrij, I., Lin, S. C., Saylors, R. L. and Manolagas, S. C. (1999), 'Stat3 activation in stromal/osteoblastic cells is required for induction of the receptor activator

of nf-kappab ligand and stimulation of osteoclastogenesis by gp130-utilizing cytokines or interleukin-1 but not 1,25-dihydroxyvitamin d3 or parathyroid hormone.', *J Biol Chem* **274**, 19301–19308.

Oki, T., Nishimura, K., Kitaura, J., Togami, K., Maehara, A., Izawa, K., Sakaue-Sawano, A., Niida, A., Miyano, S., Aburatani, H., Kiyonari, H., Miyawaki, A. and Kitamura, T. (2014), 'A novel cell-cycle-indicator, mvenus-p27k-, identifies quiescent cells and visualizes g0-g1 transition.', *Sci Rep* **4**, 4012.

Ormerod, M. G., Collins, M. K., Rodriguez-Tarduchy, G. and Robertson, D. (1992), 'Apoptosis in interleukin-3-dependent haemopoietic cells. quantification by two flow cytometric methods.', *J Immunol Methods* **153**, 57–65.

Ozdemir, B. C., Hensel, J., Secondini, C., Wetterwald, A., Schwaninger, R., Fleischmann, A., Raffelsberger, W., Poch, O., Delorenzi, M., Temanni, R., Mills, I. G., van der Pluijm, G., Thalmann, G. N. and Cecchini, M. G. (2014), 'The molecular signature of the stroma response in prostate cancer-induced osteoblastic bone metastasis highlights expansion of hematopoietic and prostate epithelial stem cell niches.', *PLoS One* **9**(12), e114530.

Palmqvist, P., Persson, E., Conaway, H. H. and Lerner, U. H. (2002), 'Il-6, leukemia inhibitory factor, and oncostatin m stimulate bone resorption and regulate the expression of receptor activator of nf-kb ligand, osteoprotegerin, and receptor activator of nf-kb in mouse calvariae', *The Journal of Immunology* **169**, 3353–3362.

Park, S. I., Kim, S. J., McCauley, L. K. and Gallick, G. E. (2010), 'Pre-clinical mouse models of human prostate cancer and their utility in drug discovery.', *Curr Protoc Pharmacol* **Chapter 14**, Unit 14.15.

Parker, C., Nilsson, S., Heinrich, D., Helle, S. I., O'Sullivan, J. M., Fosså, S. D., Chodacki, A., Wiechno, P., Logue, J., Seke, M., Widmark, A., Johannessen, D. C., Hoskin, P., Bottomley, D., James, N. D., Solberg, A., Syndikus, I., Kliment, J., Wedel, S., Boehmer, S., Dall'Oglio, M., Franzén, L., Coleman, R., Vogelzang, N. J., O'Bryan-Tear, C. G., Staudacher, K., Garcia-Vargas, J., Shan, M., Bruland, Ø. S. and Sartor, O. (2013),

'Alpha emitter radium-223 and survival in metastatic prostate cancer', *New England Journal of Medicine* **369**, 213–223.

Patterson, S. G., Wei, S., Chen, X., Sallman, D. A., Gilvary, D. L., Zhong, B., Pow-Sang, J., Yeatman, T. and Djeu, J. Y. (2006), 'Novel role of stat1 in the development of docetaxel resistance in prostate tumor cells.', *Oncogene* **25**(45), 6113–6122.

Perlmutter, M. A. and Lepor, H. (2007), 'Androgen deprivation therapy in the treatment of advanced prostate cancer', *Reviews in Urology* **9**, S3–S8.

Pittenger, M. F., Mackay, A. M., Beck, S. C., Jaiswal, R. K., Douglas, R., Mosca, J. D., Moorman, M. A., Simonetti, D. W., Craig, S. and Marshak, D. R. (1999), 'Multilineage potential of adult human mesenchymal stem cells', *Science* **284**, 143.

Pointis, G., Latreille, M. T., Mignot, T. M., Janssens, Y. and Cedard, L. (1979), 'Regulation of testosterone synthesis in the fetal mouse testis', *Journal of Steroid Biochemistry* **11**, 1609–1612.

Pollack, A. and Ciancio, G. (1990), 'Cell cycle phase-specific analysis of cell viability using hoechst 33342 and propidium iodide after ethanol preservation.', *Methods Cell Biol* **33**, 19–24.

Prates, C., Sousa, S., Oliveira, C. and Ikram, S. (2011), 'Prostate metastatic bone cancer in an egyptian ptolemaic mummy, a proposed radiological diagnosis', *International Journal of Paleopathology* **1**, 98 – 103.

Reid, L. R., Lowe, C., Cornish, J., Skinner, S. J., Hilton, D. J., Willson, T. A., Gearing, D. P. and Martin, T. J. (1990), 'Leukemia inhibitory factor: a novel bone-active cytokine.', *Endocrinology* **126**, 1416–1420.

Roberts, E., Cossigny, D. A. F. and Quan, G. M. Y. (2013), 'The role of vascular endothelial growth factor in metastatic prostate cancer to the skeleton.', *Prostate Cancer* **2013**, 418340.

Rucci, N. (2008), 'Molecular biology of bone remodelling', *Clinical Cases in Mineral and Bone Metabolism* **5**, 49–56.

Saad, F., the Zoledronic Acid Prostate Cancer Study Group, F., Gleason, D. M., Murray, R., Tchekmedyian, S., Venner, P., Lacombe, L., Chin, J. L., Vinholes, J. J., Goas, J. A. and Zheng, M. (2004), 'Long-term efficacy of zoledronic acid for the prevention of skeletal complications in patients with metastatic hormone-refractory prostate cancer', *JNCI: Journal of the National Cancer Institute* **96**, 879–882.

Saltiel, A. R. (2001), 'You are what you secrete', *Nature Medicine* **7**, 887 – 888.

Sanchez-Sweatman, O. H., Orr, F. W. and Singh, G. (1998-1999), 'Human metastatic prostate pc3 cell lines degrade bone using matrix metalloproteinases.', *Invasion Metastasis* **18**, 297–305.

Scarpace, P. J., Matheny, M., Zhang, Y., Shek, E. W., Prima, V., Zolotukhin, S. and Tümer, N. (2002), 'Leptin-induced leptin resistance reveals separate roles for the anorexic and thermogenic responses in weight maintenance', *Endocrinology* **143**, 3026–3035.

Schafer, K. A. (1998), 'The cell cycle: A review', *Veterinary Pathology* **35**, 461–478.

Sellins, K. S. and Cohen, J. J. (1987), 'Gene induction by gamma-irradiation leads to dna fragmentation in lymphocytes.', *J Immunol* **139**, 3199–3206.

Seto, D. N., Kandarian, S. C. and Jackman, R. W. (2015), 'A key role for leukemia inhibitory factor in c26 cancer cachexia.', *J Biol Chem* **290**, 19976–19986.

Shariat, S. F., Shalev, M., Menesses-Diaz, A., Kim, I. Y., Kattan, M. W., Wheeler, T. M. and Slawin, K. M. (2001), 'Preoperative plasma levels of transforming growth factor beta(1) (tgf-beta(1)) strongly predict progression in patients undergoing radical prostatectomy.', *J Clin Oncol* **19**, 2856–2864.

Sharif, G. M., Schmidt, M. O., Yi, C., Hu, Z., Haddad, B. R., Glasgow, E., Riegel, A. T. and Wellstein, A. (2015), 'Cell growth density modulates cancer cell vascular invasion via hippo pathway activity and cxcr2 signaling', *Oncogene* **34**, 5879–5889.

Shin, J. E., Park, S. H. and Jang, Y. K. (2011), 'Epigenetic up-regulation of leukemia

inhibitory factor (lif) gene during the progression to breast cancer', *Molecules and Cells* **31**, 181–189.

Simmons, J. K., Elshafae, S. M., Keller, E. T., McCauley, L. K. and Rosol, T. J. (2014), 'Review of animal models of prostate cancer bone metastasis', *Veterinary Sciences* **1**, 16–39.

Slaney, C. Y., Möller, A., Hertzog, P. J. and Parker, B. S. (2013), 'The role of type i interferons in immunoregulation of breast cancer metastasis to the bone', *Oncoimmunology* **2**, e22339.

Smith, M. R., Brown, G. A. and Saad, F. (2009), 'New opportunities in the management of prostate cancer-related bone complications', *Urologic Oncology: Seminars and Original Investigations* **27**, S1–S20.

Sosa, M. S., Parikh, F., Maia, A. G., Estrada, Y., Bosch, A., Bragado, P., Ekpin, E., George, A., Zheng, Y., Lam, H.-M., Morrissey, C., Chung, C.-Y., Farias, E. F., Bernstein, E. and Aguirre-Ghiso, J. A. (2015), 'Nr2f1 controls tumour cell dormancy via sox9- and rarbeta-driven quiescence programmes.', *Nat Commun* **6**, 6170.

Stark, G. R., Kerr, I. M., Williams, B. R. G., Silverman, R. H. and Schreiber, R. D. (1998), 'How cells respond to interferons', *Annual Review of Biochemistry* **67**, 227–264.

Sturge, J., Caley, M. P. and Waxman, J. (2011), 'Bone metastasis in prostate cancer: emerging therapeutic strategies.', *Nat Rev Clin Oncol* **8**, 357–368.

Suburu, J. and Chen, Y. Q. (2012), 'Lipids and prostate cancer.', *Prostaglandins Other Lipid Mediat* **98**, 1–10.

Sudhakar, A. (2009), 'History of cancer, ancient and modern treatment methods', *Journal of cancer science & therapy* **1**, 1–4.

Takenaka, K., Moriguchi, T. and Nishida, E. (1998), 'Activation of the protein kinase p38 in the spindle assembly checkpoint and mitotic arrest', *Science* **280**, 599 – 602.

Tallarida, R. J. (2011), 'Quantitative methods for assessing drug synergism', *Genes & Cancer* **2**, 1003–1008.

Tapscott, S. J. and Weintraub, H. (1991), 'Myod and the regulation of myogenesis by helix-loop-helix proteins.', *Journal of Clinical Investigation* **87**, 1133–1138.

Tat, S. K., Padrines, M., Theoleyre, S., Couillaud-Battaglia, S., Heymann, D., Redini, F. and Fortun, Y. (2006), 'Opg/membranous–rankl complex is internalized via the clathrin pathway before a lysosomal and a proteasomal degradation.', *Bone* **39**, 706–715.

Taylor, B. S., Schultz, N., Hieronymus, H., Gopalan, A., Xiao, Y., Carver, B. S., Arora, V. K., Kaushik, P., Cerami, E., Reva, B., Antipin, Y., Mitsiades, N., Landers, T., Dolgalev, I., Major, J. E., Wilson, M., Socci, N. D., Lash, A. E., Heguy, A., Eastham, J. A., Scher, H. I., Reuter, V. E., Scardino, P. T., Sander, C., Sawyers, C. L. and Gerald, W. L. (2010), 'Integrative genomic profiling of human prostate cancer.', *Cancer Cell* **18**, 11–22.

Tazi, H., Manunta, A., Rodriguez, A., Patard, J. J., Lobel, B. and Guillé, F. (2003), 'Spinal cord compression in metastatic prostate cancer', *European Urology* **44**, 527–532.

Thompson, B. R., Lobo, S. and Bernlohr, D. A. (2010), 'Fatty acid flux in adipocytes; the in's and out's of fat cell lipid trafficking', *Molecular and cellular endocrinology* **318**, 24–33.

Timms, B. G. (2008), 'Prostate development: a historical perspective.', *Differentiation* **76**, 565–577.

Todenhofer, T. Stenzl, A. H. L. and Rachner, T. D. (2015), 'Targeting bone metabolism in patients with advanced prostate cancer: current options and controversies.', *Int J Endocrinol* **2015**, 1–9.

Trouillas, M., Saucourt, C., Guillotin, B., Gauthereau, X., Taupin, J.-L., Moreau, J.-F. and Boeuf, H. (2009), 'The lif cytokine: towards adulthood.', *Eur Cytokine Netw* **20**, 51–62.

Turner, C. J. and Edwards, C. M. (2016), 'The role of the microenvironment in prostate cancer-associated bone disease.', *Curr Osteoporos Rep* **14**, 170–177.

Varambally, S., Yu, J., Laxman, B., Rhodes, D. R., Mehra, R., Tomlins, S. A., Shah, R. B., Chandran, U., Monzon, F. A., Becich, M. J., Wei, J. T., Pienta, K. J., Ghosh, D., Rubin, M. A. and Chinnaiyan, A. M. (2005), 'Integrative genomic and proteomic analysis of prostate cancer reveals signatures of metastatic progression.', *Cancer Cell* **8**(5), 393–406.

Vermeulen, K., Van Bockstaele, D. R. and Berneman, Z. N. (2003), 'The cell cycle: a review of regulation, deregulation and therapeutic targets in cancer.', *Cell Prolif* **36**, 131–149.

Verze, P., Cai, T. and Lorenzetti, S. (2016), 'The role of the prostate in male fertility, health and disease', *Nature Reviews Urology* **13**, 379 – 386.

Wallen, C. A., Higashikubo, R. and Dethlefsen, L. A. (1982), 'Comparison of two flow cytometric assays for cellular rna–acridine orange and propidium iodide.', *Cytometry* **3**, 155–160.

Wang, S., Gao, J., Lei, Q., Rozengurt, N., Pritchard, C., Jiao, J., Thomas, G. V., Li, G., Roy-Burman, P., Nelson, P. S., Liu, X. and Wu, H. (2003), 'Prostate-specific deletion of the murine pten tumor suppressor gene leads to metastatic prostate cancer.', *Cancer Cell* **4**, 209–221.

Wang, Z., Gerstein, M. and Snyder, M. (2009), 'Rna-seq: a revolutionary tool for transcriptomics', *Nature Reviews Genetics* **10**, 57 – 63.

Weichselbaum, R. R., Ishwaran, H., Yoon, T., Nuyten, D. S. A., Baker, S. W., Khodarev, N., Su, A. W., Shaikh, A. Y., Roach, P., Kreike, B., Roizman, B., Bergh, J., Pawitan, Y., van de Vijver, M. J. and Minn, A. J. (2008), 'An interferon-related gene signature for dna damage resistance is a predictive marker for chemotherapy and radiation for breast cancer', *Proceedings of the National Academy of Sciences* **105**, 18490.

Wen, Y.-A., Xing, X., Harris, J. W., Zaytseva, Y. Y., Mitov, M. I., Napier, D. L., Weiss, H. L., Mark Evers, B. and Gao, T. (2017), 'Adipocytes activate mitochondrial fatty acid oxidation and autophagy to promote tumor growth in colon cancer', *Cell Death & Disease* **8**, e2593.

Wittrant, Y., Theoleyre, S., Chipoy, C., Padrines, M., Blanchard, F., Heymann, D. and Redini, F. (2004), 'Rankl/rank/opg: new therapeutic targets in bone tumours and associated osteolysis.', *Biochim Biophys Acta* **1704**, 49–57.

Wu, C., Jin, X., Tsueng, G., Afrasiabi, C. and Su, A. I. (2016), 'Biogps: building your own mash-up of gene annotations and expression profiles.', *Nucleic Acids Res* **44**, D313–6.

Wu, L., Yu, H., Zhao, Y., Zhang, C., Wang, J., Yue, X., Yang, Q. and Hu, W. (2015), 'Hif-2alpha mediates hypoxia-induced lif expression in human colorectal cancer cells.', *Oncotarget* **6**, 4406–4417.

Wu, T. T., Sikes, R. A., Cui, Q., Thalmann, G. N., Kao, C., Murphy, C. F., Yang, H., Zhau, H. E., Balian, G. and Chung, L. W. (1998), 'Establishing human prostate cancer cell xenografts in bone: induction of osteoblastic reaction by prostate-specific antigen-producing tumors in athymic and scid/bg mice using lncap and lineage-derived metastatic sublines.', *Int J Cancer* **77**, 887–894.

Wu, X., Gong, S., Roy-Burman, P., Lee, P. and Culig, Z. (2013), 'Current mouse and cell models in prostate cancer research', *Endocrine-related cancer* **20**, 10.1530/ERC–12–0285.

Wyllie, A. H., Morris, R. G., Smith, A. L. and Dunlop, D. (1984), 'Chromatin cleavage in apoptosis: association with condensed chromatin morphology and dependence on macromolecular synthesis.', *J Pathol* **142**, 67–77.

Yang, M., Jiang, P., Sun, F. X., Hasegawa, S., Baranov, E., Chishima, T., Shimada, H., Moossa, A. R. and Hoffman, R. M. (1999), 'A fluorescent orthotopic bone metastasis model of human prostate cancer.', *Cancer Res* **59**, 781–786.

Young, G. J., Harrison, S., Turner, E. L., Walsh, E. I., Oliver, S. E., Ben-Shlomo, Y., Evans, S., Lane, J. A., Neal, D. E., Hamdy, F. C., Donovan, J. L., Martin, R. M. and Metcalfe, C. (2017), 'Prostate-specific antigen (psa) testing of men in uk general practice: a 10-year longitudinal cohort study', *BMJ Open* **7**, e017729.

Yu, H., Yue, X., Zhao, Y., Li, X., Wu, L., Zhang, C., Liu, Z., Lin, K., Xu-Monette, Z. Y., Young, K. H., Liu, J., Shen, Z., Feng, Z. and Hu, W. (2014), 'Lif negatively regulates

tumour-suppressor p53 through stat3/id1/mdm2 in colorectal cancers.', *Nat Commun* **5**, 5218.

Zhang, L., Yang, S., Chen, X., Stauffer, S., Yu, F., Lele, S. M., Fu, K., Datta, K., Palermo, N., Chen, Y. and Dong, J. (2015), 'The hippo pathway effector yap regulates motility, invasion, and castration-resistant growth of prostate cancer cells.', *Mol Cell Biol* **35**, 1350–1362.

Zhao, B., Wei, X., Li, W., Udan, R. S., Yang, Q., Kim, J., Xie, J., Ikenoue, T., Yu, J., Li, L., Zheng, P., Ye, K., Chinnaiyan, A., Halder, G., Lai, Z.-C. and Guan, K.-L. (2007), 'Inactivation of yap oncoprotein by the hippo pathway is involved in cell contact inhibition and tissue growth control.', *Genes Dev* **21**, 2747–2761.

Zhou, Y., Bolton, E. C. and Jones, J. O. (2015), 'Androgens and androgen receptor signaling in prostate tumorigenesis.', *J Mol Endocrinol* **54**, R15–29.

7

Appendix

Table of differentially expression genes after RNA-Seq

Gene	Log2 Fold Change	p value	Adjusted p value
LIF	5.72E+00	2.95E-30	4.92E-26
STAT1	1.10E+00	1.75E-27	9.69E-24
HELZ2	1.05E+00	1.70E-27	9.69E-24
IFI44L	1.64E+00	2.99E-25	1.24E-21
OAS2	1.25E+00	1.07E-24	3.58E-21
PARP9	9.41E-01	3.04E-22	8.45E-19
HSPA6	-1.76E+00	1.59E-19	3.78E-16
CXCL8	-1.36E+00	3.84E-19	7.99E-16
BST2	1.98E+00	3.73E-17	6.89E-14
OAS3	9.43E-01	1.48E-14	2.47E-11

Continued on next page

Table 7.1 – *Continued from previous page*

Gene	Log2 Fold Change	p value	Adjusted p value
PLSCR1	7.99E-01	4.69E-14	7.10E-11
IFI6	1.72E+00	1.10E-12	1.53E-09
APOL6	8.73E-01	3.49E-12	4.47E-09
IFI27	1.58E+00	4.86E-12	5.78E-09
SP100	7.51E-01	1.29E-11	1.34E-08
DDX60	5.26E-01	1.27E-11	1.34E-08
IRF7	1.20E+00	1.48E-11	1.45E-08
LGALS3BP	7.77E-01	1.63E-11	1.51E-08
TRIM69	9.01E-01	2.15E-11	1.88E-08
SHISA5	5.02E-01	4.67E-10	3.89E-07
DDX58	1.01E+00	9.17E-10	7.27E-07
IFITM3	7.13E-01	2.18E-09	1.65E-06
MX1	1.91E+00	2.29E-09	1.66E-06
HLA-E	5.38E-01	2.98E-09	2.06E-06
OAS1	6.76E-01	4.44E-09	2.92E-06
PARP10	1.34E+00	4.56E-09	2.92E-06
DTX3L	5.89E-01	6.04E-09	3.72E-06
GBP1	2.74E+00	7.52E-09	4.47E-06
MALAT1	-4.65E-01	1.75E-08	1.01E-05
STAT2	8.14E-01	4.02E-08	2.23E-05
HERC6	7.65E-01	4.37E-08	2.34E-05
IFITM1	2.31E+00	5.21E-08	2.71E-05
CMPK2	2.25E+00	5.63E-08	2.76E-05
SLFN5	5.16E-01	5.47E-08	2.76E-05
IFIT1	1.13E+00	8.39E-08	3.99E-05
ISG15	8.99E-01	1.06E-07	4.88E-05
PLAT	5.31E-01	1.21E-07	5.43E-05

Continued on next page

Table 7.1 – *Continued from previous page*

Gene	Log2 Fold Change	p value	Adjusted p value
NUPR1	4.98E-01	3.40E-07	1.49E-04
RBCK1	5.07E-01	1.07E-06	4.46E-04
UBE2L6	1.47E+00	1.07E-06	4.46E-04
B2M	2.78E-01	1.82E-06	7.23E-04
SAMD9L	1.34E+00	1.81E-06	7.23E-04
EIF2AK2	4.18E-01	1.96E-06	7.59E-04
IFI35	1.03E+00	2.61E-06	9.67E-04
SOX4	-3.04E-01	2.59E-06	9.67E-04
IFIH1	7.53E-01	2.69E-06	9.74E-04
GDF15	3.33E-01	2.98E-06	1.06E-03
AGR2	3.79E-01	3.89E-06	1.35E-03
TNFAIP3	-1.15E+00	4.43E-06	1.51E-03
ZNF92	-7.52E-01	5.16E-06	1.72E-03
SP110	9.93E-01	5.30E-06	1.73E-03
KLF6	-3.65E-01	6.02E-06	1.93E-03
QSOX1	2.70E-01	6.40E-06	2.01E-03
OASL	3.69E-01	9.08E-06	2.80E-03
HES4	4.44E-01	1.34E-05	4.07E-03
PDK4	-9.87E-01	1.43E-05	4.26E-03
ISG20	5.73E-01	1.63E-05	4.75E-03
SLC3A2	2.83E-01	2.07E-05	5.94E-03
LGALS1	2.51E-01	2.11E-05	5.94E-03
NA	-4.18E+00	2.43E-05	6.75E-03
TAP1	8.89E-01	2.57E-05	7.02E-03
PSME1	3.67E-01	2.66E-05	7.14E-03
PARP14	3.91E-01	2.71E-05	7.17E-03
VMP1	-2.91E-01	3.19E-05	8.12E-03

Continued on next page

Table 7.1 – *Continued from previous page*

Gene	Log2 Fold Change	p value	Adjusted p value
GOLGA8A	-4.17E-01	3.17E-05	8.12E-03
USP18	6.52E-01	3.22E-05	8.12E-03
HIST1H2BG	-8.76E-01	4.08E-05	1.01E-02
DUSP1	-5.72E-01	4.31E-05	1.06E-02
PTHLH	-1.36E+00	5.05E-05	1.22E-02
GOLGA8B	-3.94E-01	7.28E-05	1.73E-02
HAS2	-6.02E-01	7.62E-05	1.79E-02
KITLG	-5.21E-01	8.92E-05	1.89E-02
PARP12	5.78E-01	8.89E-05	1.89E-02
PSME2	3.80E-01	8.21E-05	1.89E-02
HSPH1	-3.03E-01	8.34E-05	1.89E-02
DUSP6	-3.82E-01	8.63E-05	1.89E-02
CRABP2	2.36E-01	8.70E-05	1.89E-02
RPL8	1.97E-01	8.97E-05	1.89E-02
MIR3648-2	8.99E-01	8.59E-05	1.89E-02
NA	-5.26E+00	9.08E-05	1.89E-02
GUK1	2.51E-01	9.51E-05	1.95E-02
IFITM2	3.20E-01	9.97E-05	2.02E-02
IGFBP6	3.14E-01	1.05E-04	2.10E-02
SFN	3.01E-01	1.13E-04	2.23E-02
MIR3648-1	8.40E-01	1.28E-04	2.51E-02
OGT	-3.15E-01	1.42E-04	2.74E-02
ADAR	2.39E-01	1.45E-04	2.78E-02
CXCL11	1.58E+00	1.56E-04	2.95E-02
FTH1	3.27E-01	1.62E-04	3.02E-02
RPS15	2.48E-01	1.92E-04	3.52E-02
CKB	2.64E-01	1.91E-04	3.52E-02

Continued on next page

Table 7.1 – *Continued from previous page*

Gene	**Log2 Fold Change**	**p value**	**Adjusted p value**
HSPA1A	-5.81E-01	2.02E-04	3.66E-02
MGA	-4.64E-01	2.17E-04	3.89E-02
RSAD2	1.78E+00	2.33E-04	4.14E-02
NEAT1	-2.97E-01	2.52E-04	4.42E-02
CHPF	2.99E-01	2.68E-04	4.62E-02
IL17RC	4.04E-01	2.69E-04	4.62E-02
FEM1C	-4.01E-01	2.91E-04	4.95E-02

Table 7.1: Table of differentially expression genes after RNA-Seq of LIF overexpression prostate cancer cells.